THE UNIVERSITY
of EDINBURGH

Investigation into germ cell fate determination of rat embryonic stem cells

Ryan Mathew Taylor

Thesis presented for the award of the degree of Doctor of Philosophy

The University of Edinburgh

2019

Declaration

I declare that except where stated otherwise by reference or acknowledgement, the work presented is entirely my own. This thesis has not been submitted, in whole or part, in any previous application for a degree, diploma or qualification.

Ryan Mathew Taylor
August 2019

Acknowledgements

I would like to express my sincere thanks and appreciation to Tom Burdon for giving me the opportunity to work on this project. I wish to thank him for his seemingly limitless understanding, patience, as well as his advice and support throughout this project and the writing of this thesis. I would also like to thank my other supervisors Ian and Anagha for their invaluable insight and advice over the past few years.
Special thanks go to Linda, Stephen and Tom (W), not only for their continued support and helpful advice, but for the knowledge and experience they have imparted throughout my time working in the lab. I believe without their overwhelming kindness and faith in my abilities, I do not believe I would have made it to this stage. Thank you all!
My thanks to my colleagues in Ian's lab, particularly Man and Jingchao for their dissection expertise, impartial advice and guidance when I presented my progress at their lab meetings. I would also like to thank my colleagues from the neighbouring labs at the Roslin Institute for making the Institute a friendly, happy and productive place to work.
I wish to thank the other members of the Burdon group who have come and gone during my time (Taeho, Madeline, Conn, Alex, Francesca, Zoe) for their company, stimulating conversations and for brightening up even the darkest of days.
Many thanks to Joe, Mel and everyone at Roslin Technologies for their patience, support and understanding during the write up of this thesis.
Finally, my heartfelt thanks to my family and friends, both new and old for their constant support, love and understanding throughout this adventure.

Abstract

The laboratory rat is an important experimental model in biomedical research. Rat embryonic stem cells (ESCs) are valuable for studying mammalian development and for facilitating germ line-modification of rat strains. However, the germline contribution of rat ESCs when injected into developing rat embryos can be variable, restricting their utility. This investigation addressed two key questions; could rat ESC differentiation *in vitro* be directed towards the germline, and could the proportion of cells entering the germ cell lineage be increased by manipulating the gene network of epiblast cells? The formation of the unipotent germline precursors known as primordial germ cells (PGCs) is induced by BMP4/WNT3-mediated induction of essential PGC transcription factors (TFs) BLIMP1, PRDM14 and AP2γ within the epiblast. These factors cooperate to direct a small subset of cells at the proximal posterior region of the epiblast towards a germ cell fate by re-activating expression of naïve pluripotency markers whilst upregulating PGC-specific transcription factors.
To promote differentiation of rat ESCs into the PGC fate, cells were subjected to a differentiation protocol previously developed for mouse ES-to-PGC-like cell (PGCLC) differentiation, which was modified for rat ESCs. Using this protocol, a small proportion of rat cells expressing the PGC-associated surface marker CD61 exhibited enhanced expression of PGCLC gene markers, indicating that the differentiation protocol had generated a population of rat PGCLCs.
To increase the efficiency of PGCLC differentiation, three strategies were implemented to manipulate the epiblast gene network to improve the proportion of rat ESCs entering the germline lineage. The first strategy involved the use of gene-editing technology (CRISPR/Cas9), to incorporate a PGC gene cassette expressing a transgene copy of *Blimp1* immediately downstream of the epiblast gene promotor of *Brachyury*. It was hypothesised that insertion of this gene cassette would drive expression of the *Blimp1* transgene during the epiblast phase of rat ESC fate determination and improve the number of rat PGCLCs generated during PGCLC differentiation. Indeed, the proportion of cells expressing the PGC-associated surface marker CD61 was elevated compared to the parental unmodified cell line. Additionally, $CD61^{+ve}$ cells generated from cells containing the *Blimp1* transgene displayed increased expression of early PGC markers.
The second strategy involved the conditional expression of the three key PGC transcription factors, *Blimp1, Prdm14 and Ap2γ* from stably integrated doxycycline-dependant Tet-On transposon vectors.

Stably transduced cells cultured in doxycycline during embryoid body and PGCLC differentiation protocols had a greater proportion of $CD61^{+ve}$ cells and increased PGC marker gene expression compared to the parental cell line. This was most noticeable in cells expressing *Blimp1* and either of the other two PGC transcription factors (*Prdm14* or *Ap2γ*).

Finally, CRISPR/Cas9 gene editing was also used to inactivate the rat *Otx2* transcription factor gene. Deletion of *Otx2* in mouse ESCs has been shown to increase the proportion of PGCLCs generated during germline differentiation *in vitro*. Similar to exogenous PGC transcription factor expression, rat $Otx2^{-/-}$ knock-out cells generated a greater proportion of $CD61^{+ve}$ cells compared to the parental cell line when put through a PGCLC differentiation protocol. $CD61^{+ve}$ $Otx2^{-/-}$ cells also had increased PGC transcription factor expression compared to the parental cell line, suggesting the loss of *Otx2* can help drive the expression *Blimp1*, *Prdm14* and *Ap2γ*.

In conclusion, rat ESCs subjected to a PGCLC differentiation protocol and manipulation of PGC transcription factor expression exhibited increased expression of PGC markers. However, this response was more limited than that obtained with mouse ESCs, a result which is consistent with reduced germ line transmission of rat ESCs in chimaeric rats. This difference could be due to the initial pluripotency state of rat ESCs; rat ESCs might be in a more committed primed state compared to naïve mouse ESCs, reducing their competence for germ cell lineage differentiation. Additionally, rat ESCs may require different combinations of signals or regulatory factors to ensure efficient germ cell differentiation *in vitro*. Further development of the cell lines and reagents established during this investigation should provide a better understanding of germ line differentiation in the rat.

Lay summary

Embryonic stem cells (ESCs) are a useful tool for introducing mutations into the germline, studying embryonic development, and are a source of cell types for cell replacement therapies. Using modern gene editing technologies, the genomes of ESCs can be altered at specific sequences, facilitating the introduction of mutations into the genome. Rat ESCs are isolated from a developing rat embryo, retaining their potential to become almost any cell type or tissue within the body while being propagated in a laboratory.

When injected into donor embryos, rat ESCs can incorporate into the tissue of the embryo to generate chimaeric animals. Within the chimaera, ESCs can contribute to the germline (a population of cells responsible for maintaining the reproductive cells), producing gametes and thereby facilitating the transmission of the ESC genome into the next generation. However, the contribution of rat ESCs to the germline is relatively inefficient compared to mouse ESCs in mouse chimaeras.

The aim of this investigation was to examine why rat ESCs are inefficiently incorporated into the germline and to explore options for improving their contribution to that lineage. This knowledge could be used to improve the utility of rat ESCs in transgenic research.

During early embryonic development, a small population of cells are set aside from the majority that contribute to tissues required the development of body (somatic) tissues and are directed to become the precursor cells of the germline (PGCs). These PGCs give rise to the reproductive cells, sperm and eggs. PGC formation can be induced by activating the expression of key transcription factor proteins (BLIMP1, PRDM14 and AP2γ) within the early embryonic cells; activating the expression of genes required for PGC specification whilst also restricting the expression of genes required for somatic cell types. Mouse ESCs were efficiently directed into PGCs using a specific germ cell differentiation protocol. Rat ESCs were treated with the same protocol and a small sub-population of the rat cells had increased expression of genes associated with PGCs. To improve the generation of rat PGCs, three gene-editing strategies were adopted.

The first strategy utilised gene-editing technology (CRISPR/Cas9) to place a copy of the rat *Blimp1* gene under the control of the *Brachyury* gene promoter, a gene expressed in the embryo during PGC specification. It was hypothesised that forced expression of *Blimp1* in rat ESCs during the earliest stages of PGC specification would increase the formation of rat PGCs.

Expression of *Blimp1* via the *Brachyury* promotor increased the expression of early PGC gene markers within a sub-population of cells compared to unmodified rat ESCs. This indicated that increased expression of factors involved in PGC specification can help direct rat ESCs towards the germline.

The second strategy involved conditional expression of the three key PGC transcription factor proteins (*Blimp1, Prdm14 and Ap2γ*) from an expression vector randomly integrated into the genome of rat ESCs. Expression of these transcription factor genes was induced by introducing a drug (doxycycline) into the culture medium of the cells. Activation of these genes during the germline differentiation protocol increased PGC gene marker expression within a sub-population of cells compared to unmodified rat ESCs. This was most noticeable when cells were induced to express *Blimp1* in combination with either of the other two PGC transcription factors proteins (*Prdm14* or *Ap2γ*), showing that expression of multiple PGC transcription factors increased expression of PGC markers in rat cells.

The third strategy used gene editing technology to reduce the number of rat cells which became non-germline cells (somatic cells). This was achieved by inactivating *Otx2*, a gene reported to be involved in directing cells away from the germline. In mice, loss of *Otx2* expression increased the proportion of PGCs. Loss of *Otx2* in rat ESCs decreased the expression of somatic cell gene markers, suggesting the capacity of the *Otx2* deficient cells to become somatic cells had been comprised. However, expression of PGC markers in three independent *Otx2* deficient rat ESC clones was inconsistent, making it difficult to conclude whether this strategy was useful for directing rat cells towards the germline.

In summary, although the expression of PGC transcription factors in differentiating rat ESCs increased expression of PGC gene markers, this response was more limited than that obtained with mouse ESCs. This result was consistent with the less effective germline contribution of rat ESCs in chimaeras, leading to the conclusion that under the current culture conditions the stem cell status of rat ESCs is inherently different to mouse ESC. Future studies should explore what these differences are and what factors are critical for efficient germline determination in the rat.

List of figures

Chapter 1

Chapter 3

Chapter 4

Chapter 5

Chapter 6

Chapter 7

Chapter 9

List of tables

Chapter 2

Abbreviations

AP2γ	Activating enhancer-binding protein-2 gamma
bFGF	Basic fibroblast growth factor
bp	Base pairs
BLIMP1	B-lymphocyte-induced maturation protein 1
BMP	Bone morphogentic protein
BSA	Bovine serum albumin
cDNA	Complementary deoxyribonucleic acid
CO_2	Carbon dioxide
DMEM	Dulbecco's modified Eagle's medium
DMSO	Dimethyl sulfoxide
DNA	Deoxyribonucleic acid
dpc	Days postcoitum
EDTA	Diaminetetraacetic acid disodium salt
EGCs	Embryonic germ cells.
EGF	Epidermal growth factor
EM	Embryonic mesoderm
EpiLCs	Epiblast-like cells
EpiSCs	Epiblast stem cells
ESC	Embryonic stem cell
ESRRβ	Estrogen-related receptor beta
EXE	Extra-embryonic ectoderm
FACS	Fluorescent activated cell sorter
FCS	Foetal calf serum
g	Gravitational force
GFP	Green fluorescent protein
GMEM	Glasgow's modified Eagle's medium
GSK3	Glycogen synthase kinase 3
HCl	Hydrochloric acid
ICM	Inner cell mass
iPSCs	Induced pluripotent stem cells
KCl	Potassium chloride
KH_2PO_4	Potassium dihydrogen phosphate
KSR	knock-out serum replacement
LB	Luria-Bertani

LEF1	Lymphoid enhancer binding factor 1
L-Glut	L-glutamine
LIF	Leukaemia inhibitory factor
MEF	Mouse embryonic fibroblasts
MEK	Mitogen activated protein kinase
MQ H_2O	MilliQ water
NaCl	Sodium chloride
Na_2HPO_4	Sodium hydrogen phosphate
NEAA	Non-essential amino acids
nt	Nucleotides
PBS	Phosphate-buffered saline
PBST	Phosphate-buffered saline + Triton
PFA	Paraformaldehyde
PGC	Primordial germ cell
PGCLC	Primordial germ cell-like cell
PRDM14	PR domain-containing protein 14
qRT-PCR	Quantitative reverse transcription polymerase chain reaction
RNA	Ribonucleic acid
SCF	Stem cell factor
TCF3	Transcription factor 3
TFAP2C	Transcription factor AP-2 gamma
VE	Visceral endoderm

Contents

Chapter 1 Introduction

1.1 Generation of *in vitro* cell lines from pluripotent rodent cell lines

1.1.1 The rat as a model organism

Model organisms such as rodents are used extensively in research to further our understanding of the biological processes which occur throughout growth and development. Over the last century, the laboratory rat has been used as a model for studying many aspects of mammalian biology, including physiology, immunology and toxicology (Jacob 1999, Aitman et al. 2008). There are now a large number of different inbred rat models available, giving researchers the opportunity to explore a range of different biomedical and developmental research questions (Jacob 1999, Aitman et al. 2008). A key advantage of the laboratory rat is that it is both metabolically and physiologically more similar to humans than the mouse, another popular rodent model organism (Gibbs et al. 2004, Blais et al. 2007). In stem cell biology, a gold-standard method for interrogating the pluripotency of *in vitro* cultured stem cells is to inject the cells into a blastocyst and determine whether the injected cells can contribute to the developing embryo. If these embryos survive the procedure, the offspring produced will be chimeras, animals which contain two or more genetically distinct cell types derived from more than one zygote. It has been proven that *in vitro* derived rat pluripotent stem cells can contribute to the developing germ cell layers and the germline of a host embryo, producing chimaeric rat models for future scientific study (Iannaccone et al. 1994, Buehr et al. 2008, Li et al. 2008). These characteristics, coupled with other advantages such as a fast generation time compared to larger mammalian species, makes the laboratory rat a useful model organism for scientific research.

1.1.2 Early rodent embryogenesis

The early development of the albino rat (*Mus Norvegicus Albinus*) was first described in 1915, detailing the stages of rat embryogenesis from the establishment of the early rat zygote, to the formation of the egg cylinder and its subsequent development until ~E9 days post coitum (dpc) (Huber 1915). The developmental stages of the rat embryo have since been investigated further (Butcher 1929, Nicholas & Hall 1942, Krehbiel 1962, Tarkowski 1962, Schlafke & Enders 1963), revealing a similarity in the development of the rat embryo to that of the mouse. As the embryonic structures produced during both mouse and rat embryogenesis appear consistent, it has become widely accepted that rat embryogenesis follows the same developmental pattern to that of the mouse embryo. Comparing the two species to the Carnegie staging system developed from the early work of Streeter (1942) and O'Rahilly & Müller (1987) (the 23 stages of embryo development used to standardise embryogenesis between different vertebrate species), one crucial difference between the two is rat embryogenesis is ~1-2 developmental days behind that of the mouse. For instance, the mouse embryo reaches the blastocyst stage of development at ~E3.5 dpc, compared to the rat which reaches the same stage at ~E4.5 dpc (Casanova et al. 2012). This section summarises the development of the rodent fertilised zygote up until the formation of the early germ cell progenitors. The dpc times presented represent the stages during mouse embryogenesis, as this is more widely represented in the literature compared to the rat.

Once fertilised, the rodent zygote undergoes multiple cellular divisions to form a cluster of cells (blastomeres) known as the morula (Bedzhov et al. 2014). At this stage, blastomeres are totipotent cells, meaning they are capable of differentiating into any cell type of the developing embryo including the placenta (Nichols & Smith 2009). Further cellular division and differentiation of the blastomeres within the morula gives rise to the early blastocyst at ~E3.5 dpc in mice, a heterogeneous structure composed of trophoblast cells (trophectoderm precursors cells) surrounding an inner cell mass (ICM) (Figure 1.1.1) (Bedzhov et al. 2014).

Figure 1.1.1. Formation of the mouse blastocyst. *The fertilised egg (zygote) undergoes multiple rounds of cellular divisions (between E0.5 – E2.5 dpc) to give rise to the Morula, a mass of ~16 cells (blastomeres). The cells within the morula will continue to divide and form the early blastocyst (E3.5 dpc).*

Prior to implantation, the ICM is the naïve compartment of the embryo, harbouring the pluripotent cells which will differentiate into the three germ layers, ectoderm, endoderm and mesoderm (Nichols & Smith 2009, Nichols & Smith 2011, Bedzhov et al. 2014). Cells from the ICM can be isolated and injected into the blastocyst of a recipient embryo, contributing to all three germ layers of the host embryo to form a chimaeric animal (Nichols & Smith 2009, Nichols & Smith 2011, Bedzhov et al. 2014). Just before implantation, the ICM segregates into two distinct cell types, the epiblast and hypoblast (Nichols & Smith 2009, Nichols & Smith 2011, Bedzhov et al. 2014, Irie et al. 2014) (Figure 1.1.2). The cells within the epiblast retain the ability to differentiate into the germ layers, while the hypoblast cells predominantly differentiate into the primitive endoderm (Nichols & Smith 2009, Nichols & Smith 2011, Bedzhov et al. 2014, Irie et al. 2014).

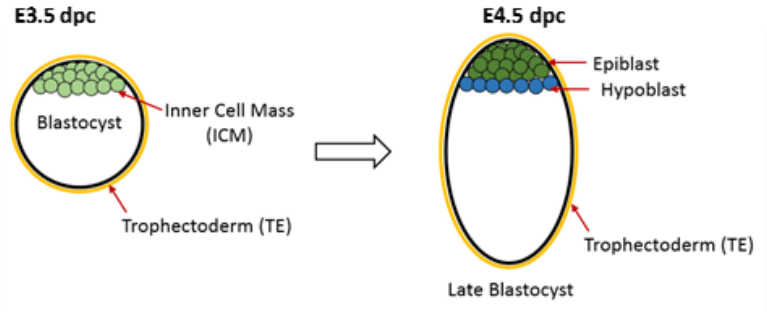

Figure 1.1.2. Late blastocyst stage of mouse. *After blastocyst formation (E3.5 – E4.5 dpc in mice), the ICM segregates into the epiblast and the hypoblast. This structure is known as the late blastocyst.*

After implantation (E4.5< dpc in mice), epiblast cells in the developing rodent embryos form a cup-shaped epithelium (egg cylinder), a structure different from the bilaminar disc seen in other mammalian species such as humans and pigs (Figure 1.1.3) (Nichols & Smith 2011, Irie et al. 2014, Irie et al. 2015, Wang et al. 2016).Analysing the gene expression profile of pre- and post-implantation embryos has revealed that the expression of naïve stem cell markers such as *Nanog* is reduced after implantation, while the expression of markers of primed cells such as *Brachyury* and *Fgf5* increases (Chambers et al. 2003).

These results suggest that the cells comprising the post-implantation embryo are more “primed” for differentiation than the naïve cells present within the pre-implantation embryo. Epiblast stem cells (EpiSCs) are pluripotent stem cells generated from the successful isolation and *in vitro* culture of the cells found within the ICM of the post implantation epiblast (Tesar et al. 2007, Brons et al. 2007). Cells isolated directly from the post-implantation epiblast or cultured *in vitro* as EpiSCs do not form chimeras when injected into a pre-implantation embryo, but they have been reported to contribute to all three germ layers ex vivo (Gardner 1985, Tesar et al. 2007, Brons et al. 2007, Rossant 2008). It has been reported that unlike ESCs, EpiSCs derived from either post-implantation embryos or via the differentiation of ESCs into EpiSCs can contribute to chimeras when injected into early post-implantation embryos (Huang Y et al. 2012). Despite the similarity in pluripotency gene expression, the cells of the post implantation embryo appear to have a different developmental potential compared to the cells of pre-implantation embryo. The majority of the cells within the epiblast will then contribute further to the embryo proper, reorganising during gastrulation and differentiating into the tissue/cell progenitors for all three germ layers (ectoderm, endoderm and mesoderm) (Nichols & Smith 2009, Nichols & Smith 2011, Bedzhov et al. 2014).

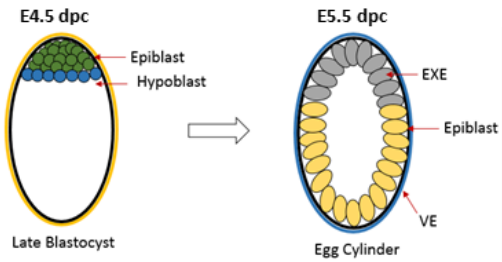

Figure 1.1.3. Formation of the egg cylinder in mice*. After implantation (E4.5 – E5.0 dpc in mice), the late blastocyst matures into the egg cylinder. Rapid proliferation of the epiblast and trophectoderm occurs, causing the cells to grow and re-order themselves into the blastocyst cavity. Cells generated from the trophectoderm make up the extra-embryonic ectoderm (EXE). The differentiating hypoblast cells surrounds the epiblast and EXE cells, forming the visceral endoderm (VE).*

However, a small proportion of cells within the post-implantation epiblast do not enter the somatic pathway but instead are fated to give rise to primordial germ cells (PGCs). PGCs are the unipotent precursor cells of gametes and first emerge in the proximal posterior region of the epiblast (Ohinata et al. 2005, Dudley et al. 2007, Rao et al. 2010, Welling & Geijsen 2013, Günesdogan et al. 2014, Irie et al. 2014). Their formation is stimulated by BMP4 and WNT3 signals generated by the extraembryonic ectoderm and visceral endoderm (Winnier et al. 1995, Ohinata et al. 2005, Rao et al. 2010, Günesdogan et al. 2014). These intercellular signals induce

the expression of PGC transcription factors which drive the cells towards the germ cell lineage (Ohinata et al. 2005, Dudley et al. 2007, Rao et al. 2010, Günesdogan et al. 2014). Once established, PGCs begin to multiply and then migrate through the developing hindgut, accumulating at the site of the embryonic gonad by mid-gestation (~E11.5 dpc in mice) (Ohinata et al. 2005, Richardson & Lehmann 2010, Günesdogan et al. 2014) (Figure 1.1.4). After migration, PGCs differentiate into the cell types which form the adult reproductive cells (Ohinata et al. 2005, Richardson & Lehmann 2010, Günesdogan et al. 2014).

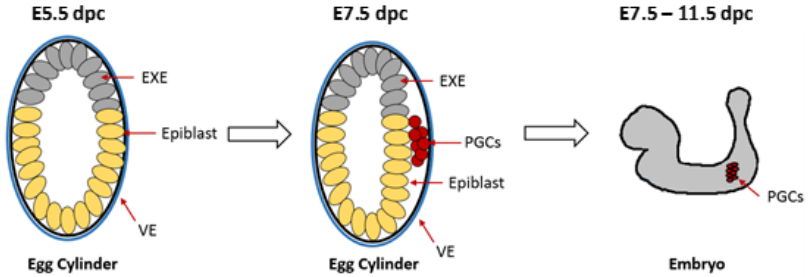

Figure 1.1.4. Generation of mouse primordial germ cells (PGCs). *A small proportion of epiblast cells in the proximal region of the rodent embryo are stimulated to differentiate into the unipotent germ cell precursor cells, primordial germ cells (PGCs) via extracellular signalling from the extra-embryonic ectoderm (EXE) and visceral endoderm (VE). These cells migrate through the developing embryo and accumulate at the embryonic gonad by ~11.5 dpc in mice.*

1.1.3 Derivation and *in vitro* culture of rodent pluripotent stem cells

1.1.3.1 Mouse pluripotent stem cells

Embryonic stem cells (ESCs) are pluripotent cells derived from the undifferentiated ICM of pre-implantation embryos. ESCs can be maintained for prolonged periods in tissue culture conditions and be induced to differentiate into the three primary germ layers, ectoderm, endoderm and mesoderm. The method for deriving and culturing mouse ESC lines *in vitro* was established by two research groups independently in 1981 (Evans & Kaufman 1981, Martin 1981). Since then, the derivation protocol has been further optimised to generate one of the most widely used mammalian ESC models in scientific research. Naïve cells contained within the mouse epiblast can be isolated from the ICM (~E3.5 dpc) and captured in a self-renewing ESC state *in vitro* by culturing them either on mouse embryonic fibroblast (MEF) feeder layers or feeder-free (e.g. on gelatin-coated plates) (Ward et al. 2002, Czechanski et al. 2014) (Figure 1.1.5). The established cell culture mediums for mouse are a basal medium supplemented with FCS (foetal calf serum) and LIF (leukaemia inhibitory factor) (Williams et al. 1988) or 2i+LIF conditions, a culture medium containing a MEK (mitogen activated protein kinase) and GSK3 (glycogen synthase kinase) inhibitor in addition to LIF (Silva et al. 2008, Ying et al. 2008).

These culture mediums have been optimised to retain the self-renewal capability associated with cells of the pre-implantation epiblast. ESCs cultured in 2i+LIF medium are characterised by the expression of the core pluripotency factors (e.g. *Nanog*) (Chambers et al. 2003), as well as widespread hypomethylation of the genome (Leitch et al. 2013, Habibi et al. 2013, Bagci et al. 2013). Cultured mouse ESCs can be injected into a blastocyst and contribute to the developing embryo to form chimeras. However, certain strains of mouse ESCs develop chimeras which have poor viability or abnormalities during development, such as the inbred strain C57BL/6 (Eggan et al. 2001). There is also reported to be variability in the germline competency of mouse ESC strains (the ability of ESCs to contribute to the germline of the embryo). For instance, the germline competency of the mouse ESC strains DBA/1Ola, BALB/c, and FVB/N are all thought to be lower than that of ESCs derived from the 129 strain of mouse strains (129/Sv, 129/SvEv, and 129/Ola) (Auerbach et a. 2000, Ware et al. 2003). This has been suggested to be due to inherent issues acquired during the derivation of these inbred strains impacting their ability to enter the germ cell lineage.

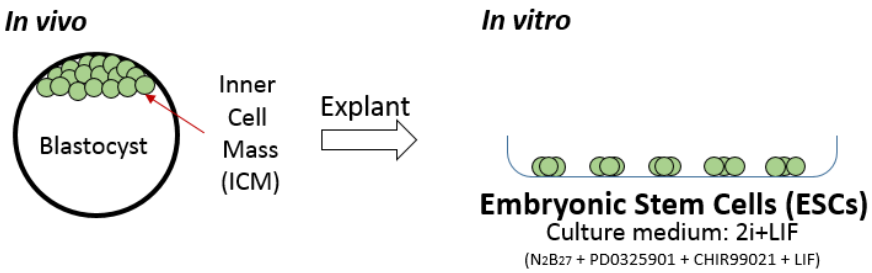

Figure 1.1.5. ESC derivation. *Cells harvested from the ICM of a pre-implantation embryo can be cultured in vitro in culture medium such as 2i+LIF.*

Primed pluripotent stem cells, referred to as epiblast-derived stem cells (EpiSCs), are derived by explanting cells from the epiblast of post-implantation embryos and culturing them in culture medium often supplemented with either FCS or knock-out serum replacement (KSR), Activin A and FGF2 (bFGF) (Tesar et al. 2007, Brons et al. 2007) (Figure 1.1.6). It is also possible to irreversibly differentiate ESCs into EpiSCs by culturing them in N_2B_{27} culture medium supplemented with Activin A and bFGF (Guo et al. 2009). EpiSCs express the core pluripotency factors found in ESCs (e.g. *Nanog*, *Oct4, Sox2*) and can form teratomas when injected into immunodeficient mice (Tesar et al. 2007, Brons et al. 2007).

However, EpiSCs have a distinct “primed” gene expression profile compared to ESCs, increased DNA methylation of gene promotors, and are not incorporated efficiently into the germline of chimaeric animals if injected into a blastocyst (Brons et al. 2007, Guo et al. 2009, Veillard et al. 2014).

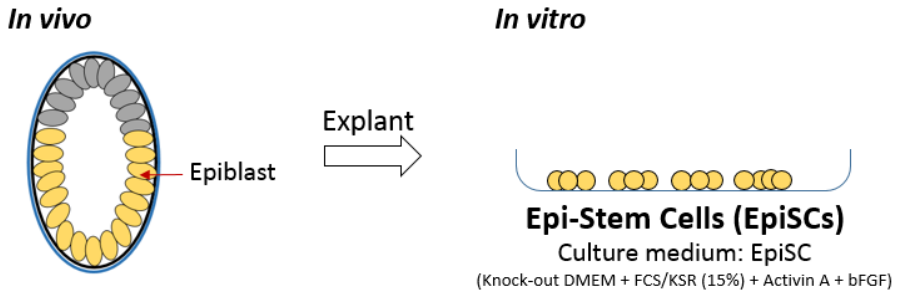

Figure 1.1.6. EpiSC derivation. *Cells isolated from the epiblast cells of a post-implantation embryo can be cultured in vitro in a chemically defined culture medium (Knock-out DMEM + Fetal Calf Serum (FCS) or Knock-out serum replacement (KSR)) supplemented with Activin A and bFGF.*

It is also possible to derive pluripotent cell lines by isolating and maintaining PGCs *in vitro* from the developing embryo (Matsui et al. 1992, Resnick et al. 1992). PGCs can be retained and will proliferate *in vitro* when the cells are cultured in DMEM with FCS supplemented with LIF and bFGF (Matsui et al. 1992, Resnick et al. 1992, Durcova-Hills et al. 2006). The explanted PGCs transition into embryonic germ cells (EGCs), cells which share similar characteristics to ESCs derived from the pre-implantation embryo, such as the ability to form chimeras when injected into an embryo (Matsui et al. 1992, Resnick et al. 1992, Labosky et al. 1994, Stewart et al. 1994) and the expression of pluripotency factors (Buhr et al. 2008, Hochedlinger 2011).

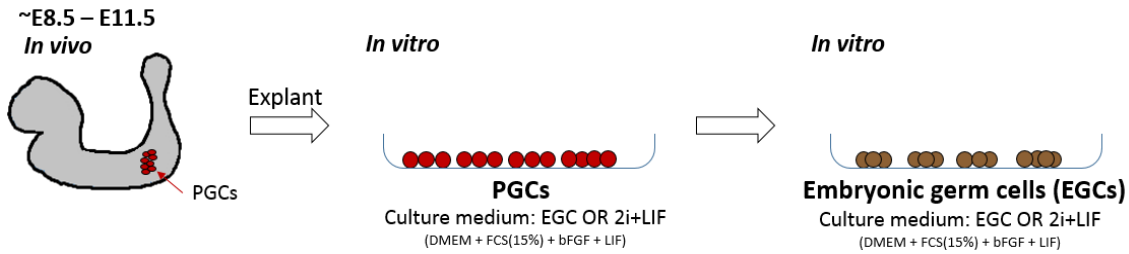

Figure 1.1.7. EGC derivation. *Primordial germ cells (PGCs) isolated from the developing embryo can be cultured in vitro in either serum culture medium or in 2i+LIF. These cells transition into embryonic germ cells (EGCs), cells with similar properties to ESCs.*

1.1.3.2 Rat pluripotent stem cells

Early attempts to derive rat ESCs from blastocysts using similar techniques as those used to generate mouse ESC lines proved unreliable, generating cell lines with high variability in their potential to form chimaeras and to contribute to the tissue of a host blastocyst (Ouhibi et al. 1995, Stranzinger 1996, Vassilieva et al. 2000, Buehr et al. 2003). These cell lines also suffered from cell heterogeneity and spontaneous differentiation during *in vitro* cell culture (Ouhibi et al. 1995, Stranzinger 1996, Vassilieva et al. 2000, Buehr et al. 2003).

Direct genetic modification of germ cells and zygotes has been demonstrated to be capable of generating genetically modified rats without the need for deriving rat ESCs (Smits et al. 2006, Geurts et al. 2009, Izsvák et al. 2010). Although these approaches proved a useful alternative to avoid the apparent issues with *in vitro* rat ESC derivation, extensive screening methods to identify suitable candidates were required and the generated cells were far more limited in their usefulness to generate reporter cell lines (Smits et al. 2006, Geurts et al. 2009, Izsvák et al. 2010).

Similar to the mouse, rat PGCs could be isolated and cultured in 2i+LIF medium *in vitro* to derive EG cell lines (Leitch et al. 2010). These EG cell lines share similar characteristics to other *in vitro*-derived pluripotent cells, such as the expression of the core pluripotency network (Leitch et al. 2010).

In 2008, the derivation and culture of genuine ESCs from the rat blastocyst was accomplished (Buehr et al. 2008, Li et al. 2008), providing another alternative source of ESCs from a model which is metabolically close to humans (Gibbs et al. 2004, Blais et al. 2007). Rat ESC derivation was performed by isolating cells from the ICM of rat blastocysts and maintaining them in serum-free 2i culture medium (culture medium containing a MEK and GSK3 inhibitor) whilst attached to a MEF feeder layer (Figure 1.1.8) (Buehr et al. 2008, Li et al. 2008).

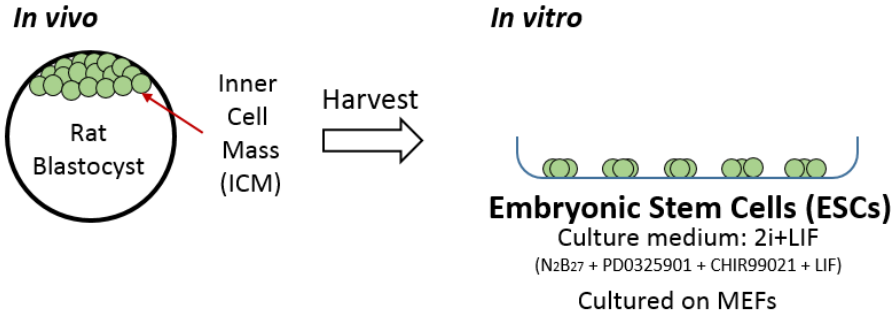

Figure 1.1.8. Rat ESC derivation. *Rat cells explanted from the ICM of a pre-implantation embryo can be cultured in vitro in 2i+LIF medium on mouse embryonic fibroblast (MEF) layers.*

These rat ESC lines have been shown to exhibit all the properties of naïve pluripotent cells such as being responsive to LIF (improving the stability of the cells in culture), a capacity for clonal expansion and have the ability to contribute to the germline of chimaeras. The addition of LIF alongside the 2i inhibitors (2i+LIF cell medium) has proven useful in retaining ESCs in a self-renewing pluripotent state by blocking MEK/ERK activity and preventing the degradation of β-catenin, a factor involved in restricting the repressive action of TCF3 (Figure 1.1.9) (Buehr et al. 2008, Li et al. 2008, Ying et al. 2008, Meek et al. 2013).

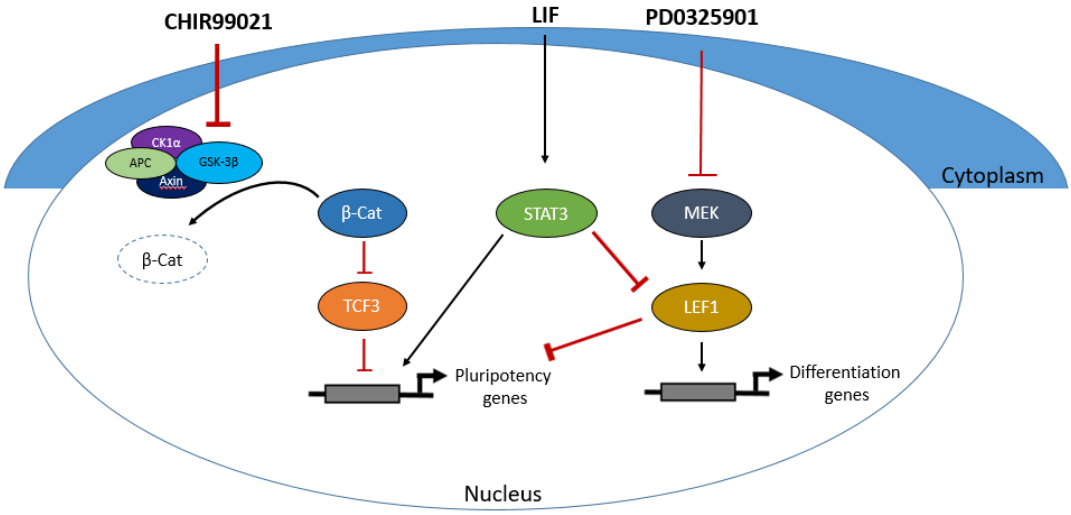

***Figure 1.1.9. Model of CHIR99021, PD0325901 and LIF mediated ESC self-renewal during 2i+LIF cell culture**. TCF3 and LEF1 are involved in driving ESC differentiation.TCF3 represses the expression of pluripotent genes, while LEF1 induces differentiation through induction of differentiation genes and suppressing pluripotency genes. Both transcription factors are downregulated by the presence of CHIR99021 and PD0325901 in the culture medium, assisting in maintaining ESC self-renewal. CHIR99021 increases β-catenin (β-Cat) stability by reducing wnt signalling inhibition, inhibiting TCF3 mediated suppression of pluripotency genes. LIF/STAT3 signalling assists in the suppression of Lef1 expression, while also maintaining the expression of pluripotency genes.*

Despite the relative success in the derivation and maintenance of rat ESC lines, there are still multiple issues to be resolved to better improve their usefulness as an ESC model. Although rat ESCs express the core pluripotency factors, increased expression of lineage specific genes suggests that rat ESCs may be more 'primed' for differentiation than mouse ESCs (Blair et al. 2011, Hong et al. 2013). 2i+LIF culture conditions can maintain rat ESCs in a pluripotent and self-renewal state *in vitro*, but spontaneous differentiation can still occur during standard cell culture (Buehr et al. 2008, Li et al. 2008, Meek et al. 2013). It has also been noted in our laboratory and by colleagues that there is a problem with karyotypic instability of rat ESCs, as well as greater variability in the germline competency of rat ESCs compared to mouse ESCs (data not published).

To generate transgenic animals, it is important that ESCs are incorporated into the germline of a developing embryo to facilitate the transmission of the ESC genome into the next generation. However, reports have shown variable success rates in the generation of chimaeric animals, with some strains of rat being more efficient at germline transmission than others (Buehr et al. 2008, Li et al. 2008, Ueda et al. 2008, Li et al. 2008, Zhao et al. 2010). This variability in germline transmission can restrict the utility of rat ESCs as a tool for scientific research. Therefore, a better understanding of the ESC genetic background and the conditions required for rat germline determination both *in vitro* and *in vivo* is required.

1.2 Derivation of the germline

1.2.1 Primordial germ cells (PGCs)

Mammalian germ cell specification begins after blastocyst implantation, where a small proportion of post-implantation cells found in the proximal posterior region of the embryo are diverted from differentiating into somatic precursor cells and instead differentiate into the unipotent germline precursor cells, referred to as PGCs (Ohinata et al. 2005, Dudley et al. 2007, Rao et al. 2010, Welling & Geijsen 2013, Günesdogan et al. 2014, Irie et al. 2014).

An investigation performed in mouse embryos by Saitou et al (2003) found that once established, the developing PGCs can be separated into two separate categories, Fragilis^{+ve}/Stella^{-ve} or Fragilis^{+ve}/Stella^{+ve}. Cells positive for both genes (found in the centre of PGC clusters) are thought to be the cells destined for the germ cell lineage, as the presence of *Stella* is a hallmark of PGCs (Saitou et al 2003).

Once formed, the PGC progenitors will multiply and then migrate through the developing hindgut and accumulate at the site of the embryonic gonad by mid-gestation, ~E11.5 dpc in mice (Ohinata et al. 2005, Richardson & Lehmann 2010, Günesdogan et al. 2014) and ~E13 dpc in rats (Kemper & Peters 1987). Migrating germ cells in mice retain *Stella* expression (Yeom et al. 1996), but also have a strong repression of homeobox genes (e.g. *Hoxa1*, *Hoxb1*) (Saitou et al. 2003), despite the opposite being true in neighbouring somatic cells. The expression of the pluripotency factor *Oct4* has also been detected in migratory PGCs of both mice and rats (Yeom et al. 1996, Encinas et al. 2012). This retention of pluripotency gene expression alongside the repression of differentiation markers is what gives the PGCs the pluripotency potential necessary to generate the germline during embryogenesis.

1.2.2 Driving forces in PGC specification

To direct the differentiation of epiblast cells towards the germ cell lineage, the BMP and WNT signalling cascades induce the expression of three transcription factors required for PGC specification, BLIMP1 (PRDM1), PRDM14 and AP2γ (TFAP2C) (Figure 1.2.1) (Ohinata et al. 2005, Dudley et al. 2007, Rao et al. 2010, Welling & Geijsen 2013, Günesdogan et al. 2014).

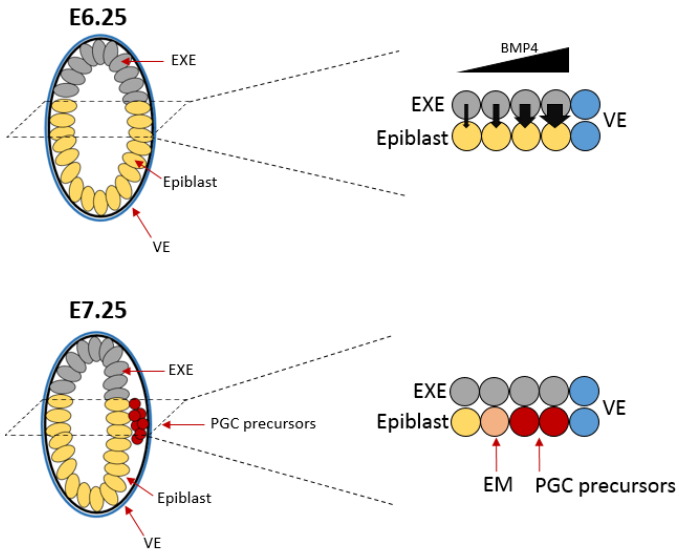

Figure 1.2.1. Rodent PGC specification. *At ~E6.25 in the mouse post-implantation embryo, signalling molecules (e.g. BMP4) are secreted from the extraembryonic ectoderm (EXE) and visceral endoderm (VE), activating signal pathways which drives the differentiation of epiblast cells in the proximal region of the egg cylinder towards the embryonic mesoderm (EM) or PGC precursor cells*

1.2.2.1 *BLIMP1: The transcriptional repressor*

BLIMP1 (B-lymphocyte-induced maturation protein 1 or PR domain-containing protein 1 (PRDM1)) belongs to the PRDM SET domain family of proteins and is induced by the BMP4-SMAD1/5 signalling pathway (Ohinata et al. 2005, Dudley et al. 2007, Fog et al. 2012, Günesdogan et al. 2014) (Figure 1.2.2). BLIMP1 has been reported to be important in mature adult cells; decreased *Blimp1* expression in human testicular germ cell tumours (Eckert et al. 2008) and in B Cell Lymphoma restores the ability of mature adult cells to enter a pluripotent state (Mandelbaum et al. 2010). *Blimp1* expression is undetectable at the pre-implantation stage of embryogenesis (Chu et al. 2011), but is detected within the developing PGC progenitor cells and the visceral endoderm (VE) in the mouse post-implantation embryo (Ohinata et al. 2005, Vincent et al. 2005).

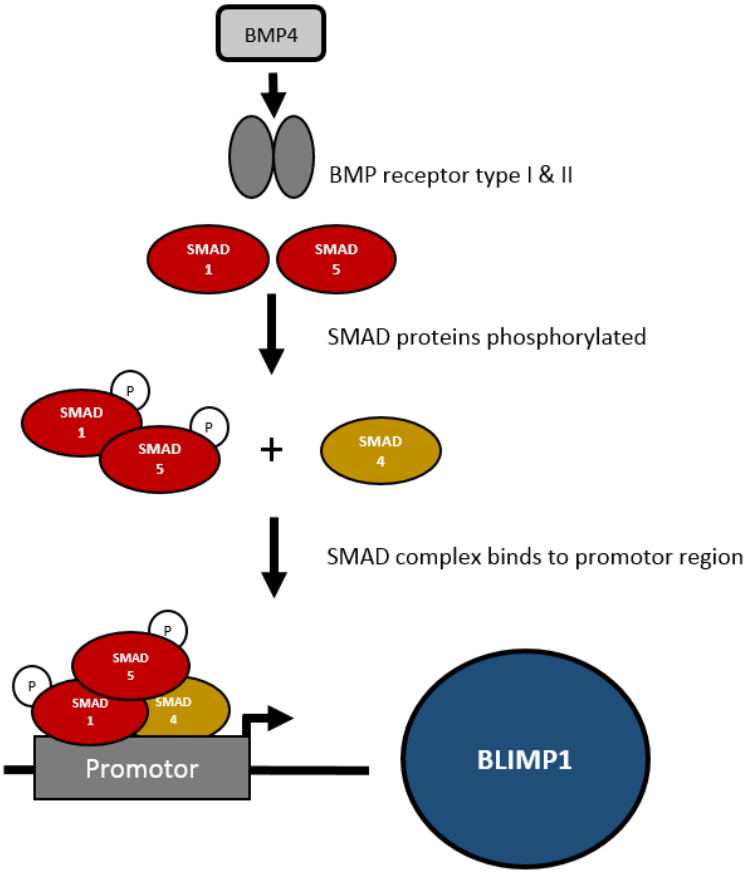

Figure 1.2.2. BMP4 signalling activates Blimp1 expression. *BMP4 binds to a BMP receptor, inducing the phosphorylation of members of the SMAD family (SMAD1 & SMAD5). This phosphorylation activity induces the formation of the SMAD complex (SMAD4 associated with phosphorylated SMAD1 and SMAD5) at the promotor region of the Blimp1 gene, inducing the expression of the Blimp1 transcription factor.*

The BLIMP1 transcription factor is involved in the silencing of the somatic pathway during embryogenesis, driving cells at the proximal posterior region of the epiblast to differentiate into the germ cell lineage (Ohinata et al. 2005, Bikoff et al. 2009, John & Garrett-Sinha 2009, Schäfer et al. 2011). BLIMP1 lacks histone methyl-transferase activity in their conserved PR/SET domain (Fog et al. 2012), suggesting it does not directly influence histone methylation. Instead, it is reported that BLIMP1 acts as a platform, recruiting histone modifying factors such as PRMT5 and histone deacetylases (HDACs) to promoter regions, inducing the silencing of target genes (Bikoff et al. 2009, Nagamatsu et al. 2011). This role assists in the repression of factors which promote the formation of the somatic lineages, such as the homeobox genes (e.g. *Hoxa1*/*Hoxb1*) and de novo methyltransferases (e.g. *Dnmt3a*/*Dnmt3b*) (Ohinata et al. 2005, Bikoff et al. 2009, John & Garrett-Sinha 2009, Schäfer et al. 2011).

Inhibiting these factors prevents differentiation of the epiblast cells into somatic cells and assists the re-activation of pluripotent factors necessary for PGC development (Figure 1.2.3).

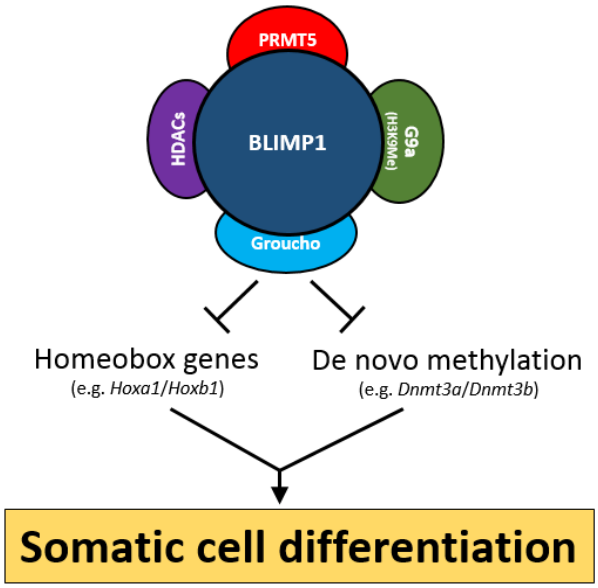

***Figure 1.2.3. BLIMP1 inhibits somatic differentiation**. The BLIMP1 transcription factor acts as a scaffold, recruiting histone modifying enzymes and their co-factors to promotor regions of genes which drive somatic cell differentiation. Recruitment of these factors induces epigenetic repression of these genes, restricting somatic cell differentiation of these cells.*

It is reported BLIMP1 is key to early specification and generation of PGCs, as it is the first of three PGC transcription factors to be active during PGC specification in the post-implantation embryo (~E6.25 dpc in the mouse) (Ohinata et al. 2005). Loss or downregulation of *Blimp1* due either to mutation or impaired BMP or WNT signalling, can reduce the proportion of epiblast cells transitioning into the PGC lineage, as well as inhibiting the proliferation of already established PGCs (Ohinata et al. 2005, 2009). Loss of *Blimp1* expression has no influence on the derivation or growth of *in vitro* mouse ESCs from *Blimp1*$^{-/-}$ knock-out embryos (Bao et al. 2012). However, overexpression of *Blimp1* within mouse ESCs can adversely affect ESC colony growth (Nagamatsu et al. 2011), suggesting there is a threshold of *Blimp1* expression, above which the repressive activity negatively impacts ESC growth.

1.2.2.2 *PRDM14: The critical regulator*

PRDM14 (PR domain-containing protein 14) is also a member of the PRDM family of proteins and is induced by the BMP4-SMAD1/5 signalling pathway (Ohinata et al. 2005, Dudley et al. 2007, Fog et al. 2012, Günesdogan et al. 2014). *Prdm14* is a key component of the pluripotency transcription network and is expressed exclusively within PGCs and pluripotent cells (Yamaji et al. 2008, Chia et al. 2010). Similar to BLIMP1, PRDM14 lacks histone methyl-transferase activity in the conserved PR/SET domain (Fog et al. 2012). After embryo implantation, *Prdm14* expression is detected in cells contained within the proximal region of the epiblast and is induced at ~E6.75 dpc, shortly after the initiation of *Blimp1* expression at ~E6.25 dpc (Ohinata et al. 2005,Yamaji et al. 2008). Both BLIMP1 and PRDM14 are required to drive the differentiation of ESCs towards the PGC lineage (Bikoff et al. 2009, Yamaji et al. 2013, Nakaki et al. 2014). PRDM14 is involved in silencing de novo methyltransferases (e.g. *Dnmt3a*/*Dnmt3b*) and FGF receptors via the recruitment of polycomb repressor complexes (such as PRC2) (Yamaji et al. 2013, Nakaki et al. 2014). This prevents hypermethylation of genes encoding transcription factors required for PGC development and genes required to maintain stem cell self-renewal (Figure 1.2.4) (Nakaki et al. 2014).

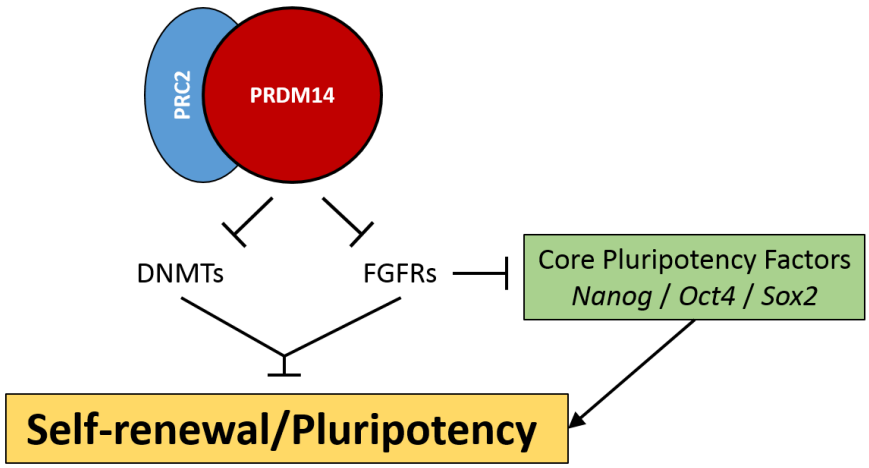

Figure 1.2.4. PRDM14 inhibits expression of pluripotency gene repressors. *The association of PRDM14 with the polycomb repressor complexes (e.g. PRC2) induces epigenetic silencing of de novo methyltransferases (e.g. Dnmt3a/Dnmt3b) and FGF receptors. This silencing reduces DNA methylation and allows for the re-activation of pluripotency factors required for self-renewal and PGC specification.*

However, PRDM14 is also involved in the re-activation of pluripotent factors during PGC differentiation by co-operating with the transcription factors NANOG and Estrogen-Related Receptor Beta (ESRRβ) at enhancer elements of target genes (Yamaji et al. 2013, Nakaki et al. 2014).

This dual repressive and active function of PRDM14 assists the establishment of self-renewing PGCs (Yamaji et al. 2013, Nakaki et al. 2014). Mice lacking functional expression of *Prdm14* are viable but they are infertile due to the lack of germ cells (Nakaki et al. 2014). In the absence of functional BMP4 and WNT3 signalling cascades, differentiated mouse cells have reduced *Prdm14* and *Blimp1* expression, resulting in little to no germ cell formation (Bagci & Fisher 2013). It is hypothesised that epiblast cells destined for the PGC lineage were able to repress the somatic mesodermal program due to the presence of functional BLIMP1 activation, but PGC progenitors lacking *Prdm14* expression are lost due to their inability to re-acquire self-renewal capability (Ohinata et al. 2009, Nakaki et al. 2014).

1.2.2.3 *AP2γ: The mediator*

AP2γ (or TFAP2C) is a member of the family of AP2 transcription factors and is a downstream target of the BLIMP1 transcription factor (Eckert et al 2005, Kurimoto et al. 2008, Schäfer et al. 2011). It is expressed in several locations throughout the developing embryo, including PGCs and the trophectoderm (Auman et al. 2002, Kurimoto et al. 2008, Schäfer et al. 2011). *Ap2γ* is expressed at ~E7.25 dpc in mouse PGCs, after the induction of both *Blimp1* and *Prdm14* gene expression (Kurimoto et al. 2008, Schäfer et al. 2011). *Ap2γ* is reported to be involved in the suppression of genes which induce terminal differentiation, apoptosis and factors which slow cellular growth (Schäfer et al. 2011, Günesdogan et al. 2014). The AP2γ transcription factor is enriched at promotor/enhancer binding sites of both BLIMP1 and PRDM14 (Günesdogan et al. 2014). A complete loss of *Ap2γ* expression is embryonic lethal, resulting in the loss of the developing embryo at ~E6.5 due to defects in the development of the placenta (Auman et al. 2002, Werling & Schorle. 2002). However, inducing the loss of *Ap2γ* transcription factor expression in the mouse via a floxed *Ap2γ* gene results in the loss of PGCs at ~E8.5 dpc, producing infertile offspring (Weber et al. 2010). The loss of *Ap2γ* can also result in de-repression of mesoderm markers such as *Hoxa1* and *Hoxb1*, and a failure to upregulate genes associated with PGC specification, such as *Stella* and *Nanos3* (Figure 1.2.5) (Auman et al. 2002).

The AP2γ transcription factor is considered to be an important mediator of PGC specification, either by ensuring self-renewal and the continued proliferation of PGCs by either acting as a co-factor for both BLIMP1 and PRDM14, or by directly assisting the upregulation of pro-PGC and/or downregulation of pro-somatic genes.

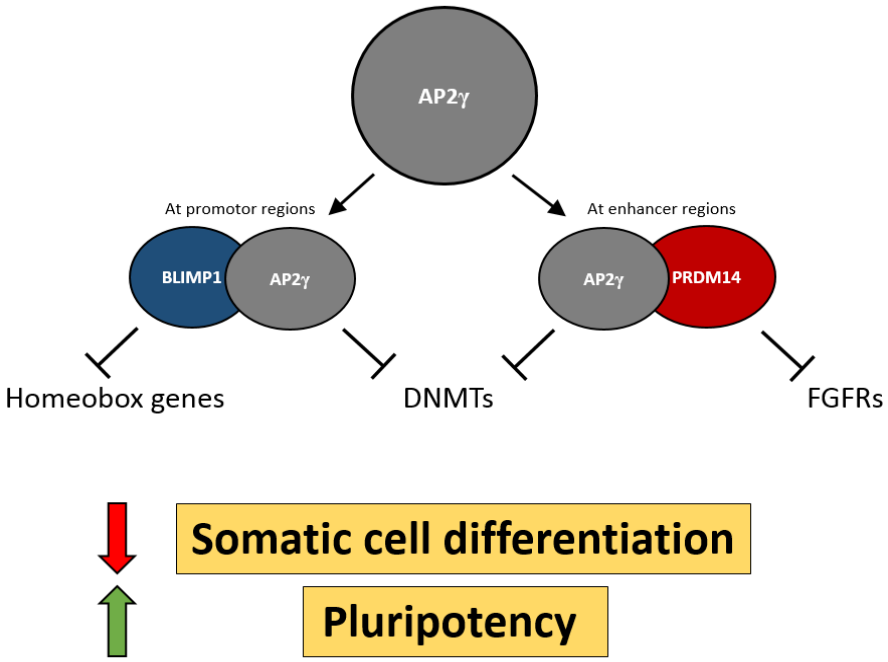

Figure 1.2.5. AP2γ supports BLIMP1 and PRDM14 activity. *AP2γ associates with BLIMP1 and PRDM14 at their sites of activity, supporting the suppressive/active function in PGCs to repress somatic cell differentiation and retain cell pluripotency.*

1.2.2.4 *The role of the Wnt signalling cascade*

Both the BMP4 and WNT3 signalling pathways are required for successful PGC specification (Ohinata et al. 2005, Dudley et al. 2007, Günesdogan et al. 2014). While BMP4 is required for the activation of *Blimp1* and *Prdm14* expression during the early stages of PGC specification (Ohinata et al. 2005, Dudley et al. 2007, Günesdogan et al. 2014), the WNT3 signalling cascade is reported to sustain the expression of the PGC transcription factors via the mesodermal factor *Brachyury* (Rivera-Pérez & Magnuson 2005, Rao et al. 2010, Aramaki et al 2013). $WNT3^{-/-}$ mice have impaired WNT3/β-catenin signalling in EpiLCs (Armaki et al. 2013). *Brachyury* is a downstream target of the WNT3/β-catenin signalling cascade, primarily expressed in the post-implantation epiblast and within the primitive streak during gastrulation (Rivera-Pérez & Magnuson 2005). BRACHYURY is also involved in the formation of the mesoderm during embryogenesis and the differentiation of epiblast cells into the somatic lineage (Winnier et al. 1995, Rivera-Pérez & Magnuson 2005).

It is reported that the BRACHYURY transcription factor can interact with the regulatory factors driving *Blimp1* and *Prdm14* expression, positively influencing the expression of both PGC transcription factors (Aramaki et al 2013) (Figure 1.2.6).

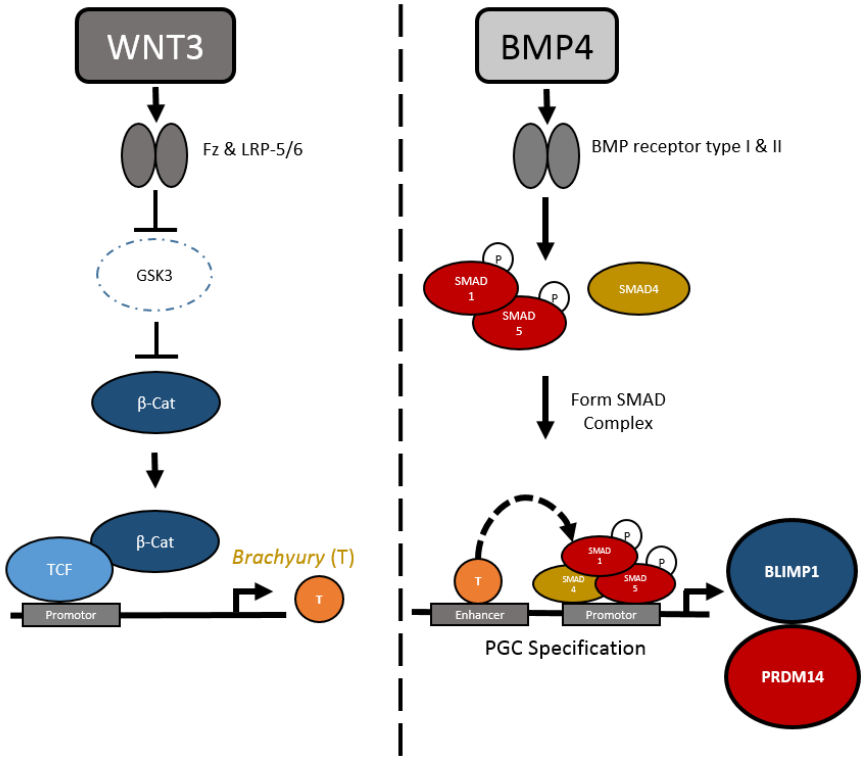

Figure 1.2.6. WNT3 signalling sustains Blimp1 and Prdm14 expression during PGC specification*. Wnt3 binds to a frizzled receptor, inhibiting GSK3 activity. Reduced GSK3 stabilises β-catenin (β-cat) expression, which associates with TCF to induce the expression of Brachyury. The BRACHYURY transcription factor (T) then binds to the enhancer elements upstream of the Blimp1 and Prdm14 genes, maintaining their expression as PGCs migrate through the embryo to the site of the embryonic gonad.*

Loss of functional BRACHYURY protein has a negative effect on the expression of all three PGC transcription factors (BLIMP1, PRDM14, AP2γ) during the late streak stages of mouse embryogenesis (~E7.0) (Aramaki et al 2013). It is therefore suggested that although BMP4 signalling alone is sufficient to initiate *Blimp1* and *Prdm14* expression in the early stages of PGC specification (Ohinata et al. 2005, Dudley et al. 2007, Günesdogan et al. 2014), BRACHYURY is required to ensure the successful maturation of the developing PGCs and to retain PGC transcription factor expression during their migration towards the genital ridges (Aramaki et al 2013). However, it has been proposed that *Brachyury* is not required for the generation of human *in vitro* derived-PGC like cells (PGCLCs) and it is instead the WNT-driven expression of EOMEs which helps drive human germ cell fate determination (Kojima et al. 2017, Chen et al. 2017).

Perhaps these results suggest that it is not the specific action of *Brachyury* that helps to drive the expression PGC factors, but the generation of a PGC-progenitor niche environment via functional WNT signalling and the activation of its downstream targets.

1.2.3 Generation of *in vitro*-derived PGCLCs

Mouse ESCs can be induced to differentiate into the germ cell lineage by a two-step protocol developed by Hayashi et al (Hayashi et al. 2011, Hayashi & Saitou 2013). ESCs are differentiated into primed epiblast-like cells (EpiLCs) and then induced to form primordial germ cell-like cells (PGCLCs) (Figure 1.2.7) (Hayashi et al. 2011, Hayashi & Saitou 2013).

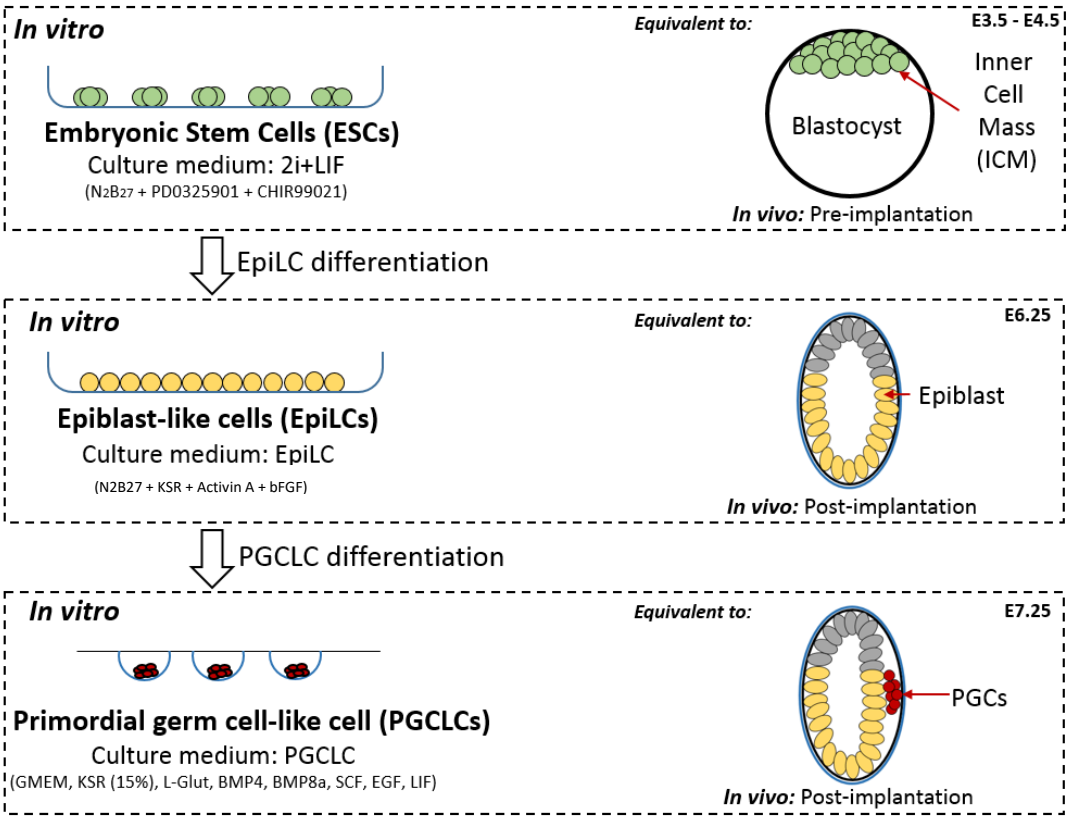

Figure 1.2.7. The "Hayashi" PGCLC differentiation protocol. *ESCs represent the cells found in the ICM of a pre-implantation blastocyst. EpiLCs have similar characteristics and differentiation potential to the epiblast cells of a post-implantation embryo. Cells cultured in suspension in PGCLC medium, referred to as PGC-like cells (PGCLCs), share similar characteristics to the migratory PGCs found in the post implantation embryo.*

EpiLC differentiation medium, a basal medium containing bFGF and Activin A, is used to direct the differentiation of ESCs into a primed epiblast-like state (Hayashi et al. 2011, Hayashi & Saitou 2013). Although they share similar characteristics to the post-implantation embryo, the transcriptome of EpiLCs is considered to be distinct from EpiSCs (Ohinata et al. 2009). The EpiLC state is considered to be a necessary transitionary phase of mouse PGCLC differentiation, making the cells more responsive to the germ cell inducers present during the second stage of the protocol (Hayashi et al. 2011, Hayashi & Saitou 2013). EpiLCs are then transferred into PGCLC medium in suspension culture to form multiple small aggregates (Hayashi et al. 2011, Hayashi & Saitou 2013). The PGCLC differentiation medium contains a cocktail of cytokines (BMP4, BMP8a, SCF, EGF, LIF) which are reported to assist cellular differentiation into the germ cell lineage (Hayashi et al. 2011, Hayashi & Saitou 2013). Mouse PGCLCs can be isolated from the resulting cell pools by fluorescent activated cell sorting (FACs), based on co-expression of the surface markers SSEA-1 and CD61 (Hayashi et al. 2011, Hayashi & Saitou 2013). Isolation of PGCLCs is confirmed by qRT-PCR analysis, checking for the expression of the key PGC transcription factors (*Blimp1, Prdm14, Ap2γ*) and PGC associated marker genes (*Nanos3, Dazl*, etc) (Hayashi et al. 2011, Hayashi & Saitou 2013).
The PGCLC differentiation protocol described above has also been successfully adapted for other model systems, including porcine (Wang et al. 2016) and human (Meyenn et al. 2016) induced pluripotent stem cells (IPSCs). Despite being a well-established scientific model, there currently is no published report showing successful rat ESC differentiation into PGCLCs.

1.3 Aims

Mouse cells can be differentiated *in vitro* into the germ cell lineage and can successfully contribute to the germline in chimeras (Hayashi et al. 2011, Hayashi & Saitou 2013). Although EGCs lines can be derived from rat embryos by dissociating cells from genital ridges and culturing them in 2i+LIF culture conditions (Leitch et al. 2010), there is currently no published data showing successful generation of rat PGCLCs from *in vitro* cultured rat ESCs. Therefore, could similar differentiation cues be used to direct the differentiation of rat ESCs towards the germline? This investigation has two aims; 1) to direct the differentiation of rat ESCs to the germline using a PGCLC differentiation protocol, and 2) to improve the number of cells directed towards the PGC lineage by manipulating the gene network of epiblast cells. To accomplish the first of these aims, the PGCLC differentiation protocol developed by Hayashi et al (2011, 2013) was tested and adapted for rat ESC culture. To achieve the second aim, the epiblast gene network of rat ESCs was manipulated by using gene editing technology to 'hijack' or 'rewire' epiblast gene expression to direct cells towards the germ cell lineage and to direct cell differentiation away from the somatic lineage.

In addition, expression of key PGC transcription factors via a dox-inducible Tet-On piggyBac transposon vector was used to drive PGCLC differentiation. Both approaches built upon the current model of *in vitro* PGC specification, and attempted to improve understanding of mechanisms regulating rat ESC differentiation potential.

Chapter 2 Materials and Methods

2.1 General solutions

LB agar

1% w/v Bacto-trytone (Difco, 211705), 0.5% w/v Bacto-yeast extract (Difco, 212750), 1% w/v NaCl, 1.5% w/v Bacto-agar (Difco, 214010), made to pH 7 and autoclaved

LB medium

1% w/v Bacto-trytone, 0.5% w/v Bacto-yeast extract, 1% w/v NaCl, Made to pH 7 and autoclaved

Cell lysis buffer

100mM Tris-HCL (pH 8.5), 5mM EDTA (pH 8.0), 0.2% w/v SDS, 200mM NaCl. Solution made up to 500mls, filter sterilised using a 0.22µM filter and stored at room temperature for up to one year.

PBS

137mM NaCl, 2.7mM KCl, 4.3mM Na_2HPO_4, 1.47mM KH_2PO_4, made to pH7.4

PBS-T

PBS, 0.1% v/v Tween-20

PFA (4%)

4% w/v in PBS, dissolved at 70^{o}C for 2 hours

TAE (50x)

2M Tris, 50mM EDTA, made to pH 7.7

2.2 Cell culture solutions & culture mediums

2.2.1 Cell culture reagents

Table 2.2.1. List of reagents used during cell culture.

Reagent	Company	Reference code
Activin A	Peprotech	120-14
B_{27} supplement	Gibco™	12587-010
β-mercaptoethanol	Invitrogen™	21985-023
bFGF	Invitrogen™	13256-029
BMP4	R&D Systems	314-BP-010
BMP8b	R&D Systems	1073-BP-010
Chicken serum	Gibco™	16110082
CHIR99021*	Axon Medchem	1386
DMEM/F12 (1:1)	Gibco™	21331-020
DMSO	Sigma-Aldrich™	D2650
Epidermal growth factor (EGF)	R&D Systems	2028-EG-010
ESGRO® LIF	Millipore	ESG1106
Fetal Calf Serum (FCS)	Gibco™	10270-106
GMEM	Invitrogen™	11710-035
Knockout Serum Replacement (KSR)	Invitrogen™	10828-028
L-glutamine (L-Glut)	Gibco™	25030-024
N_2 supplement	Gibco™	17502-048
Neurobasal	Gibco™	21103-049
Non-essential amino acids (NEAA)	Gibco™	11140035
Optimem	Gibco™	11058021
PD0325901**	Axon Medchem	1408
Stem cell factor (SCF)	R&D Systems	455-MC-010
Sodium pyruvate	Gibco™	11360039
Trypsin-EDTA 0.5% (wt/vol)	Invitrogen™	15400-054

2.2.2 Culture mediums

N_2B_{27} Medium

DMEM/F12 (1:1), Neurobasal, 0.5% N_2 supplement, 1% B_{27} supplement, 2mM L-Glut, 0.1mM β-mercaptoethanol. Filter sterilised (0.22µM filter) and stored at 4°C for up to four weeks.

Rat ESC growth medium - 1i medium

N_2B_{27} medium, 1µM PD0325901. Filter sterilised (0.22µM filter) and stored at 4°C for up to two weeks.

Rat ESC growth medium - 2i+Lif medium

N_2B_{27} medium, 1µM PD0325901, 2µM CHIR99021, 1000U/ml ESGRO® LIF. Filter sterilised (0.22µM filter) and stored at 4°C for up to two weeks.

Epi-like cell differentiation medium (EpiLC medium)

N_2B_{27} medium, 20ng/ml Activin A, 12ng/ml bFGF, and 1% KSR. Filter sterilised (0.22µM filter) and made fresh before each use.

Serum-free GK15 medium (GK15 medium)

GMEM, 15% KSR, 0.1mM NEAA, 1mM sodium pyruvate , 0.1mM β-mercaptoethanol, 2 mM L-glut. Filter sterilised (0.22µM filter) and stored at 4°C for up to two weeks.

Primordial germ cell differentiation medium (PGCLC medium)

GK15 medium, 50ng/ml BMP4, 1000U/ml ESGRO® LIF, 10 ng/ml SCF, 50 ng/ml BMP8a, and 10 ng/ml EGF. Filter sterilised (0.22µM filter) and made fresh before each use.

Feeder medium

GMEM, 10% FCS, 1x NEAA, 1mM sodium pyruvate, 2mM L-glutamine, 0.1nM β-mercaptoethanol. Filter sterilised (0.22µM filter) and stored at 4°C for up to four weeks

Phosphate buffered saline (PBS) (Tissue culture grade)

Prepared from commercially available PBS tablets dissolved in tissue grade water and autoclave sterilised.

TVP (trypsin)

0.025% trypsin, 1mM EDTA, 1% chicken serum in PBS. Filter sterilised (0.22µM filter) and stored at -20ºC for up to one year. Aliquots thawed and stored at 4ºC for up to two weeks.

Cell freezing mix (2x stock)

20% FCS and 20% DMSO added to N_2B_{27}. Filter sterilised (0.22µM filter) and stored at 4ºC for up to two weeks.

2.3 Cell culture

2.3.1 Cell attachment substrates

Gelatin from porcine skin (Sigma-Aldrich™, G1890-100G)

Gelatin from porcine skin (0.1% w/v) was introduced to tissue grade water and autoclave sterilised.

Laminin (Sigma-Aldrich™, L1010)

Laminin was pipetted into 100µl aliquots from Engelbreth-Holm-Swarm murine sarcoma basement membrane and stored at -20ºC.

Fibronectin (Millipore, FC010)

Human plasma fibronectin was diluted to 16µg/ml in 1xPBS, separated into 50µl aliquots and stored at 4ºC.

2.3.2 Mouse embryonic fibroblasts (MEFs) feeder layers

CF1 (Gibco™, A34181)

MEFs derived from Carworth CF-1 colony mice. Primarily used for routine passaging of ESCs.

DR4 (Gibco^{TM}, A34966)

MEFs derived from mice generated from an intercross of multiple strains, 129/SvJae + OlaHsd + BALB/c + C57BL/6. Used when required to culture cells in the presence of puromycin.

2.3.3 Gelatin coating

Wells were coated in 0.1% gelatin for five minutes at room temperature in a tissue culture hood. Gelatin was aspirated and the wells allowed to dry for approximately five minutes.

2.3.4 Laminin coating

Wells were coated with 10µg/ml Laminin for at least one hour prior to use at 37^{o}C. Laminin solution was aspirated and the well washed three times with 1x PBS. The final 1x PBS wash was left and removed immediately prior to plating cells.

2.3.5 Fibronectin coating

Wells were coated with 16.6µl/ml fibronectin for at least two hours prior to use at 37^{o}C. Fibronectin solution was aspirated immediately prior to plating cells.

2.3.6 Passaging *in vitro* cultured ESCs

The culture medium was aspirated and a minimal volume of TVP added to cover the cells (typically 200µl per well of a 24-well plate). Cells were incubated at 37^{o}C, 5% CO_2 for three minutes and then dispersed to a single cell suspension using a pipette (confirm by observing under a light microscope). Cell suspensions were transferred to a sterile tube containing 10-20x volume of N_2B_{27} medium and the cells pelleted by centrifugation at 1200rpm for 4 minutes. The supernatant was aspirated and the cells resuspend in their standard culture medium to an appropriate density, as recommended by the chosen cytometric method (typically 1 x 10^6 / ml using a haemocytometer). Cells plated at a density of 1 - 1.5 x 10^5/cm^2 onto a monolayer of γ-irradiated MEFs in the appropriate medium. After 24 hours, half of the culture medium was removed and replaced with fresh culture medium. Cells were passaged every 48 hours or before ~90% well confluency had been reached.

2.3.7 Freezing and thawing *in vitro* cultured cells

2.3.7.1 Freezing cells

Single cell suspensions were prepared as described during passaging of *in vitro* cultured ESCs. Cells were pelleted and resuspended in appropriate culture medium, transferring at least $5x10^5$ cells to a cryovial (Nunc™ Cryotube, Thermo Scientific™, 375418) in 500µl culture medium. Added an equal volume of 2x freezing mix, gently pipetting to ensure uniform distribution of cells. Cryovials were stored at -80ºC overnight or up to one month. For long term storage, vials were transferred to -150ºC within one week of -80ºC storage.

2.3.7.2 Thawing cells

Frozen cyrovials were collected from -150ºC storage on dry-ice and thawed in a 37ºC water bath. The cell stock was transferred into 10mls of pre-warmed (37ºC) N_2B_{27} in a 15ml sterile falcon tube and pelleted by centrifugation at 1200rpm for 4 minutes. Supernatant was aspirated and the pellet gently resuspended in appropriate cell culture medium. The cell suspension was transferred onto a monolayer of γ-irradiated MEFs containing cell culture medium (typically 2-4 x 10^5 frozen cell stock/cm^2). Any left-over cells were recovered by rinsing the 15ml falcon tube with cell culture medium and transferred to the same well. Cells were incubated at 37ºC, 5% CO_2 overnight and the medium replaced with fresh culture medium the following morning.

2.3.8 Lipofectamine transfection of ESCs

ESC transfections were performed using Lipofectamine™ LTX with PLUS™ reagent (Invitrogen™, 15338100), using a protocol adapted from the manufacturer's instructions. Donor DNA mixes were prepared for each individual transfection event containing up to 500ng/µl donor DNA (1:1 Hybase (250ng) to donor vector (250ng)) and 1µl of plus™ reagent. The mixture made up to 50µl with Optimem. Transfection reagent was prepared by mixing 2µl Lipofectamine™ LTX with 48µl Opti-MEM™ for each individual transfection reaction. 50µl of transfection reagent was added to 50µl Donor DNA mix and incubated for 30 minutes at room temperature. 1 x 10^5 ESCs were introduced into a 24 well containing a monolayer of γ-irradiated MEFs in with 500µl of 2i+LIF medium. Before the cells had a chance to attach to the feeder layer, 100µl DNA:LTX mix was added and mixed gently to ensure equal distribution. Cells were incubated in the transfection medium overnight at 37ºC, 5% CO_2.

The transfection medium was exchanged for fresh culture medium the following morning and the cells allowed to recover over 3-4 days. Half of the culture medium was removed and replaced with fresh medium every 24 hours.

2.3.9 Embryoid body (EB) differentiation protocol (rat ESCs)

2.3.9.1 Generating aggregates

Single cell suspensions were prepared as described during passaging of *in vitro* cultured ESCs ~2.4 x 10^6 cells were introduced into a well of a 400 AggreWell™ plate (StemCell Technologies, 34415) in 2mls 2i+LIF medium, pelleted into microwells by centrifugation for 1 minute at 100xg and incubated for 48 hours. This cell density ensured each microwell contained ~2,000 cells. After 24 hours, 1.5mls culture medium was aspirated and fresh 2i+LIF medium added. After 48 hours, cellular aggregates formed within each microwell were collected in 15ml falcon tubes and allowed to pellet by gravity. The culture medium was aspirated and replaced with 5mls of feeder medium. Aggregates were gently pipetted up and down to prevent clumping while not breaking up the aggregates into single cells. The resulting cell suspensions were transferred to 6-well ultra-Low attachment plates and cultured for an extended period of time. Care was taken to ensure the aggregates were spread evenly across the well to reduce clumping.

2.3.9.2 Plating down aggregates onto gelatin coated plates

After 4 days culture in 6-well ultra-Low attachment plates, suspended aggregates were collected in 15ml falcon tubes and allowed to pellet by gravity. The culture medium was aspirated and the aggregates resuspended in 1ml of feeder medium. Aggregates were transferred to 6-well tissue culture grade plates coated and supplemented with 4mls fresh Feeder medium. Care was taken to ensure aggregates were distributed evenly across the plate to reduce clumping. Aggregates were allowed to attach to the gelatin layer were cultured for up 15 days.

2.3.10 Epiblast-like cell (EpiLC) differentiation protocol

During the course of this investigation, variations of this method were tested. The following is a general protocol used to induce EpiLC differentiation of ESCs adapted from that used by Hayashi et al (2013).

12-well culture plates were coated with the designated attachment substrate (e.g. Fibronectin, MEFs) up to 24 hours prior to starting the EpiLC differentiation protocol. 1 - 2 × 10^5 ESCs were transferred into the coated 12-well culture plates and cultured for 48-72 hours in 1ml of EpiLC differentiation medium at 37ºC, 5% CO_2. The culture medium was aspirated and exchanged for fresh EpiLC medium after 24 hours.

2.3.11 Primordial germ cell-like cell (PGCLC) differentiation

During the course of this investigation, variations of this method were tested. The following is a general protocol used to induce PGCLC differentiation of cells which have been subjected to the EpiLC differentiation protocol, adapted from that used by Hayashi et al (2013).

Cells were first put through the EpiLC medium differentiation protocol as described above (2.3.10). Tissue culture grade 15cm dishes were filled with 10-15mls of 1x PBS and stored at 37ºC, 5% CO_2 1 hour prior to PGCLC differentiation. The EpiLC differentiation medium was aspirated and the cells washed three times with 1x PBS solution to ensure its complete removal. Cells were trypsinised using 200µl of TVP and the detached cellular supernatant transferred to a 15-ml falcon tube with 10-20x GK15 medium. The falcon tube was centrifuged at 500x*g* for 3 min at room temperature, and the supernatant removed. The cell concentration was adjusted to 6.7 × 10^4 cells per ml with PGCLC differentiation medium. 40-50 hanging drops consisting of 30µl of the cell suspension (~2 x 10^3 cells per drop) were pipetted onto the lids of the prepared tissue culture grade 15cm dishes. The hanging drop plates were incubated at 37ºC, 5% CO_2 for 48 hours. The cells within each hanging drop are noted to form small aggregates during the 48 hour incubation. After 48 hours, hanging drops were washed from the lids of the 15cm dishes with GK15 medium and collected in 15ml falcon tubes. Aggregates were allowed to pellet by gravity at room temperature and the supernatant aspirated. Aggregates were re-suspended in PGCLC differentiation medium and divided between multiple 3cm plates. ~20 aggregates were added to each 3cm plate to reduce risk of clumping while maintaining enough aggregates to promote cell survival.

Plates were incubated at 37ºC, 5% CO_2 for ~96 hours and shook at random intervals to reduce clumping of aggregates and attachment to the bottom of the plate. Fresh PGCLC medium was introduced to each plate after 48 hours.

2.3.12 Karyotyping cells

2.3.12.1 Preparation

Fixative solution (3:1, Methanol : Acetic acid) was prepared and cooled to -20ºC 2 hours prior to karyotyping. Any remaining solution could be stored up to 1 week at -20ºC for future use. 0.56% KCl solution (1.12g KCl in 200mls dH2O) was prepared and incubated at 37ºC, 5% CO_2 for 1 hour prior to karyotyping. Any remaining solution was stored at room temperature for future use.

2.3.12.2 Incubation

KaryoMAX™ Colcemid™ solution (10ug/ml) (Gibco™, 15212-012) was added at a ratio of 1:100 to the fresh culture medium (0.1mg/ml final concentration). The culture medium was aspirated from the wells to be karyotyped and was replaced with enough Colcemid/media mixture to cover the bottom of the well. The plates were incubated 37ºC, 5% CO_2 for 2 – 3 hours.

2.3.12.3 Collection

The Colcemid/media mixture was aspirated from each well and the cells trypsinized with TVP. Single cell suspensions were generated by triturating in N_2B_{27} medium. The resulting cell suspensions were centrifuged at 1200rpm for 4 minutes in a 15ml falcon tube and the resulting supernatant aspirated.

2.3.12.4 Swell

The cells pellets were resuspended in 5mls 0.56% KCl (37ºC) and incubated for 10-15 minutes at room temperature. 100µl of cold fixative was added drop-wise to the falcon tubes and the tube inverted several times to ensure proper mixture. The resulting cell suspension was centrifuged at 1200rpm for 4 minutes and supernatant aspirated.

2.3.12.5 Fix

1ml cold fixative solution was added slowly along the side of the 15ml falcon tube and incubated for 30 minutes on ice. The resulting suspension was centrifuged at 1200rpm for 4 minutes and the supernatant aspirated.

2.3.12.6 Preparation of slides and Imaging

Small drops (~10µl) of cell suspension were dropped onto the surface of clear glass slides. Drops were allowed to spread and dry without disturbance. Glass coverslips were mounted onto the slides using VECTASHIELD® Mounting Medium with DAPI (Vector labortoies, H-1200). 20-50 images of burst cells taken for each slide/cell line at 630x under oil. Chromosomes were counted using the image processing programme 'ImageJ'. Counts were used to estimate the percentage of karyotypically normal and abnormal cells within the population.

2.4 Cloning

DNA fragments were generated either via PCR amplifications, restriction enzyme digests or were built by an external company. Generated DNA fragments were resolved on TAE agarose gels to determine if its size met expectations. If a single fragment was generated, samples were purified using ExoSAP-IT™ PCR clean-up (Applied Biosystems, 78200.200.UL) following manufactures instructions. Otherwise, the desired fragment was excised from the agarose gel and purified using Wizard® SV Gel and PCR Clean-Up System (Promega, A9281).

2.4.1 TOPO cloning

Purified DNA fragments were added to a PCR reaction mix with a non-proofreading Taq Polymerase (NEB, M0273S) and incubated in a thermocycler for 15 minutes at 72ºC. 4µl of PCR reaction mix cloned into the pCR™8/GW/TOPO® vector following the TOPO® TA Cloning kit manufacturer's instructions (Invitrogen™, K2500-20)

2.4.2 Gibson cloning

Table 2.4.1. Gibson cloning master mix

Reagent	Volume (µl)	Final Concentration
1M Tris-HCL	40	100mM
1M $MgCl_2$	4	10mM
dNTPs (100mM)	3.2	0.2mM (each)
NEB Taq Polymerase (2U/µl)	5	25U/mL
T5 Exonuclease (10 U/µl)	0.32	8U/mL
dH_2O	147.8	

Gibson cloning method:

10µl aliquot of Gibson cloning master mix was thawed on ice for each vector to be ligated. The linearised vector and DNA fragments were added together at a ratio of 1:3 and 1:5 p/mols. Concentration of vector ranged between 50ng-150ng and the total volume was made up to 20ul with dH_2O. The Gibson cloning reactions were incubated at 50^{o}C for 60 minutes. Samples were then either transferred to ice for immediate transformation or stored at -20^{o}C for transformation at a later date.

2.4.3 Bacterial transformations

2.4.3.1 Standard transformation

Previously derived/verified vectors were typically transformed at 50ng/µl into 100µl of competent DH5α cells (Invitrogen™, 18265017). Aliquots of bacterial culture were thawed on ice ~5 minutes prior to transformation. The DNA vectors to be transfected were pipetted into the DH5α aliquots and incubated on ice for a further 30 minutes. Vector/bacterial mixes were heatshocked at 42^{o}C for 1 minute and then placed back on ice for 2 minutes. 900µl of LB medium was added and the vector/bacterial mixes incubated on a 37^{o}C shaker for 1 hour. 100, 250 and 500µl of vector/bacterial mixes were plated onto 9cm LB agar dishes containing the appropriate antibiotic necessary for selection of successful transformants. Even spreading of the bacteria was accomplished using disposal plastic bacterial spreaders. Dishes were incubated overnight at 37^{o}C to allow colony growth. Colonies were picked in LB medium containing the appropriate antibiotic necessary for selection of successful transformants.

2.4.3.2 High competency transformation

Vectors generated by Gibson cloning were transformed into NEB® 5-alpha Competent *E. coli* (NEB, C2987H) as this is recommended in the protocols followed for Gibson cloning. The method used is very similar to that described in 2.4.3.1, with the following changes:

- 3µl of Gibson master mix was added to a 50µl aliquot of high competency bacteria
- 950µl of SOC medium is added to the vector/bacteria mix after heatshock.
- 50µl and 250µl of vector/bacterial mixes were plated onto 9cm LB agar dishes containing the appropriate antibiotic necessary for selection of successful transformants.

2.5 Sample preparation

2.5.1 Plasmid vector isolations

2.5.1.1 Minipreps

Colonies from LB agar dishes were picked and cultured overnight at 37^{o}C in 3mls of LB medium containing the appropriate antibiotic necessary for selection of successful transformants. The next day, pellets of bacteria were made and re-suspended in 600µl nuclease-free H_2O. The transformed vector was then isolated using the PureYield™ Plasmid Miniprep System (Promega, A122), following manufacturer's instructions.

2.5.1.2 Midipreps

Colonies from LB agar dishes were picked and cultured overnight at 37^{o}C in 50mls of LB medium containing the appropriate antibiotic necessary for selection of successful transformants. The transformed vector was then isolated using the PureLink™ HiPure Plasmid Midiprep Kit (Invitrogen^{TM}, K210004), following manufacturer's instructions.

2.5.2 Genomic DNA isolation

Genomic DNA was isolated from cells either in suspension or attached to a basal membrane using the following method. Cells in suspension were spun at 1200rpm for 4 minutes to pellet cells. The supernatant was aspirated and an appropriate volume of ESC lysis buffer and 100µg/ml proteinase K (Invitrogen™, AM2548) added. Cells were left at 37^{o}C overnight or 50^{o}C for between 1-6 hours to promote cell lysis. The lysate was transferred to an Eppendorf with an equal volume of isopropanol and centrifuged at 8,000xg for 10 minutes at room temperature. The supernatant was removed and the pellet washed twice with 500µl 70% ethanol, followed by centrifugation at 8,000xg for 2 minutes at room temperature. After the second ethanol wash, the supernatant was removed and the pellet allowed to air-dry for 5-10 minutes. The pellet was resuspended in dH_2O overnight at 4^{o}C to assist resuspension.

2.5.3 RNA isolation

2.5.3.1 Extraction from tissue

Small sections of tissue were mixed with 700µl of RLT buffer (Qiagen, 79216) with β-mercaptoethanol. Mixes were subjected to multiple rounds of syringe-and-needle homogenization until the majority of the tissue had dissolved into the RLT buffer. A QIAshredder was used to ensure further homogenisation following manufacturer's instructions (Qiagen, 79654). RNA was isolated from tissue using the RNeasy™ Mini Kit (Qiagen, 74104) following the manufacturer's instructions. The optional DNase treatment step was performed, following manufacturer's instructions (Qiagen, 79254).

2.5.3.2 Extraction from cells

Previously isolated cells were pelleted at 150xg for 5 minutes. The supernatant was removed and the cell pellet re-suspended in 1x PBS. The cells were pelleted a second time at 300xg for 3 minutes and the supernatant removed. Cell pellets were then either transferred to ice for RNA extraction or were stored at -20^{o}C for future extraction. RNA was isolated from tissue using the RNeasy™ Mini Kit (Qiagen, 74104) following the manufacturer's instructions. The optional DNase treatment step was performed, following manufacturer's instructions (Qiagen, 79254).

2.5.4 cDNA synthesis

cDNA synthesis from RNA samples was performed using Superscript™ First Strand Synthesis system for RT-PCR (Invitrogen™, 11904-018) following manufacturer's instructions.

2.5.5 Protein isolation

2.5.5.1 Attached Cells

The culture medium was aspirated and the cells washed three times with 1x PBS. 1ml cold RIPA buffer (Thermo Scientific™, 89900) with Halt Protease Inhibitor Cocktail Kit (Thermo Scientific™, 78410) was added to each well and the plate incubated on ice for 15 minutes. The lysate was collected and transferred to a microcentrifuge tube, centrifuging at ~14,000xg for 15 minutes at 4^{o}C to pellet the cell debris. The supernatant was then transferred to a new microcentrifuge tube for analysis.

2.5.5.2 Cells in suspension

Cells were pelleted by centrifugation at 2500xg for 5 minutes at room temperature in 15ml Falcon tube. The supernatant was aspirated and the cells washed three times with sterile 1x PBS, followed by centrifugation at 2500xg at room temperature for 5 minutes. 1ml cold RIPA buffer (Thermo Scientific™, 89900) with Halt Protease Inhibitor Cocktail Kit (Thermo Scientific™, 78410) was added and the falcon tube placed on a rotatory shaker for 15 minutes at 4^{o}C. The resulting cell solution was centrifuged at ~14,000xg for 15 minutes at 4^{o}C to pellet the cell debris. The supernatant containing the isolated protein was transferred to a microcentrifuge tube for further analysis.

2.6 Detection and quantitative methods

2.6.1 Routine PCR

Routine PCR was performed using Q5® High-Fidelity DNA Polymerase (NEB, M0491) following the manufacturer's protocol. All reaction components were kept on ice during set up and quickly transferred to a thermocycler.

Table 2.6.1. Components of routine PCR master mix

Component	Volume	Final concentration
5X Q5 Reaction Buffer	10 µl	1X
10 mM dNTPs	1 µl	200 µM
10 µM Forward Primer	2.5 µl	0.5 µM
10 µM Reverse Primer	2.5 µl	0.5 µM
Template DNA	variable	<1,000 ng
Q5 High-Fidelity DNA Polymerase	0.5 µl	0.02 U/µl
Nuclease-Free Water	to 50 µl	N/A

The volume of template DNA used varied depending on the concentration required. Used either 1ng – 1ug of Genomic DNA or 1ng – 10ng of Plasmid DNA.

Table 2.6.2. Thermocycling conditions for routine PCR

Step	Temperature	Time (secs)
Initial Denaturation	98°C	30
25–35 Cycles	98°C 50–72°C 72°C	5–10 10–30 30 per kb
Final Extension	72°C	120
Hold	4–10°C	

2.6.2 Quantitative RT-PCR (qRT-PCR)

cDNA samples were typically diluted 1:50, with 8µl per replicate used for qRT-PCR analysis. Analysis was performed using Brilliant III Ultra-Fast SYBR® Green qRT-PCR Master Mix (Aligent Technologies, 600882), following manufacturer's instructions. qRT-PCR reactions performed using a MX-3000 thermocycler (Aligent Technologies).

Table 2.6.3. Thermocycling conditions for qRT-PCR

Step	Temperature	Time (secs)
Initial Denaturation	95°C	120
Cycle extension (40 cycles)	95°C 60°C	5–10 10–30
Dissociation curve	95°C 25°C	15 30

2.6.2.1 qRT-PCR Primers (Specificity to both mouse and rat)

Table 2.6.4. qRT-PCR primer sequences

Gene	Primer (For/Rev)	Sequence
β-Actin	For	TGACAGGATGCAGAAGGAGA
	Rev	GTACTTGCGCTCAGGAGGAG
Ap2γ	For	GACTGTCACCACCGGAATG
	Rev	TTTTGTCCAACTTCTCCCTCA
Blimp1	For	TCCCAAGAATGCCAAGAGGA
	Rev	CTCCCGGGCAGAGTGAGTT
Brachyury	For	TCAGCAAAGTCAAACTCACCA
	Rev	CCAACTCTCACGATGTGAATC
Dazl	For	TGGATGAAACCGAAATCAGGAG
	Rev	TCTTCTGCACATCCACGTCA
Dnmt3b	For	AGCGCCTCAAGACAAATAGCT
	Rev	CGGTCTTCCAGATTGCCCTT
Elf5	For	ACGCAGGAGGAGTTCATTGA
	Rev	TGACTCTTGATGCCACTTGT
Fgf5	For	GGGATTGTAGGAATACGAGGAG
	Rev	CGCGGACGCATAGGTATTAT
Gapdh	For	ATGACTCTACCCACGGCAAG
	Rev	TGGGTTTCCCGTTGATGACC
Gata3	For	CGGGTTCGGATGTAAGTCGA
	Rev	CTTGATAAGGGGCCGGTTCT
Gata4	For	TGAGGGCGAGCCTGTTTGCAA
	Rev	ATTCAGATTCTTGGGCTTCC

Gata6	For	TCATCACGACGGCTTGGACTG
	Rev	GCCAGAGCACACCAAGAATCC
Nanog	For	TACCTCAGCCTCCAGCAGAT
	Rev	GCAATGGATGCTGGGATACT
Nanos3	For	CAAGACTGGTTGGGGCTCTG
	Rev	GACTCGCCATTGTGTTTGCA
Oct4	For	GAAGTTGGAGAAGGTGGAACC
	Rev	GTGTACCCCAAGGTGATCCTC
Otx2	For	CCAGGGTGCAGGTATGGTTT
	Rev	GCCACTTGTTCCACTCTCTG
Prdm14	For	CAGTCTTCCAGCCTGAACAAG
	Rev	TTGCACTTGAAGGGCTTCTC
Sox17	For	CTTTATGGTGTGGGCCAAAG
	Rev	CCAAGGTCAACGCCTTCCA
Stella	For	TCGGATTGAGCAGAGACAAA
	Rev	TGGCAGAAAGTGCAGAGACA
Tcf15	For	GCTCCATCTGCACCTTCTG
	Rev	GGCTACACCCCTCACTTTCA
Vasa	For	GCAGCTTTTCTCTTGGCTATTT
	Rev	CAGCTCTTACACAAGTCCCA
Wnt3	For	CCTGGTCCCCAAGCAACT
	Rev	CATGCACGAAGGCCGATTC

2.6.3 Statistical tests

Unless otherwise stated, the statistical test used on quantifiable data was the Student's T-Test.

2.6.4 DNA sequencing

500-750ng of purified DNA was mixed with 6.4pmoles of sequencing primer, made up to a total volume of 6µl with dH_2O. Sequencing was carried out by Edinburgh Genomics using BigDye v3.1 Terminator Cycle Sequencing Kit (Thermofisher P/N AB0384/240; BS034042) and analysed on a 3730*xl* DNA Analyzer (Applied Biosystems™, 3730*xl*).

2.6.5 Alkaline Phosphatase staining (Sigma-Aldrich™)

Alkaline Phosphatase staining was performed using an alkaline phosphatase staining kit (Sigma-Aldrich™, 86R-1kT), following the manufacturer's instructions

with minor changes. Solutions for Alkaline Phosphatase staining were made up as follows:

2.6.5.1 Fixative

5ml citrate solution, 13ml acetone, 1.6ml formaldehyde (37%). Prepare fresh.

2.6.5.2 Stain

200µl sodium nitrite solution + 200µl FRV-alkaline solution. Incubated for two minutes at room temperature then added 9ml MQ water. Added 200µl naphthol AS-BI alkaline solution, mixed and was used immediately.

2.6.5.3 Protocol

Extracted tissue was washed with 1x PBS and fixed with fixative solution for five minutes to ensure fixative had had time to permeate throughout the tissue. The tissue was washed with 5ml MQ H_2O 3 times to ensure the fixative had been removed. The staining solution was added for 15-30 minutes at room temperature in the dark. After staining, the tissue was washed with MQ H_2O 3 times to ensure the staining solution had been removed. The last MQ H_2O was left to ensure the sample did not dry out.

2.6.6 Immunocytochemistry

2.6.6.1 Solutions

Fixative

Dissolved paraformaldehyde (4% w/v) in PBS at 70^{o}C for two hours. Aliquoted and stored solution at -20^{o}C for up to four weeks

PBST

Triton X100 (0.3% v/v) in PBS.

Blocking solution

Dissolved bovine serum albumin (1% w/v) and serum (10% v/v) (from the same species as the secondary Ab was raised in) in PBST.

2.6.6.2 Fixation of cells

The cell culture medium was aspirated and each well washed twice with 1x PBS. The fixative solution was added to each well and incubated for 15-20 minutes at room temperature. Fixative solution was aspirated, and the wells washed three

times for 1-2 minutes each in 1x PBS. If the plates were to be stored at this stage, the last 1x PBS wash was left, the plate sealed with parafilm and then stored at 4ºC.

2.6.6.3 Permeabilisation/Blocking

Cells were permeabilised by adding enough ice-cold Methanol to cover the bottom of the well and incubating the plate at -20ºC for 10 minutes. The methanol was aspirated and the cells washed three times for 1-2 minutes each in 1x PBS. Blocking solution was added to each well and left for 1 hour at room temperature.

2.6.6.4 Primary antibody staining

The primary antibody was diluted in the blocking solution at the recommended ratio. The blocking solution was removed from the cells and the primary antibody dilution added at the manufacturers recommended ratio. Primary antibody staining took place overnight at 4ºC, with the plate sealed with parafilm to reduce condensation.

2.6.6.5 Secondary antibody staining

The plate was removed from 4ºC and each well washed four times for 5 minutes with PBST. Secondary antibody was diluted in blocking solution to the manufacturers recommended ratio. Diluted secondary antibody was added to each well and incubated for 1 hour at room temperature in the dark as fluorescent antibodies are light sensitive. After incubation, each well washed four times for 5 minutes with PBST.

2.6.6.6 DAPI staining and imaging

DAPI was diluted 1:10,000 in PBST and added as part of the final wash noted above. After final PBST wash, the wells were washed twice with 1x PBS. Fluorescent images were taken of each well, the plates sealed in parafilm, and stored at 4ºC.

2.6.7 Flow Cytometry and Fluorescent activated cell sorting (FACs)

If fluorescent antibody staining was not required (e.g. Looking for expression of fluorescent marker from incorporated vector), single cell suspensions were made and resuspended in 2% FACs buffer (2% FCS in 1x PBS). If fluorescent antibody staining was required, single cell suspensions were blocked with 10% FACs buffer for 30 minutes to avoid nonspecific antibody binding. 1 – 5 x 10^5 cells were stained with a fluorescent antibody for 1 hour in 10% FACs buffer. Cells were washed 3 times with 2% FACs buffer and re-suspended in 2% FACs buffer.

Flow cytometry was performed on a BD LSR Fortessa (16 colour Analyser) with High Throughput Sampler. FACs was performed on a BD FACS Aria IIIu 4-laser/11 detector Cell Sorter, operated by Roslin Bioimaging and Flow Cytometry department. The gating strategy used was consistent throughout this investigation and so has been summarised here. First, forward (FSC-A) versus side scatter (SSC-A) was plotted to identify the cells of interest with the expected size and granularity of the cells. To remove doublets, forward scatter height (FSC-H) was plotted against forward scatter area (FSC-A) and a gate drawn so that only single cells were analysed further. Finally, the live cells were then sorted from the dead by staining the cells with DAPI. Only the cells which stained negative for DAPI (450/50) were analysed further. Further gating, alterations or deviations from this gating strategy are detailed in the relevant chapters.

2.6.8 Antibodies and Dyes

Table 2.6.5. List of antibodies used for Flow, FACs or Immunostaining cells

Antigen	Concentration	Species	Specificity	Marker	Ref
SSEA-1	1:100	Mouse (IgM)	Mouse/ Human	Alexa 647	Biolegend, 125607
CD61	1:1000	Armenian Hamster (IgG)	Mouse/Rat	PE	Biolegend, 104307
OTX2	1:100	Goat (IgG)	Human	N/A	RD system, AF1979
BRACHYURY	1:100	Goat (IgG)	Mouse/Rat/ Human	N/A	Santa Cruz, sc-17745
Goat IgG (2^o antibody)	1:1000	Rabbit (IgG)	Goat IgG	Alexa 647	Invitrogen™, A27018
Goat IgG (2^o antibody)	1:1000	Rabbit (IgG)	Goat IgG	Alex 488	Invitrogen™, A27012

Dead cell stain: DAPI fluorescent dye (1:10, 000) - Invitrogen™, D1306

Chapter 3 Cytokine-mediated induction of germline differentiation in embryonic stem cells

3.1 Introduction

Primordial germ cells (PGCs), the unipotent precursor cells to germ cells can not only be isolated from the genital ridges of developing embryos of mouse and rats (Matsui et al. 1992, Resnick et al. 1992, Durcova-Hills et al. 2006, Leitch et al. 2010), but can also be derived *in vitro* by directing mouse pluripotent embryonic stem cells (ESCs) towards the germline by activating the same signalling pathways involved in guiding *in vivo* epiblast cells towards PGCs, e.g. the BMP pathway (Ohinata et al. 2005, Ohinata et al. 2009, Hayashi et al. 2011, Hayashi & Saitou 2013). Mouse ESCs can be induced to differentiate into an epiblast-like cell (EpiLC) fate in a basal medium containing basic fibroblast growth factor (bFGF) and activin A (Hayashi et al. 2011, Hayashi & Saitou 2013). These cytokine factors drive the differentiation of ESCs and generate flat monolayers of epithelium-like cells, thought to be similar to the epiblast of the early post-implantation embryo (Hayashi et al. 2011, Hayashi & Saitou 2013). Induction of ESCs into an EpiLC 'differentiation primed' state is essential for the cells to respond appropriately to germ cell inducers (Hayashi et al. 2011). In contrast, more immature pluripotent cells exposed to cytokines associated with inducing germline competency (e.g. BMP4) do not differentiate, remaining in the naïve state and retaining their self-renewal capabilities (Ying et al 2003, Hayashi et al. 2011). EpiLCs are then placed into a suspension culture to form multiple small aggregates in medium containing a cocktail of cytokines that direct differentiation towards a germ cell fate (BMP4, BMP8a, SCF, EGF, LIF) (Hayashi et al. 2011, Hayashi & Saitou 2013). These differentiated cells share many characteristics of their *in vivo* counterparts, and so are referred to as primordial germ cell-like cells (PGCLCs) (Hayashi et al. 2011, Hayashi & Saitou 2013). PGCLCs can then be isolated from aggregates by staining for co-expression of the surface markers SSEA-1 and CD61 and performing fluorescent-activated cell sorting (FACs) (Hayashi et al. 2011, Hayashi & Saitou 2013). The identity of the purified cells can then be confirmed by qRT-PCR analysis of key PGC transcription factors (*Blimp1, Prdm14 and Ap2γ*), as well as by the presence of PGC associated marker genes (e.g. *Nanos3, Dazl*, etc) (Hayashi et al. 2011, Hayashi & Saitou 2013). This PGCLC differentiation protocol has been successfully adapted for both

porcine (Wang et al. 2016) and human induced pluripotent stem cells (IPSCs) (Meyenn et al. 2016), showing that IPSCs generated from these species can be directed towards the germline using similar cocktails of cytokines as the mouse ESCs.

Embryonic germ cell lines (EGCs) can be derived from rat embryos by dissociating the cells of harvested genital ridges, pre-culturing them for 2-3 days in serum based medium (DMEM-F12 medium. 15% FCS, 0.1% NEAA, 4 mM glutamate, 2 mM sodium pyruvate, 0.1 mM 2-mecaptanethanol and LIF) and then expanding the cultures in 2i+LIF conditions (N2B27 medium, 1 µM PD0325901, 3 µM CHIR99021 and LIF) (Leitch et al. 2010). However, currently there is no published data showing successful generation of rat PGCLCs from rat ESCs. This chapter details the experiential approaches taken to induce the formation of rat PGCLCs using a similar differentiation protocol to that used for mouse ESCs.

3.2 Rat PGC marker expression

3.2.1 Expression of PGC markers in rat genital ridges

To track the transition of rat cells entering a PGC-like fate, it was important to confirm that the markers commonly used to identify PGCs were also expressed in the germ cells of the developing rat embryo. Embryos were collected from the uteri of female pregnant rats between E11.5 – 16.5 dpc in order to sample rat PGCs at different stages of their maturation. Embryos dissected at E11.5 - E13.5 dpc were too small to confidently identify the genital ridges (data not shown). However, genital ridges dissected from E14.5, E15.5 and E16.5 dpc rat embryos were readily harvested under a dissection microscope (Figure 3.2.1). Alkaline phosphatase (AP) staining has been used previously to determine the presence of PGCs (Hayashi et al 2011). AP staining of the extracted genital ridges showed a positive speckled stain throughout the genital ridge tissue, suggesting these genital ridges did contain PGCs.

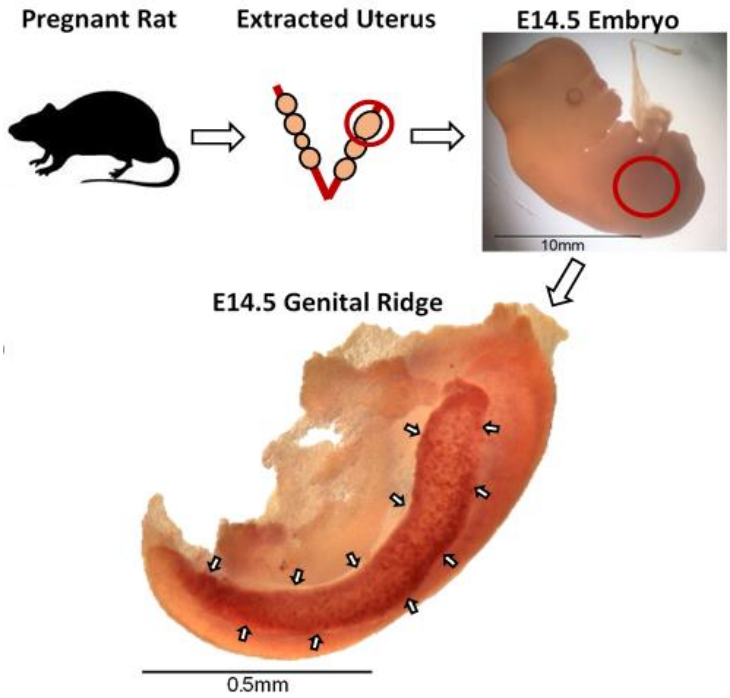

Figure 3.2.1. Dissection of rat genital ridges from an E14.5 dpc embryo*. Embryos were gathered from the uterine of pregnant rats and dissected to collect the genital ridges. Harvested genital ridges (outlined by white arrows) were stained for alkaline phosphatase to identify the presence of the pluripotent PGCs.*

The genital ridges extracted from embryos of a pregnant rat were pooled and processed for RNA extraction. qRT-PCR analysis was performed on the samples gathered from genital ridges of E14.5, E15.5 and E16.5 dpc embryos and the adult ovary and testis tissues, as controls (Figure 3.2.2).

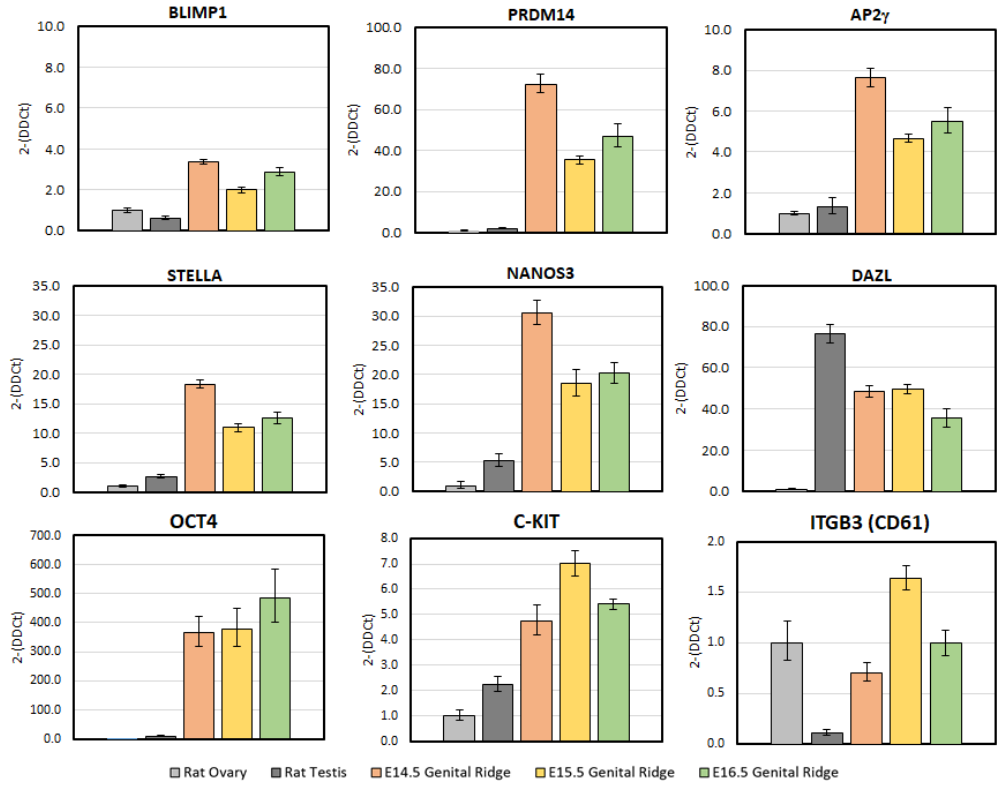

Figure 3.2.2. qRT-PCR analysis of rat genital ridges. *Samples were collected from the genital ridges of E14.5, E15.5 and E16.5 dpc embryos and compared to samples taken from adult rat ovary and testis tissue. Data shown is the average of two experimental replicates (6 litters in total). All data was normalised to the house keeping gene GAPDH (dCT) and fold change was calculated by normalising gene expression to that detected in rat ovary tissue (2-DDCT). Bars represent mean of the two experimental replicates ± SD.*

Elevated levels of the PGC transcription factors (*Blimp1, Prdm14, Ap2y*), PGC gene markers (*Nanos3, Dazl*) and stem cell markers (*Stella, Oct4*) were detected in genital ridge samples compared to those from adult rat tissue. Expression of *Dazl* in rat testis has been reported previously (Rocchietti et al. 2000), and therefore elevated expression of this gene in the testis compared to the rat ovary was not unexpected. These results confirmed that rat PGCs do express the standard PGC gene markers commonly found in mouse. The surface markers C-KIT and ITGβ3 (CD61) have been used previously to identify and separate PGCs from the genital ridges of mice, and isolate PGC-like cells from differentiated *in vitro* human cells (Hayashi & Saitou 2013, Meyenn et al. 2016). CD61 has been noted to be expressed in the ovaries of mice (Burns et al. 2002), so it was not surprising to see high level expression of this gene within the rat ovary tissue.

C-KIT has been identified on the surface of both human and mouse PGCs (Keshet et al. 1991, Høyer et al. 2005, Hayashi et al 2011). Therefore, the expression of both of these factors in the genital ridge samples are consistent with rat PGC expressing these surface markers.

3.2.2 Basal expression of PGC transcription factors in rat ESCs

To establish the base line expression of PGC related factors (e.g. *Blimp1*, *Prdm14*, and *Ap2γ*) in rat ESCs, RNA transcript levels were analysed in self-renewing rat ESC cultures maintained in 2i+LIF by qRT-PCR (Figure 3.2.3). Basal expression of the PGC transcription factors and marker genes from rat genital ridges was compared to the expression in both mouse and rat ESCs. The qRT-PCR data was generated from the average transcript expression of three independent replicates of dark agouti rat ESCs (DA) and 129/OLA mouse ESCs (Figure 3.2.4). Oligonucleotide primer pairs for each gene were selected so they exactly matched both the rat and mouse target sequences, thus ensuring that qRT-PCR analysis could be performed using the same primer set, and allow direct quantitative comparison of gene expression between the species.

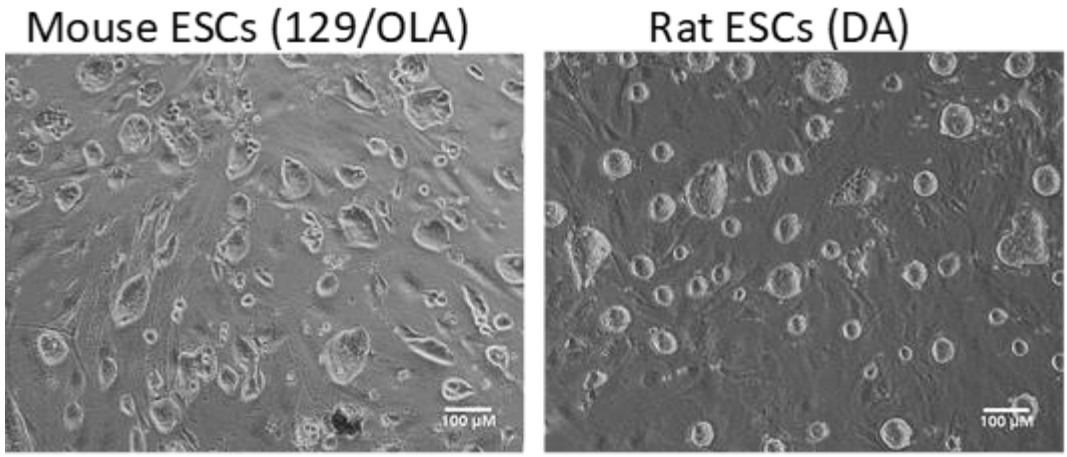

Figure 3.2.3. Bright field photographs of rat and mouse ESCs. *Photographs taken show 1x10^5 cells seeded onto MEF layers and cultured in 2i+LIF medium for 24 hours.*

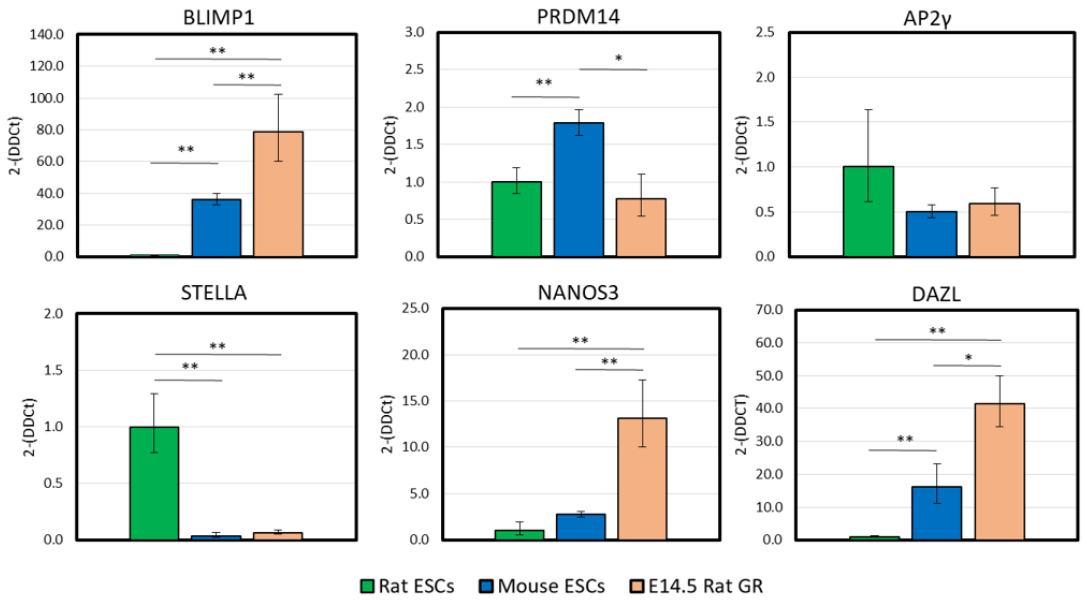

Figure 3.2.4. qRT-PCR analysis of mouse and rat ESCs compared to rat E14.5 dpc genital ridges. *Samples were taken from the genital ridges of E14.5 rat embryos dpc (E14.5 Rat GR) and were compared to rat (Rat ESCs) and mouse (Mouse ESCs) ESCs. All data was normalised to the house keeping gene GAPDH (dCT) and fold change was calculated by normalising gene expression to that seen in the rat ESCs (2-DDCT). Bars represent the average transcript expression of three independent replicates generated from one rat (DAK31) and one mouse (129/OLA) cell line ± SD. *P<0.05, **P<0.01.*

Rat and mouse ESC populations showed a significantly lower expression of two PGC transcription factors (*Blimp1*, *Ap2y*) and two PGC marker genes (*Nanos3*, *Dazl*) compared to rat genital ridges. *Prdm14* expression was significantly higher in mouse ESCs, whereas rat ESCs had a significantly higher expression of *Stella* compared to both rat genital ridges and mouse ESCs.

A notable difference between mouse and rat ESCs was that rat ESCs had 5-fold decrease in *Blimp1* expression compared to mouse ESCs. BLIMP1 is thought to be the key transcription factor necessary for initiating PGC specification in a specific population of epiblast cells (Ohinata et al. 2005), and therefore its low level of expression might affect the ability of rat ESCs to transition into a PGCLC fate.

3.3 Primordial germ cell-like (PGCLC) differentiation of mouse ESCs

129/OLA mouse ESCs cultured in the same standard 2i+LIF conditions as rat ESCs were subjected to a PGCLC differentiation protocol adapted from the method used by Hayashi et al (2011, 2013) (Figure 3.3.1). Although mouse ESC culture is often performed in feeder-free conditions (cultured in the absence of an irradiated feeder cell layer), colonies which have been derived and cultured on MEF layers in 2i+LIF medium were used for this experiment in order to closely match the initial starting conditions of the rat ESCs. Performing the differentiation protocol on mouse cells cultured in the rat ESC culture conditions would eliminate differences in culture condition as a variable in the formation of rat PGCLCs.

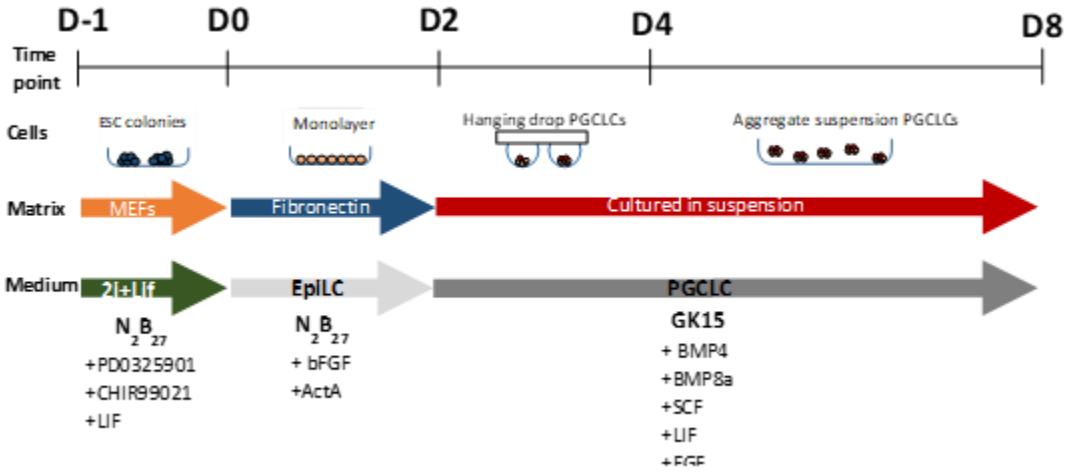

Figure 3.3.1 Schematic of the mouse PGCLC differentiation protocol. *Mouse ESCs cultured in 2i+Lif conditions on a MEF layer were transferred onto a fibronectin layer with EpiLC differentiation medium for 2 days. These cells were pipetted into hanging drops containing ~2,000 cells in PGCLC culture medium. After 2 days of culture, aggregates were collected and transferred into fresh PGCLC culture medium in 6-well low adhesion plates for 4 days.*

3.3.1 EpiLC differentiation of mouse ESCs

129/OLA mouse ESCs cultured in 2i+LIF medium on MEF layers were transferred to 12-well plates coated with fibronectin at a cell density of 1 x 10^5 cells per ml. The cells were then cultured in EpiLC culture medium (N_2B_{27} + bFGF + Activin A) for 2 days, with the medium being replaced with fresh EpiLC medium after 24 hours to replenish bFGF and Activin A. Cells were photographed after 2 days of EpiLC differentiation to record the morphology of the differentiating cells, and compared with those described by Hayashi et al (2011, 2013). Mouse ESCs cultured in EpiLC medium for 2 days formed a flat monolayer, quite different to the domed individual colonies seen in wells of mouse ESCs cultured in 2i+LIF medium on MEF layers (Figure 3.3.2).

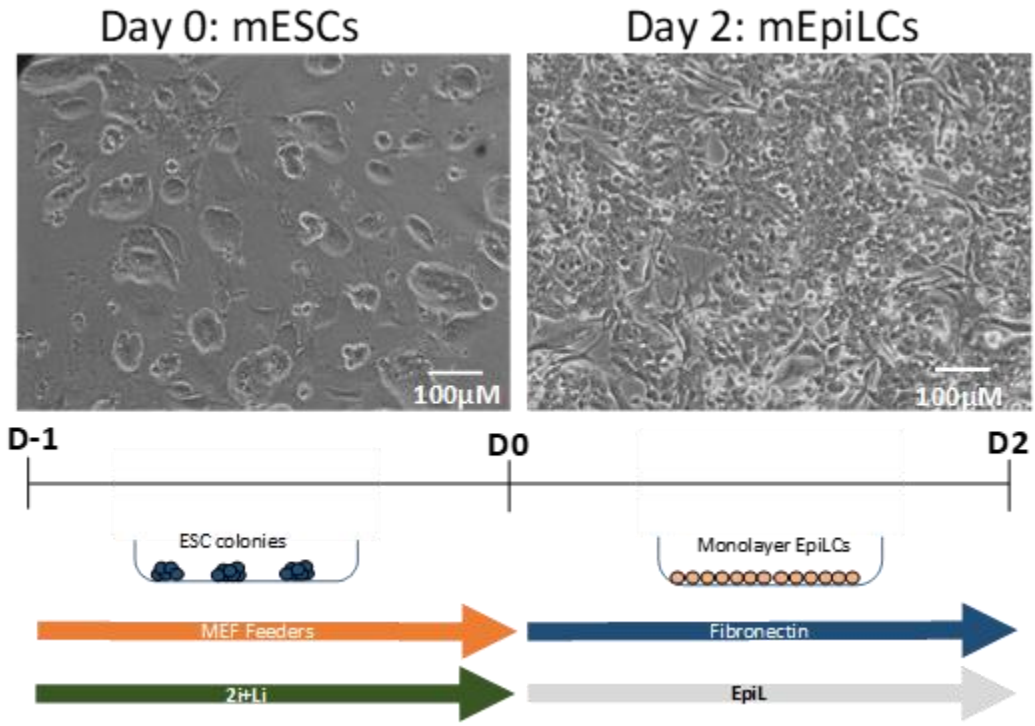

Figure 3.3.2. Bright field images of mouse cells after the 2 day EpiLC differentiation protocol. *Images were taken prior to (Day 0 – left panel) and 2 days (Day 2 – right panel) after cells had been cultured on laminin in EpiLC differentiation medium.*

Mouse cells were harvested after 24 and 48 hours of EpiLC differentiation and RNA processed for qRT-PCR analysis. The expression of gene markers associated with EpiLC differentiation were analysed to assess the progression of the cultures to the EpiLC fate. qRT-PCR analysis identified a significant drop in pluripotency and naïve markers (*Nanog*, *Klf4* and *Prdm14*) when cultured in EpiLC medium compared to the mouse ESCs prior to differentiation (Figure 3.3.3).

Gene markers characteristic of EpiLCs (*Otx2*, *Tcf15* and *Fgf5*) were significantly higher in cells cultured in EpiLC medium compared to mouse ESCs (Figure 3.3.3). This data suggested that these mouse cells were responding in a similar manner to what has been reported previously (Hayashi et al. 2011, Hayashi & Saitou 2013) and were being driven out of the naïve state towards an EpiLC fate.

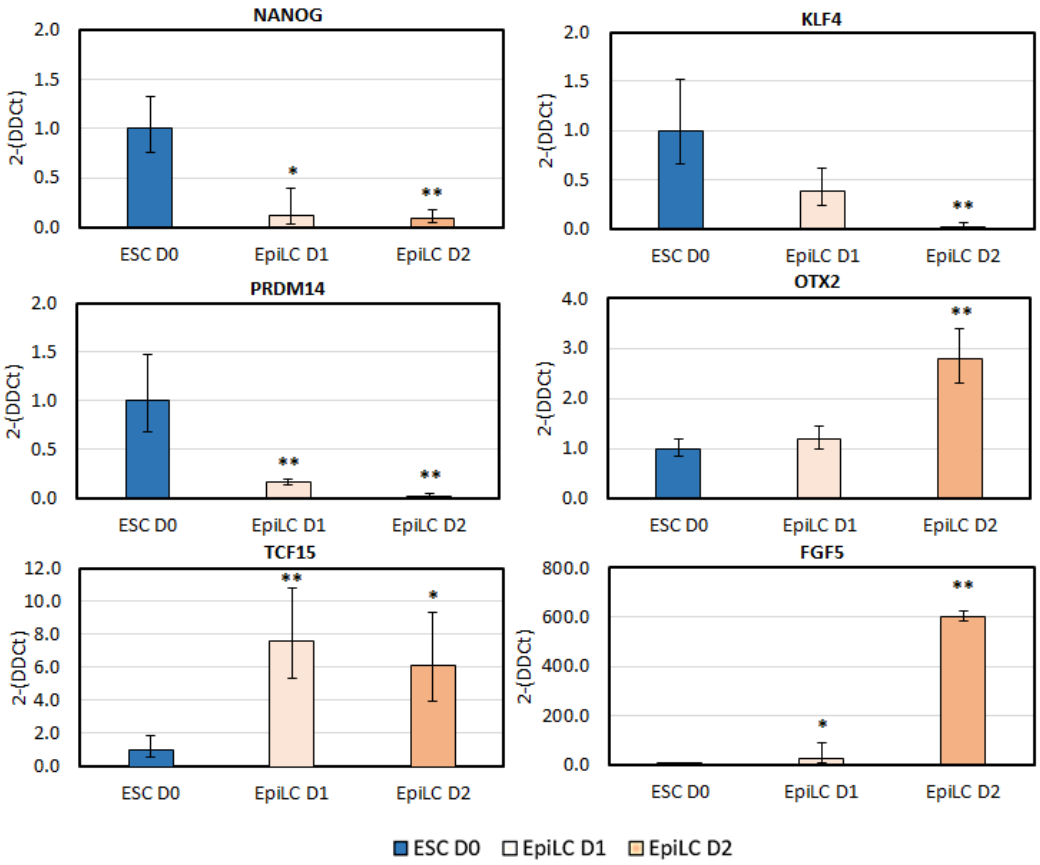

Figure 3.3.3 qRT-PCR of mouse cells undergoing the EpiLC differentiation protocol. *129/OLA mouse cells were harvested after 0, 1 and 2 days culture on fibronectin in EpiLC differentiation medium. All data was normalised to the house keeping gene β-actin (dCT) and fold change was calculated by normalising gene expression to that seen in mouse ESCs (ESC D0) cultured in 2i+LIF medium (2-DDCT). Bars represent the mean of three independent experiments performed with 129/OLA ESCs ± SD. *p<0.05, **p<0.01 to ESC D0.*

3.3.2 PGCLC differentiation of mouse cells

Mouse cells cultured in EpiLC medium for 2 days were collected and suspended in hanging drops of PGCLC medium (GMEM +KSR(15%) +L-Glut +BMP4 +BMP8a +SCF +EGF +LIF) on the lids of 15cm dishes. Each hanging drop consisted of ~2,000 EpiLCs contained within a 30µl drop of PGCLC medium. Dishes containing the suspended hanging drops were incubated for 2 days to promote aggregation of the EpiLCs. After 2 days, aggregates were transferred into 6-well low adhesion plates with fresh PGCLC medium to retain the aggregates in suspension and incubated for a further 4 days. Bright field photographs of these cellular aggregates were taken after 2 and 6 days of culture in PGCLC medium (Figure 3.3.4). Aggregation of EpiLCs occurred within 24 hours in hanging drop suspension and the cells formed large spheroid structures by the time they had completed the PGCLC differentiation protocol at day 8 (Figure 3.3.4).

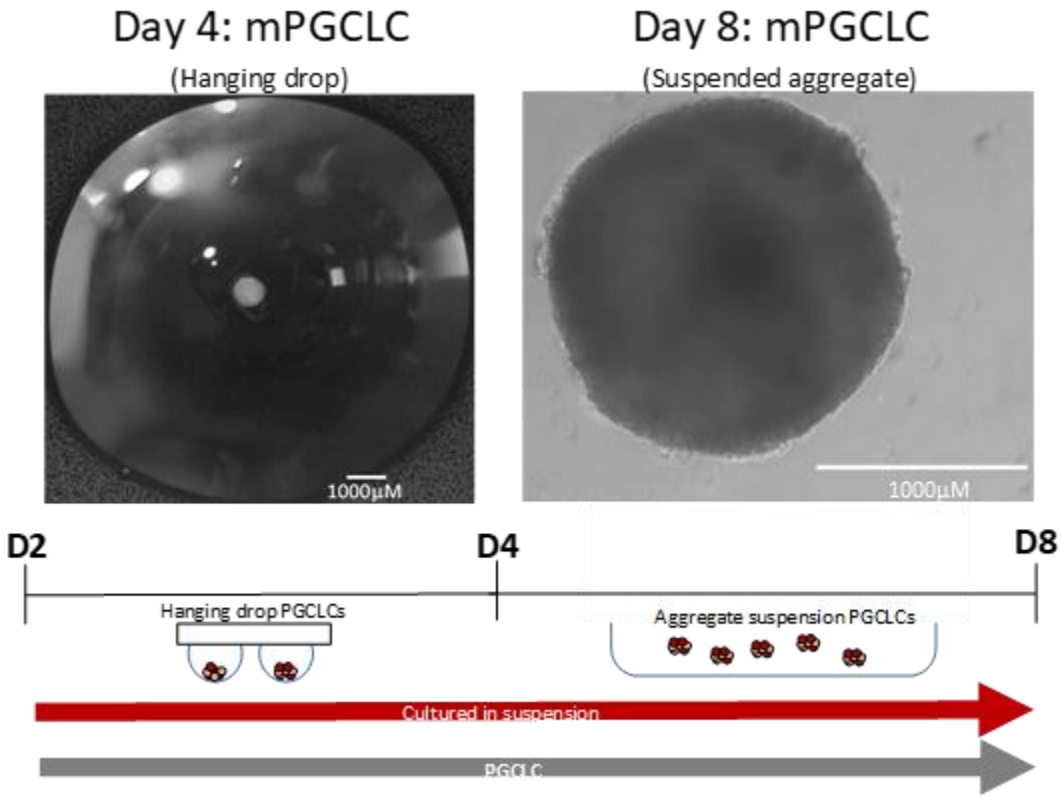

Figure 3.3.4. Bright field photographs of mouse aggregates undergoing the PGCLC differentiation protocol. *Images were taken 2 days after hanging drop set up (left panel) and 4 days of culture in 6-well low adhesion plates (right panel).*

To identify the presence of PGCLCs within the aggregates, aggregates were carefully dispersed by trituration and the cell suspensions stained with fluorescent antibodies for the surface markers SSEA-1 (CD15) and CD61. The gating strategy detailed in section 2.6.7 was used. The remaining cells were gated to isolate populations of double negative, single stained and double stained populations by plotting CD61 (586/15A) versus SSEA-1 (670/14A) using fluorescent activated cell-sorting (FACs). The gates were set against unstained mouse ESCs. Mouse ESCs cultured in 2i+LIF medium alongside the PGCLC differentiation protocol were used as a SSEA-1^{+ve}/CD61^{-ve} control. Mouse ESCs are positive for the SSEA-1 marker, so it was expected that during PGCLC differentiation there would be a global loss of this marker. Any PGCLCs present within the aggregates would be positive for both SSEA-1 and CD61, as described in the literature (Hayashi et al. 2011, Hayashi & Saitou 2013). Flow cytometry plots generated during cell sorting are displayed in Figure 3.3.5.

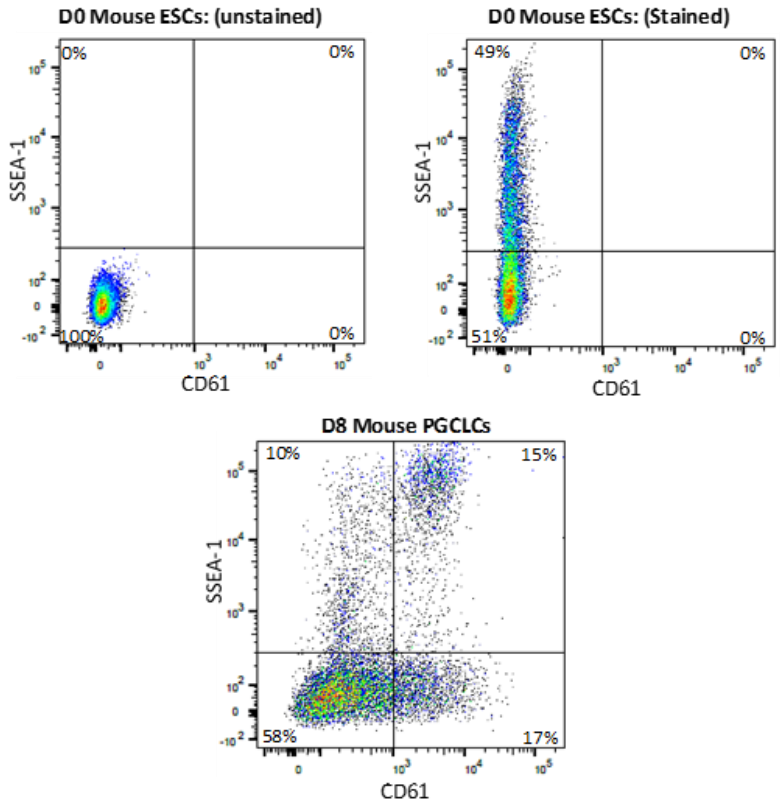

Figure 3.3.5. Flow cytometry plots of 129/OLA mouse cells after undergoing a PGCLC differentiation protocol. *Mouse ESCs cultured in 2i+LIF and cells which had been stimulated to differentiate using the PGCLC differentiation protocol were stained for SSEA-1 and CD61. Percentages represent total proportion of the population which were either positive or negative for SSEA-1 and CD61 surface markers.*

Interestingly, 129/OLA mouse ESCs cultured in 2i+LIF medium on MEFs showed a 50:50 split of SSEA-1^{+ve} and SSEA-1^{-ve} cells. A similar profile has been observed in both rat and mouse cell lines cultured on MEF layers within our lab, suggesting this may be a consequence of the MEF / 2i+LIF culture condition. Another potential factor was the presence of MEFs in the same culture well as the mouse ESCs, contributing to the SSEA^{-ve} population and thereby generating the 50:50 split of SSEA-1^{+ve} and SSEA-1^{-ve}.

Cells which had undergone the PGCLC differentiation protocol had a reduced population of SSEA-1^{+ve} / CD61^{-ve} cells compared to the ESC control and a general shift towards the CD61^{+ve} state. A distinct population of SSEA1^{+ve} / CD61^{+ve} cells was identified after PGCLC differentiation.

Cells which had been separated into these four quadrants were harvested and their RNA processed for qRT-PCR analysis in order to determine the distribution of PGC marker genes within the different populations. The quality of the RNA gathered from the SSEA-1^{+ve} / CD61^{-ve} population of cells which had undergone the PGCLC differentiation protocol was too poor for qRT-PCR and so was not analysed.

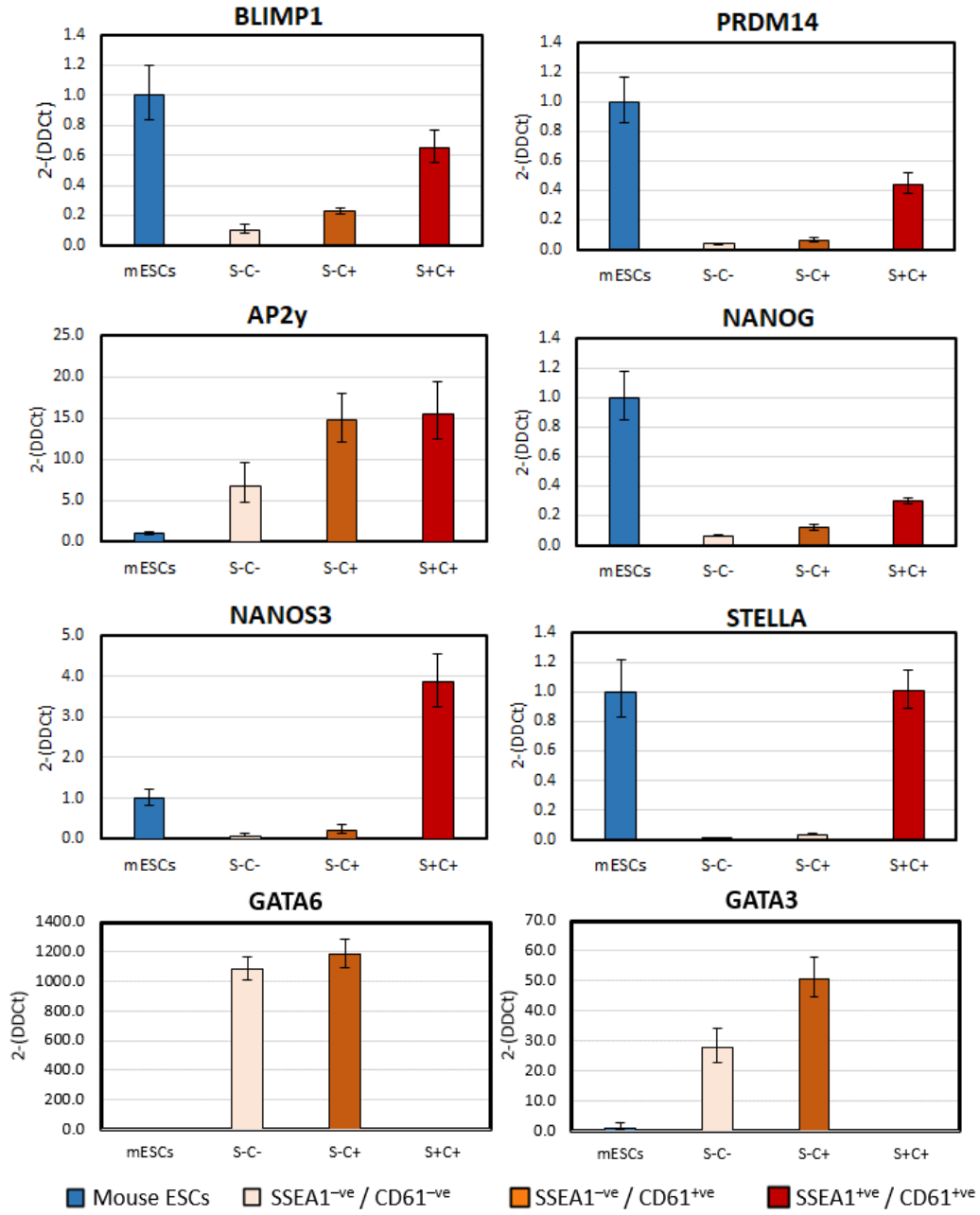

Figure 3.3.6. qRT-PCR of stained populations after undergoing a PGCLC differentiation protocol. *Mouse cells stained for SSEA-1 and CD61 were sorted by FACs into double negative, single and double positive populations. All data was normalised to the house keeping gene β-actin (dCT) and fold change was calculated by normalising gene expression to that seen in the mouse ESCs (mESCs) cultured in 2i+LIF medium (2-DDCT). S- = SSEA-1^{-ve}, C- = CD61^{-ve}, S+ = SSEA-1^{+ve}, C+ = CD61^{+ve}. Bars represent mean of two independent experiments performed with 129/OLA cells ± SD.*

The SSEA-1^{+ve} / CD61^{+ve} population showed the greatest expression of the PGC transcription factors *Blimp1* and *Prdm14* compared to the other sorted populations. This population also showed the highest transcript expression of the PGC marker *Nanos3* and pluripotency markers *Nanog* and *Stella* compared to all other sorted populations. Additionally, there was no detectable expression of either the definitive endoderm marker *Gata6* or trophectoderm marker *Gata3* in SSEA-1^{+ve} / CD61^{+ve} cells when compared to the other sorted populations. These results therefore confirmed that the PGCLC differentiation protocol applied to mouse cells cultured in 2i+LIF on MEFs did produce cells with a PGCLC-like profile similar to that described in the literature (Hayashi et al. 2011, Hayashi & Saitou 2013).

3.4 Epiblast-like (EpiLC) differentiation of rat ESCs

3.4.1 Attachment of rat ESCs to a basement membrane

Before mouse ESCs are induced to differentiate into PGCLCs, they are transitioned into an EpiLC fate, ensuring they are sensitised to the differentiation cues activated by the cocktail of cytokines present in the PGCLC culture medium (Hayashi et al. 2011, Hayashi & Saitou 2013). The EpiLC differentiation protocol employs a fibronectin substratum to enable attachment and differentiation of cells towards the EpiLC fate. Rat DAK31 cells (dark agouti) were plated into tissue culture plates coated with different basement membranes; MEFs ($1.5x10^4$ cells/cm^2), fibronectin (16.7 µg/ml) or laminin (10 µg/ml). Rat ESCs were also cultured as suspended aggregates in aggrewells® to determine their survival in a non-adherent environment. In all conditions rat ESCs were seeded at a density of $1x10^5$ cells and cultured for 48 hours in 2i+LIF medium (Figure 3.4.1).

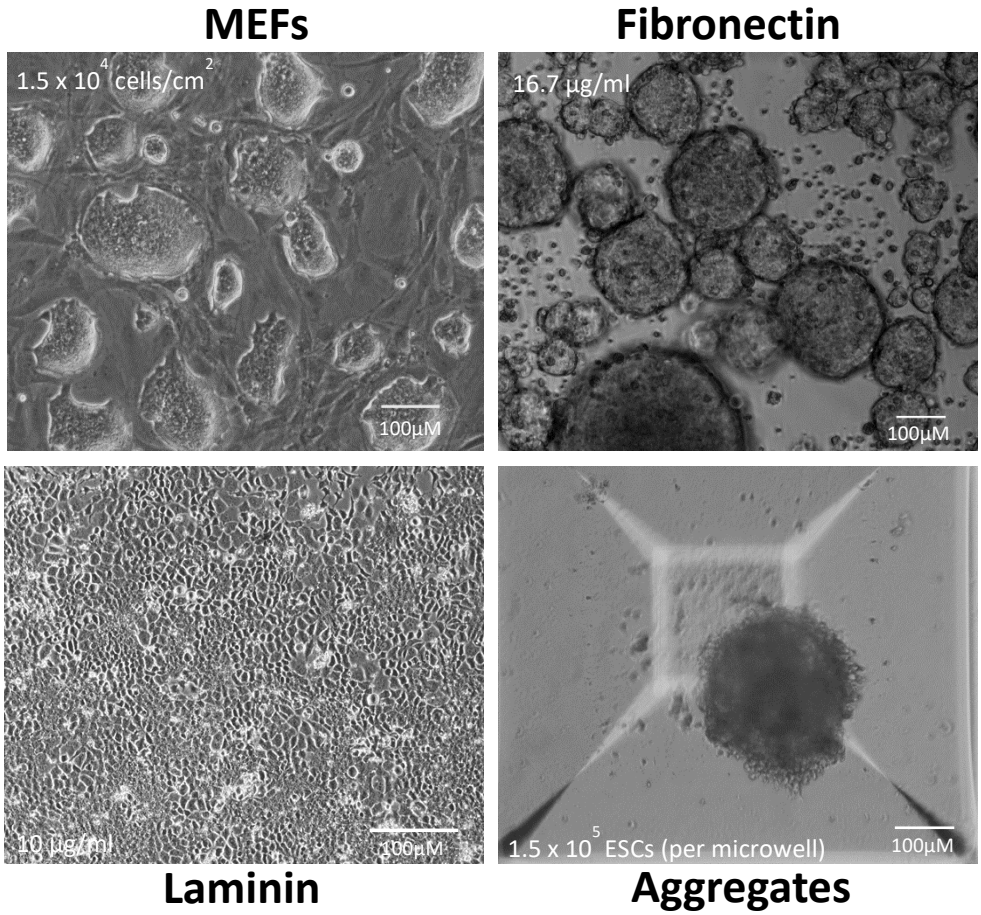

Figure 3.4.1. Bright field microscopy photographs of rat ESCs cultured on different basement membranes. *Cells were seeded at a density of $1x10^5$ per well and were cultured for 2 days in 2i+LIF medium within tissue culture wells. For aggregate suspension, cells were passaged into the aggrewells® so that each microwell depression contained $1x10^5$ cells.*

After 48 hours, there was no evidence of attachment of the rat ESCs to the fibronectin layer. The cells floated in the culture medium, aggregating together to form spheroids. Several different concentrations of fibronectin were tested in both 2i+LIF and EpiLC medium to try to improve attachment. However, no condition promoted attachment of rat ESCs to the fibronectin layer. Rat ESCs were capable of attaching to both the MEF and laminin substratum layers, however. Cells cultured on MEFs formed tight, domed colonies while those cultured on laminin formed a flat monolayer. Rat ESCs readily formed spheroid aggregates in suspension culture in the aggrewells®.

3.4.2 Inducing rat cell differentiation (EpiLC differentiation)

As rat ESCs did not attach to fibronectin, they were plated instead into 12-well plates coated with laminin or containing MEFs. $1x10^5$ cells/well were cultured in EpiLC medium for up to 3 days. Rat ESCs were also cultured in aggrewell plates at a density representing ~$1x10^5$ cells per microwell depression. This density of starting cells was chosen to replicate the mouse EpiLC differentiation protocol. Cells were photographed every 24 hours to record their response to the EpiLC medium and ascertain whether there was any noticeable differences in cell morphology or growth between the different populations. Rat ESCs cultured in laminin coated plates attached to the basement membrane as a flat monolayer rather than domed colonies (Figure 3.4.2). Cellular debris was apparent after 24 hours in EpiLC medium, but those remaining cells showed a flattened morphology (Figure 3.4.2). Rat ESCs grown in suspension quickly formed small aggregates which did not grow in size during the 3-day culture (Figure 3.4.2). Cell debris indicative of cell death was present at the bottom of all microwells and attached to the outer surface of each aggregate (Figure 3.4.2).

ESCs cultured on MEF layers in the presence of EpiLC medium formed domed colonies during the first 48 hours of EpiLC differentiation (Figure 3.4.2). However, by day 3, there were patches of morphologically flat cells reminiscent of mouse EpiLC differentiation (Figure 3.4.2). Cells cultured on MEFs with EpiLC medium also showed greater evidence of cellular debris compared with all other basement substrates tested (Figure 3.4.2).

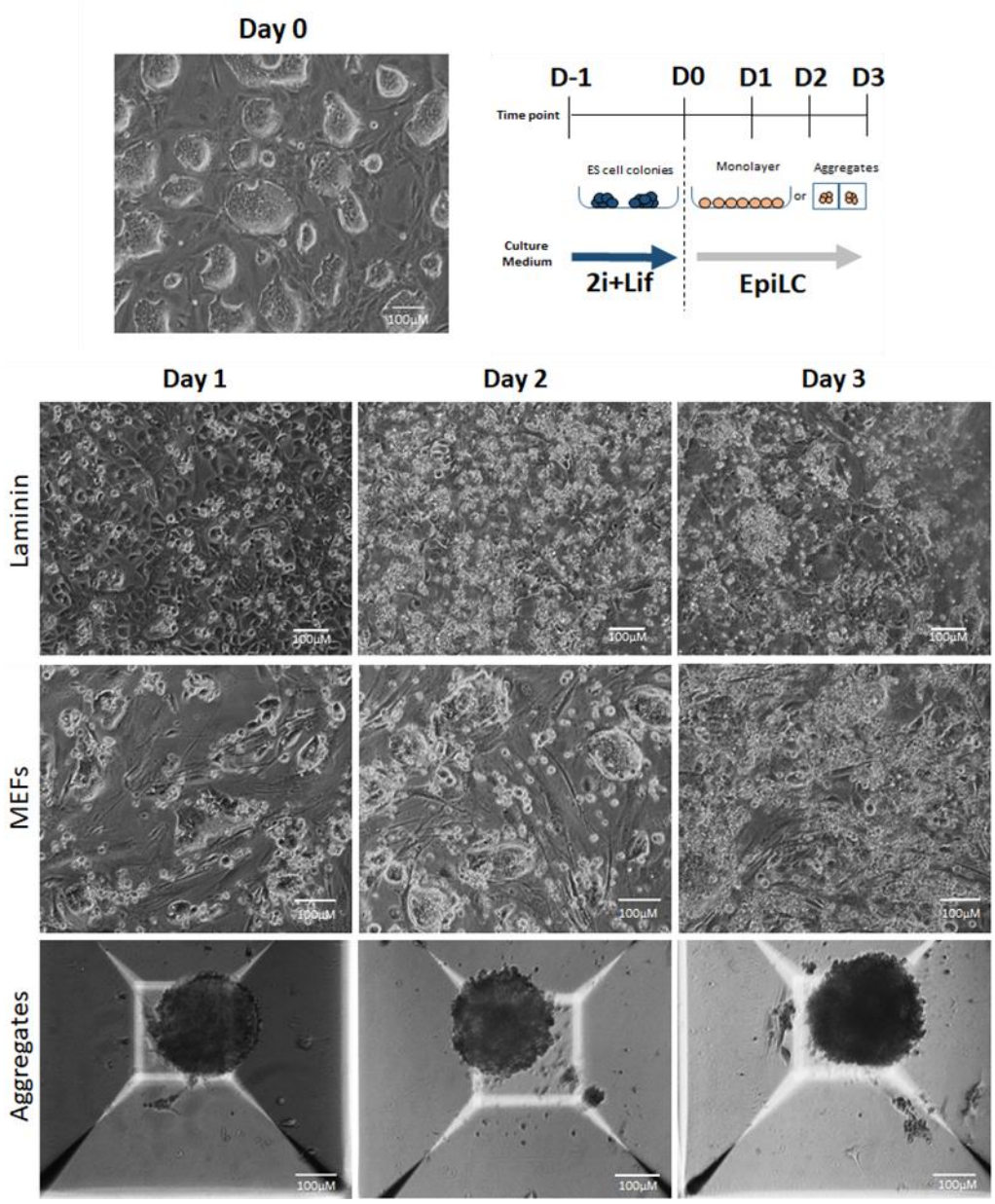

Figure 3.4.2. Bright field microscopy photographs of rat ESCs undergoing an EpiLC differentiation protocol. *$1x10^5$ rat ESCs were cultured for 3 days in EpiLC medium in tissue culture wells coated with Laminin (10µg/ml), MEFs ($1.5x10^4$ cells/cm^2) or cultured in suspended aggregates.*

Rat cells cultured in EpiLC medium were harvested at 24 hour time points over 3 days. qRT-PCR analysis was performed to quantify the expression of markers commonly associated with EpiLC differentiation.

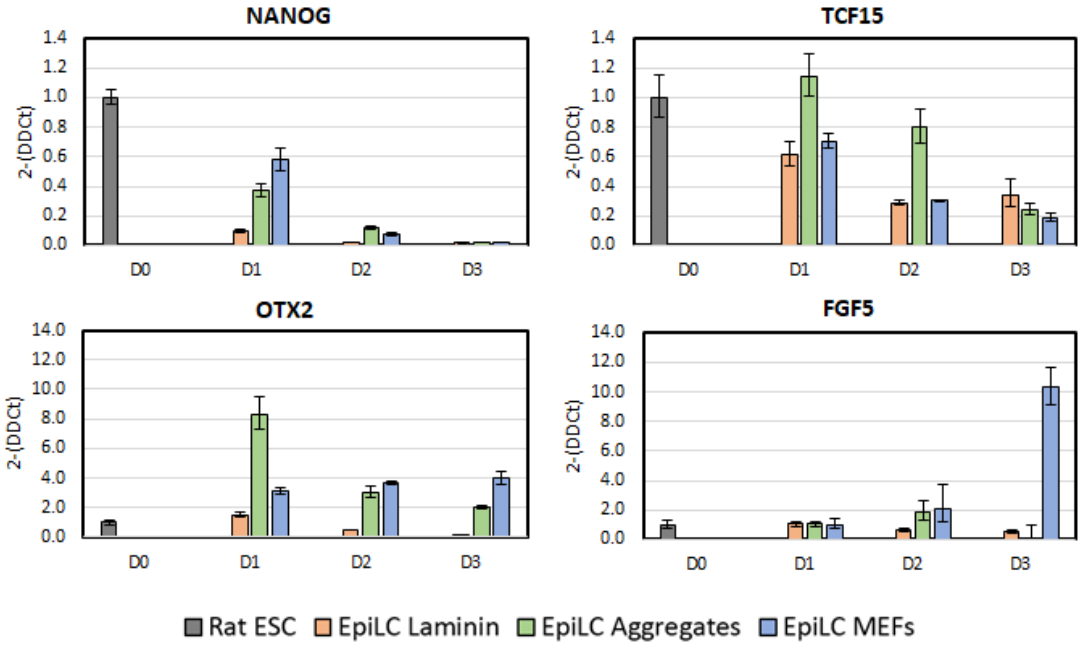

Figure 3.4.3. q-RT PCR of rat ESCs undergoing an EpiLC differentiation protocol. *$1x10^5$ rat ESCs were cultured for 3 days in EpiLC medium in wells coated with Laminin (10µg/ml), MEFs ($1.5x10^4$ cells/cm^2) or cultured in suspended aggregates. Cells were harvested at 24 hour time points. The data shown is the average of two experimental replicates of rat DAK31 ESCs cultured in EpiLC medium for 3 days. All data was normalised to the house keeping gene β-actin (dCT) and fold change was calculated by normalising gene expression to that seen in rat ESCs cultured in 2i+LIF medium on MEFs (2-DDCT). Bars represent mean of two independent experiments performed with DAK31 ESCs ± SD.*

During the 3-day EpiLC differentiation protocol, all cell treatments displayed a substantial reduction in *Nanog* transcript expression and by day 3, there was little or no detectable *Nanog* expression from any of the cell treatments (Figure 3.4.3).
It is reported that expression of *Tcf15* during EpiLC differentiation of mouse ESCs increases within the first 24 hours of culture, and then falls as the cells transition out of the naïve state (Hayashi et al. 2011). In the rat cells, no rise in *Tcf15* expression was detected, only a gradually reduction in all conditions during the EpiLC differentiation protocol (Figure 3.4.3). *Otx2* gene expression increased within the first 24 hours of being cultured in EpiLC medium within suspended aggregates and then gradually declined over the next 48 hours (Figure 3.4.3). The expression of *Otx2* in cells cultured on laminin decreased gradually over the 3 days, becoming almost undetectable after 3 days culture in EpiLC medium (Figure 3.4.3). ESCs cultured on MEF layers in EpiLC medium displayed increased levels of *Otx2*, which was maintained throughout the 3-day protocol (Figure 3.4.3). Expression of the growth factor *Fgf5* did not change in any culture condition during the first 48 hours of EpiLC differentiation (Figure 3.4.3).

However, between 48-72 hours, cells cultured on MEF layers showed a sharp increase in *Fgf5* (Figure 3.4.3), suggesting there was a proportion of cells entering an epiblast-like fate. Based on the induction of EpiLC markers, it seemed that the protocol originally optimised for the mouse system to induce EpiLC differentiation (Hayashi et al. 2011, Hayashi & Saitou 2013) could not be simply translated to rat ESCs without modification. The best differentiation response came from rat cells cultured on MEFs during a 3-day protocol of EpiLC differentiation. This condition not only produced cells with the characteristic flattened monolayer morphology typical of mouse EpiLCs (Figure 3.4.2), but also displayed increased expression of *Otx2* and *Fgf5* compared to the rat ESCs (Figure 3.4.3).

3.4.3 Inducing rat cell differentiation after pre-treatment (EpiLC differentiation)

Induction of both *Otx2* and *Fgf5* within rat ESCs grown on MEFs in EpiLC medium suggested that this condition might support EpiLC differentiation of rat ESCs. However, the induction of both of these genes was far lower than that compared to mouse ESCs (Figure 3.4.4).

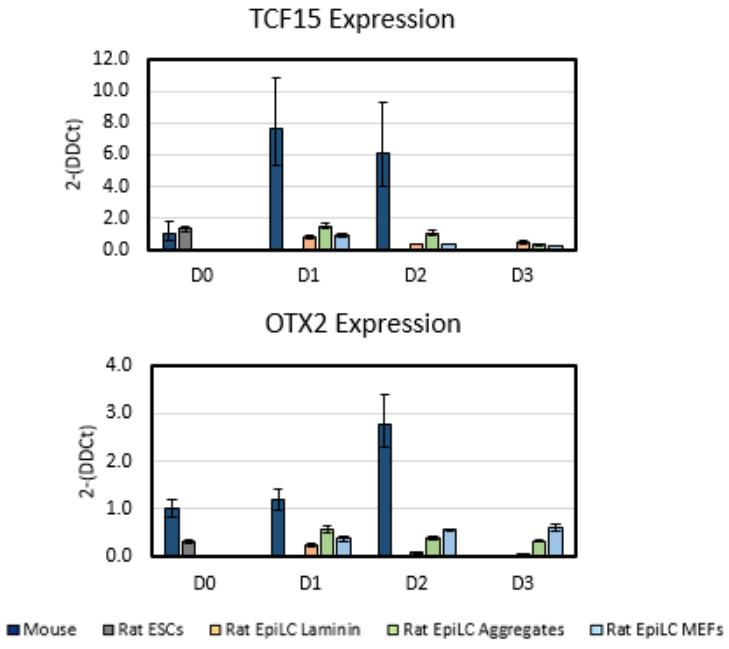

Figure 3.4.4. qRT-PCR of mouse and rat ESCs undergoing an EpiLC differentiation protocol. The mouse (129/OLA) data shown is the average of three experimental replicates mouse cells, whereas the rat (DAK31) is the average of two experimental replicates. All data was normalised to the house keeping gene β-actin (dCT) and fold change was calculated by normalising gene expression to that seen in mouse ESCs cultured in 2i+LIF medium on MEFs (2-DDCT). Bars represent mean of independent experiments ± SD.

The OTX2 transcription factor is thought to be a critical determinant for EpiLC differentiation of mouse ESCs (Acampora et al 2013, Yang et al. 2014). The basal expression of *Otx2* within rat ESCs was interrogated to identify whether rat and mouse ESCs both expressed *Otx2* at a similar level prior to being cultured in EpiLC medium. Three independent rat ESC lines (2x dark agouti, 1x Sprague-dawley) were cultured on MEF layers in 2i+LIF medium for 2 days alongside 3 independent mouse ESC lines (2x 129/OLA, 1x E14). qRT-PCR analysis showed that the basal expression of *Otx2* in rat ESCs was far lower than that in the mouse ESC lines (Figure 3.4.5).

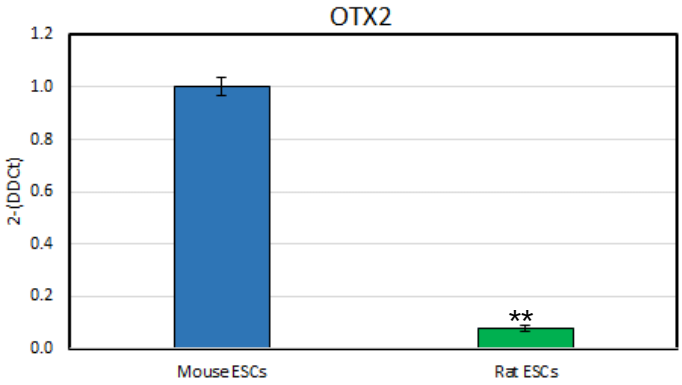

Figure 3.4.5. qRT-PCR displaying basal Otx2 expression within mouse and rat ESCs. *$1.5x10^5$ mouse and rat ESCs were cultured for 2 days in 2i+LIF on MEF layers. Cells were harvested after 48 hours. All data was normalised to the house keeping gene β-actin (dCT) and fold change was calculated by normalising gene expression to that seen in mouse ESCs cultured in 2i+LIF medium on MEFs (2-DDCT). Bars represent mean of three independent mouse and rat cell lines ± SD. **p<0.01 to Mouse ESCs.*

During the establishment of the rat ESC culture conditions in our laboratory, *Otx2* transcript expression was found to increase when ESCs were cultured in 1i medium, a culture medium containing only PD0325901 without CHIR99021 or LIF. 3 independent rat ESC lines (2x DA, 1x SD) were cultured on MEF layers in 2i+LIF and 1i medium for 3 days. These cells were then harvested and their RNA processed for qRT-PCR analysis. After 3 days culture in 1i medium, there was a substantial rise in *Otx2* transcript expression compared to cells cultured in 2i+LIF medium (Figure 3.4.6).

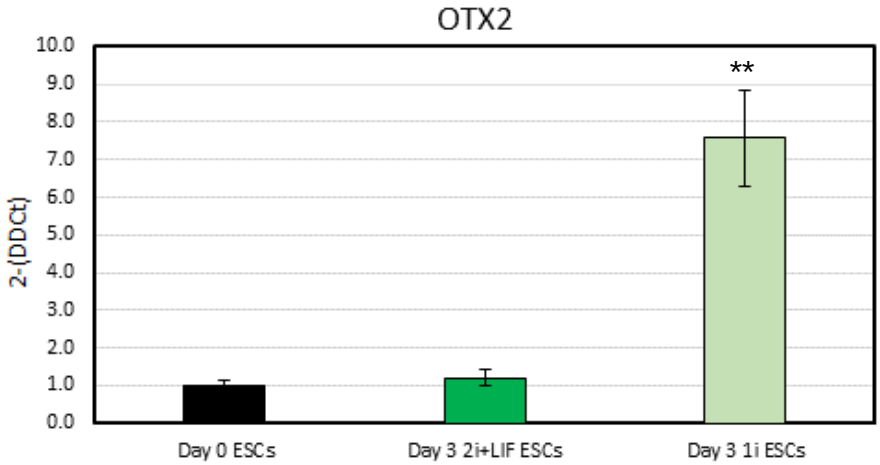

Figure 3.4.6. qRT-PCR displaying Otx2 expression within rat ESCs cultured in 2i+LIF and 1i culture medium. *1.5x10^5 rat ESCs were cultured for 3 days in 2i+LIF and 1i medium on MEF layers. Cells were harvested after 3 days and the transcript expression (2-DDCt) normalised to the population of rat ESCs prior to the 3 day culture (Day 0 ESCs) hours. Bars represent mean of three independent rat cell lines ± SD. **P<0.01 to Day 0 Rat ESCs.*

To determine if increased *Otx2* expression assisted transition into the EpiLC fate, rat ESCs were pre-cultured in 1i medium for 3 days prior to the 3-day EpiLC differentiation protocol. Cells were cultured on either a laminin layer, MEF layer or in suspended aggregates to identify if any of these conditions showed greater expression of EpiLC markers after 1i pre-culture. Cells were photographed every 24 hours to observe their response to being cultured in EpiLC medium. ESCs cultured on laminin coated plates formed flat monolayers, similar to the cells cultured in 2i+LIF medium prior to EpiLC medium (Figure 3.4.7). However, cells pre-cultured in 1i medium had a flatter morphology (Figure 3.4.7) compared to their 2i+LIF counterparts (Figure 3.4.2). Cellular aggregates formed from cells pre-cultured in 1i medium (Figure 3.4.7) appeared smaller and had greater cellular debris within each microwell compared to those cells pre-cultured in 2i+Lif medium prior to EpiLC medium (Figure 3.4.2).

After 3 days of being cultured in EpiLC medium on MEFs, cells pre-cultured in 1i medium displayed a flat monolayer morphology with very little cellular debris (Figure 3.4.7) when compared to the cells pre-cultured in 2i+LIF medium (Figure 3.4.2). Rat cells which had been pre-cultured in 1i medium and then cultured for 3 days in EpiLC medium on different basement substrates were harvested at 24 hour time points after being photographed (Figure 3.4.7).

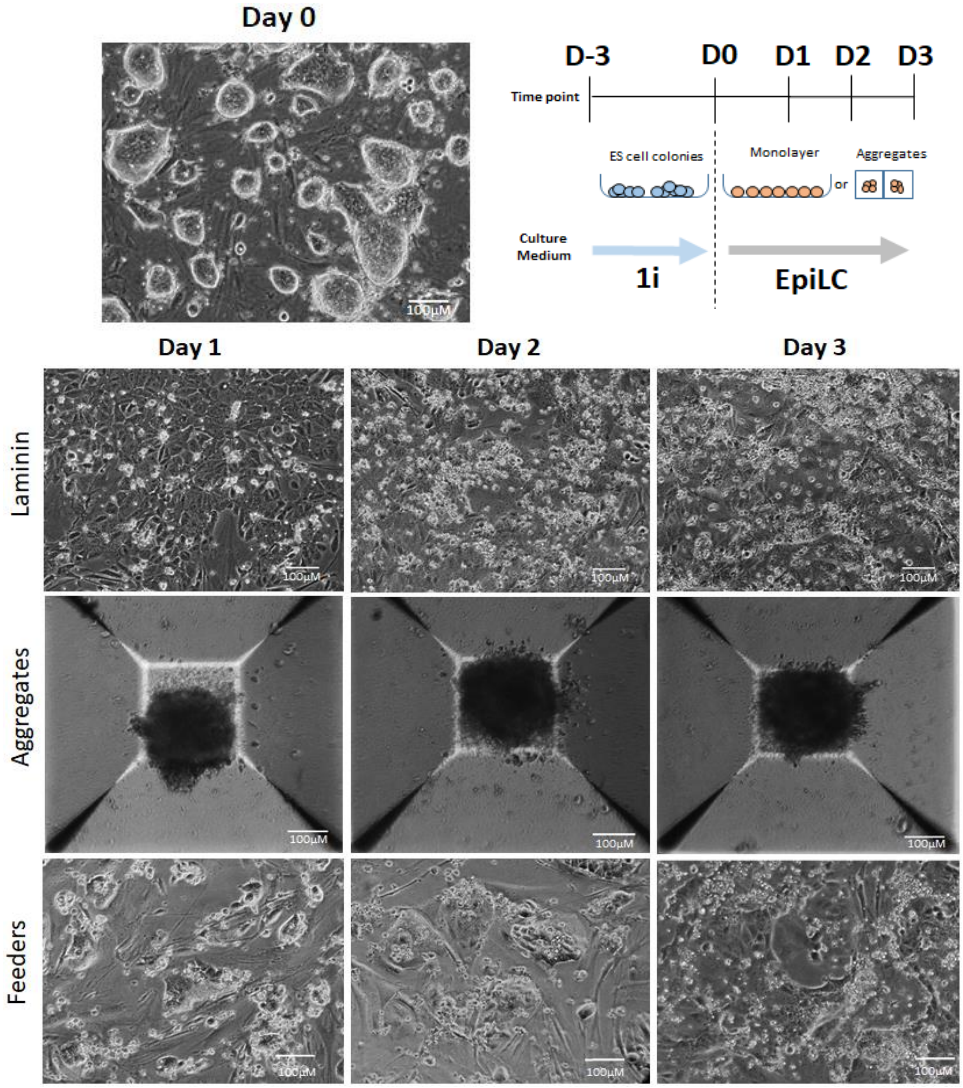

Figure 3.4.7. Bright field microscopy photographs of rat ESCs undergoing an EpiLC differentiation protocol after 3 days of 1i medium pre-culture. *1x10^5 rat ESCs were pre-cultured for 3 days in 1i medium on MEFs. 1x10^5 were then transferred into EpiLC medium in wells coated with Laminin (10µg/ml), MEFs (1.5 x 10^4 cells/cm^2) or cultured in suspended aggregates.*

qRT-PCR analysis was performed for cells which had either been pre-cultured in the presence (2i+LIF) or absence (1i) of CHIR99021 and LIF. No substantial difference in *Nanog*, *Tcf15* and *Otx2* transcript expression from cells pre-cultured in 1i medium compared to those pre-cultured in 2i+LIF (Figure 3.4.8).

However, 1i pre-cultured cells in all conditions had double the expression of *Fgf5* after being cultured in EpiLC medium for 3 days compared to cells pre-cultured in 2i+LIF medium (Figure 3.4.8). This increased *Fgf5* expression was most noticeable in cells which had been cultured on MEF layers (Figure 3.4.8).

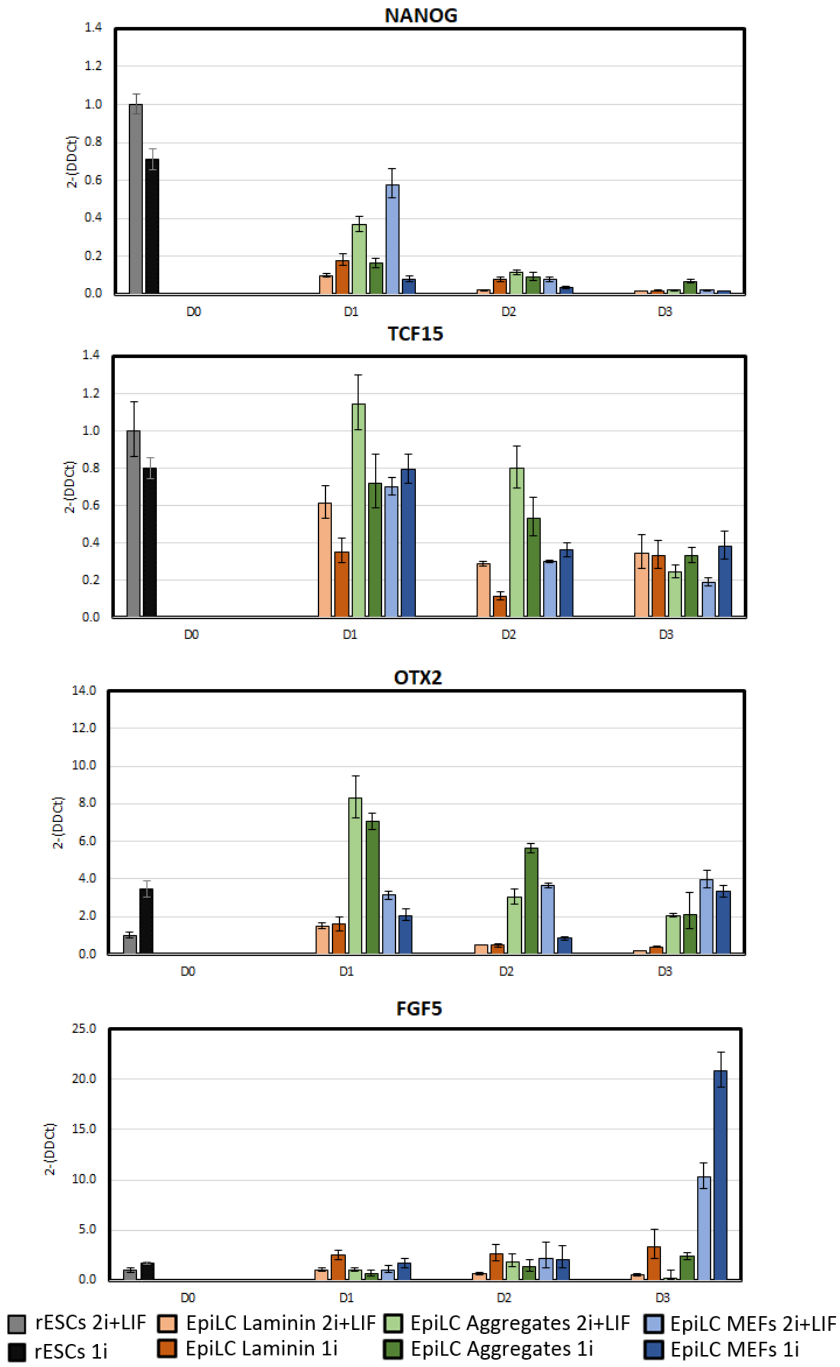

Figure 3.4.8. q-RT PCR of rat ESCs undergoing an EpiLC differentiation protocol with or without 1i medium pre-culture. *Cells undergoing EpiLC differentiation for 3 days were harvested at 24 hour time points. The data shown is the average of two experimental replicates performed on the same DAK31 ESC line. All data was normalised to the house keeping gene β-actin (dCT) and fold change was calculated by normalising gene expression to that seen in rat ESCs cultured in 2i+LIF medium on MEFs (2-DDCT). Bars represent the mean of two independent experiments performed in rat DAK31 ± SD.*

3.4.4 Summary of rat EpiLC differentiation

The loss of *Nanog* expression and the changes in morphology of rat cells subjected to the EpiLC differentiation protocol indicated that they were being directed out of the naïve ESC state under these conditions. However, it was difficult to conclude whether these cells were actually entering an EpiLC fate. The expression of *Fgf5* indicated that at least a small portion of these cells were adopting an epiblast fate. The greatest induction of this gene occurred when cells were pre-cultured in 1i medium and then co-cultured with MEFs during the EpiLC differentiation protocol. Based on these results, it was decided that prior to PGCLC differentiation, rat ESCs would be cultured with either 2i+LIF or 1i medium on MEF layers prior to undergoing the EpiLC differentiation protocol (Figure 3.4.9). These conditions were chosen as a 3 day culture in EpiLC medium on MEFs appeared to show the greatest induction of *Fgf5* expression in the experiments performed. Because it was still unclear at this point whether the 1i medium pre-culture might impair further differentiation, it was considered prudent to test both treatments when attempting to differentiate these cells towards a PGCLC fate.

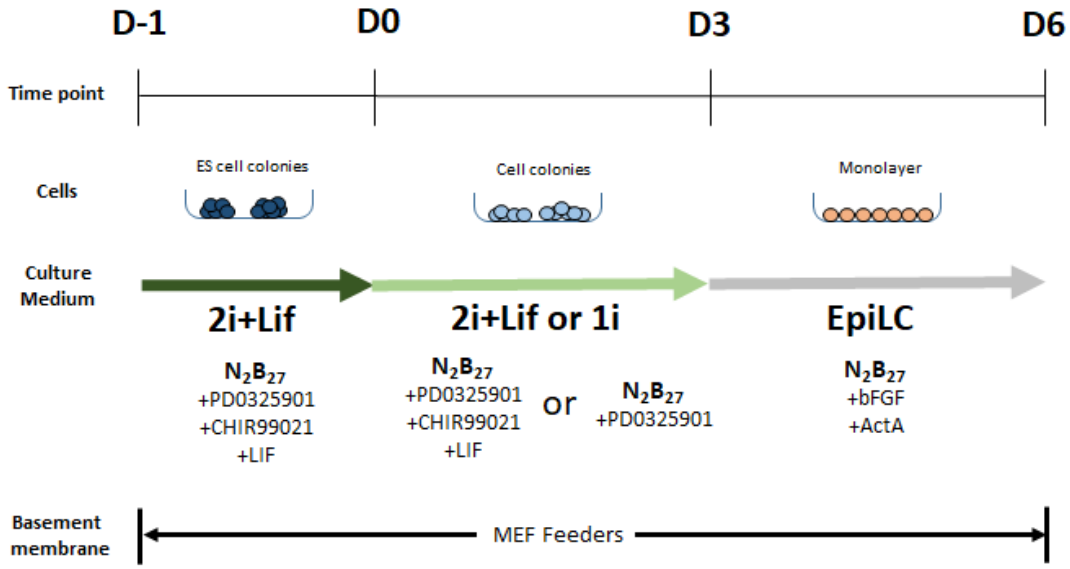

Figure 3.4.9. Revised EpiLC differentiation protocol for rat ESCs. *Rat ESCs cultured in 24-well plates with 2i+Lif conditions on a MEF layer are transferred into 24-well plates with fresh MEF layers and pre-cultured in either 2i+LIF or 1i medium for 3 days. These pre-cultured cells are then moved onto 12-well plates coated with MEF layers and cultured with EpiLC differentiation culture medium for 3 days.*

3.5 Primordial germ cell-like (PGCLC) differentiation of rat ESCs

3.5.1 Rat PGCLC differentiation protocol

The PGCLC differentiation protocol shown in Figure 3.5.1 was tested in rat DAK31 ESCs. This was to determine if rat ESCs could efficiently differentiate towards a PGC-like fate. The DAK31 cell line was chosen as it has been previously shown to be germline competent when injected into rat embryos (Blair et al. 2012) and does not express any fluorescent marker which could complicate immunostaining and analysis by flow cytometry. This protocol was adapted from the PGCLC differentiation protocol reported in the literature to drive mouse cells towards PGCLCs (Hayashi et al. 2011, Hayashi & Saitou 2013), and a method used for differentiating 129/OLA mouse ESCs in our laboratory.

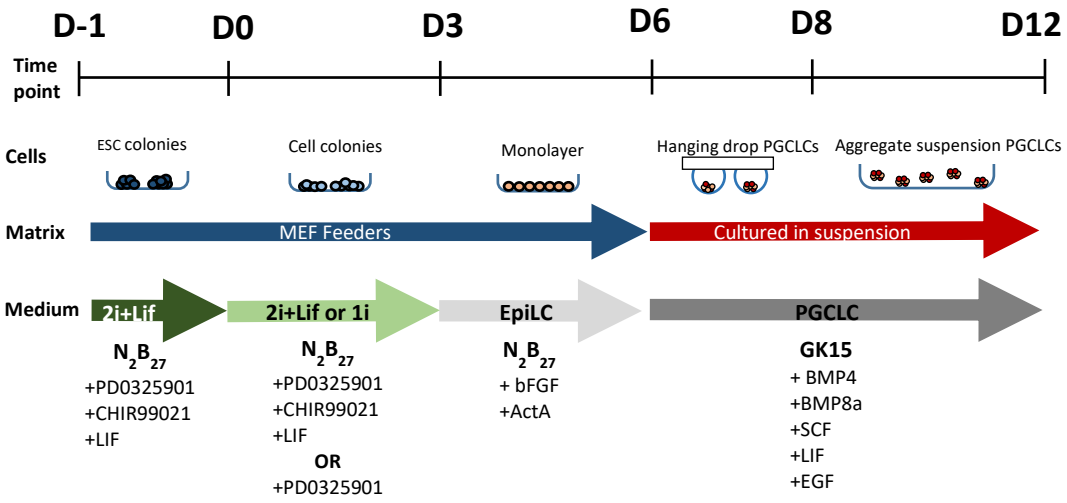

Figure 3.5.1. PGCLC differentiation protocol applied to rat ESCs. *Cells were first induced to differentiate using the revised EpiLC differentiation protocol described in section 3.4.4. The cells were then pipetted into hanging drops containing ~2,000 cells in PGCLC culture medium. After 2 days of culture, aggregates were collected and transferred into fresh PGCLC culture medium in 6-well low adhesion plates for 4 days.*

DAK31 ESCs were transferred to fresh MEF layers and pre-cultured for 3 days in either 2i+LIF or 1i medium. After 3 days, $1x10^5$ cells were passaged 12-well plates coated with fresh MEF layers in EpiLC medium. Cells were incubated for 3 days, with the EpiLC medium being replaced with fresh medium every 24 hours to replenish the bFGF and activin A. Cells were photographed after 3 days in EpiLC culture medium. Both 2i+LIF and 1i medium pre-cultured cells showed a flattened morphology compared to the domed rat ESC colonies under standard rat ESC culture conditions (Figure 3.5.2).

Wells of pre-cultured cells showed evidence of differentiation in the form of small, cobblestone patches (Figure 3.5.2 - white arrows). Although the cells pre-cultured in 1i medium appeared to grow slower, there was less cellular debris present in this treatment compared to cells pre-cultured in 2i+LIF medium (Figure 3.5.2).

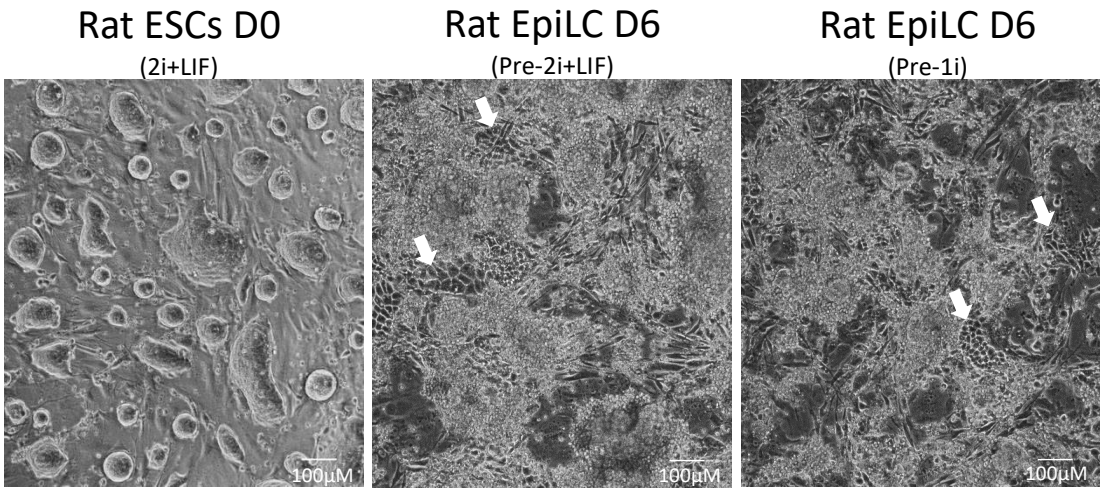

Figure 3.5.2. Bright field microscopy photographs of rat ESCs after 3 days culture in EpiLC differentiation medium. *DAK31 cells pre-cultured in either 2i+LIF (Pre-2i+LIF) or 1i medium (Pre-1i) for 3 days were seeded at a density of 1x10^5 on MEF layers in EpiLC medium and incubated for 3 days. White arrows highlight patches of 'cobblestone' differentiation after being cultured in EpiLC medium. Images taken are cells cultured in standard rat ESCs culture conditions (D0) and cells which had been cultured in EpiLC medium (D6).*

Cells which had undergone the EpiLC differentiation protocol were transferred into hanging drops of PGCLC culture medium. Each hanging drop consisted of ~2,000 cells contained within 30µl PGCLC culture medium. Dishes containing the suspended hanging drops were incubated for 2 days to promote aggregation of the cells. Cells which had been pre-cultured in 2i+LIF medium and 1i medium but had not been cultured in EpiLC differentiation medium were also transferred to hanging drops to observe whether the efficiency of aggregate formation was affected by culturing the cells in EpiLC differentiation medium. Cell aggregates were photographed after 2 days using bright field microscopy. Cells which had not been through the EpiLC differentiation protocol produced either multiple tiny aggregates or a single small aggregate surrounded by cellular debris (Figure 3.5.3). Cells exposed to EpiLC differentiation medium however produced on average one single aggregate within each hanging drop (Figure 3.5.3). Aggregates formed from cells pre-cultured in 1i medium were on average larger compared to those in 2i+LIF medium after the cells had been cultured in EpiLC culture medium (Figure 3.5.3).

Hanging drop cultures from cells pre-cultured in 2i+LIF medium contained noticeable levels of cellular debris surrounding the main aggregates (Figure 3.5.3). This debris was less evident in the hanging drops formed from the 1i pre-cultured cells (Figure 3.5.3). Finally, it was interesting to note that the size of the aggregates formed from differentiating rat cells were far smaller than those generated from mouse cells (Figure 3.3.4), suggesting that the rat cells were either not growing under these conditions or that cell death restricted the growth of these aggregates, maintaining them at a similar size.

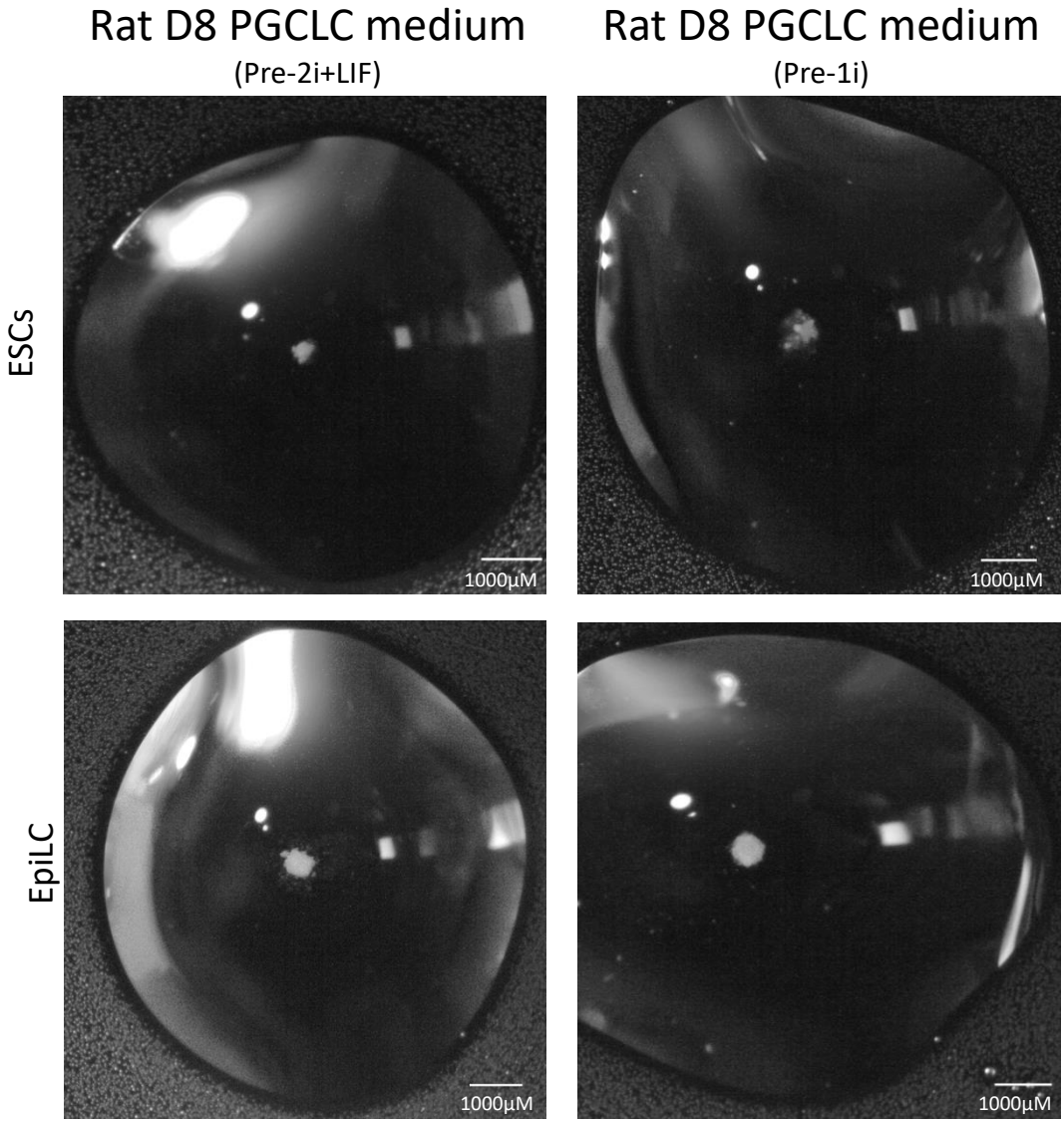

Figure 3.5.3. Bright field microscopy photographs of hanging drops containing rat cell aggregates after 2 days culture. *Photographs were obtained 2 days after hanging drops were set up. Each drop of PGCLC medium (30μl) contained ~2,000 cells. The top panels show rat cells which have been taken from pre-cultured wells and placed immediately into PGCLC hanging drops. The bottom panels show rat cells which have been pre-cultured in 2i+LIF or 1i medium, induced to differentiate by culturing in EpiLC medium for 3 days and then transferred to hanging drops containing PGCLC medium.*

After 2 days in hanging drops, the aggregates were transferred into 6-well low adhesion plates and remained in suspension for a further 4 days. During this period the aggregates were monitored daily and bright field photographs were taken on the final day of PGCLC culture. There appeared to be little noticeable difference in the growth or survival of either of the pre-cultured populations after the 4-day culture (Figure 3.5.4). Both pre-cultured populations exhibited significant signs of cell death (Figure 3.5.4), and did not appear to increase in size during the PGCLC differentiation protocol, unlike the mouse aggregates (Figure 3.3.4).

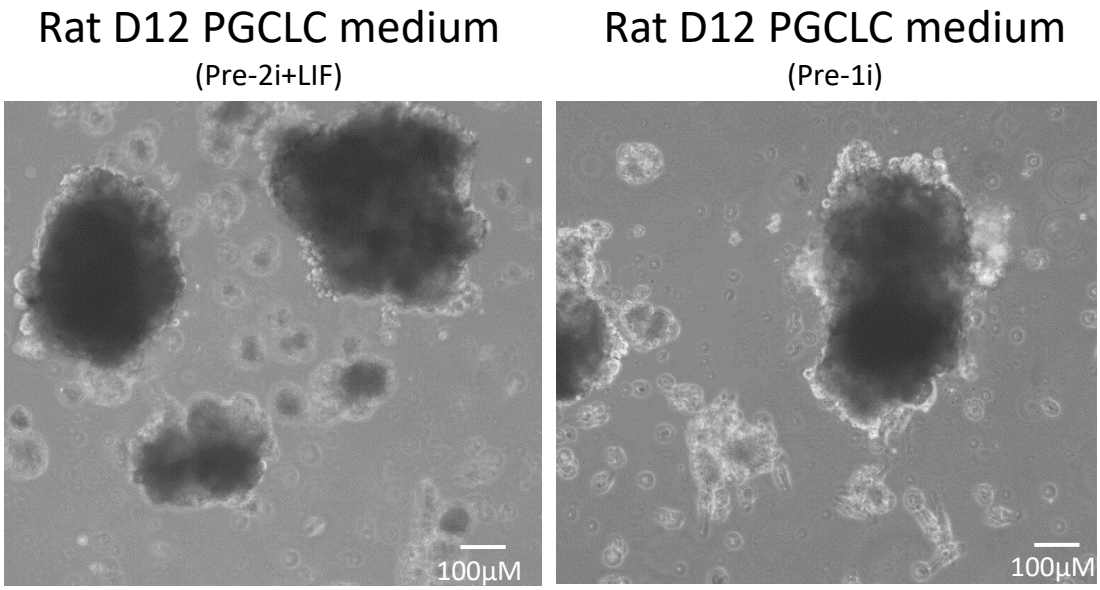

Figure 3.5.4. Bright field photographs of rat aggregates after 6 days culture in PGCLC differentiation medium. *Aggregates cultured in hanging drops of PGCLC medium for 2 days were transferred to 6-well low adhesion plates in fresh PGCLC medium and cultured for a further 4 days.*

3.5.2 Analysis of PGC markers from rat cells

Aggregates formed by the end of the 12 day protocol were carefully broken apart by gentle pipetting (trituration) and the cell suspensions stained with fluorescent antibodies for SSEA-1 and CD61. These surface markers were used to monitor the differentiation status of the cells and sort the pools by FACs into populations of cells which were either unstained, single stained, or double stained for both surface markers. A population of cells which are both SSEA-1^{+ve} / $CD61^{+ve}$ is reported to be generated after mouse ESCs are induced to differentiate via the PGCLC differentiation protocol (Hayashi et al. 2011, Hayashi & Saitou 2013). It was hoped that by isolating these separate populations in the rat cells, rat PGCLCs could be identified by increased expression of pluripotency markers and expression of PGC marker genes. Co-expression of the markers SSEA-1 (CD15) and germ cell nuclear antigen 1 (GCNA1) have been noted to identify mouse PGCs (Hayashi et al. 2011, Encinas et al. 2012). However, it has been reported that these markers, were not detectable in rat PGCs within the genital ridges (Encinas et al. 2012). Nonetheless, it was still of interest to see if this applied to rat cells subjected to the PGCLC differentiation protocol, with the differentiation of rat ESCs being monitored by the loss of the SSEA-1 surface marker. Similar to their mouse counterparts, rat ESCs are known to be positive for SSEA-1, and during the differentiation protocol, it was expected that the majority of these cells would lose SSEA-1 expression. The gating strategy detailed in section 2.6.7 was used. The remaining cells were gated to isolate populations of double negative, single stained and double stained populations by plotting CD61 (586/15A) versus SSEA-1 (670/14A) using fluorescent activated cell-sorting (FACs). The FACs plots generated during the analysis of rat cells are shown in Figure 3.5.5. Rat DAK31 ESCs cultured in standard 2i+LIF culture conditions were used as a rat ESC control, representing the surface marker expression of rat cells prior to PGCLC differentiation. The gates were set against unstained DAK31 ESCs.

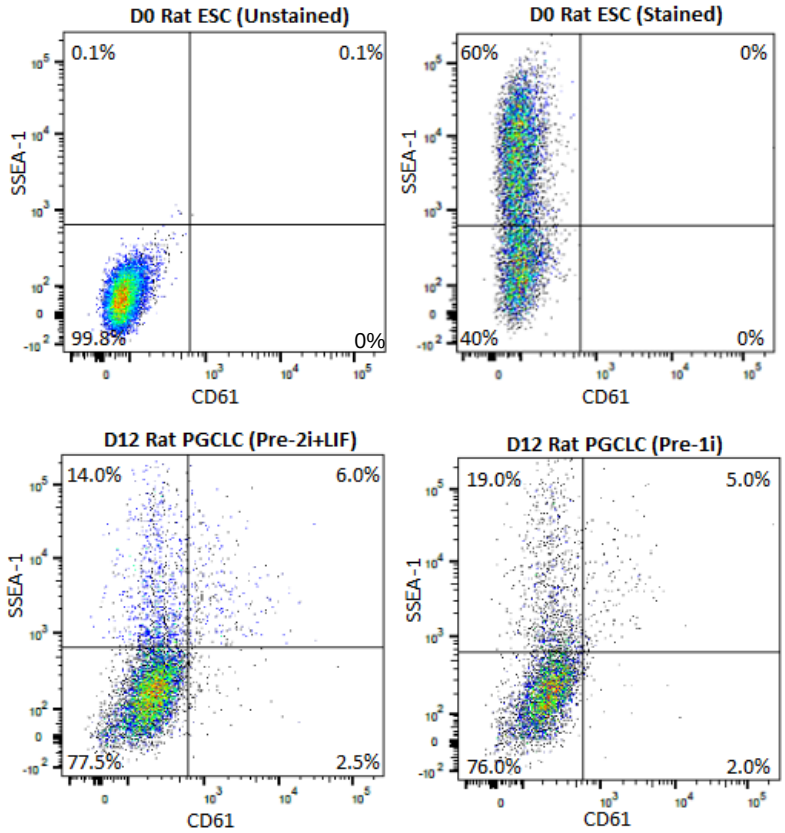

Figure 3.5.5. Flow cytometry plot of DAK31 rat cells after PGCLC differentiation. *Rat ESCs cultured in 2i+LIF and pools of rat cells induced to differentiate using the PGCLC differentiation protocol were stained for SSEA-1 and CD61 surface markers. Percentages represent total proportion of the population which were either positive or negative for SSEA-1 and CD61 surface markers.*

Similar to the 129/OLA mouse ESCs shown previously (Figure 3.3.5), rat ESC cultures maintained in 2i+LIF on MEFs possessed both SSEA-1^{+ve} and SSEA-1^{-ve} cells (Figure 3.5.5). This profile is consistent with other ESC lines cultured within the laboratory, suggesting that this might be a consequence of culturing rodent ESCs on MEF layers with 2i+LIF medium instead of a feeder-free environment. This difference could also be compounded by staining mixed cell populations containing both ESCs and MEFs, where ESCs are SSEA-1^{+ve} while the MEFs are SSEA-1^{-ve}. Cells which had been induced to differentiate by being subjected to the PGCLC differentiation protocol showed a general loss of SSEA-1^{+ve} cells within the whole population (Figure 3.5.5). There was a population of SSEA-1^{+ve} / CD61^{+ve} cells present in rat cell pools after PGCLC differentiation (Figure 3.5.5). However unlike the mouse cells, rat ESC pre-cultured in either condition did not show a distinct population of SSEA-1^{+ve} / CD61^{+ve} cells when compared to the stained ESCs; showing instead a general shift of the whole population towards increased CD61^{+ve} presence (Figure 3.5.5).

Although the proportion of SSEA-1^{+ve} / CD61^{+ve} cells in pools pre-cultured in either 2i+LIF or 1i medium was not substantially different, there was a greater proportion of SSEA-1^{+ve} cells in pools pre-cultured in 1i medium (Figure 3.5.5). There was little variation in the percentages of each population between the 3 experimental repeats performed in the rat DAK31 cell line.

These individual populations were analysed for expression of PGC related transcripts. The qRT-PCR data represents the average of three experimental replicates performed in the rat DAK31 cell line. All stained populations of cells after PGCLC differentiation had significantly greater *Blimp1* expression compared to rat ESCs (Figure 3.5.6). The most marked increase in *Blimp1* expression was observed in the SSEA-1^{-ve} / CD61^{+ve} population of cells pre-cultured in 2i+LIF medium (Figure 3.5.6). However, this population also had the greatest variation in *Blimp1* expression between the three experimental replicates (Figure 3.5.6).

In all but one of the sorted cell populations, there was a significant drop in *Prdm14* expression compared to ESCs (Figure 3.5.6). The SSEA-1^{-ve} / CD61^{+ve} population of cells pre-cultured in 2i+LIF medium retained a similar expression of *Prdm14* compared to ESCs (Figure 3.5.6).

Ap2y expression remained fairly consistent between the different populations, with only the population of SSEA-1^{-ve} / CD61^{+ve} cells pre-cultured in 2i+LIF showing a significant rise in expression after PGCLC differentiation compared to rat ESCs (Figure 3.5.6).

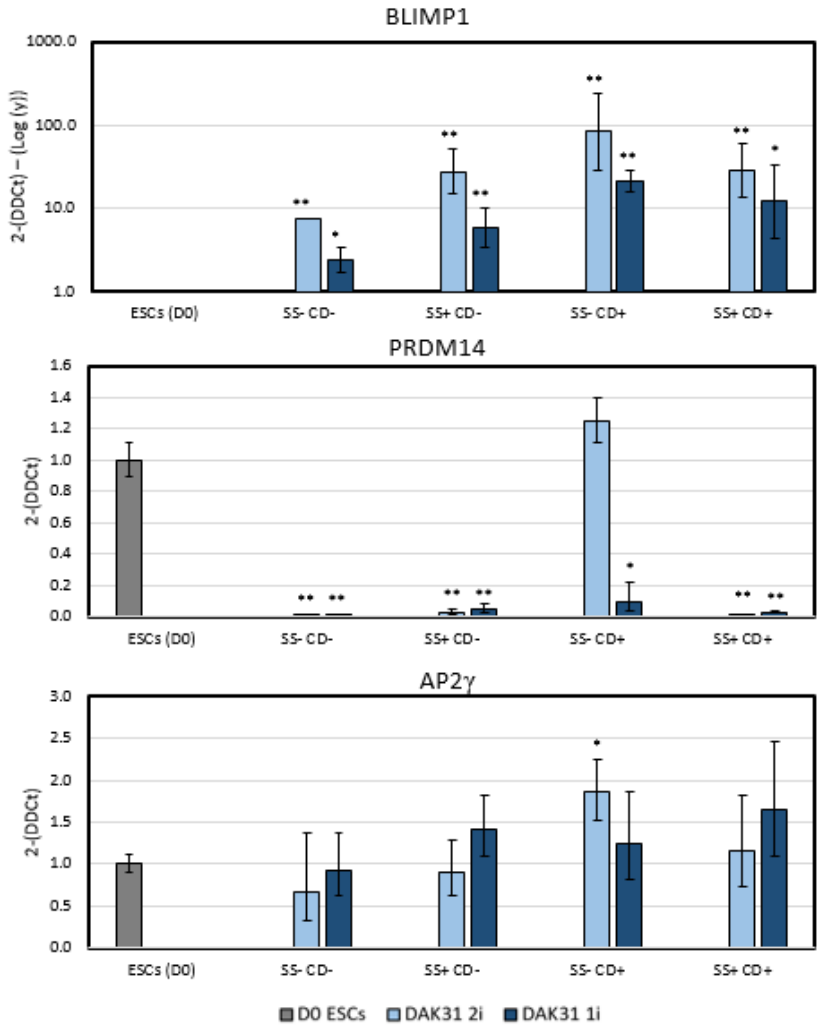

Figure 3.5.6. qRT-PCR analysis of the expression of PGC TFs in SSEA1/CD61 stained populations of rat cells subjected to a PGCLC differentiation protocol. *Rat cells which had undergone PGCLC differentiation and had been stained for SSEA-1 and CD61 were sorted by FACs into double negative, single and double positive populations. All data was normalised to the house keeping gene β-actin (dCT) and fold change was calculated by normalising gene expression to that seen in the rat ESCs (ESCs (D0)) cultured in 2i+LIF medium (2-DDCT).The y-axis for BLIMP1 expression is presented as a log scale. SS- = SSEA-1^{-ve}, CC- = CD61^{-ve}, SS+ = SSEA-1^{+ve}, CC+ = CD61^{+ve}. Bars represent mean of three independent experiments performed with DAK31 cells ± SD. *P<0.05, **P<0.01 to ESCs (D0).*

Expression of the pluripotency markers, *Oct4*, *Nanog* and *Stella* was on average significantly reduced in sorted cells derived after the PGCLC differentiation protocol when compared to rat ESCs (Figure 3.5.7). *Nanog* expression in the population of SSEA-1^{-ve} / CD61^{+ve} cells pre-cultured in 2i+LIF medium was slightly elevated compared to rat ESCs (Figure 3.5.7). However, this population also displayed a significant variation in *Nanog* expression between the three independent experiments (Figure 3.5.7). Expression of *Oct4* within the SSEA-1^{+ve} / CD61^{-ve} cells pre-cultured in 1i medium was equivalent to the expression within rat ESCs (Figure 3.5.7).

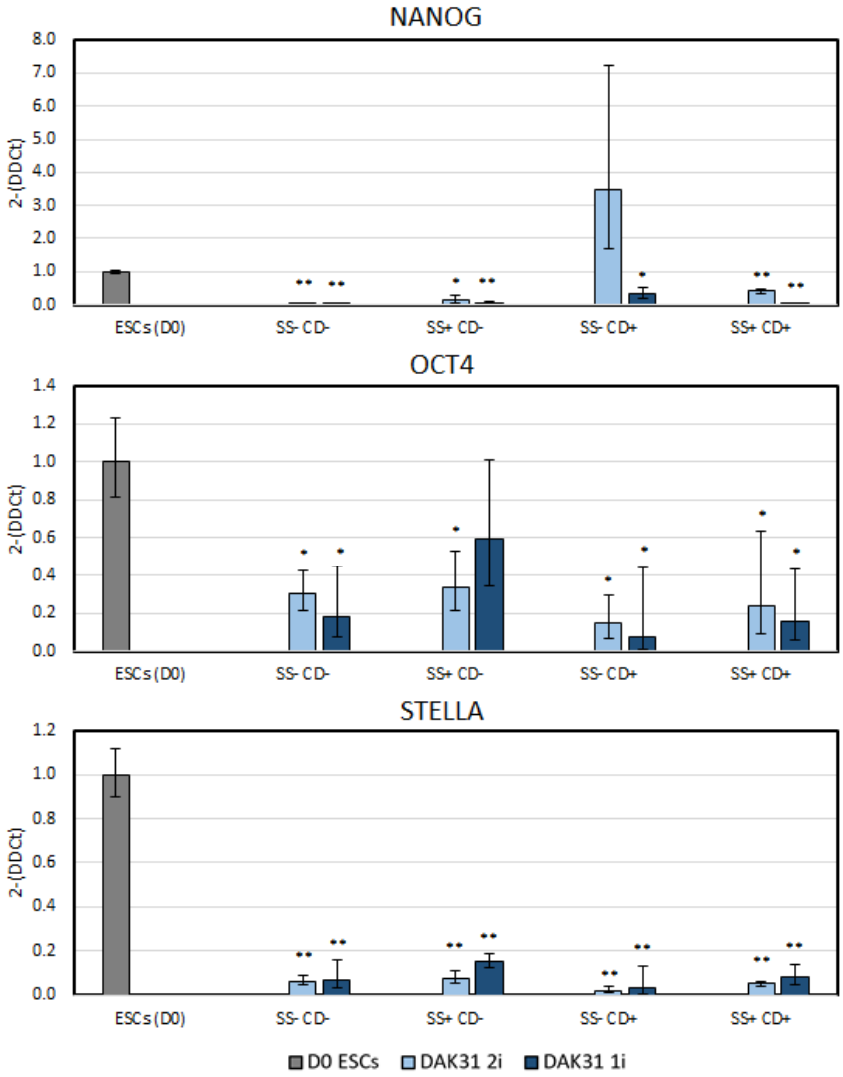

Figure 3.5.7. qRT-PCR analysis of expression of pluripotency genes in SSEA1/CD61 stained populations of rat cells subjected to a PGCLC differentiation protocol. *Rat cells which had undergone PGCLC differentiation and had been stained for SSEA-1 and CD61 were sorted by FACs into double negative, single and double positive populations. All data was normalised to the house keeping gene β-actin (dCT) and fold change was calculated by normalising gene expression to that seen in the rat ESCs (ESCs (D0)) cultured in 2i+LIF medium (2-DDCT). SS- = SSEA-1^{-ve}, CC- = CD61^{-ve}, SS+ = SSEA-1^{+ve}, CC+ = CD61^{+ve}. Bars represent mean of three independent experiments performed with DAK31 cells ± SD.*P<0.05, **P<0.01 to ESCs (D0).*

qRT-PCR data generated showed no evidence of significantly increased expression of any of the PGC markers compared to the rat ESCs (Figure 3.5.8). *Nanos3* transcript level was significantly reduced in both the SSEA-1^{-ve} / CD61^{-ve} and SSEA-1^{+ve} / CD61^{+ve} populations compared to rat ESCs (Figure 3.5.8). There was also no detectable *Nanos3* expression in SSEA-1^{-ve} / CD61^{+ve} cells pre-cultured in 2i+LIF medium (Figure 3.5.8). The remaining populations expressed lower levels of *Nanos3* transcript compared to rat ESCs (Figure 3.5.8). *Dazl* expression from SSEA-1^{-ve} / CD61^{+ve} cells pre-cultured in 2i+LIF medium was higher than that in rat ESCs (Figure 3.5.8).

Dazl transcript expression was not detected in either SSEA-1^{+ve} / CD61^{+ve} populations and was reduced in all other populations when compared to rat ESCs (Figure 3.5.8). In almost all cases, *Vasa* transcript was significantly lower than that in rat ESCs; only the population of SSEA-1^{-ve} / CD61^{+ve} cells pre-cultured in 2i+LIF medium retained a similar expression of *Vasa* to the rat ESCs (Figure 3.5.8)

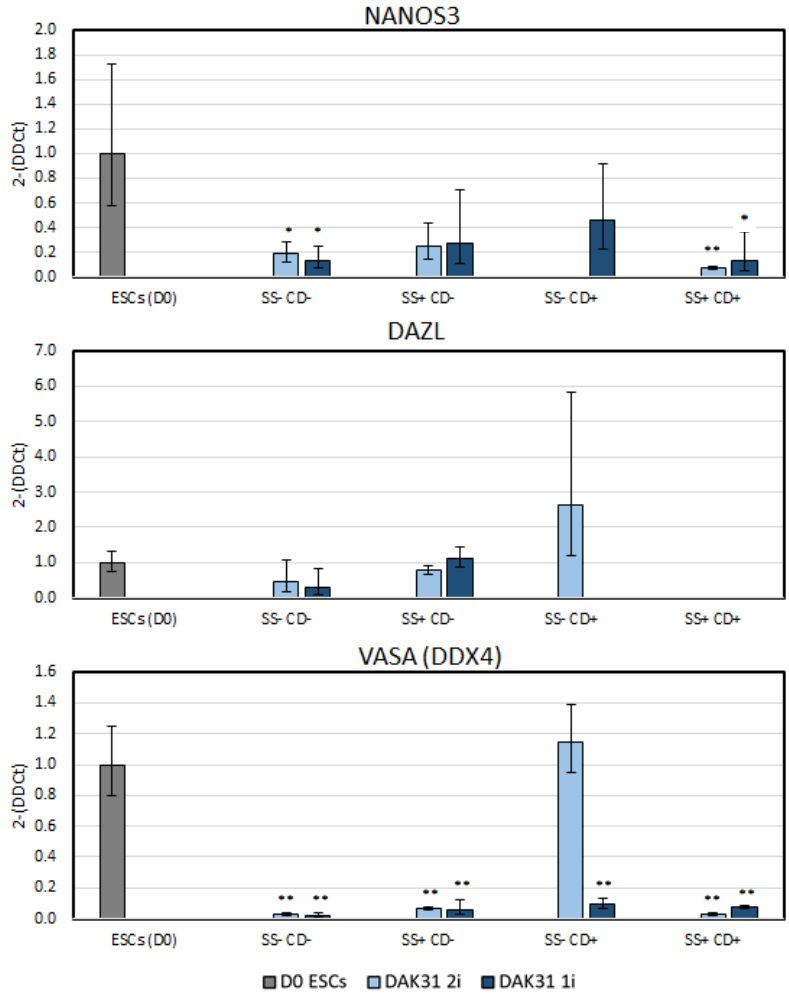

Figure 3.5.8. qRT-PCR analysis of PGC marker gene expression in SSEA1/CD61 stained populations of rat cells subjected to a PGCLC differentiation protocol. *Rat cells which had undergone PGCLC differentiation and had been stained for SSEA-1 and CD61 were sorted by FACs into double negative, single and double positive populations. All data was normalised to the house keeping gene β-actin (dCT) and fold change was calculated by normalising gene expression to that seen in the rat ESCs (ESCs (D0)) cultured in 2i+LIF medium (2-DDCT). SS- = SSEA-1^{-ve}, CC- = CD61^{-ve}, SS+ = SSEA-1^{+ve}, CC+ = CD61^{+ve}. Bars represent mean of three independent experiments performed with DAK31 cells ± SD. *P<0.05, **P<0.01 to ESCs (D0).*

Transcript expression of markers of endoderm (*Gata4*, *Gata6*) and trophectoderm (*Gata3*) were also analysed to determine whether a proportion of the differentiating cells were directed towards these lineages during the PGCLC differentiation protocol. Expression of both *Gata4* and *Gata6* was upregulated in all stained populations compared to the expression seen in rat ESCs (Figure 3.5.9).

However, there appeared to be no noticeable differences in the expression of these markers between the 2i+LIF and 1i medium pre-cultured cell pools (Figure 3.5.9). *Gata3* expression was higher in all stained populations compared to rat ESCs (Figure 3.5.9). The population of SSEA-1^{-ve} / CD61^{+ve} cells generated from pools pre-cultured in 1i medium was greater than those pre-cultured in 2i+LIF medium (Figure 3.5.9). This expression data suggested that subjecting these cells to a PGCLC differentiation protocol was directing a proportion of the cells towards endoderm and trophectoderm lineage rather than the PGCLC lineage.

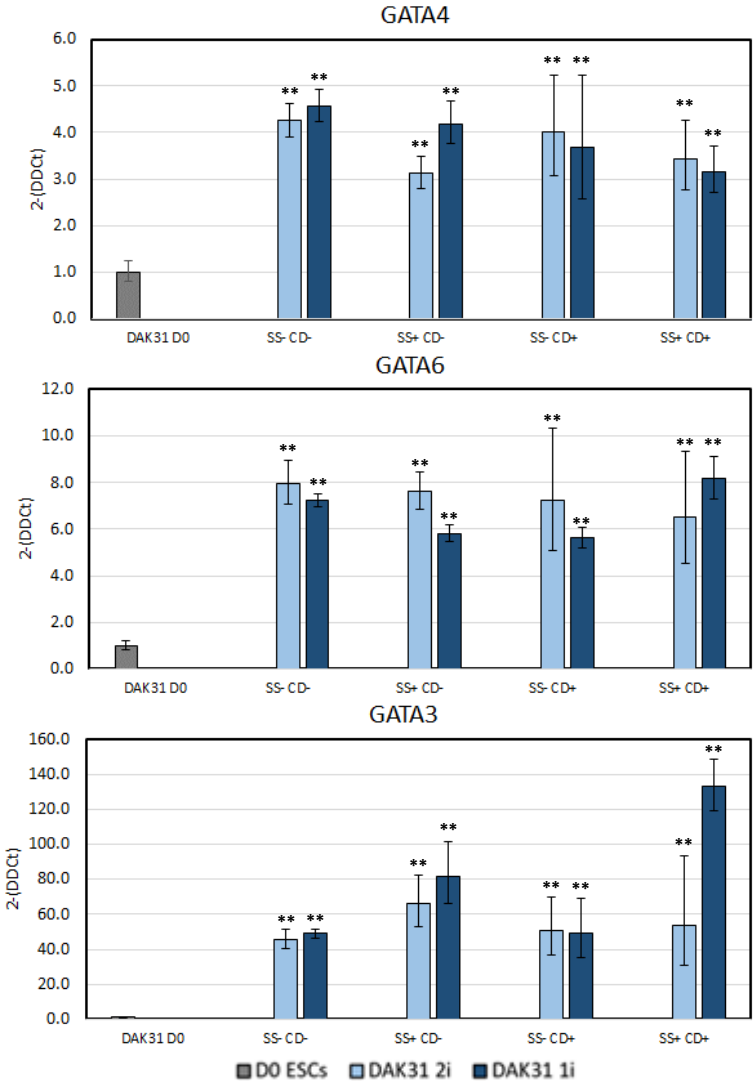

Figure 3.5.9. qRT-PCR analysis of expression of endoderm and trophectoderm markers in SSEA1/CD61 stained populations of rat cells subjected to a PGCLC differentiation protocol. *Rat cells which had undergone PGCLC differentiation and had been stained for SSEA-1 and CD61 were sorted by FACs into double negative, single and double positive populations. All data was normalised to the house keeping gene β-actin (dCT) and fold change was calculated by normalising gene expression to that seen in the rat ESCs (ESCs (D0)) cultured in 2i+LIF medium (2-DDCT). SS- = SSEA-1^{-ve}, CC- = CD61^{-ve}, SS+ = SSEA-1^{+ve}, CC+ = CD61^{+ve}. Bars represent mean of three independent experiments performed with DAK31 cells ± SD. *P<0.05, **P<0.01 to ESCs (D0).*

The data generated from rat cell pools subjected to the PGCLC differentiation protocol highlighted that in its current state, the protocol does not seem to reliably drive rat cells towards the germ cell lineage. Although mouse PGCLCs are characterised being both SSEA-1^{+ve} / CD61^{+ve} cells, this population of rat ESCs did not appear to show the upregulation of PGC transcription factors or PGC marker genes. Interestingly, the SSEA-1^{-ve} / CD61^{+ve} population of cells pre-cultured in 2i+LIF medium consistently expressed the highest levels of PGC transcription factors and gene markers, suggesting that this population of cells might harbour rat PGCLCs.

3.6 Chapter 3 discussion

Rat ESCs are demonstrably pluripotent and have been shown to have the capability of contributing to the germline in chimaeric animals (Buehr et al. 2008, Li et al. 2008). Mouse ESCs can be differentiated *in vitro* into PGCLCs, cells similar to the unipotent germ line precursor cells present within the developing epiblast embryo (Hayashi et al. 2011, Hayashi & Saitou 2013). Although variations of this differentiation protocol have been used to produce PGCLCs from other mammalian species (Wang et al. 2016, Meyenn et al. 2016), there is no published evidence of rat ESCs being successfully differentiated into PGCLCs. The aim in this chapter was to determine whether the PGCLC differentiation protocol described by Hayashi et al (2011, 2013) could direct rat ESC differentiation into the PGC lineage.

3.6.1 Mouse ESCs cultured in identical conditions as rat ESCs can be differentiated into PGCLCs using the PGCLC differentiation protocol developed by Hayashi et al

To establish the Hayashi protocol in our laboratory, we first applied it to mouse ESCs established and grown in the same conditions as our rat ESCs. Mouse PGCLCs are identified by co-expression of the surface markers SSEA-1 and CD61 (Hayashi et al. 2011, Hayashi & Saitou 2013). A distinct population of SSEA-1^{+ve}/$CD61^{+ve}$ PGCLCs was purified from our mouse cells by FACs and shown to have upregulated PGC transcription factor (*Blimp1*, *Prdm14*, *Ap2γ*) and PGC specific marker (e.g. *Nanos3*) gene expression. These results match the previously reported characteristics of mouse PGCLCs (Hayashi et al. 2011, Hayashi & Saitou 2013). The percentage of SSEA-1^{+ve}/$CD61^{+ve}$ PGCLCs generated from our mouse ESCs (~15%) was within the range shown by Hayashi et al (8-15%) (Hayashi et al. 2011, Hayashi & Saitou 2013).

These mouse cells were used as a positive control for the rat PGCLC differentiation experiments, showing that any differences between the responses of the rat and mouse ESCs were not due to the culture conditions used to derive and maintain the ESCs.

3.6.2 Rat cells subjected to the EpiLC differentiation protocol had low expression of epiblast markers compared to mouse ESCs

Direct application of the Hayashi protocol to rat ESCs was not successful, suggesting that the protocol could not be simply translated from mouse to rat ESCs without additional modification. During the EpiLC stage of the differentiation protocol, two key differences between the responses of the mouse and rat ESCs were observed. Firstly, rat ESCs were unable to attach to fibronectin layers. Fibronectin is the substratum used to induce EpiLC differentiation of mouse cells prior to PGCLC differentiation (Hayashi et al. 2011, Hayashi & Saitou 2013). Attachment to fibronectin requires the integrin receptor α5β1 on the cell surface (Wu et al. 1993, Zhang et al. 1993). However, both α5 and β1 integrins are expressed at low levels in rat ESCs (Li et al. 2008, Yaoyao et al. 2017), providing an explanation why rat cells would not attach to fibronectin coated wells. Laminin and MEF layers were used as alternative basement substratum to facilitate attachment of rat cells, as both have been shown previously to support rat ESC growth (Buehr et al. 2008, Li et al. 2008). Rat cells cultured on MEF layers in EpiLC medium showed the greatest transcript expression of the Epiblast marker *Fgf5* compared to cells cultured on laminin or in suspended aggregates. This result suggested that not only was attachment of the cells important for driving Epiblast marker expression, attachment of rat ESCs to MEFs was the most suitable condition of the three to assist directed differentiation towards the Epiblast-like state.

The second difference between mouse and rat cells was that the expression of markers associated with EpiLC differentiation (e.g. *Tcf15* and *Otx2*) were not induced in rat cells after being cultured in EpiLC medium. TCF15 is important for early epiblast differentiation in mice, inhibiting *Nanog* and driving *Otx2* expression as cells transition out of the naïve state (Davies et al. 2013). It is also reported that active *Tcf15* expression assists in the repression of endoderm markers during cell differentiation (Davies et al. 2013). Therefore, the lack of *Tcf15* expression in rat ESCs could have allowed a greater proportion of cells to differentiate towards the endoderm lineage rather than becoming EpiLCs. The role of the OTX2 transcription factor during EpiLC differentiation is to redirect OCT4 binding to genomic regulatory elements of Epiblast-related genes and driving the cells out of the naïve state (Yang et al. 2014, Buecker et al. 2014).

Further analysis of the basal expression of *Otx2* in our rat ESCs showed there was a substantially reduced expression of *Otx2* in rat ESCs compared to the mouse cells. This low initial expression of *Otx2* in rat ESCs could have negatively impacted the capacity of rat cells to differentiate into EpiLCs or indicate that the rat ESCs were not in the same initial pluripotency state as the mouse ESCs. Previous studies have shown that increasing Wnt-signalling in mouse cells by the addition of high concentrations of CHIR99021 to the culture medium can reduce the expression of *Otx2* transcript (Zhang et al. 2018). Increased β-catenin activity has been identified in rat ESCs compared to the mouse during standard 2i+LIF culture conditions (Meek et al. 2013), therefore, the low basal expression of *Otx2* in rat ESCs may have been due to increased Wnt-signalling within rat ESCs compared to the mouse. Rat ESCs cultured in medium lacking the Wnt-signalling inhibitor CHIR99021 and LIF (1i medium) had increased *Otx2* gene expression compared to cells cultured in 2i+LIF medium. When subjected to EpiLC differentiation medium, cells pre-cultured in 1i medium had no substantial difference in *Tcf15* expression compared to 2i+LIF pre-cultured cells. However, elevated *Fgf5* expression was detected in cells which had been pre-cultured in 1i medium compared to 2i+LIF medium. This result suggested that this pre-culture condition may have improved the differentiation of rat ESCs towards the epiblast fate.

Overall, the low expression of *Tcf15* and *Otx2* during the EpiLC differentiation protocol made it difficult to confirm if rat ESC differentiation was being directed towards the EpiLC fate. Exploring the expression of other factors used in the identification of EpiLCs in other mammalian species (e.g. *Rab15* in porcine IPSCs (Wang et al. 2016)) or the markers present in the *in vivo* rat epiblast during embryogenesis may help identify the presence of rat EpiLCs in future investigations. Additionally, female mouse EpiLCs lack H3K27me3 enrichment (Hayashi et al. 2012) and are reported to have a similar epigenetic status to mouse ESCs (Takahashi et al. 2018), suggesting that epigenetic profiling could potentially be used in future investigations to distinguish the presence of rat EpiLCs from a pool of differentiated cells.

3.6.3 CD61^{+ve} rat cells have increased PGC marker expression after being subjected to the PGCLC differentiation protocol

The surface markers SSEA-1 and CD61 have been used to identify mouse PGCLCs from differentiated ESC cultures (Hayashi et al. 2011, Hayashi & Saitou 2013). However, immunohistochemistry staining of the genital ridges of rat embryos (E13 - E19 dpc) showed that rat PGCs do not express SSEA-1 on their surface, unlike the PGCs within the genital ridges of mice (Encinas et al. 2012). Therefore SSEA-1 was used in this investigation to monitor the loss of undifferentiated stem cells during the differentiation protocol rather than as a marker of rat PGCLCs. As expression of *Cd61* was present in tissue harvested from the genital ridge of rat embryos, it was assumed that the population of cells expressing CD61 on their cell surface could also harbour PGCLCs generated during the differentiation protocol. PGC markers were detected in CD61^{+ve} rat cells, although the level of expression was lower than that generated from mouse cells.

Rat cells subjected to the PGCLC differentiation protocol had increased expression of the endoderm marker *Gata6* and trophectoderm marker *Gata3*. In mice, expression of these markers was elevated in all cells except the distinct SSEA1^{+ve}/CD61^{+ve} population of PGCLCs. This suggests that rat PGCLCs generated during the differentiation protocol were not isolated from the heterogeneous differentiated population of cells and remained a small sub-population within the CD61^{+ve} population. This would explain why PGC marker expression was lower than that generated by the mouse. However, this result could also be due to inefficient PGCLC differentiation of the rat cells. *Tcf15* expression is reported to represses endoderm marker expression (Davies et al. 2013), while the primitive endoderm of the developing mouse embryo has been shown to lack OTX2 protein (Boroviak et al. 2018). Additionally, rat cells harvested from the epiblast and cultured *in vitro* have been shown to have more evidence of endoderm differentiation than their mouse counterparts (Nichols et al. 1998), suggesting rat cells may be more primed for differentiation into certain lineages than mouse cells. Therefore, the absence of *Otx2* and *Tcf15* induction in cells already pre-primed for differentiation may have driven rat cell differentiation towards other lineages such as endoderm instead of the PGCLC fate.

Rat cells pre-cultured in 2i+LIF medium had increased PGC marker expression compared to cells pre-cultured in 1i medium, showing that culturing rats cells in 1i medium prior to the differentiation protocol did not improve the proportion of cells which differentiated into the germ cell lineage.

A recent study in mouse ESCs showed that the loss of *Otx2* expression prior to differentiation produced a greater number of PGCLCs (Zhang et al. 2018).

As the expression of *Otx2* was raised in rat ESCs pre-cultured in 1i medium, could the loss of *Otx2* expression have a similar impact on PGCLC determination in rat cells? The data generated suggests that the *in vitro* differentiation protocol described by Hayashi et al (2011, 2013) is not suitable for driving rat PGCLC differentiation. As it is possible for rat ESCs to be engrafted into chimeras with variable success (Buehr et al. 2008, Li et al. 2008), the inefficiency of generating rat PGCLCs is likely due to the culture conditions not being appropriate for driving germ cell differentiation of rat ESCs. Therefore, could PGCLC differentiation of rat ESCs be improved by manipulating the epiblast gene network of rat ESCs during the differentiation protocol? As the expression of the *Blimp1* transcription factor within rat ESCs is low, it was of interest to explore whether increasing its expression could direct a greater proportion of rat ESCs towards the germ cell lineage during differentiation.

Chapter 4 Directing differentiation by 'rewiring' the expression of *Blimp1* via the *Brachyury* promotor

4.1 Introduction

The PGCLC differentiation protocol described by Hayashi et al did not efficiently induce PGCLC formation in rat ESCs. However, overexpression of PGC transcription factors within mouse epiblast-like cells can promote adoption of the PGCLC fate (Nakaki et al. 2013). This chapter details an alternative experimental approach to 'hijack' or 'rewire' the epiblast transcriptional programme to place an exogenous copy of a PGC transcription factor (TF) under the control of an epiblast promoter. It is hypothesised that activation of the epiblast promotor during cellular differentiation will drive the expression of the PGC TF, increasing the efficiency of epiblast cells entering the germ cell lineage when subjected to the PGCLC differentiation protocol.

The BRACHYURY (T) transcription factor is primarily expressed in the late epiblast stage, within the proximal region of the embryo and within the primitive streak, the regions with the highest expression of WNT3 (Rivera-Pérez & Magnuson 2005). The *Brachyury* gene is a downstream target of the WNT signalling cascade, and is activated as ESCs transition out of the naïve state and differentiate towards the more primed epiblast fate (Aramaki et al. 2013, Günesdogan et al. 2014). It is involved in the formation of the mesoderm during embryogenesis and the differentiation of epiblast cells into the somatic lineage (Rivera-Pérez & Magnuson 2005). BRACHYURY has also been reported to interact with the regulatory regions of *Blimp1* and *Prdm14* genes (Aramaki et al. 2013). The association of BRACHYURY with these regulatory regions is thought to enhance the expression of PGC transcription factors as PGC precursor cells migrate towards the embryonic genital ridges (Aramaki et al. 2013). As BRACHYURY is linked with both the differentiation of epiblast cells (Rivera-Pérez & Magnuson 2005) and PGC specification (Aramaki et al. 2013), the *Brachyury* promotor was deemed a suitable candidate for driving the expression of exogenous PGC TFs in the posterior epiblast.

BLIMP1 is the first of the three PGC TFs to be active during PGC specification in the post implantation embryo (~E6.25 in the mouse) and is essential for early PGC specification, ensuring that the default somatic pathway is silenced so that the epiblast cells within the proximal region of the embryo are directed towards the germ cell lineage (Ohinata et al. 2005, Dudley et al. 2007, Fog et al. 2012, Günesdogan et al. 2014).

The aim was to use homologous recombination to insert a cDNA copy of the BLIMP1 transcription factor downstream of the *Brachyury* promotor. To accomplish this targeted insertion, a CRISPR/Cas9 gene editing strategy would be implemented to improve the recombination frequency and promote efficient recovery of correctly targeted clones. The intended outcome was to generate rat ESC clones containing a heterozygous insertion of exogenous *Blimp1* cDNA within the *Brachyury* locus so as not to completely disrupt the expression of *Brachyury*.

4.2 Gene-editing strategy for editing the *Brachyury* locus

4.2.1 CRISPR/Cas9 gene editing overview

Clustered Regularly Interspaced Short Palindromic Repeats (CRISPR)/CAS9 gene editing is a gene targeting technique with two primary components, a CRISPR-associated endonuclease (Cas nuclease) and guide RNA (gRNA or sgRNA) (Cong et al. 2013, Mali et al. 2013). The gRNA acts as a scaffold for the Cas nuclease, guiding it to the specified region of the genome (Cong et al. 2013, Mali et al. 2013). If this targeted region is directly followed by a protospacer-adjacent motif (PAM), the Cas nuclease cleaves the DNA by inducing a double strand break (DSB) (Cong et al. 2013, Mali et al. 2013). DNA repair mechanisms such as non-homologous end joining (NHEJ) or homology directed repair (HDR) can then promote the re-joining of the cut strands (Cong et al. 2013, Mali et al. 2013, Hsu et al. 2014). A template sequence/vector with homology to either side of the DSB is co-transfected with Cas nuclease and gRNA, acting as a template for HDR repair and introducing genetic modifications into the targeted region of the genome (Cong et al. 2013, Mali et al. 2013, Hsu et al. 2014).

4.2.2 CRISPR/Cas9 strategy to be implemented

To place a rat *Blimp1* transgene under the control of the *Brachyury* promotor, a CRISPR/Cas9 nuclease strategy was designed to target the ATG start codon of the *Brachyury* gene. Targeted cleavage at the ATG site would assist homologous recombination of the *Blimp1* cDNA into the region downstream of the *Brachyury* promotor (Figure 4.2.1).

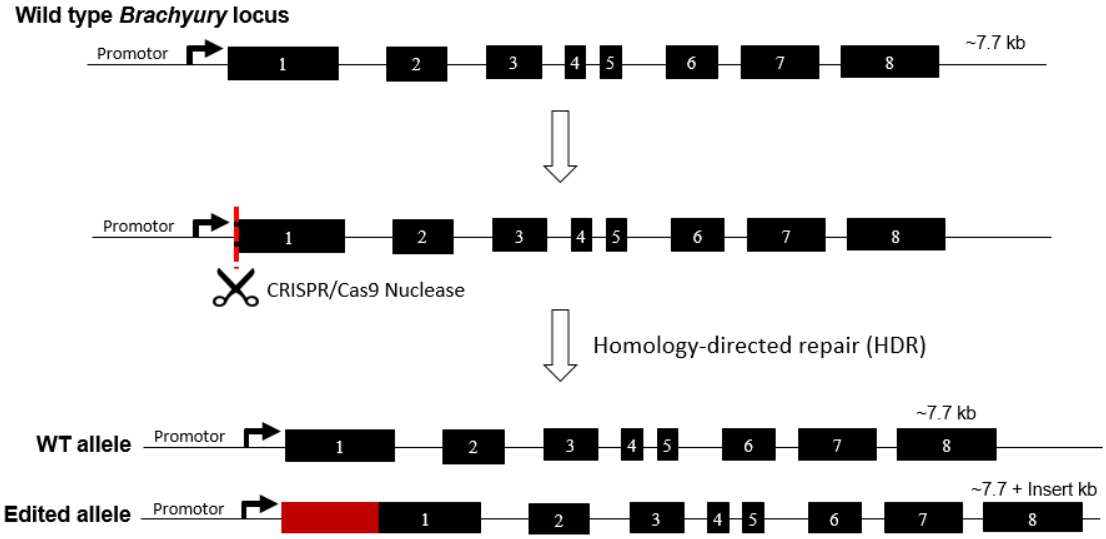

Figure 4.2.1. Strategy for 'hijacking' the Brachyury promotor. *CRISPR gRNA was designed so Cas9 nuclease was recruited downstream of the Brachyury promotor. A HDR template containing a rat Blimp1 transgene with homology arms spanning either side of the cut region was co-transfected with the Cas9 nuclease and gRNA to assist incorporation of the Blimp1 transgene via HDR repair. Heterozygous clones containing a WT allele, and an edited Brachyury allele containing the BLIMP1 cDNA (red box) would be identified and used for further investigation.*

Using the CRISPR Design tool produced by the Zhang Lab (crispr.mit.edu), two gRNA sequences with PAM sites within 30 base pairs of the *Brachyury* ATG start codon were identified and chosen to target the Cas9 nuclease to the ATG site of *Brachyury* locus (

Figure 4.2.2).

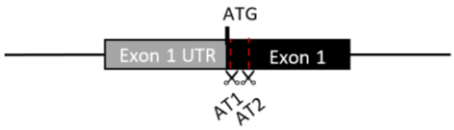

gRNA Name	Sequence (-PAM, 20bp + G)	PAM	DSB location (After ATG site, bp)
AT1	**(G) TGGCGGGAGGATGAGCTCCC**	**CGG**	**10**
AT2	**(G) CCCTGCGCTCTCTGTGCCCG**	**GGG**	**27**

Figure 4.2.2. gRNA sequences designed to target ATG initiation codon within exon 1 of the Brachyury locus. *Both AT1 and AT2 gRNAs targeted regions within 30bps of the ATG site and inside*

exon 1 of Brachyury. Each gRNA sequence was 21 base pairs long, with 20 base pairs of homology before the PAM sequence. A 'G' was added to the 5' end of each gRNA sequence to ensure efficient expression of the gRNA from the U6 promotor of the PX458 vector.

4.3 Generation of Cas9 nuclease vectors designed to target the *Brachyury* locus

4.3.1 Insertion of gRNA sequences into PX458 Cas9 nuclease

The Cas9 nuclease used during this investigation was a human codon optimised *S. pyogenes Cas9 (*SpCas9) nuclease expressed from the PX458 Cas9 mCherry vector (Figure 4.3.1), provided by the Hohenstein group (Roslin Institute).

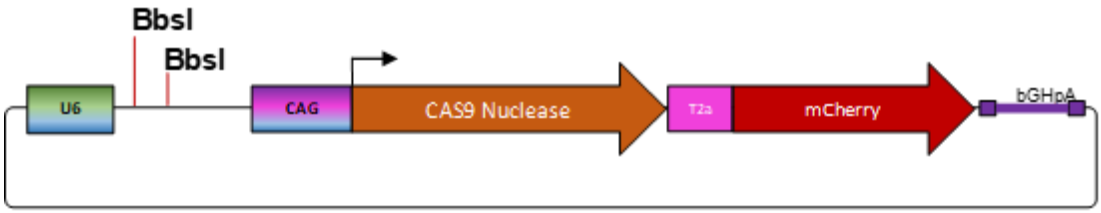

Figure 4.3.1. Px458 mCherry CRISPR vector. *A CAG enhancer/promoter (CAG) drove the expression of a CRISPR/Cas9 nuclease (CAS9 Nuclease), which was coupled to a 2A peptide (T2A) and mCherry fluorescent protein (mCherry). Upstream of this cassette was a Human U6 promotor (U6) which drove the expression of the chimaeric gRNA scaffold. gRNA sequences were introduced into the plasmid by linearization of the vector via BbsI digestion (BbsI) and ligation of an oligonucleotide containing the gRNA sequence. The vector co-expressed both the Cas9 nuclease and gRNAs required to target Cas9 nuclease DSBs.*

The PX458 vector was designed to co-express Cas9 nuclease and mCherry fluorescent protein. A gRNA sequence was inserted into the same vector downstream of a human U6 promotor via restriction digest and ligation. Once inserted the PX458 vector was capable of driving the expression of the gRNA sequence in addition to the nuclease and mCherry protein. Insertion of the gRNA sequences was performed as presented in Figure 4.3.2. Two complementary strands of oligonucleotides matching the sense and anti-sense sequences of each gRNA were synthesised. The sense strand was designed to have a 5'-CACC overhang, while the anti-sense strand a 5'-CAAA overhang. Sense and anti-sense sequences were annealed together overnight to form double-stranded gRNA sequences. Insertion of these gRNA sequences was performed by linearization of the PX458 vector by BbsI restriction digest, followed by incubation of linearised vector and gRNA with T4 ligase.

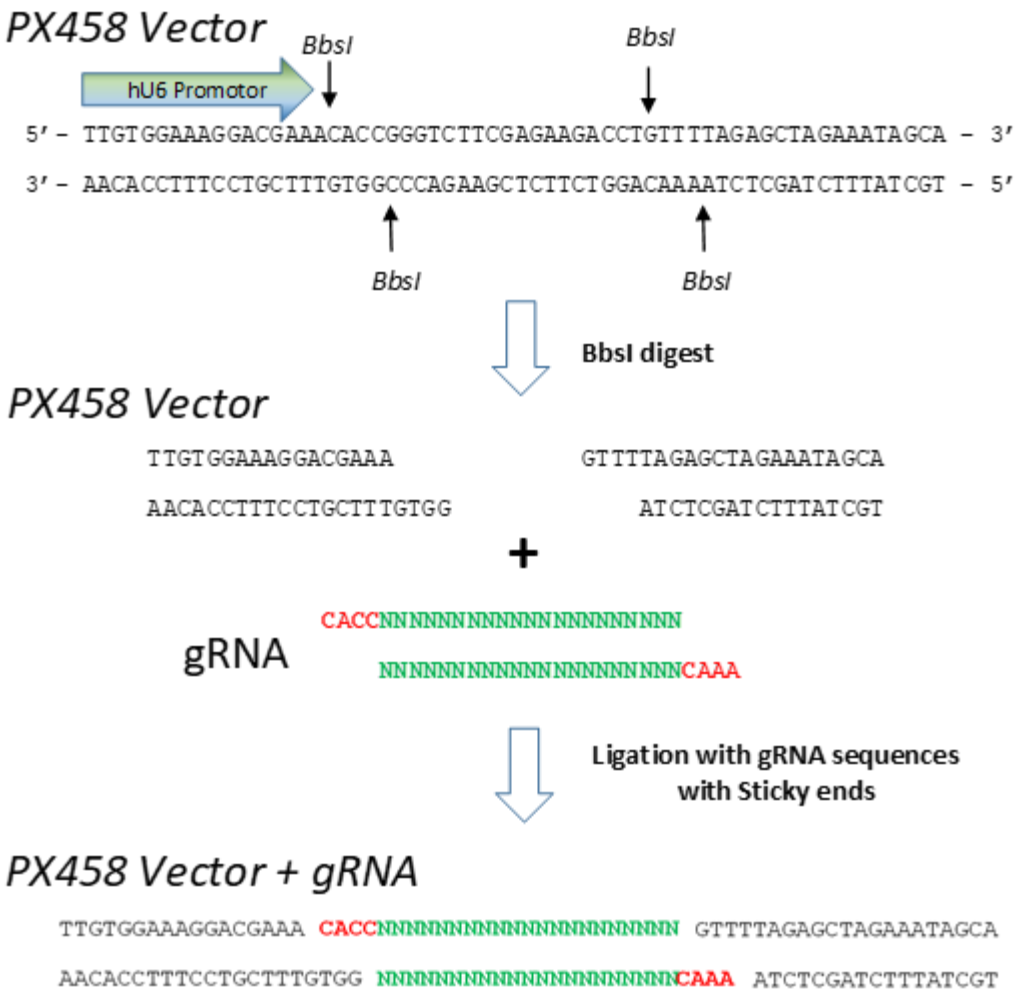

Figure 4.3.2. Strategy for insertion of gRNA into PX458 vector. *The PX458 mCherry CRISPR vector was linearized with BbsI, producing overhangs or "sticky ends" which would not ligate back together. The oligonucleotides strands (encoding for the gRNA) with matching 5' overhangs were introduced and ligated to form a circular vector (PX458 vector) containing Cas9 nuclease, mCherry and gRNA.*

4.3.2 CRISPR/Cas9 nuclease induced cutting of the *Brachyury* locus

Due to the variability in NHEJ and the formation of indels during CRISPR/Cas9 gene editing, it can be difficult to visualise and assess the efficiency of the Cas9 nuclease induced DSB at the target region. Sanger sequencing can be used to determine whether indels have occurred at the target region after CRISPR/Cas9 gene editing. However, it would be time consuming and expensive to use this to report on the efficiency of Cas9 nuclease induced cutting at the target region. To monitor the generation of CRISPR/Cas9 induced DSB at the ATG site of *Brachyury*, another set of Cas9 nuclease vectors were designed to induce DSBs in the intronic sequence downstream of the exon 1 of *Brachyury*.

When the gRNA sequences successfully target Cas9 nuclease to the correct regions, co-transfection of AT1 or AT2 with any of the intron targeting PX458 vectors (IN1, IN2, IN3) should generate a deletion. This deletion can be detected by PCR amplification of the genomic DNA of transfected cells. A small band represented cells which had been cleaved at both genomic target sites (Figure 4.3.3). Efficiency of Cas9 nuclease cutting was estimated by the relative intensity of the PCR bands generated by each combination of AT or IN vectors.

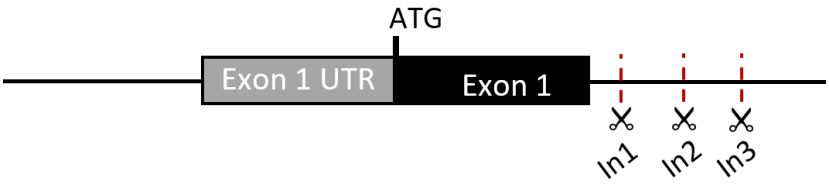

gRNA Name	Sequence (-PAM, 20bp + G)	PAM	DSB location (After ATG site, bp)
IN1	**(G) CGTGCGGCAAGCCGGCAGTC**	**TGG**	**233**
IN2	**(G) AAACTTTCCCTGACGAAACC**	**TGG**	**272**
IN3	**(G) CTCTGAGTTAACAGCCCCCA**	**GGG**	**326**

Figure 4.3.3. gRNAs designed to target genomic regions downstream of exon 1 of the rat Brachyury sequence. *Three gRNAs were designed to target varying regions downstream of exon 1 of Brachyury. Each gRNA sequence was 21 base pairs long, with 20 base pairs of homology before the PAM sequence. A 'G' was added to the 5' end of each gRNA sequence to ensure efficient expression of the gRNA from the U6 promotor of the PX458 vector.*

The parental rat DAK31 ESC line was co-transfected with different combinations of AT PX458 vector and IN PX458 vector. DAK31 ESCs were chosen as they contained no fluorescent marker which could interfere with mCherry immunofluorescence screening of the transfected cell pools. Successful transfection was determined by the presence of mCherry expression from the PX458 vectors 24 hours post transfection (Figure 4.3.4).

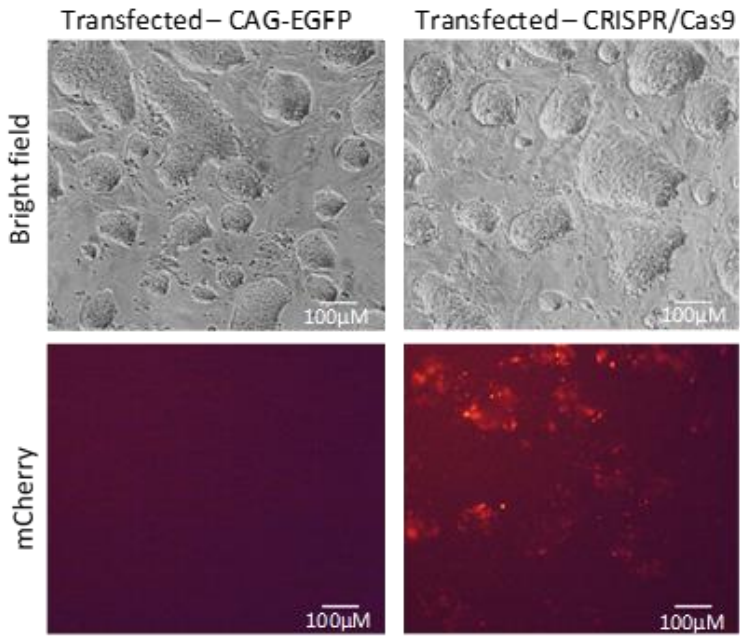

Figure 4.3.4. PX458 vector transfection of rat DAK31 cell pools. *Rat DAK31 ESCs were transfected with either a vector containing CAG-EGFP or the PX458-mCherry Cas9 nuclease vector. After 24 hours, mCherry expression was observed from PX458 vector transfected cells, but not from CAG-EGFP transfected cells.*

Genomic DNA (gDNA) was isolated 48 hours post transfection and used as a template for PCR amplification of the *Brachyury* locus. Oligonucleotides were designed to bind to regions ~300bp upstream and ~500bp downstream of the *Brachyury* ATG site, producing a wild type PCR band of ~800bp (Figure 4.3.5A). Gel electrophoresis was performed to confirm the presence of Cas9 nuclease induced cutting within the locus (Figure 4.3.5B). Every combination of AT-PX458 and IN-PX458 vector showed evidence of a faint band matching the size of a DSB-mediated deletion within the *Brachyury* gene (~445-590bp) and an intense wild type band (~800bp). DAK31 cells transfected with AT1-PX458 had more intense edited (MUT) PCR bands compared to those pools transfected with the AT2-PX458 vector (Figure 4.3.5B). Therefore, it was decided that the AT1-PX458 vector would be used for the insertion of exogenous *Blimp1* cDNA downstream of the *Brachyury* gene.

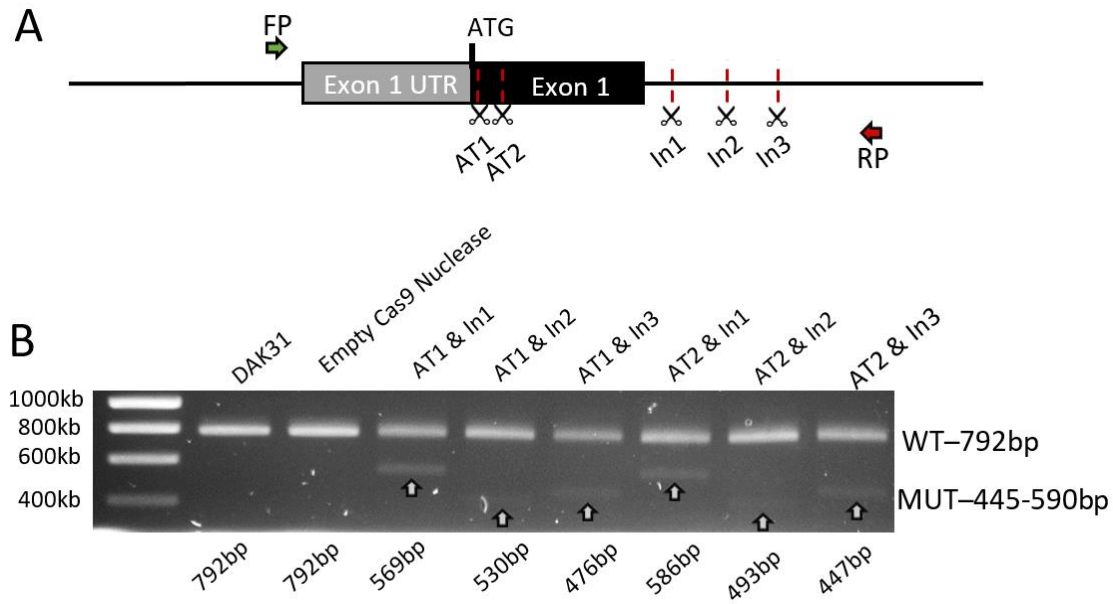

Figure 4.3.5. Screening for successful deletion within genomic DNA from the Brachyury locus of rat ESCs transfected with CRISPR/Cas9 PX458 vectors. *(A) Schematic showing target sites of gRNA and the binding locations of the PCR oligonucleotides on the Brachyury locus. (B) Agarose electrophoresis gel showing amplified PCR bands from CRISPR/Cas9 transfected cells. PCR fragments from un-transfected DAK31 ESCs and cells transfected with PX458 vector containing no gRNA sequence (Empty) were used as negative controls.*

4.4 Generation of rat ESC clones expressing BLIMP1 from the endogenous *Brachyury* promotor

4.4.1 Generating the HDR template for CRISPR Cas9-mediated insertion of Blimp1 cDNA

To enable precise insertion of the *Blimp1* cDNA downstream of the rat *Brachyury* promoter, a vector was constructed with homology arms spanning either side of the DSB induced by the AT1-PX458 vector within the *Brachyury* locus. A 2.1kb region of the rat *Brachyury* gene spanning ~1kb either side of the *Brachyury* start codon was PCR amplified from genomic DNA isolated from rat ESCs (Figure 4.4.1A). The amplified region was cloned into a TA cloning vector (Figure 4.4.1A) and sequence verified. Inverse PCR amplification of the resulting TA vector was performed to produce a linearised vector which did not have the *Brachyury* ATG start site or the AT1-PX458 Cas9 nuclease cut site (Figure 4.4.1B). This ensured that the Cas9 nuclease was not targeted to the HDR template vector when co-transfected into the rat ESCs, which would have disrupted the vector by inducing a DSB and reduced the efficiency of *Blimp1* cDNA insertion. The linearised vector was purified using a gel electrophoresis purification kit to remove any residue TA vector.

A BLIMP1-2a-mCherry cassette was generated by PCR amplification from a Tet-On piggyBac transposon vector containing a *Blimp1* cDNA and mCherry fluorescent protein expression cassette (see Chapter 5 for further details). Inclusion of the mCherry fluorescent marker was considered beneficial as activation of exogenous gene expression from the *Brachyury* locus could then be monitored and analysed by immunofluorescence imaging and flow cytometry. The exogenous rat *Blimp1* cDNA was previously synthesised to match the sequence displayed on the Ensembl database (ENSRNOT00000076541.1). Homology to the linearised 2.1kb TA-*Brachyury* vector was introduced during PCR amplification of the BLIMP1-2a-mCherry cassette (Figure 4.4.1B). Gibson cloning was performed to incorporate the BLIMP1-2a-mCherry sequence into the linearised TA vector containing the *Brachyury* homology arms. The resulting vector, referred to as the HDR template vector, was sequenced to verify that the BLIMP1-2a-mCherry had been inserted correctly into the HDR template vector.

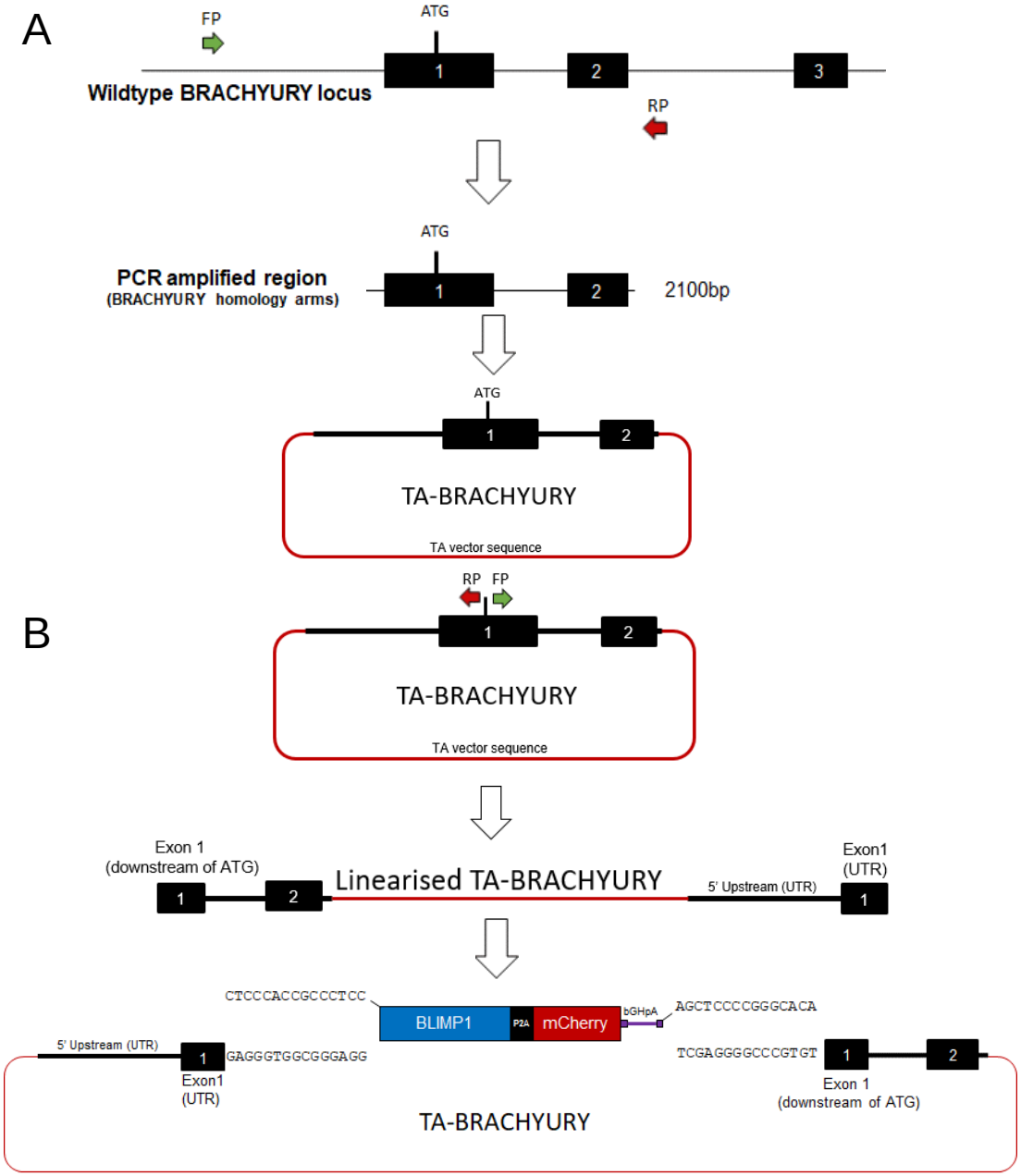

Figure 4.4.1 Generation of BRACHYURY-BLIMP1 HDR template vector. *(A) Genomic DNA from rat DAK31 ESCs was PCR amplified to produce a 2100bp fragment spanning Brachyury exon 1. This fragment was inserted into a TA cloning vector following the manufacturers cloning protocol. (B) Inverse PCR was used to amplify TA-vector containing the Brachyury homology arms. Oligonucleotides were designed so the reverse primer would bind upstream of the ATG start codon, while the forward primer bound approximately 40bp downstream of ATG start codon. PCR amplification of BLIMP1-2a-mCherry cassette was performed to introduce 15bp homology arms to both the 5' and 3' ends of cassette. Homology arms were designed to match linearised ends of previously generated TA Brachyury homology arm vector. Gibson cloning annealed the two fragments together to generate a HDR template vector with homology arms to the Brachyury gene either side of a BLIMP1-2a-mCherry cassette.*

4.4.2 CRISPR-Cas9 nuclease-induced gene editing of rat ESCs

The aim was to generate rat ESC clones which were heterozygous for BLIMP1-2a-mCherry insertion into the *Brachyury* locus, and also retained a functional *Brachyury* WT allele (Figure 4.4.2).

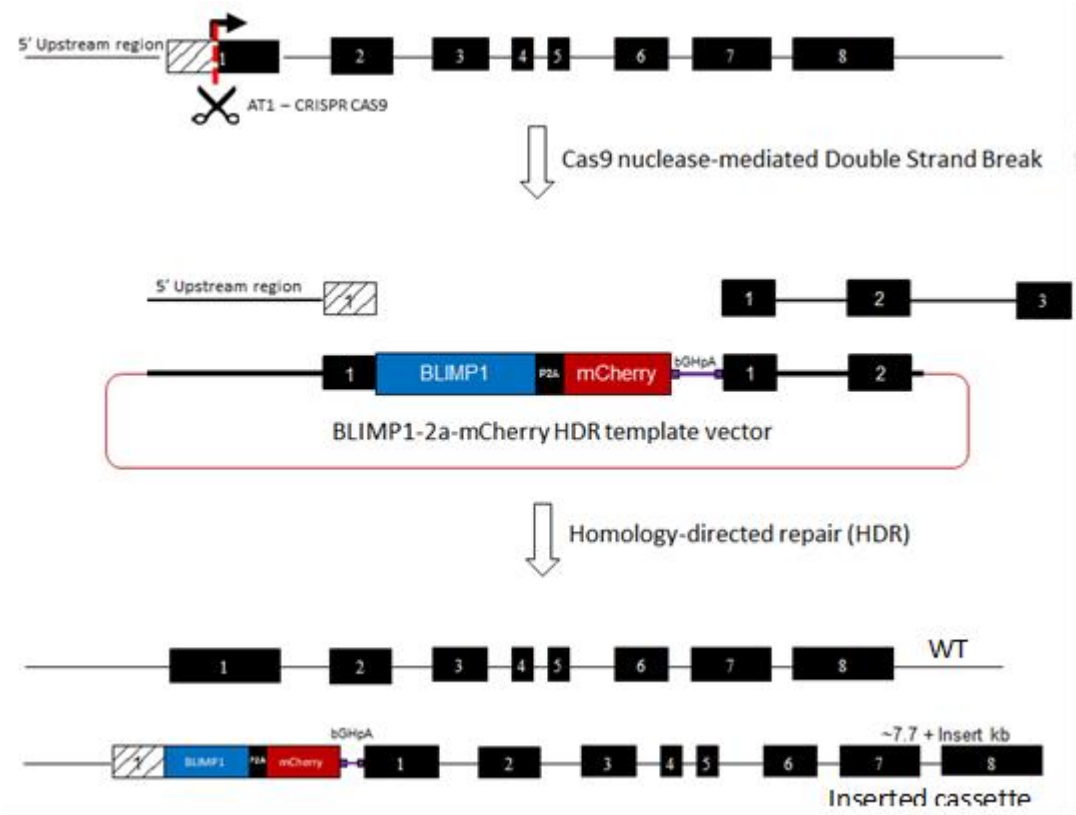

Figure 4.4.2. Schematic showing the insertion of BLIMP1-2a-mCherry sequence into the BRACHYURY locus via Homology directed repair. *The AT1 PX458 vector was designed to express both the Cas9 nuclease enzyme and the gRNA which targeted the Cas9 nuclease to the ATG region of the Brachyury locus. When co-transfected with the HDR template vector (Figure 4.4.1), the BLIMP1-2a-mCherry cassette was incorporated into the cut region by homology-directed repair.*

DAK31 ESCs were co-transfected with the AT1-PX458 Cas9 nuclease vector (

Figure 4.2.2) and the BLIMP1-2a-mCherry HDR template vector (Figure 4.4.1). 48 hours post transfection, ~300 mCherry positive ESCs from the transfected cell pool were single cell sorted into the wells of four 96 well plates. The gating strategy detailed in section 2.6.7 was used. The remaining cells were gated to isolate populations of mCherry^{+ve} cells by plotting mCherry (610/20A) versus side scatter area (SSC-A). The gates were set against untransfected rat ESCs. The flow cytometry plots generated during the FACs of these mCherry positive populations are shown in Figure 4.4.3. These single cells were cultured in 2i+LIF medium and allowed to recover for 7 days.

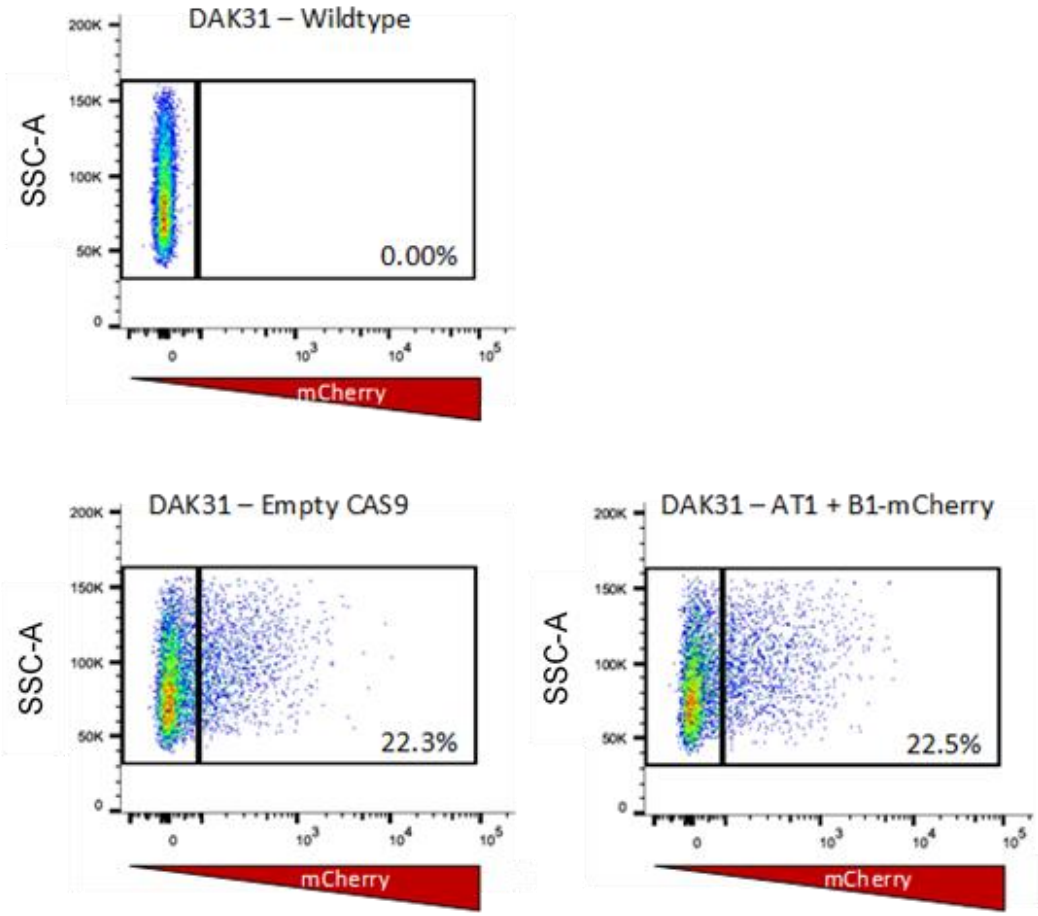

Figure 4.4.3. Flow cytometry plots of PX458 transfected cells. *Cells transfected with the PX458 vector were separated into mCherry positive and negative populations. The percentages shown indicate the proportion of mCherry positive cells within the transfected cell pools.*

Of these sorted mCherry positive cells, 100 single cell clones survived the single cell plating procedure and generated large enough colonies to propagate further. After a further 2 weeks, 20 clones were passaged further from 24-well plates. Aliquots of the 20 clones were frozen and screened for insertion of the BLIMP1-2a-mCherry sequence by PCR amplification using purified genomic DNA. The PCR oligonucleotides were designed so they would bind outside of the homology arms contained in the HDR template to ensure the amplified regions were from the rat genome and not derived from HDR template vector. If insertion of the BLIMP1-2a-mCherry cassette was successful, a PCR band of ~7.2kb would be generated. A visual representation of the PCR screen and the resulting PCR amplified bands from 3 of the analysed clones is shown in Figure 4.4.4.

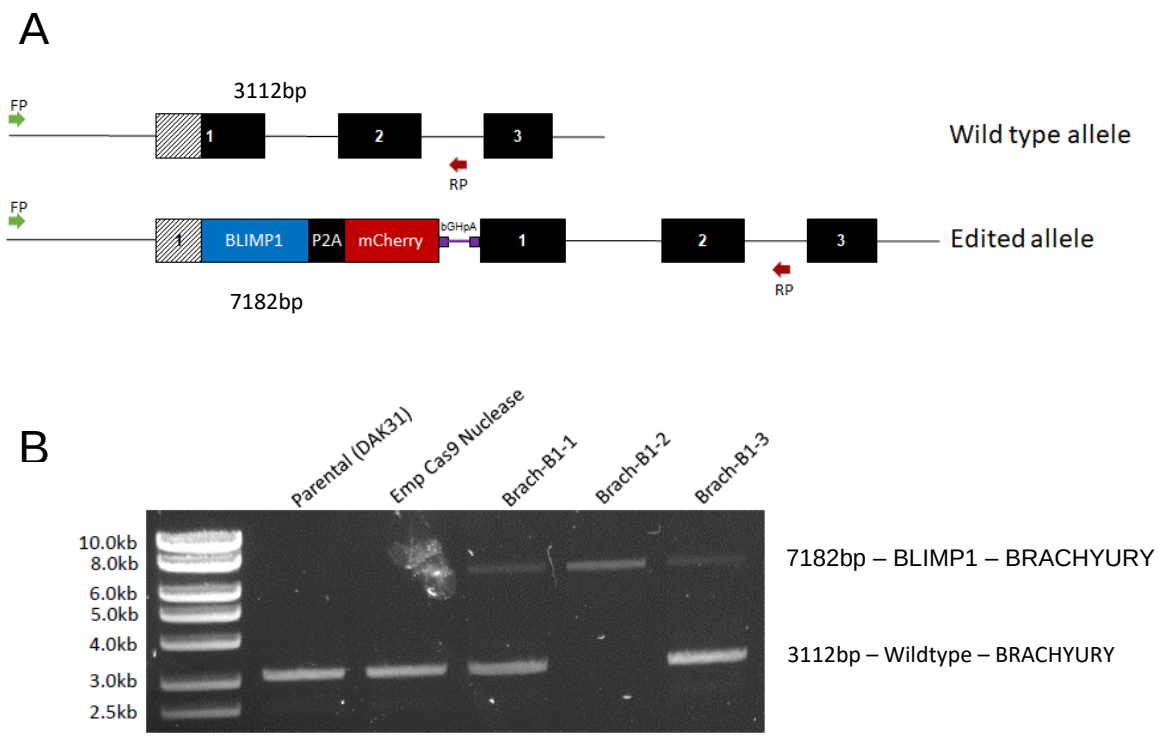

Figure 4.4.4. PCR screen for the insertion of the Blimp1-2a-mCherry cassette. *(A) Schematic showing the binding sites of the screening oligonucleotides on both the WT and edited Brachyury alleles. (B) Gel electrophoresis of PCR amplified regions from 3 transfected cell line clones (Brach-B1-1, 2 & 3). Insertion of BLIMP1-2a-mCherry increased the size of the PCR band by ~4070bps. Pools of the parental cell line (Parental (DAK31)) and cells transfected with a PX458 vector without a gRNA sequence (Emp Cas9 Nuclease) were used as PCR controls.*

Of the 20 clones screened by PCR, 8 generated an amplified band which matched the expected size if the BLIMP1-2a-mCherry cassette had been successfully inserted downstream of the *Brachyury* promotor. Of these 8 clones, 5 retained a wildtype sized amplicon as well as and the edited *Brachyury* allele.

A secondary PCR screen was used to confirm insertion of the BLIMP1-2a-mCherry cassette in the *Brachyury* locus. The 8 clones were screened with oligonucleotides designed to bind outside of the *Brachyury* homology arm and within the BLIMP1-2a-mCherry cassette. PCR bands are only amplifiable if the BLIMP1-2a-mCherry cassette was present within the *Brachyury* locus. All remaining clones had an amplified band with both PCR oligonucleotide sets, while the parental and cells transfected with an empty Cas9 vector did not generate an amplified band. A visual representation of the PCR screen and the resulting PCR amplified bands from 3 of the analysed clones is shown in Figure 4.4.5. 3 clones (renamed BRACH-B1-1, 2 and 3) were determined to be karyotypically normal (between 75%-80% of cells of each clone).

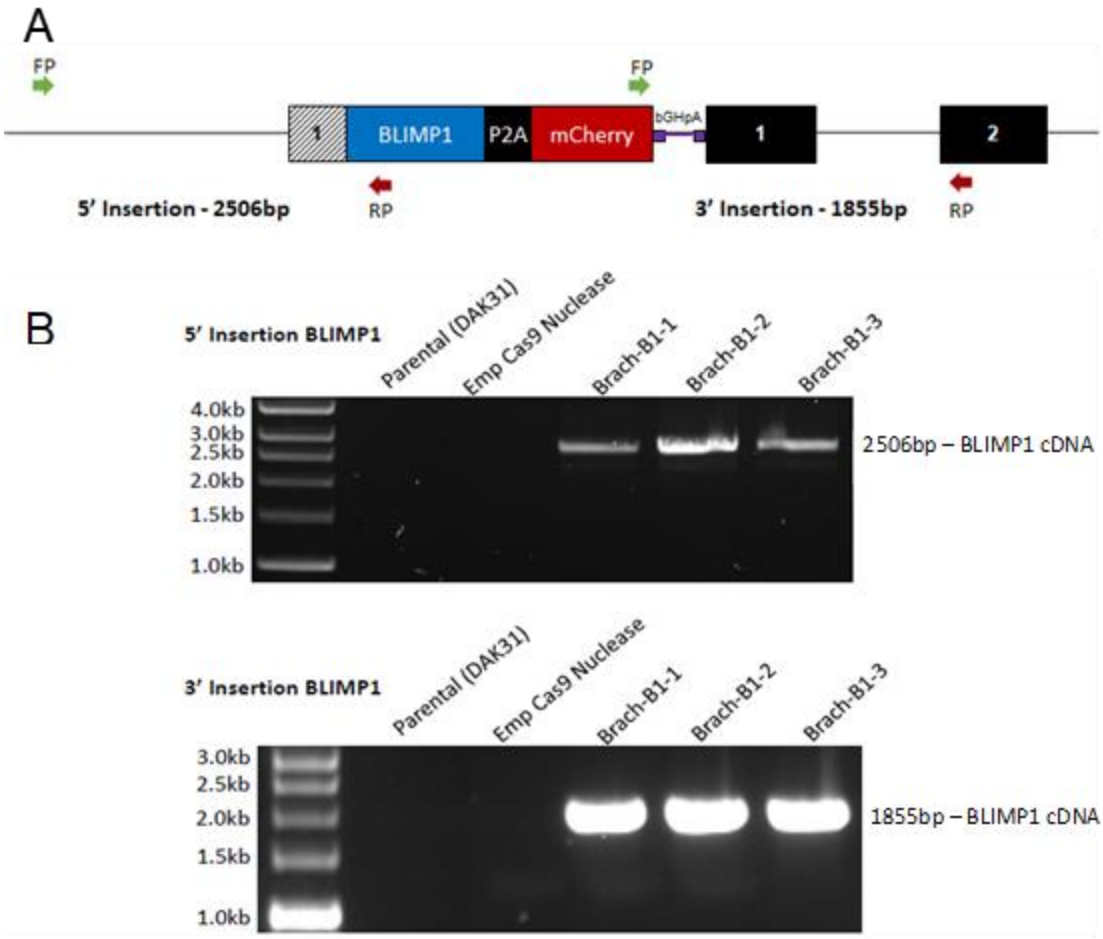

Figure 4.4.5. Internal PCR screen to confirm insertion of Blimp1-2a-mCherry cassette into the Brachyury locus. *(A) Schematic showing the regions amplified if the BLIMP1-2a-mCherry cassette has been successfully inserted into the Brachyury locus (B) Gel electrophoresis of the PCR amplified regions. Insertion of BLIMP1-2a-mCherry was identified by the presence of a PCR band with both sets of oligonucleotides. The parental and cells transfected with PX458 without a gRNA sequence were used as negative controls.*

BRACH-B1-1 did not display any substantial differences in growth or morphology compared to the parental DAK31 cell line when cultured in standard 2i+LIF medium. BRACH-B1-2 and BRACH-B1-3 however grew noticeably slower and the colonies were smaller and rounder than the parental line (Figure 4.4.6).

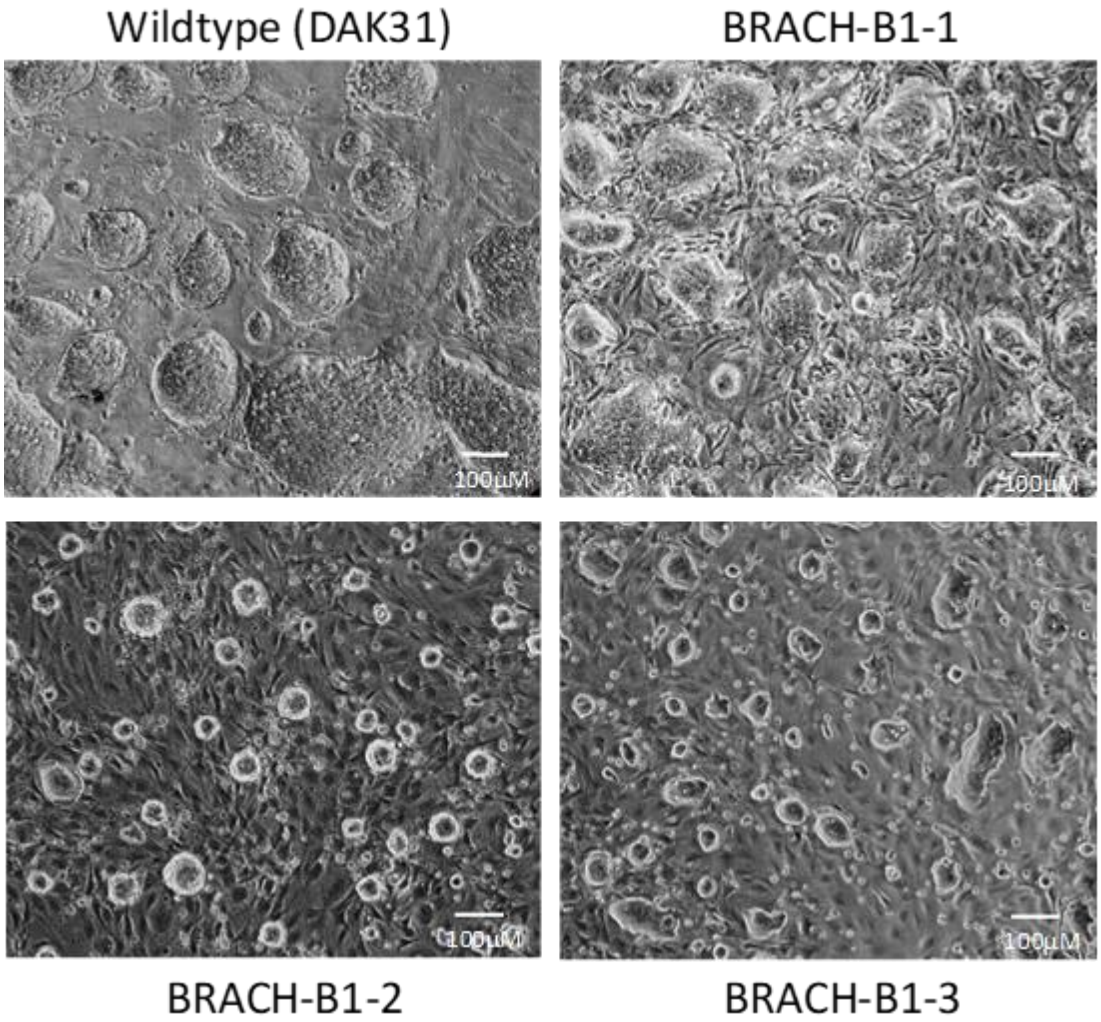

Figure 4.4.6. Bright field microscopy images of BRACH-B1 clones. *Photographs were taken of the karyotypically normal clones containing at least one allele of Brachyury containing the BLIMP1-2a-mCherry sequence. The top panel shows the parental WT cell line. All cells were seeded at 1.5 x 10^5 cells and cultured for 2 days in 2i+LIF culture medium.*

4.4.3 Sequencing of the edited *Brachyury* alleles from the BRACH-B1 clones

PCR amplification of the BRACHYURY locus had shown that within these isolated clones, all three had one allele which contained the BLIMP-2a-mCherry cassette. Sanger sequencing was performed on the amplified bands from the second PCR screen (Figure 4.4.5) with oligonucleotides designed to sequence the joining regions between the *Brachyury* locus and the BLIMP1-2a-mCherry cassette. Sequence traces generated from the 5' insertion site of the BLIMP1-2a-mCherry gene sequence matched the expected reference sequence (Figure 4.4.7).

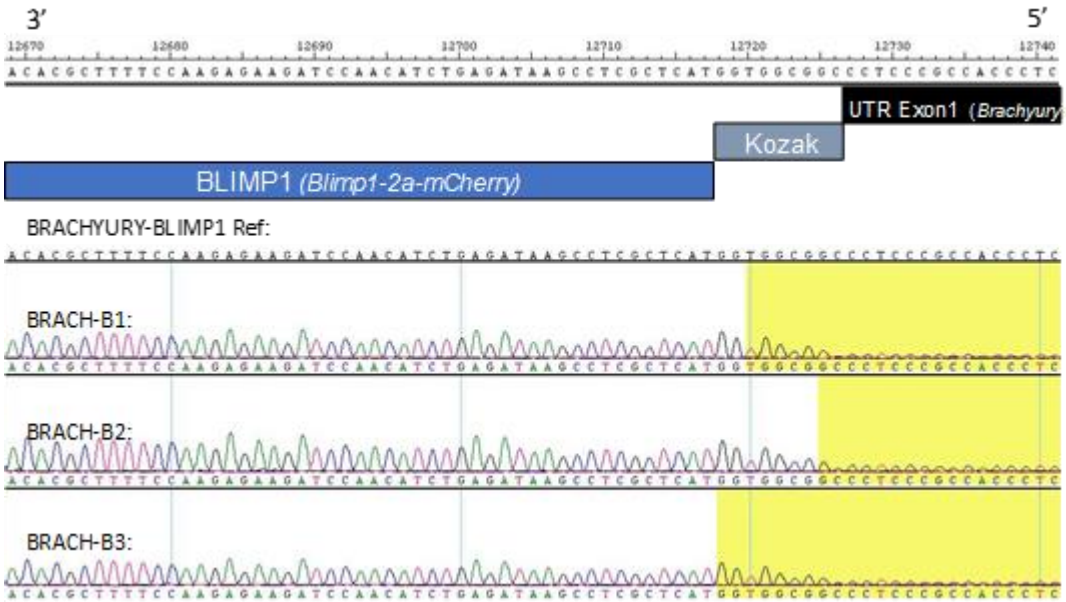

Figure 4.4.7. Sanger Sequencing report generated at the 5' insertion site of the BRACH-B1 clones. *Sequencing report generated in the 3' – 5' direction. Blue box = Blimp1 transgene of Blimp1-2a-mCherry cassette, Grey box = Kozak sequence of Blimp1-2a-mCherry cassette, Black box = Exon 1 of endogenous Brachyury (UTR region upstream of ATG start codon).*

Sequence traces generated from the 3' insertion site of the BLIMP1-2a-mCherry showed seamless insertion of the BLIMP1-2a-mCherry cassette into the *Brachyury* locus (Figure 4.4.8) in all three clones.

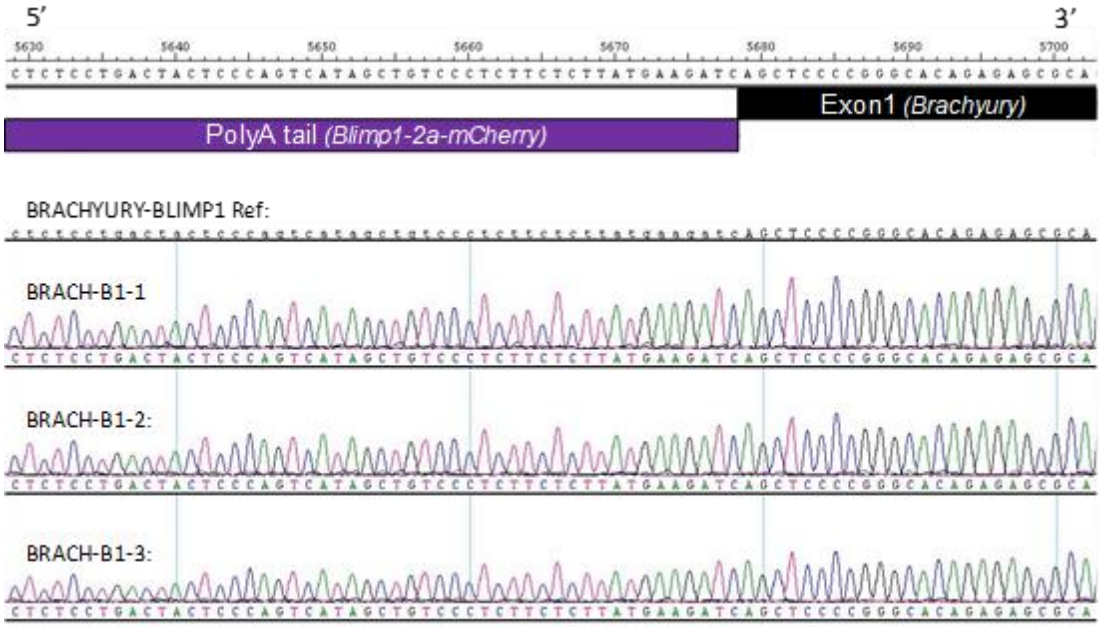

Figure 4.4.8. Sanger Sequencing report generated at the 5' insertion site of the BRACH-B1 clones. *Sequencing report generated in the 5' – 3' direction. Purple box = PolyA tail of Blimp1-2a-mCherry cassette, Black box = Exon 1 of endogenous Brachyury (downstream of ATG start codon).*

4.4.4 Sequencing of the non-HDR *Brachyury* allele within the BRACH-B1 clones

PCR amplification of the targeted region in the BRACH-B1-2 clone suggested there was no wild type *Brachyury* allele within the clonal population, implying that either the BLIMP1-2a-mCherry cassette had been inserted into both alleles of *Brachyury* or that NHEJ had removed one or both PCR oligonucleotide binding regions, preventing the amplification of the region with the screening oligonucleotides (Figure 4.4.4). BRACH-B1-1 and BRACH-B1-3 were sequenced to identify whether either of these clones had a wild type copy of the *Brachyury* gene. Sanger sequencing was performed on the smaller amplified bands (~3112 bps) generated from the first PCR screen (Figure 4.4.4) with oligonucleotides designed to span the CRISPR cut site at the *Brachyury* locus.

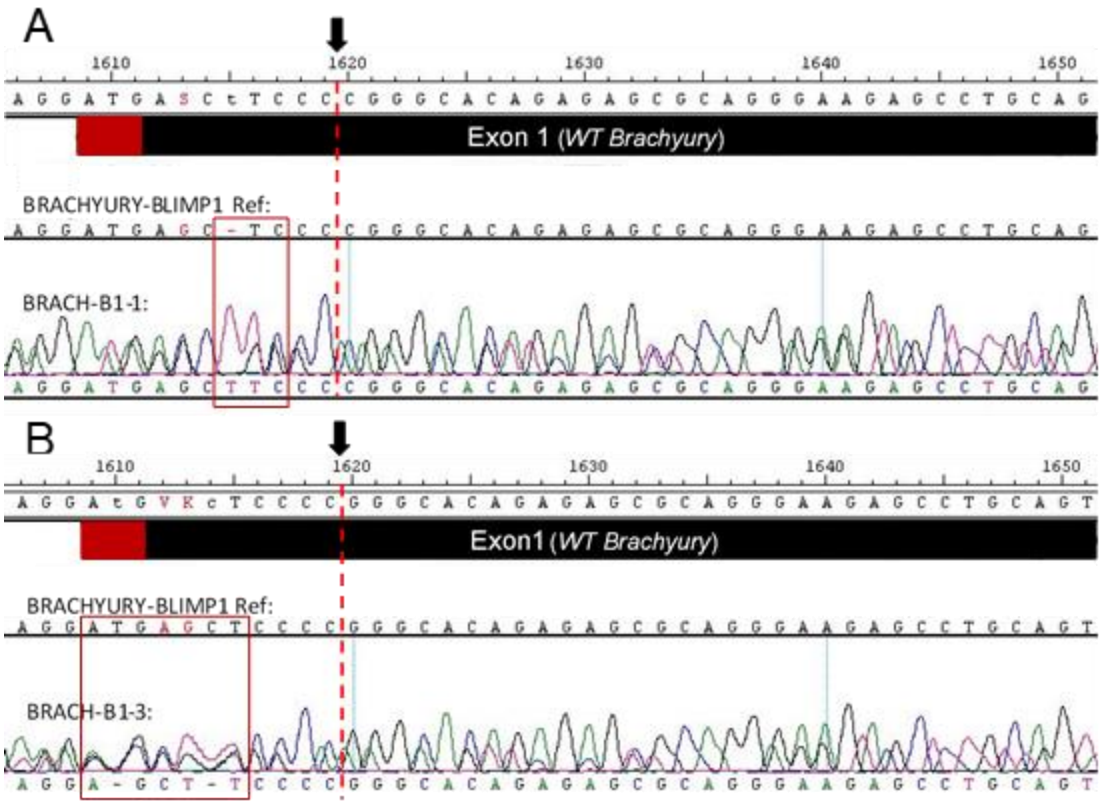

Figure 4.4.9. Sanger Sequencing report of the 5' ATG site allele Brachyury of the 'wildtype' in the BRACH-B1 clones. *Sequencing report generated in the 5' – 3' direction. Red box = ATG start codon, Black box = Exon 1 of endogenous Brachyury. Black arrow/red dotted line represents CRISPR/Cas9 cut site at position '+10' downstream of the Brachyury ATG site, highlighted regions (red outline) indicates indels present in the sequence after CRISPR gene editing. Evidence of multiple traces within each sample suggests that not all clones within the population had the same mutation, hence why the trace was more difficult to read. (A) BRACH-B1-1. A 'T' has been inserted at position +7 (B) BRACH-B1-3. 2 deletions were present at positions +2 and +6, and 2 further changes identified at position +4 and +5.*

The sequence trace for both BRACH-B1-1 and BRACH-B1-3 had modifications near the ATG start site of *Brachyury* (Figure 4.4.9). BRACH-B1-1 had a deletion of a 'T' nucleotide 7 bases downstream of the ATG codon (+7) (Figure 4.4.9A). While BRACH-B1-3 had evidence of four base changes; two deletions at positions 2 bases (+2) and 6 bases (+6) downstream of ATG and either two substitutions, 'A' to 'C' and 'G' to 'T' or an insertion of a 'CT' at 4 bases downstream of the ATG (+4 and +5) (Figure 4.4.9B). These modifications within both clones produced a frameshift mutation, indicating that all three generated BRACH-B1 clones were likely to be *Brachyury* knock-outs. Additionally, both clones had evidence of multiple traces, suggesting that these populations might be comprised of more than one single clone. Despite all three BRACH-B1 clones being effectively *Brachyury* nulls, they were analysed further to identify if the inserted *Blimp1* and mCherry cDNA could be expressed from the *Brachyury* locus.

4.5 Expression of the BLIMP-2a-mCherry cassette

4.5.1 Inducing the BLIMP1-2a-mCherry cassette by CHIR99021 titration

It has been previously shown that rat ESCs cultured in high concentrations of CHIR99021 differentiate due to over-activation of β-catenin signalling (Meek et al. 2013). This increases the expression of differentiation markers, including the epiblast gene *Brachyury* (Meek et al. 2013). To confirm that CHIR99021 induces high levels of *Brachyury* gene expression in DAK31 cells, samples were harvested after 16 and 72 hours of induction with 2-8μM CHIR99021 and levels of *Brachyury* transcripts were measured by qRT-PCR analysis (Figure 4.5.1). The qRT-PCR data generated showed that increasing the concentration of CHIR99021 increased expression of *Brachyury*, with cells cultured in 8μM CHIR99021 showing the highest level of *Brachyury* transcript after 16 and 72 hours. All 3 BRACH-B1 clones were subjected to a CHIR99021 titration for 72 hours alongside the parental DAK31 cell line (Figure 4.5.2).

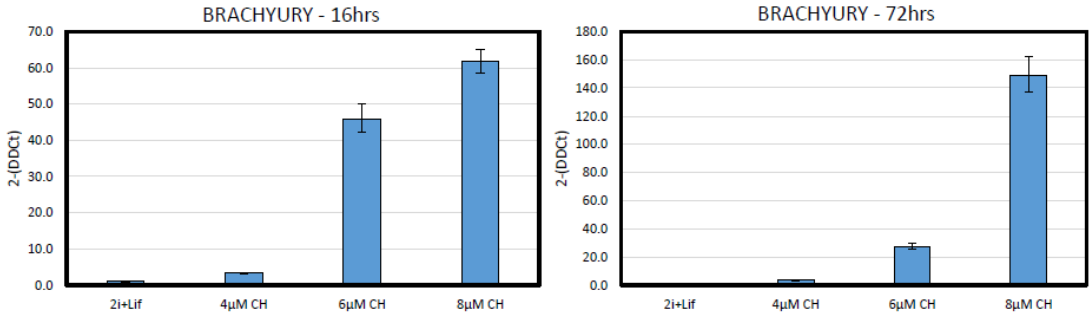

Figure 4.5.1. qRT-PCR analysis of WT DAK31 cells after CHIR99021 titration. *Cells were harvested after 16 and 72 hours of culture in varying concentrations of CHIR99021. All data was normalised to the house keeping gene β-actin (dCT) and fold change was calculated by normalising gene expression to cells cultured in 2i+LIF (2-DDCT).CH = CHIR99021. Data shown is the average of two independent experiments performed in the DAK31 cell line ± SD.*

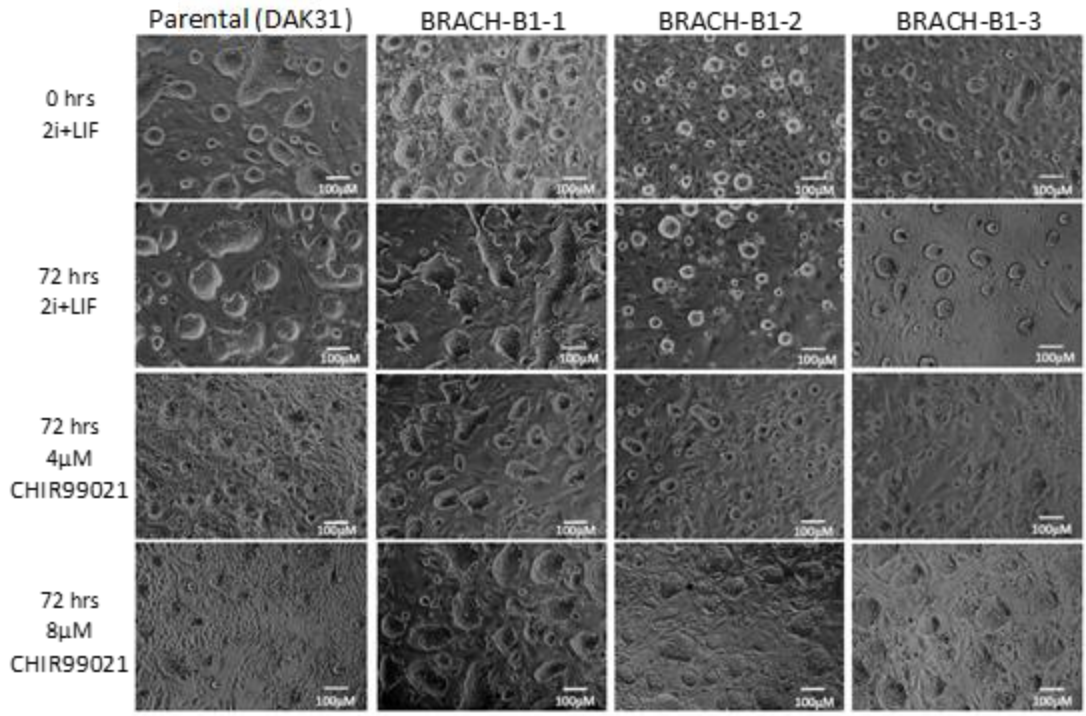

Figure 4.5.2. Bright field microscopy photographs of WT DAK31 and BRACH-B1 clones undergoing CHIR99021 titration. *Photographs were taken at day 0 (when cells were cultured in 2i+LIF conditions) and after 72 hours of culture in varying concentrations of CHIR99021. 2i+LIF medium contained 2μM CHIR99021.*

The parental cell line differentiated as expected in high concentrations of CHIR99021, showing evidence of cellular differentiation. However, BRACH-B1-1 did not exhibit any substantial morphological changes when cultured in medium with a high concentration of CHIR99021 compared to cells cultured in 2i+LIF medium. Both BRACH-B1-2 and BRACH-B1-3 clones produced flatter colonies when cultured in high concentration of CHIR99021 compared to standard 2i+LIF medium, but had little evidence of differentiation when compared to the parental.

Cells treated with high concentrations of CHIR99021 were fixed and immunostained for the presence of BRACHYURY protein. The parental DAK31 cell line cultured in medium containing 8μM CHIR99021 stained positive for BRACHYURY protein (Figure 4.5.3). However, all three BRACH-B1 clones had no discernible BRACHYURY staining when treated with 8μM CHIR99021.

Immunofluorescence staining of all three BRACH-B1 clones showed that either all three clones were *Brachyury* knock-out cell lines, or that they are less responsive to CHIR99021-induced differentiation.

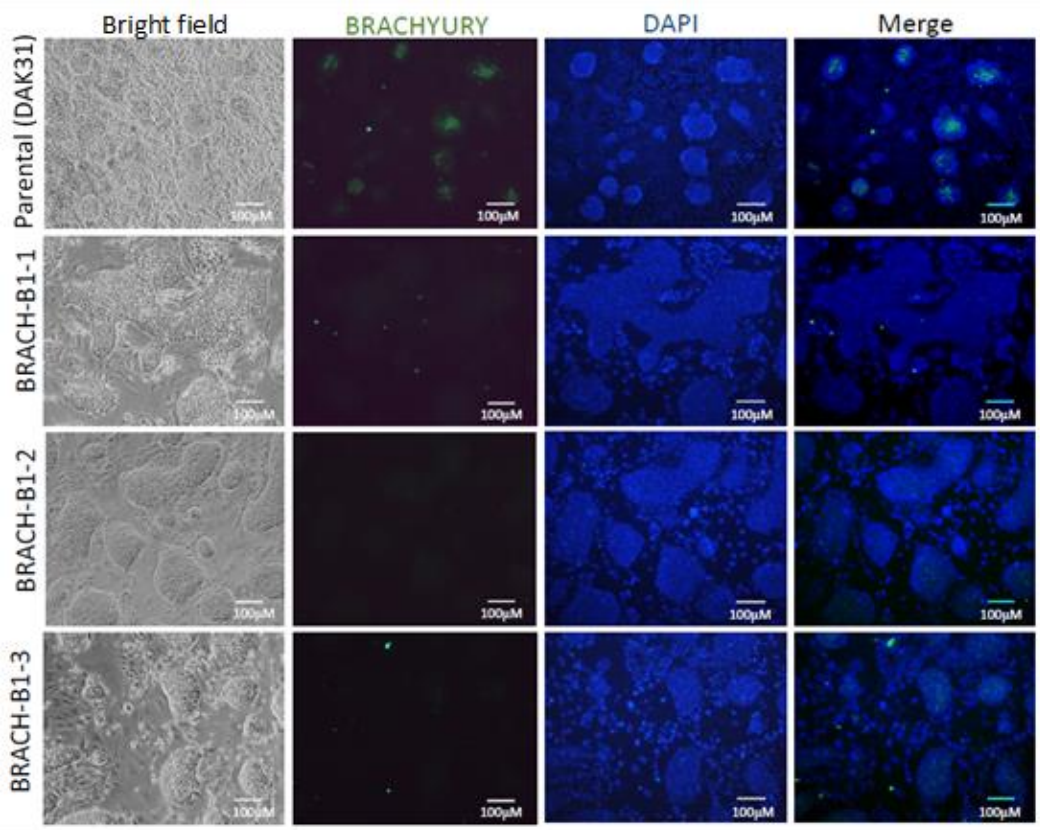

Figure 4.5.3. Immunofluorescence staining of DAK31 and BRACH-B1 clones cultured with 8µM CHIR99021. *BRACHYURY (green) protein expression was identified in the parental DAK31 cell line, but not in any of the BRACH-B1 clones. DAPI (blue) was performed as an immunostain control.*

The remaining culture wells were analysed by fluorescence microscopy and flow cytometry to identify mCherry fluorescence produced from the BLIMP1-2a-mCherry cassette as detailed previously. mCherry was not detected in any clones by fluorescence microscopy. However, flow cytometry analysis confirmed low levels of mCherry in all BRACH-B1 clones cultured in medium containing 8µM CHIR99021 (Figure 4.5.4).

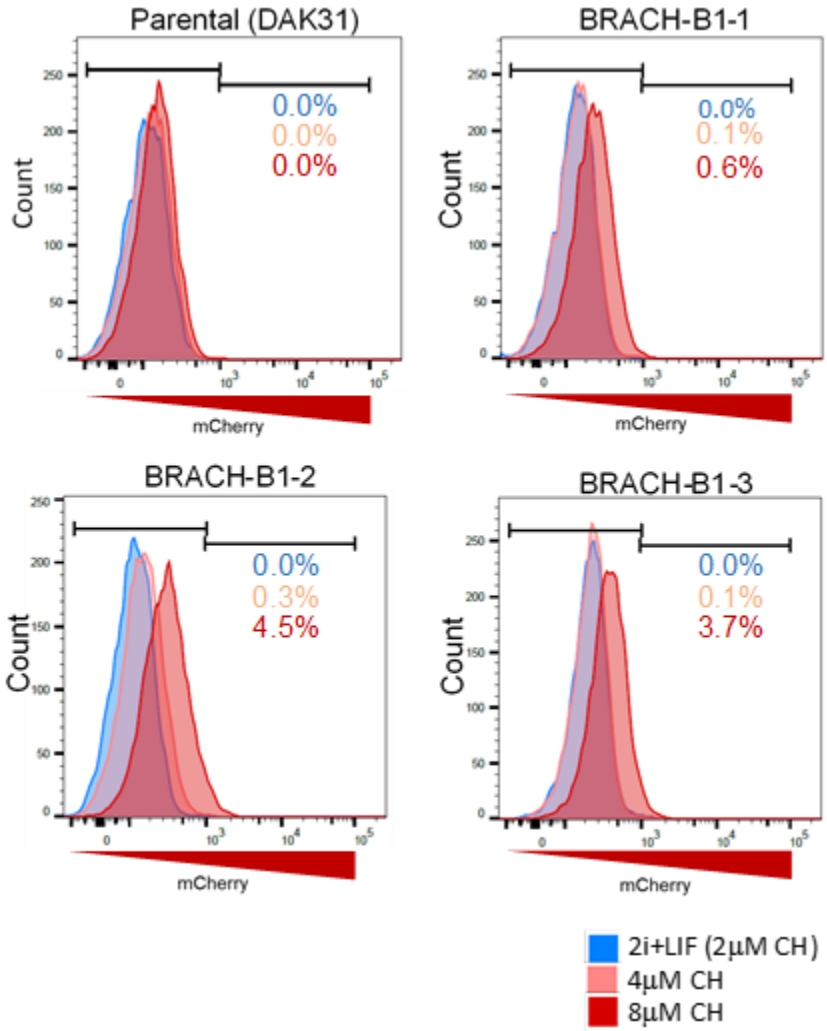

Figure 4.5.4. Flow cytometry plots of BRACH-B1 clones after CHIR99021 titration. *Pools of the 3 BRACH-B1 clones, alongside a parental control, were cultured for 72 hours with standard 2i+LIF (2µM) medium, or cell culture medium containing 4µM or 8µM CHIR99021 (CH). Peaks represent the level of mCherry expression detected from each cell pool.*

qRT-PCR analysis was performed to determine whether the expression of *Blimp1*, *Ap2γ* (downstream target of BLIMP1) and *Nanos3* (PGC marker) were upregulated in BRACH-B1 clones cultured in response to high concentrations of CHIR99021. *Blimp1* transcript levels increased substantially in all BRACH-B1 clones compared to the parental cell line when cultured medium containing 8µM CHIR99021 (Figure 4.5.5). Expression of *Ap2γ* was elevated in the BRACH-B1-3 clone when cultured in medium containing 8µM CHIR99021. However, *Ap2γ* expression in both BRACH-B1-1 and BRACH-B1-2 was similar to the expression in the parental cell line in all conditions.

When cultured in medium containing 8μM CHIR99021, all three BRACH-B1 clones had higher levels of *Nanos3* transcript expression compared to the parental cells in the same medium conditions. However, this expression level did not surpass that in the ESCs cultured in 2i+LIF medium.

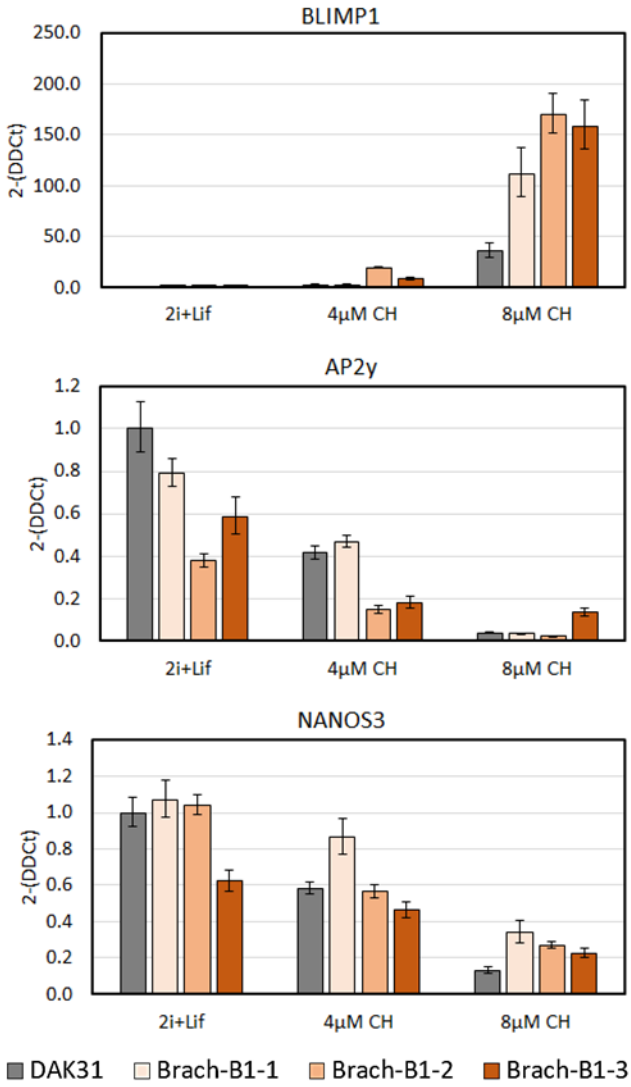

Figure 4.5.5. qRT-PCR analysis of WT DAK31 and BRACH-B1 clones treated with CHIR99021. *Cells from the parental (DAK31) or BRACH-B1 clones were harvested after 72 hours culture in varying concentrations of CHIR99021. The data presented was an average of two independent experiments. All data was normalised to the house keeping gene β-actin (dCT) and fold change was calculated by normalising gene expression to DAK31 cells cultured in 2i+LIF medium (2-DDCT)CH = CHIR99021. Data shown is mean ± SD.*

Overall, data generated from the CHIR99021 titration showed that the *Brachyury* promotor was able to induce the expression of the BLIMP1-2a-mCherry cassette within the BRACH-B1 clones. However, the low mCherry expression from the BRACH-B1 clones suggested that the expression from the *Brachyury* promotor was very weak during CHIR99021 induced activation of *Brachyury*.

4.5.2 Induction of the BLIMP1-2a-mCherry cassette in cells undergoing an Embryoid body (EB) differentiation protocol

To determine whether the BLIMP1-2a-mCherry cassette could be activated without directly stimulating the *Brachyury* promotor using the GSK3i CHIR9901, BRACH-B1 clones were induced to differentiate by being put through an undirected Embryoid body (EB) differentiation protocol (Figure 4.5.6).

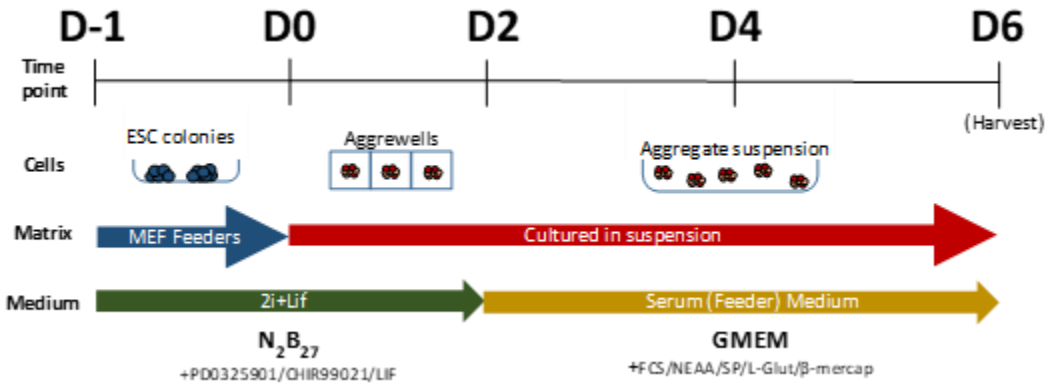

Figure 4.5.6. Schematic of the rat EB differentiation protocol. *Rat ESCs cultured in 2i+Lif conditions on a MEF layer were transferred to an aggrewell™ plate at a cellular density equivalent to 3,000 cells per microwell depression. After 2 days, these cells were transferred from the aggrewell™ plate to 6-well low adhesion plates with serum medium. These aggregates were retained in this condition for a further 4 days and then harvested at day 6.*

BRACH-B1 clones and the parental DAK31 cell line were cultured in suspension with 2i+LIF medium for 2 days to allow aggregation. Culturing rat ESCs in suspension with serum medium directly after being cultured in self-renewal conditions (2i+LIF on MEF layers) promoted extensive cell death, therefore, this 2i+LIF intermediate aggregation step was introduced to increase cell survival. After 2 days, the 2i+LIF medium was replaced with culture medium containing serum and the aggregates maintained in suspension for a further 4 days to drive differentiation of the cells. EBs were monitored for mCherry expression using fluorescent microscopy. mCherry fluorescence was detected from all 3 BRACH-B1 clones from day 5 and 6 of the EB differentiation protocol (Figure 4.5.7).

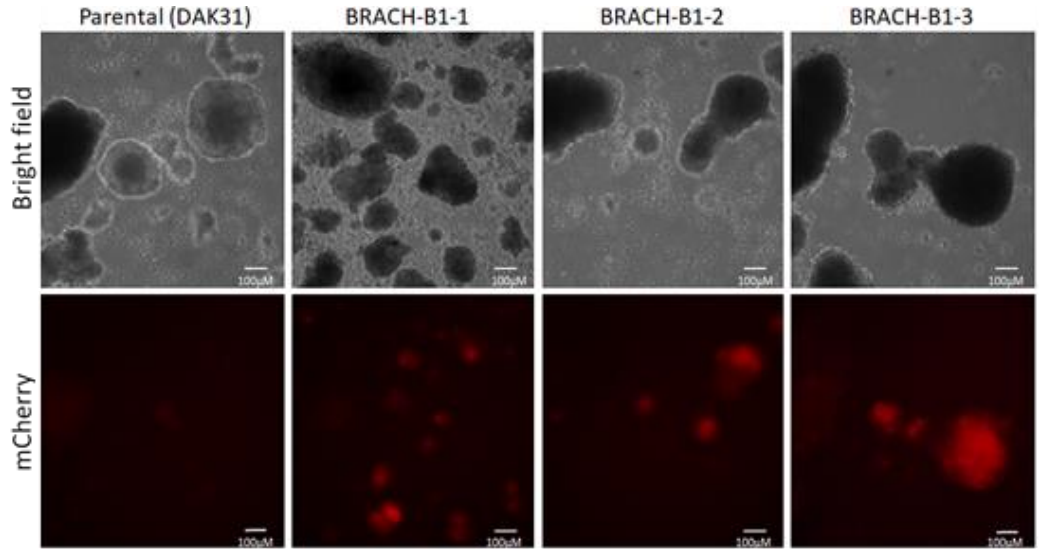

Figure 4.5.7. Brightfield and fluorescent microscopy photographs of the parental DAK31 and BRACH-B1 clones undergoing EB differentiation. *Photographs were taken after cells from the parental or BRACH-B1 clones had been subjected to an EB differentiation protocol for 6 days.*

qRT-PCR analysis was performed to identify whether *Blimp1* transcript expression had been induced within the BRACH-B1 clones after the EB differentiation protocol. *Blimp1* transcript levels increased several-fold in all three BRACH-B1 clones compared to the parental cell line after the 6-day protocol (Figure 4.5.8). Expression of *Ap2γ* did increase in the BRACH-B1-1 and BRACH-B1-3 clones compared to the parental cell line, but was lower in the BRACH-B1-2 clone (Figure 4.5.8). *Nanos3* transcript expression was slightly increased in the BRACH-B1-1 clone when compared to the parental (Figure 4.5.8). However, *Nanos3* expression in BRACH-B1-2 cells was similar to the parental cell line, and was reduced in BRACH-B1-3 cells (Figure 4.5.8). The qRT-PCR data, coupled with the fluorescence photographs taken after the cells had undergone the EB differentiation protocol indicated that the *Brachyury* promotor was able to drive the expression of the BLIMP1-2a-mCherry cassette.

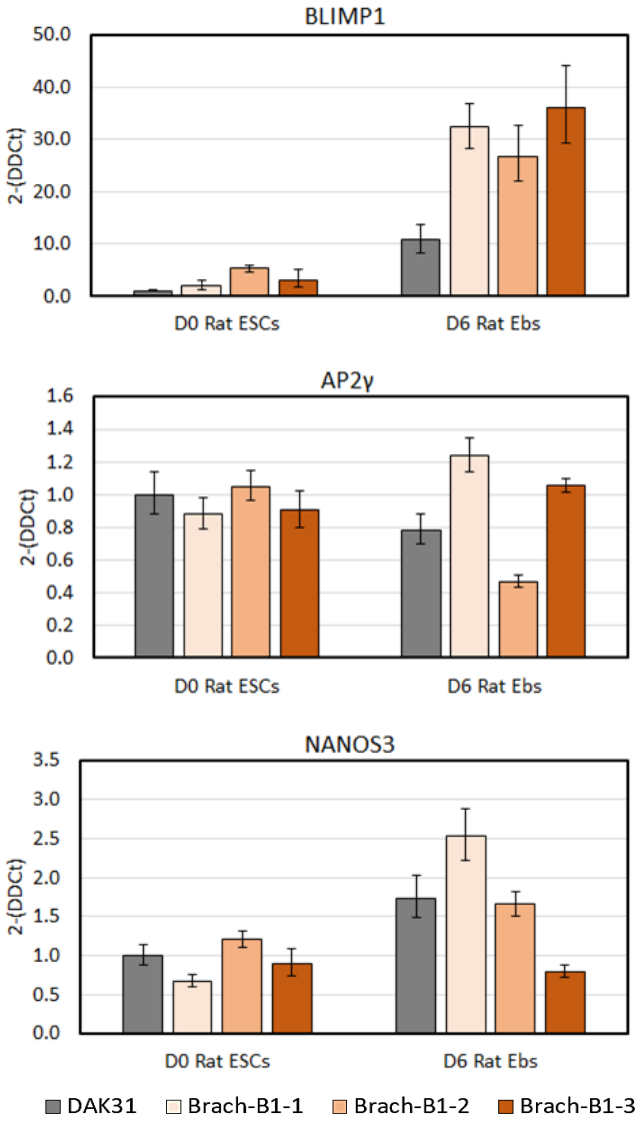

Figure 4.5.8. qRT-PCR analysis of WT DAK31 and BRACH-B1 clones undergoing EB differentiation. *Cells were harvested after the 6-day EB differentiation protocol. Data was normalised to the house keeping gene β-actin (dCT) and the fold change was calculated by normalising gene expression to the parental DAK31 ESCs (D0) (2-DDCT). Data is the average of two independent experiments generated from the parental DAK31 and BRACH-B1 clones ± SD.*

4.5.3 Induction of the BLIMP1-2a-mCherry cassette in cells undergoing a PGCLC differentiation protocol

The BRACH-B1 clones were subjected to the PGCLC differentiation protocol (Figure 4.5.9) to observe whether the expression of *Brachyury* driven *Blimp1* cDNA could enhance differentiation of rat ESCs towards a PGCLC fate.

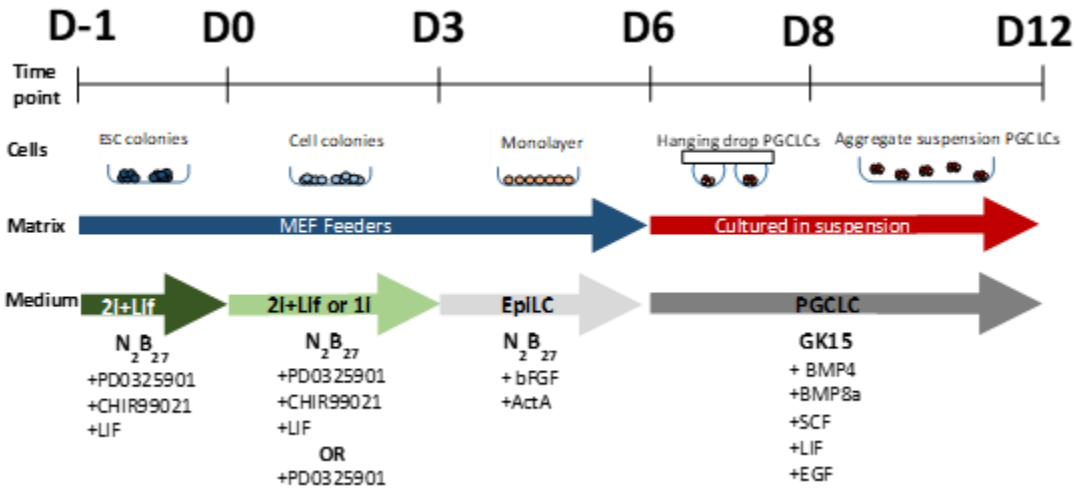

Figure 4.5.9 Schematic of the rat PGCLC differentiation protocol used for differentiation of BRACH-B1 clones. *Rat ESCs cultured in 2i+Lif or 1i medium conditions on a MEF layer were transferred onto fresh MEF feeder layers and cultured in EpiLC differentiation medium for 3 days. These cells where then pipetted into hanging drops containing ~2,000 cells in PGCLC medium. After 2 days, the hanging drops were collected and placed into fresh PGCLC medium in 6-well low adhesion plates for a further 4 days.*

BRACH-B1 clones and the parental DAK31 cell line were pre-treated for 3 days in 2i+LIF or 1i culture medium on MEF feeder layers. After the pre-treatment, cells were transferred to 12-well plates coated with fresh MEFs and maintained in EpiLC culture medium for a further 3 days. The EpiLC medium was changed every 24 hours to replenish active bFGF. Cells were photographed by bright field microscopy at the end of day 6 of the protocol to observe any morphological differences between the BRACH-B1 clones at this stage of the differentiation protocol (Figure 4.5.10). After 3 days culture in EpiLC medium, there was a large amount of cellular debris present in wells of BRACH-B1-1 cells pre-cultured in 2i+LIF medium compared to cells pre-cultured in 1i medium (Figure 4.5.10). However, no obvious differences could be identified between BRACH-B1-2 or BRACH-B1-3 cells pre-cultured in either 2i+LIF or 1i (Figure 4.5.10). No mCherry fluorescence was visible by fluorescence microscopy from any BRACH-B1 clone during the 3-day culture in EpiLC medium (data not shown).

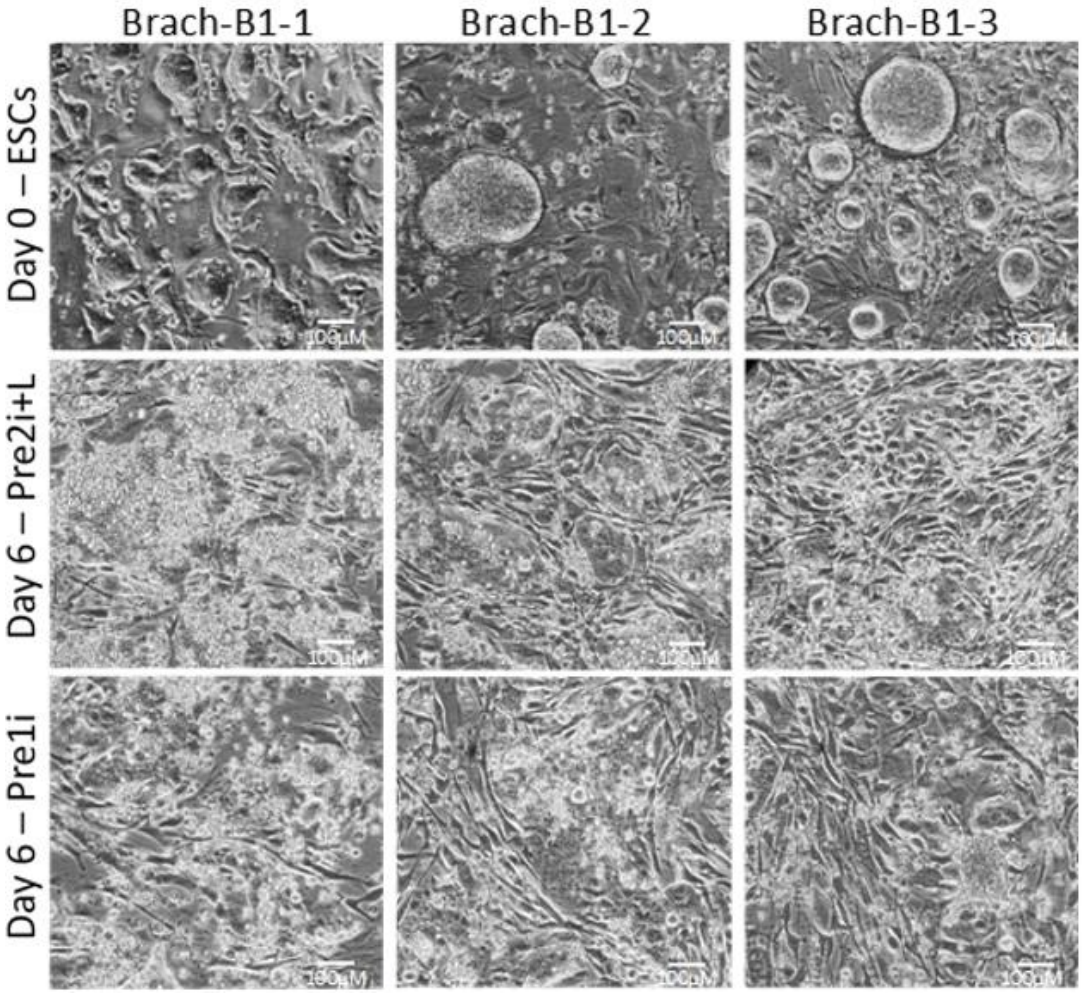

Figure 4.5.10. Bright field microscopy of BRACH-B1 clones after a 3-day culture in EpiLC medium. *Cells were photographed prior to pre-treatment (Day 0) and at day 6 of the differentiation protocol (Day 6). Pools of cells had either been pre-cultured in 2i+LIF (Pre2i+L) or 1i medium (Pre1i) for 3 days prior to being cultured for a further 3 days in EpiLC medium.*

Cells which had been subjected to the 3-day EpiLC differentiation protocol were transferred into hanging drops of PGCLC culture medium. Each hanging drop consisted of ~2,000 cells contained within 30µl PGCLC culture medium. Dishes containing the suspended hanging drops were incubated for 2 days to promote aggregation of the cells. After 2 days in hanging drops, the aggregates were transferred into 6-well low adhesion plates and retained in suspension for a further 4 days. The aggregates were observed daily and bright field photographs taken on the final day of PGCLC culture (Figure 4.5.11). Fluorescence microscopy was performed each day to assess mCherry expression in BRACH-B1 clones. Very faint mCherry fluorescence was observed after day 11 of the PGCLC differentiation protocol (Figure 4.5.11).

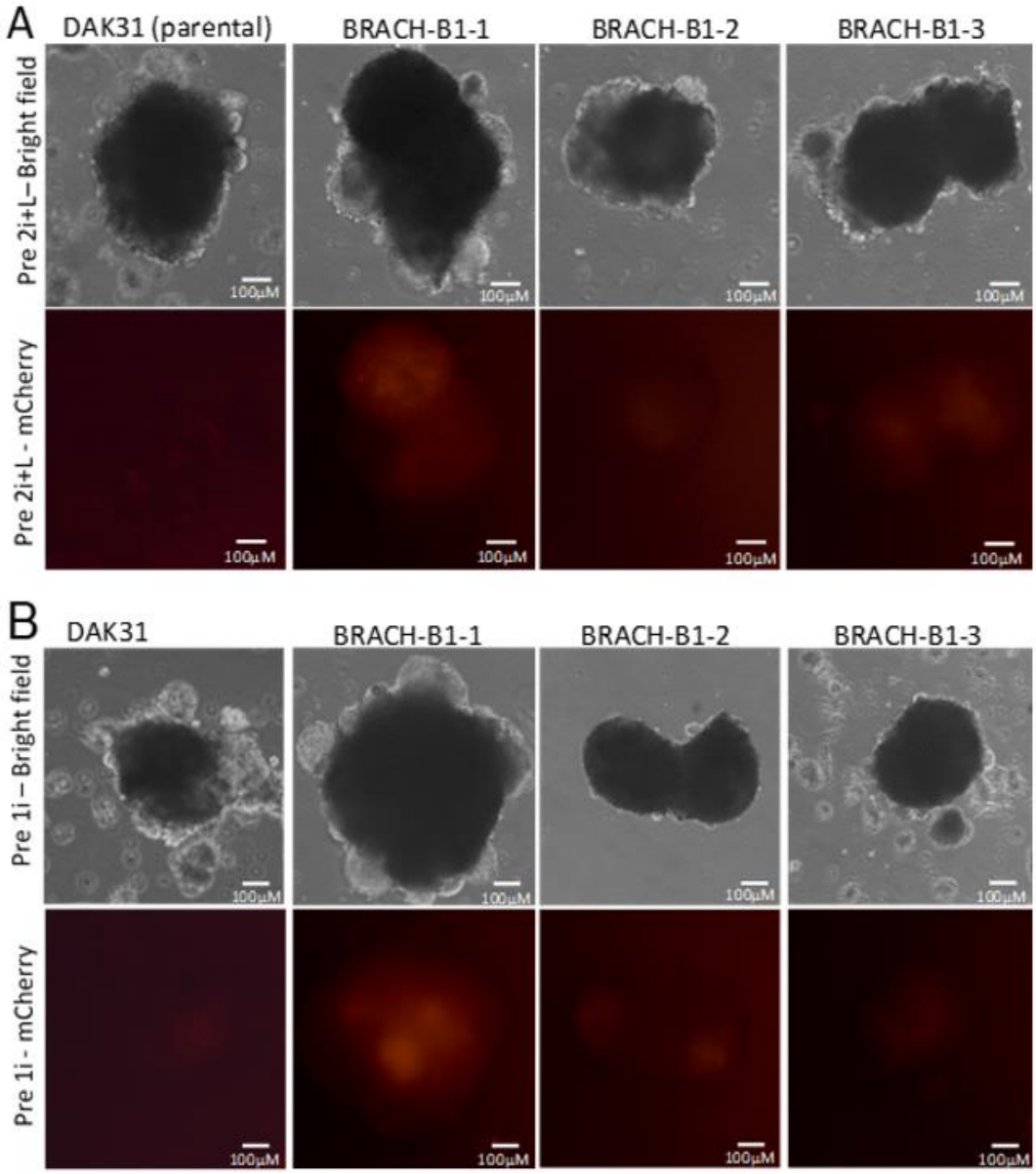

Figure 4.5.11. Bright field and wide field fluorescence microscopy of BRACH-B1 clones at day 12 of PGCLC differentiation. *(A) Aggregates from cells pre-cultured in 2i+LIF medium. (B) Aggregates from cells pre-cultured in 1i medium.*

At day 12 of the PGCLC differentiation protocol, the aggregates were broken apart by gentle pipetting (trituration) and the cell suspensions stained with fluorescent antibodies for SSEA-1 and CD61. These surface markers were used to monitor the differentiation status of the cells and sort the pools into populations of cells which were either unstained, single stained, or double stained for both surface markers by FACs. The gating strategy detailed in section 2.6.7 was used. The remaining cells were gated to isolate populations of double negative, single stained and double stained populations by plotting CD61 (586/15A) versus SSEA-1 (670/14A). DAK31 ESCs cultured in standard 2i+LIF culture conditions were used as an ESC control, representing the surface marker expression of rat cells prior to undergoing the PGCLC differentiation protocol. The gates were set against unstained DAK31 ESCs. The flow cytometry plots generated during the analysis of the BRACH-B1 and DAK31 cells are shown in Figure 4.5.12.

All BRACH-B1 clones had a greater proportion of $CD61^{+ve}$ cells (Figure 4.5.12B) compared to the parental DAK31 cell line (Figure 4.5.12A).The BRACH-B1-1 clone produced two distinct populations of cells (Figure 4.5.12B). These distinct populations were present in cells pre-cultured in either 2i+LIF or 1i medium, suggesting there was a proportion of BRACH-B1-1 cells which had remained in the ESC state even after being subjected to the PGCLC differentiation protocol. Both BRACH-B1-2 and BRACH-B1-3 showed a large proportion of $SSEA\text{-}1^{-ve}/CD61^{+ve}$ cells in both pre-cultured pools but a similar sized population of $SSEA\text{-}1^{+ve}/CD61^{+ve}$ cells compared to the parental DAK31 cell line.

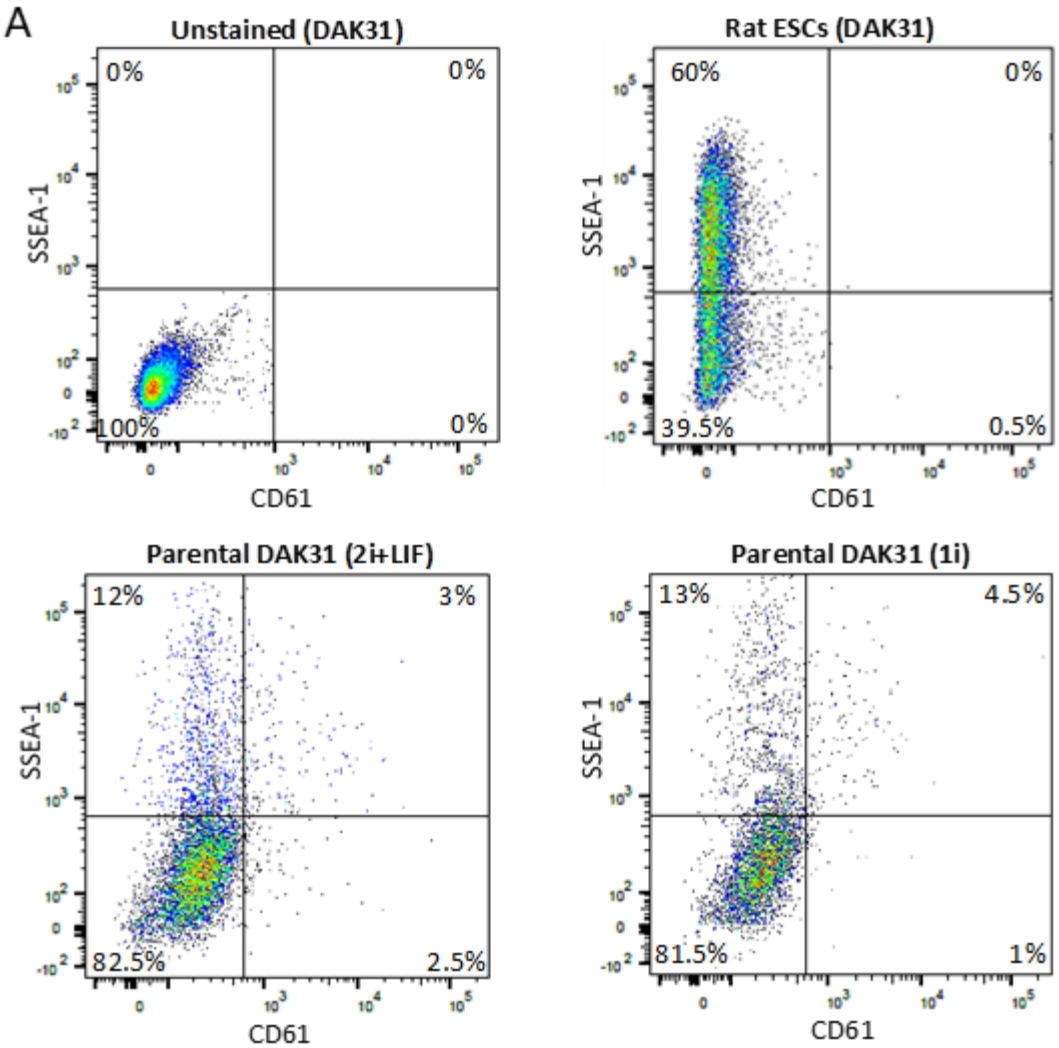
A
Unstained (DAK31)
0%
0%
100%
0%
SSEA-1
CD61
Rat ESCs (DAK31)
60%
0%
39.5%
0.5%
SSEA-1
CD61
Parental DAK31 (2i+LIF)
12%
3%
82.5%
2.5%
SSEA-1
CD61
Parental DAK31 (1i)
13%
4.5%
81.5%
1%
SSEA-1
CD61

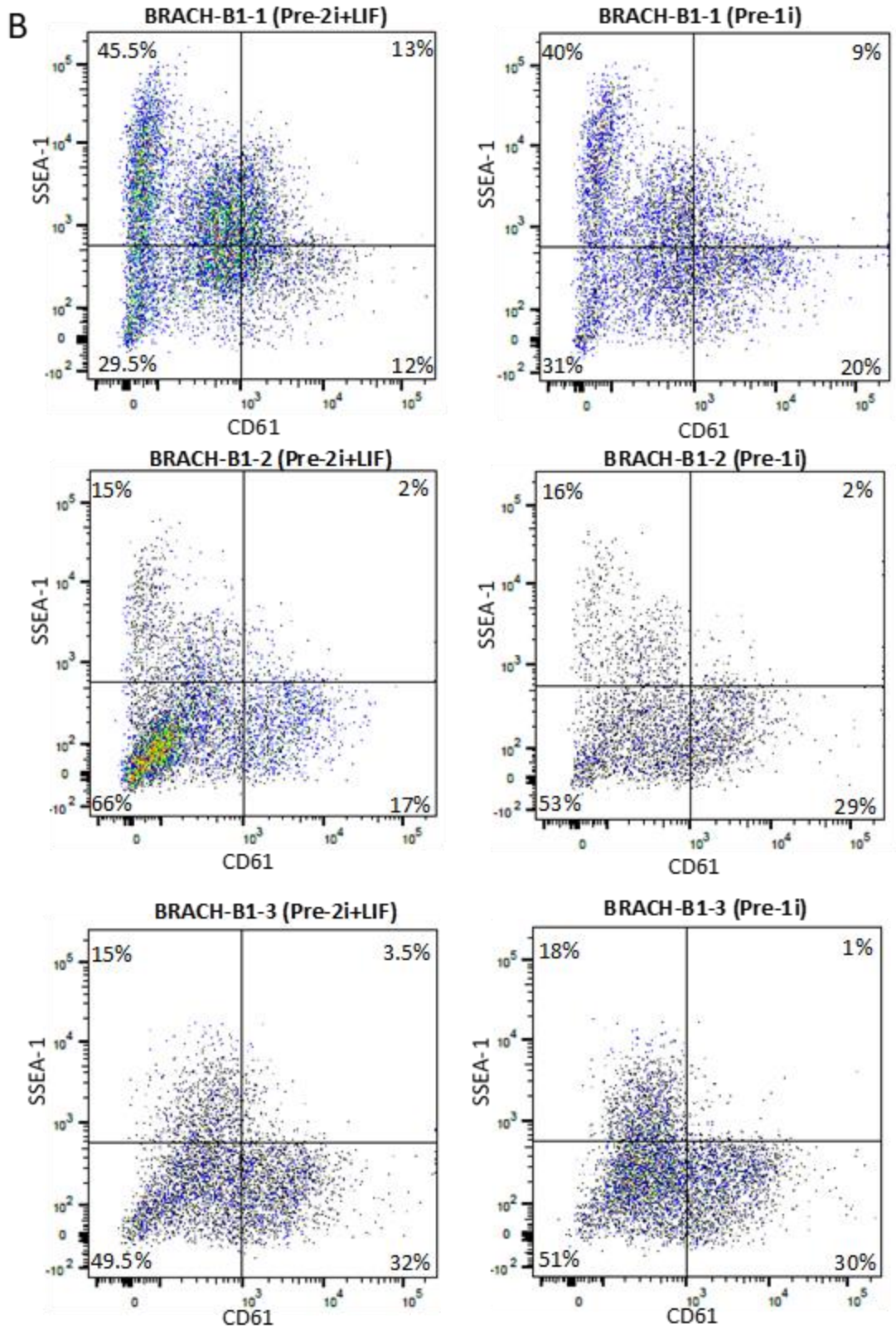

Figure 4.5.12. FACs plots for B1-HDR clones undergoing PGCLC differentiation. *Cells which had undergone the PGCLC differentiation protocol were stained for the presence of SSEA-1 and CD61. Each plot shows the percentage of the population which stained positively for one, both or neither of these antibodies. (A) Parental DAK31 ESCs and those undergoing PGCLC differentiation. (B) BRACH-B1 clones undergoing PGCLC differentiation.*

These stained populations were isolated by FACs and analysed for expression of PGC related markers via qRT-PCR. It was hypothesised that there would be an increased expression of PGC markers within differentiated BRACH-B1 cells compared to the parental line. The figures shown represent qRT-PCR data generated from a single experiment, with the average transcript expression being calculated from 3 technical replicates (Figure 4.5.13 - Figure 4.5.16). qRT-PCR data from the SSEA-1^{+ve}/CD61^{-ve} populations is absent due to the poor yield of purified RNA from the parental, BRACH-B1-2 and BRACH-B1-3 cell lines.

There was a substantial increase in *Blimp1* expression from the SSEA-1^{-ve}/CD61^{+ve} BRACH-B1-1 cells pre-cultured in 1i medium (Figure 4.5.13). However, all other populations of BRACH-B1-1 cells had similar *Blimp1* expression to the parental cell line. BRACH-B1-2 cells pre-cultured in 2i+LIF medium had elevated *Blimp1* transcript in all sorted populations when compared to the parental line. BRACH-B1-3 cells pre-cultured in 1i medium showed an increase in *Blimp1* transcript in the SSEA-1^{-ve}/CD61^{-ve} population, but showed no substantial difference to the parental cell line in any other stained population.

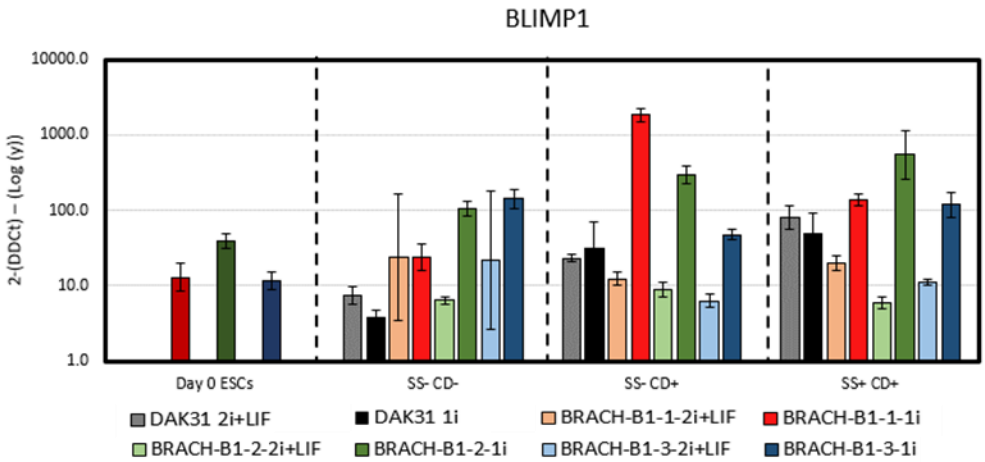

Figure 4.5.13. qRT-PCR analysis of the expression of Blimp1 transcript in SSEA1/CD61 stained populations of rat DAK31 and BRACH-B1 clones subjected to the PGCLC differentiation protocol. *Cells were harvested on day 12 of the PGCLC differentiation protocol and separated into SSEA-1 (SS) and CD61 (CD) stained populations. All data was normalised to the house keeping gene β-actin (dCT) and fold change (log scale) was calculated by normalising gene expression to Day 0 DAK31 ESCs (2-DDCT). Data shown is the mean of technical triplicates generated from one experiment ± SD.*

Nanog transcript expression in BRACH-B1-1 and BRACH-B1-2 clones was considerably greater in all sorted populations pre-cultured in 1i medium compared to the parental cell line (Figure 4.5.14). Prior to undergoing the PGCLC differentiation protocol (Day 0 ESCs), the basal expression of *Nanog* in BRACH-B1-2 cells was higher than that measured in the parental cell line (Figure 4.5.14). Increased *Nanog* expression after undergoing the PGCLC differentiation protocol indicated that these clones were switching on *Nanog* expression during the differentiation protocol. Elevated levels of *Nanog* transcripts were detected in BRACH-B1-3 cells pre-cultured in 1i medium within SSEA-1^{-ve}/CD61^{-ve} sorted cells, but no increased transcript was seen in any other sorted population of this clone compared to the parental (Figure 4.5.14).

The basal expression of *Oct4* in ESCs of all three BRACH-B1 clones prior to the PGCLC differentiation protocol (Day 0 ESCs) was substantially lower than the parental cell line (Figure 4.5.14). BRACH-B1-1 cells subjected to the PGCLC differentiation protocol had increased expression of *Oct4* transcript compared to the parental cell line within the SSEA-1^{-ve}/CD61^{-ve} population (Figure 4.5.14). However, *Oct4* transcript expression was practically undetectable in the BRACH-B1-2 and BRACH-B1-3 clones in all stained populations and in both CD61^{+ve} populations of BRACH-B1-1 cells.

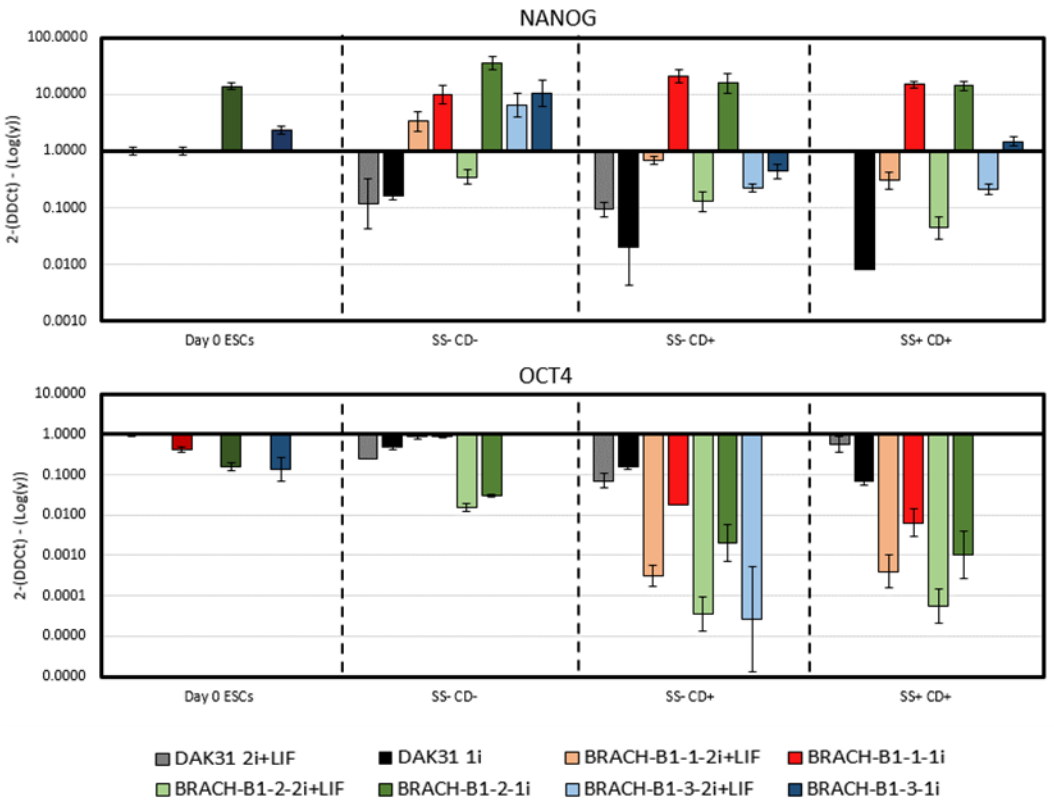

Figure 4.5.14. qRT-PCR analysis of the expression of pluripotency genes in SSEA1/CD61 stained populations of rat DAK31 and BRACH-B1 clones subjected to the PGCLC differentiation protocol. *Cells were harvested after the 12 day PGCLC differentiation protocol and separated into SSEA-1 (SS) and CD61 (CD) stained populations. All data was normalised to the house keeping gene β-actin (dCT) and fold change (log scale) was calculated by normalising gene expression to Day 0 DAK31 ESCs (2-DDCT). Data shown is the mean of technical triplicates generated from one experiment ± SD.*

Nanos3 transcript expression in both CD61^{+ve} populations of BRACH-B1-1 and BRACH-B1-2 cells pre-cultured in 1i medium was considerable higher than the levels seen in the parental cell line (Figure 4.5.15). Cells pre-cultured in 2i+LIF medium from BRACH-B1-1 and BRACH-B1-3 also showed a substantial rise in *Nanos3* transcript in the SSEA-1^{-ve}/CD61^{-ve} population compared to the parental cell line (Figure 4.5.15).

Dazl transcript expression in the SSEA-1^{-ve}/CD61^{-ve} and SSEA-1^{-ve}/CD61^{+ve} populations of BRACH-B1-1 cells pre-cultured in 1i medium was greater than the parental cell line (Figure 4.5.15). However, BRACH-B1-2 cells showed similar expression of *Dazl* to the parental cell line (Figure 4.5.15). No *Dazl* transcript expression was detected in any BRACH-B1-3 stained cell pool (Figure 4.5.15). Basal expression of *Vasa* transcript in ESCs of all three BRACH-B1 clones prior to the PGCLC differentiation protocol (Day 0 ESCs) was substantially lower than that in the parental cell line (Figure 4.5.15).

A rise in *Vasa* transcript was observed in the SSEA-1^{-ve}/CD61^{-ve} population of BRACH-B1-1 cells compared to the parental cell line (Figure 4.5.15). However, all other stained populations from all three BRACH-B1 clones had similar *Vasa* expression to the parental cell line (Figure 4.5.15).

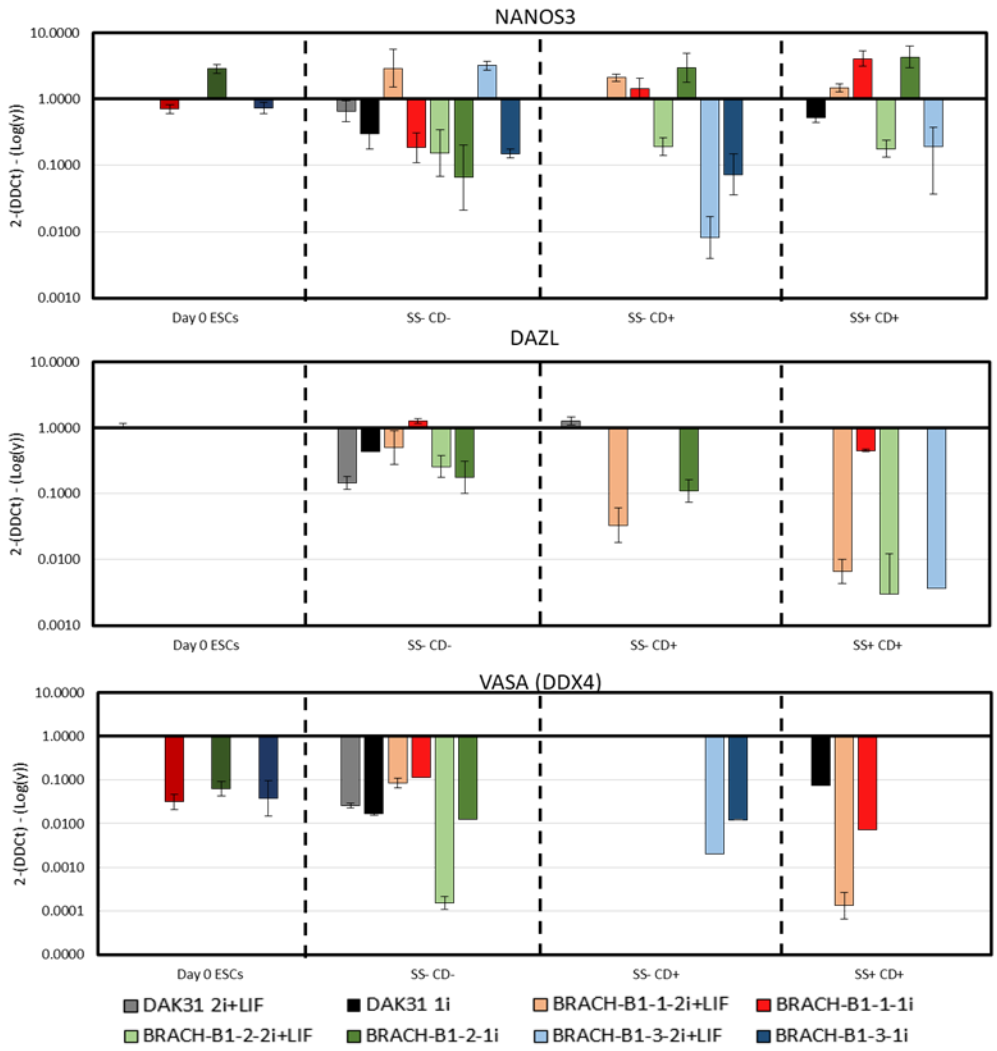

Figure 4.5.15. qRT-PCR analysis of the expression of PGC marker genes in SSEA1/CD61 stained populations of rat DAK31 and BRACH-B1 clones subjected to the PGCLC differentiation protocol. *Cells were harvested after the 12 day PGCLC differentiation protocol and separated into SSEA-1 (SS) and CD61 (CD) stained populations. All data was normalised to the house keeping gene β-actin (dCT) and fold change (log scale) was calculated by normalising gene expression to Day 0 DAK31 ESCs (2-DDCT). Data shown is the mean of technical triplicates generated from one experiment ± SD.*

Transcript expression of markers of endoderm (*Gata4*, *Gata6*) and trophectoderm (*Gata3*) were also analysed to determine whether expression of *Blimp1* cDNA or the loss of *Brachyury* expression influenced the proportion of the BRACH-B1 clones differentiating towards these lineages.

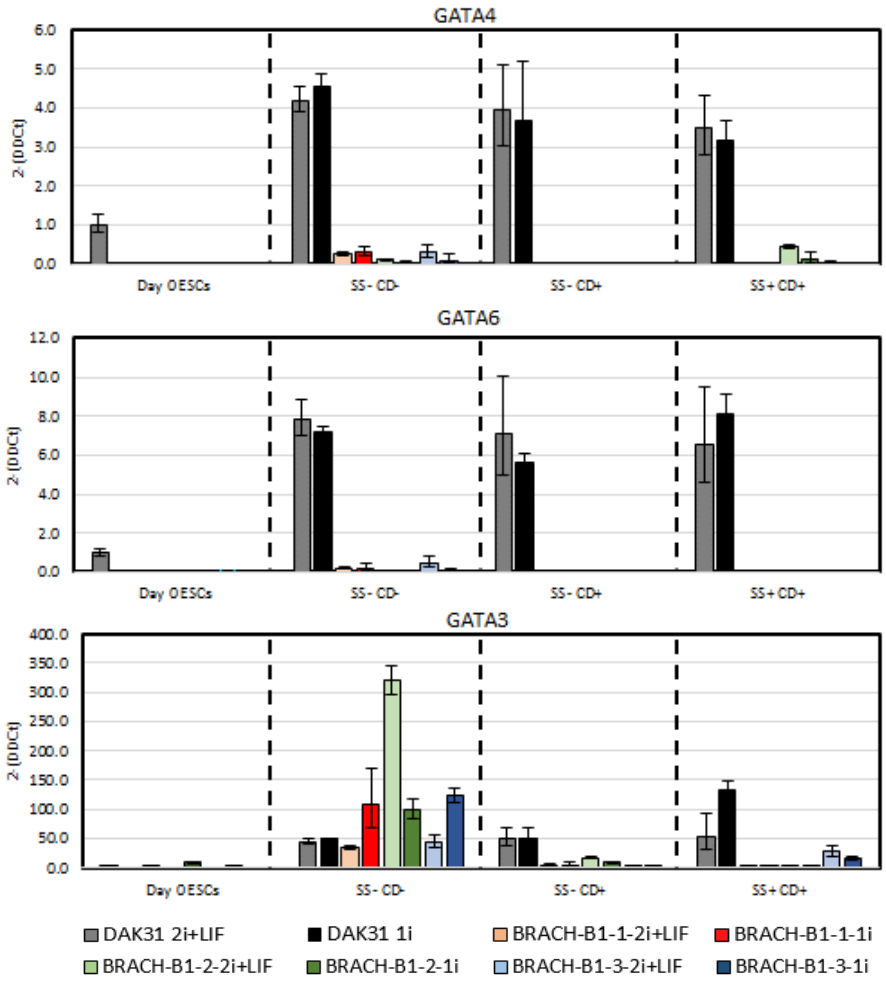

Figure 4.5.16. qRT-PCR analysis of the expression of endoderm (Gata4 and Gata6) and trophectoderm (Gata3) marker genes in SSEA1/CD61 stained populations of rat DAK31 and BRACH-B1 clones subjected to the PGCLC differentiation protocol. *Cells were harvested after the 12 day PGCLC differentiation protocol and separated into SSEA-1 (SS) and CD61 (CD) stained populations. All data was normalised to the house keeping gene β-actin (dCT) and fold change was calculated by normalising gene expression to Day 0 DAK31 ESCs (2-DDCT). Data shown is the mean of technical triplicates generated from one experiment ± SD.*

Both *Gata4* and *Gata6* transcript expression were greatly reduced in all stained populations of the BRACH-B1 cells compared to the parental cell line (Figure 4.5.16). Either the disruption of the *Brachyury* locus via the insertion of the cassette or the expression of the *Blimp1* cDNA was negatively impacting the differentiation of BRACH-B1 clones towards the endoderm lineage.

Gata3 expression was elevated in the SSEA-1^{-ve}/CD61^{-ve} population of all BRACH-B1 clones compared to the parental cell line, with the greatest expression observed from BRACH-B1-2 cells pre-cultured in 2i+LIF medium (Figure 4.5.16). However, all CD61^{+ve} BRACH-B1 cells had reduced *Gata3* expression compared to the parental cell line (Figure 4.5.16).

The qRT-PCR data presented above has been generated from a single experiment, so should be considered a preliminary study on the response of the BRACH-B1 clones to a PGCLC differentiation protocol. In summary, there is evidence of increased early PGC marker expression from BRACH-B1 clones.

4.6 Chapter 4 discussion

The BLIMP1 transcription factor plays an essential role in directing the differentiation of cells within the most proximal posterior region of the epiblast away from the somatic cell fate and towards the germ cell fate (Ohinata et al. 2005, Bikoff et al. 2009, John & Garrett-Sinha 2009, Schäfer et al. 2011). Rat ESCs express very low levels of BLIMP1 in comparison with mouse ESCs, even when cultured in identical *in vitro* cell culture conditions. The aim of this chapter was to determine whether increasing the expression of *Blimp1* within differentiating rat ESCs could direct differentiation towards a PGC fate. To accomplish this, a transgene copy of the *Blimp1* transcription factor was inserted downstream of the *Brachyury* promotor. This would allow induction of the *Blimp1* transgene to occur in differentiating epiblast rat cells, where *Brachyury* expression is induced. The hypothesis was that rat ESCs expressing *Blimp1* transgene would generate a greater proportion of PGCLCs compared to the parental cell line.

4.6.1 A BLIMP1-2a-mCherry transgene cassette was successfully integrated into the rat genome downstream of *Brachyury*

Insertion of the BLIMP1-2a-mCherry cassette into the *Brachyury* locus was highly efficient, with approximately 40% of transfected rat ESC clones having an appropriately modified *Brachyury* allele. Of these, 3 clones possessed a normal karyotype. Functionality of the inserted BLIMP1-2a-mCherry cassette was demonstrated by the induction of mCherry fluorescence and *Brachyury* transgene transcripts through the induction of high levels of β-catenin activity using the GSK3 inhibitor CHIR99021, a condition previously shown to induce *Brachyury* expression in rat ESCs (Meek et al. 2013). Expression of the mCherry component of the BLIMP1-2a-mCherry cassette was detected in all clones by fluorescence microscopy and flow cytometry analysis. These results showed that the CRISPR/Cas9 gene editing technique used was capable of efficiently knocking-in a transgene cassette into the rat genome, and that the transgene cassette was activated by inducing the endogenous gene promotor of *Brachyury*.

4.6.2 Overexpression of *Blimp1* induced a small increase in the expression of early PGC marker genes during rat ESC differentiation

As this expression cassette was designed to rely upon activation of an endogenous promoter without external input, the BLIMP1-2a-mCherry knock-in clones were subjected to two differentiation protocols that normally induce transcription of *Brachyury*. During undirected EB differentiation, increased *Blimp1* transcripts and mCherry fluorescence were detected in clones containing the BLIMP1-2a-mCherry cassette compared to the parental cell line. However, there was no increased expression of the PGC specific marker gene *Nanos3*, suggesting the expression of the *Blimp1* transgene did improve rat cell differentiation towards the germ line. Cell clones subjected to the PGCLC differentiation protocol had increased $CD61^{+ve}$ cells compared to the parental cell line. As CD61 was detected within the genital ridges of rat embryos, this increased population of $CD61^{+ve}$ cells might indicate a greater proportion of rat ESCs being directed towards the PGC fate. Increased expression of both *Nanog* and *Nanos3* was detected in $CD61^{+ve}$ cells of two cell clones compared to the parental cell line. However, the expression of other commonly associated markers of PGCs (*Vasa*, *DazL, Oct4*) remained unchanged or were reduced in $CD61^{+ve}$ cells expressing *Blimp1* transgene. *Nanos3* is considered to be an early marker of PGC specification, while *Vasa* (*Ddx4*) and *DazL* are classified as late stage markers of PGCs (Hayashi et al. 2011, Hayashi & Saitou 2013, Chen et al. 2014). This suggests that similar to what has been shown in the mouse (Ohinata et al. 2005, Bikoff et al. 2009, John & Garrett-Sinha 2009, Schäfer et al. 2011), BLIMP1 is required for early PGC specification, but increasing its expression alone is not capable of driving the expression of more mature PGC markers. It would be of interest to test whether the efficiency of germline transmission of these cell clones harbouring the BLIMP1-2a-mCherry cassette was improved compared to the parental cell line when injected to form chimeras.

4.6.3 Knock-out of *Brachyury* gene expression may have had a larger impact on rat cell differentiation during the PGCLC differentiation protocol than *Blimp1* transgene expression

Although there was improvement in the expression of early PGC markers in the cell clones, other PGC markers were not influenced by the expression of the *Blimp1* transgene during differentiation. Additionally, there was large variability in the overall gene expression between the different cell clones. One reason for this may have been the unintended loss of *Brachyury* gene expression. Sanger sequencing and immunostaining for BRACHYURY protein revealed all clones were *Brachyury* knock-outs, having either a double insertion of the transgene cassette or multiple mutations in the second allele resulting in the absence of BRACHYURY protein. Loss of functional BRACHYURY protein has been shown to reduce *Blimp1*, *Prdm14* and *Ap2γ* expression in PGCLCs during the late streak stage of mouse embryogenesis (~E7.0) (Aramaki et al. 2013). Additionally, the expression of *Brachyury* within EpiLCs increases the expression of *Blimp1* and *Prdm14* when the cells are subjected to PGCLC differentiation (Aramaki et al. 2013). However, there is also evidence suggesting that *Brachyury* expression is not required for the generation of human PGCLCs (Kojima et al. 2017). The loss of functional *Brachyury* expression in human iPSCs was shown to have little effect on the expression of PGC markers in cells undergoing a PGCLC differentiation protocol compared to wildtype cells (Kojima et al. 2017). WNT-driven *Eomes* expression activated both *Sox17* and *Blimp1* gene expression, directing human iPSC differentiation towards human PGCLCs (Kojima et al. 2017). Therefore, the loss of *Brachyury* may not impact the ability of rat ESCs to differentiate into the germ cell lineage.

Interestingly, the expression of endoderm and trophectoderm markers were reduced within the $CD61^{+ve}$ populations of all three cell clones compared to the parental cell line. *Gata3* is normally upregulated in trophoblast stem cells and thought to be important for the development of the trophectoderm lineage during development (Ray et al. 2009, Home et al. 2009). The expression of *Brachyury* during gastrulation is reported to be important for the migration of ESCs out of the primitive streak to form the mesoendoderm (Rashbass et al. 1991, Wilson et al. 1997, Showell et al 2004). *In vivo*, $Brachyury^{-/-}$ null cells have defects in their cellular migration, leading to their accumulation within the primitive streak and eventual loss due to cellular apoptosis (Rashbass et al. 1991, Wilson et al. 1997, Showell et al 2004).

A study performed in human stem cells identified that loss of the BRACHYURY protein resulted in reduced expression of trophoblast and mesoderm markers when cultured in conditions designed to promote trophoblast generation (Bernardo et al. 2011). Therefore, the reduction of *Gata3* expression and reduced levels of the endoderm markers *Gata4* and *Gata6* in all cell clones during the PGCLC differentiation protocol might be due to the loss of the functional *Brachyury* expression within these cells. For future investigations, transgene cassettes would be designed so that insertion into the gene locus would not disrupt endogenous gene expression. By using 2A peptide or IRES sequences, expression of the endogenous gene and the transgene cassette can be linked, allowing for the co-expression of both when the endogenous promotor is activated. Alternatively, the use of other potential host gene targets to drive transcription factor expression should be considered to reduce any potential disruption to PGC specification.

Chapter 5 Directing differentiation via doxycycline-regulated expression of PGC transcription factors

5.1 Introduction

A previous study performed in mouse ESCs found that if transgene copies of the key PGC transcription factors (*Blimp1, Prdm14* and *Ap2γ*) were co-expressed in mouse EpiLCs, a proportion of these cells would then transition into a PGCLC fate (Nakaki et al. 2013). The proportion of PGCLCs generated from these cells was increased when transgene expression was induced during the PGCLC protocol described by Hayashi et al (Hayashi & Saitou 2013, Nakaki et al. 2013). If PGC transcription factors transgenes were expressed before the cells had transitioned into EpiLCs, the cells reverted back to or were maintained in the naïve state; while expressing the factors too late during the PGCLC differentiation protocol had no influence on the number of cells entering the PGCLC fate (Nakaki et al. 2013). The results presented in chapter 3 showed that simply applying the protocol used by Hayashi et al did not improve the contribution of rat ESCs to the PGC lineage. However, could the proportion of rat cells entering the germ cell lineage be improved by combining ESC differentiation with overexpression of key PGC transcription factors?

In this chapter, I present an experimental approach designed to manipulate the gene network of rat ESCs using a doxycycline-inducible Tet-On piggyBac transposon system. Transgene copies of the PGC transcription factors, BLIMP1, PRDM14 and AP2γ were placed under the regulation of a doxycycline-induced vector, and expressed during the differentiation of rat cells. The influence PGC transcription factor transgene expression had on transfected cells was monitored using quantitative measurement of PGC marker expression. Within this chapter, references to the Tet-On piggyBac transposon vectors will be shortened to “Tet-On” vectors.

5.2 Cloning PGC transcription factors into a Tet-On piggyBac transposon vectors

5.2.1 Tet-On piggyBac transposon system

The Tet-On piggyBac transposon backbone vector used during this investigation was provided by the Mcgrew group (Roslin Institute) (Glover et al. 2013). A schematic of the Tet-On vector and how the activation of gene expression is induced by doxycycline is shown in Figure 5.2.1.

When transfected into a cell line, the Tet-On vector is randomly integrated into the genome through the action of a co-transfected transposase enzyme (HYBASE) (Glover et al. 2013). Once integrated, the CAG promotor drives the expression of an rtTA3 protein, which under standard culture conditions has no influence on the host cell. However, when doxycycline is added to the culture medium, the rtTA3 protein forms a complex with doxycycline, allowing it to interact with and activate a TRE promotor, inducing the expression of a downstream gene of interest.

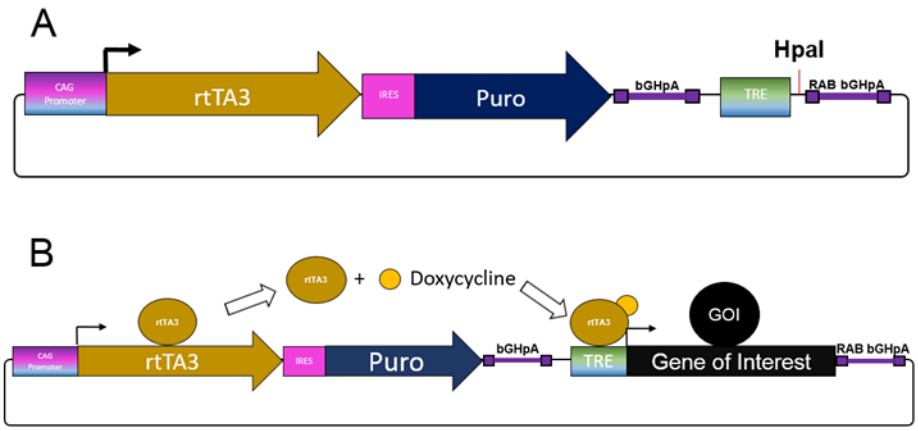

Figure 5.2.1: PB CAG rtTA3 TRE-Empty vector, as described by Glover et al. 2013. *(A) PB Tet-On vector contains a CAG enhancer/promoter (CAG Promotor) that drives the expression of a 3rd generation reverse tetracycline transactivator (rtTA3). This rtTA3 element is coupled to an Internal Ribosome Entry Site (IRES) and puromycin resistance gene (Puro). Downstream from this is a minimal tetracycline response element promoter (TRE), whose activation relies on the binding of rtTA3 bound to doxycycline. The HpaI restriction site (HpaI) can be cut to allow insertion of gene cassette to be driven by the TRE promotor. Downstream of this restriction site is a Rabbit Beta-globin PolyA signal (Rab bGHpA). (B) During standard culture conditions, rtTA3 cannot bind to the TRE reporter (TRE). When introduced to the medium, doxycycline binds to rtTA3 and induces a conformational change that allows association of rtTA3 with the TRE promotor. Binding of rtTA3 to the TRE promotor induces expression of downstream gene of interest.*

5.2.2 Generation of single PGC transcription factor expressing Tet-On vectors

The objective was to clone various combinations of PGC transcription factor cDNA into the Tet-On vector system. A 2A peptide was inserted between each transgene in the gene sequence to allow re-initiation of tandem open reading frames during translation (Liu et al. 2017). Rat BLIMP1 cDNA was synthesised by GeneArt Gene Synthesis (ThermoFisher Scientific), using the gene sequence on the Ensembl database (ENSRNOT00000076541.1). A 2A peptide was added downstream of the *Blimp1* sequence, followed by a mCherry cDNA sequence. The mCherry fluorescent marker was used for monitoring Tet-On vector activation when doxycycline was introduced to the culture medium. The complete BLIMP1-2A-mCherry cDNA sequence was PCR amplified from the GeneArt synthesis vector, with the amplifying primers adding homology to the Tet-On vector by primer overhangs. A kozak consensus sequence was also introduced by PCR primer overhangs to the 5' region upstream of the *Blimp1* sequence. The Tet-On vector was linearised using the restriction enzyme HpaI and the BLIMP1-2A-mCherry gene sequence inserted into the vector via Gibson cloning (Figure 5.2.2).

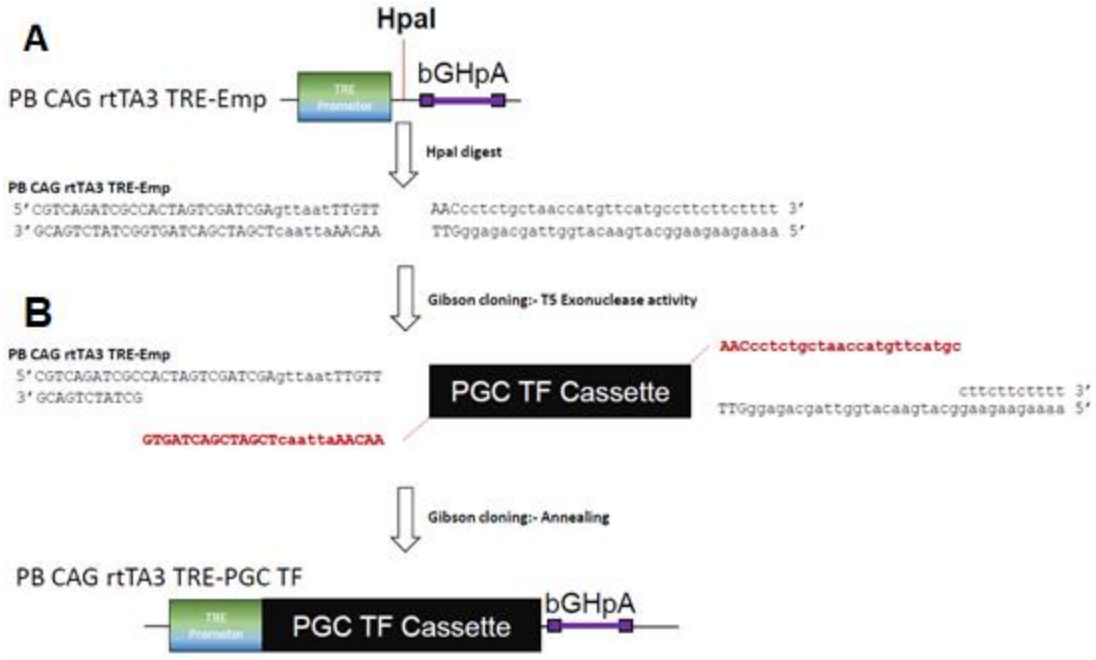

Figure 5.2.2. Strategy for generating Dox-inducible expression of PGC transcription factors. *(A) The empty Tet-On vector (PB CAG rtTA3 TRE-Emp) is linearised by a blunt end enzymatic digest with the HpaI restriction enzyme. (B) Gibson cloning is performed to incorporate a gene cassette (PGC TF Cassette) into the cut site. T5 exonuclease creates single-strand DNA overhangs, revealing the complementary sequence for the homology* arms present on the cassette. This allows the DNA fragment to subsequently anneal to each other, generating a re-circularised *vector with the gene cassette downstream of the Doxycycline dependant promotor (TRE promotor).*

Sanger sequencing of the resulting expression vector confirmed the insertion of the BLIMP1-2A-mCherry cassette into the Tet-On vector. Once verified, reverse PCR amplification was used to generate a linearised Tet-On vector lacking the *Blimp1* transgene.

This linearised vector was used to generate Tet-On vectors which would express rat *Prdm14* or *Ap2γ* in the presence of doxycycline. The rat *Prdm14* and *Ap2γ* genes were PCR amplified from cDNA generated from rat ESCs using oligonucleotides designed to the *Prdm14* (ENSRNOT00000034525.5) and *Ap2γ* (ENSRNOT00000006991.5) mRNA sequences from the Ensembl database. Homology to the Tet-On vector and the 2A-mCherry region was introduced during PCR amplification by primer overhangs. Gibson cloning was used to ligate the PGC transcription factor transgenes into the previously linearised 2A-mCherry Tet-On vector (Figure 5.2.3).

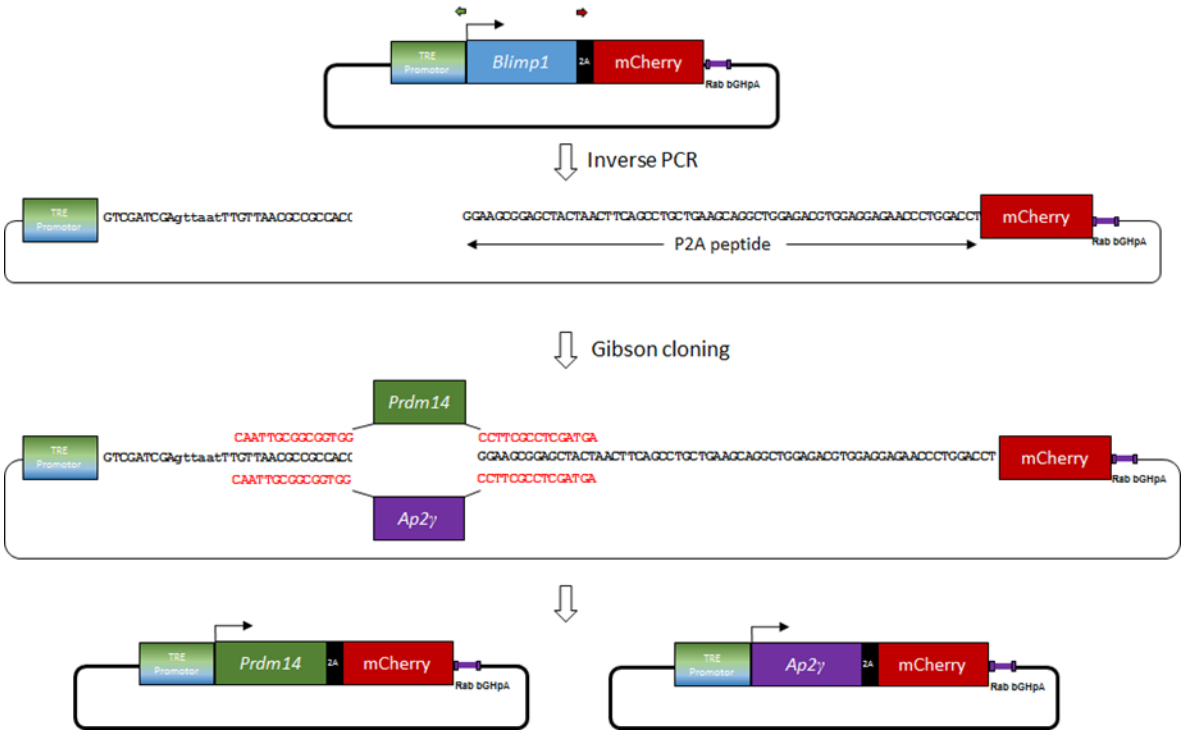

Figure 5.2.3. Ligation of Prdm14/Ap2y into the Tet-On vector. *Inverse PCR of the previously generated BLIMP1-2A-mCherry vector removes the Blimp1 transgene from the sequence while linearising the vector. Prdm14 or Ap2γ transgenes with homology arms to the linearised vector are annealed together to form a* re-circularised *expression vector by Gibson cloning.*

5.2.3 Generation of multiple PGC transcription factor expressing Tet-On vectors

Vectors containing two or all three PGC transcription factors were generated by Gibson cloning with multiple gene fragments. Each PGC transcription factor was amplified from sequence verified vectors, each gaining homology to their respective partner by PCR overhangs. During a “three-way” or “four-way” Gibson cloning reaction, each fragment would orientate themselves so that the cDNA sequence produced would be in the right orientation due to the homology arms. Each cDNA sequence was separated by a 2A peptide to ensure co-expression from a single Tet-On vector (Figure 5.2.4).

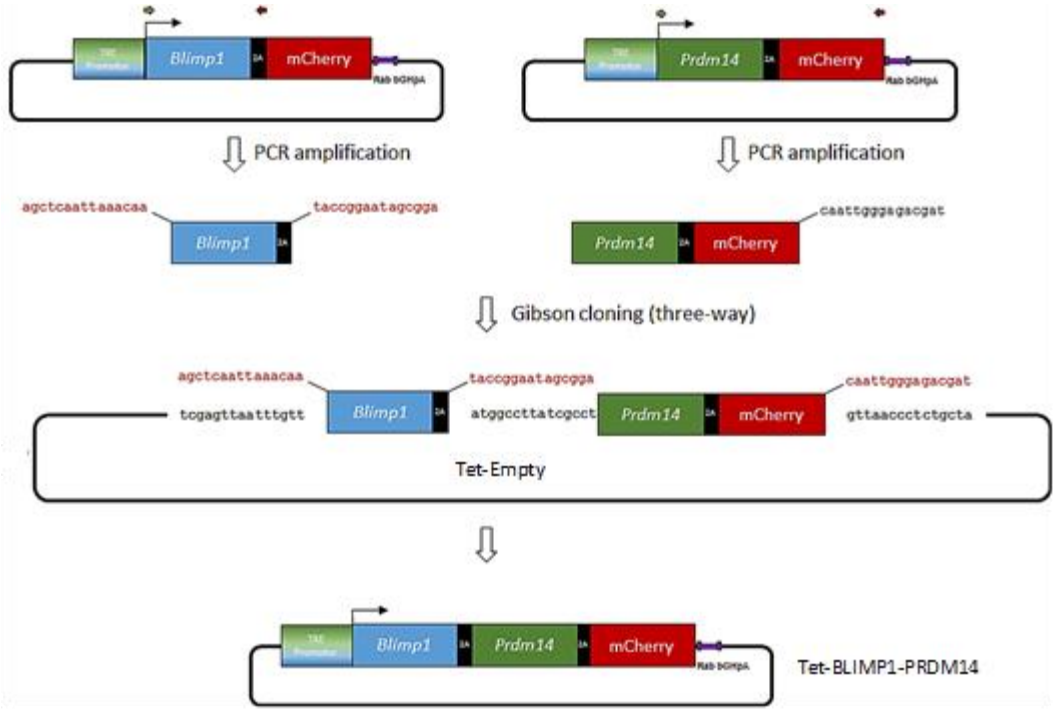

Figure 5.2.4. Schematic of how vectors containing multiple PGC transcription factors were generated. *Displayed is a “Three-way” Gibson cloning reaction, where three individual fragments are joined together to form one circular vector.*

5.2.4 List of generated Tet-On vectors generated

A list of the PGC transcription factor vectors generated is displayed in Table 5.2.1.

Table 5.2.1 Tet-On vectors constructed to express PGC transcription factors in the presence of doxycycline.

Vector name	Purpose	Fluorescence marker
Tet-EMPTY	Empty vector to act as control	None
Tet-BLIMP1	Express rat BLIMP1	mCherry
Tet-PRDM14	Express rat PRDM14	mCherry
Tet-AP2γ	Express rat AP2γ	mCherry
Tet-BLIMP1-PRDM14	Express rat BLIMP1 & PRDM14	mCherry
Tet-BLIMP1-AP2γ	Express rat BLIMP1 & AP2γ	mCherry
Tet-BLIMP1-PRDM14-AP2γ	Express all 3 rat PGC transcription factors	mCherry

5.3 Producing stably transfected rat ESC pools with Tet-inducible PGC transcription factors

5.3.1 Transfection of rat ESC pools with the Tet-On vectors

Three independent rat ESC lines, two dark agouti (DAK31 and E3) and one Sprague-Dawley (A4), were transfected with the generated Tet-On vectors using Lipofectamine LTX. A Tet-On vector containing no gene insert at the HpaI site (Tet-Empty) was used as both a puromycin-resistant positive control and doxycycline negative control. The transposase enzyme HYBASE was co-transfected at a 1:1 ratio with the Tet-On vectors to ensure incorporation of the vectors into the ESC genome. Transfections using a range of plasmid DNA concentrations were tested, with 500ng/ml total plasmid DNA in a 24-well having the best transfection efficiency whilst limiting the cell death evident at higher DNA/LTX concentrations. Therefore, 250ng/ml of each Tet-On vector was co-transfected with 250ng/ml of HYBASE. Transfected cell pools were then subjected to puromycin selection (1µg/ml) to isolate cells with stable integration of the Tet-On vector. Cells were routinely passaged every 2 days into 24-well plates containing MEFs in 2i+LIF medium at a cell density of 1.5×10^5 cells. Pools of stably transfected cells showed similar growth and morphology to the parental wildtype after 2 days of culture. However, pools containing Tet-On vectors with multiple PGC transcription factors did show a slower growth rate than the parental, resulting in smaller colonies after 2 days of growth (Figure 5.3.1).

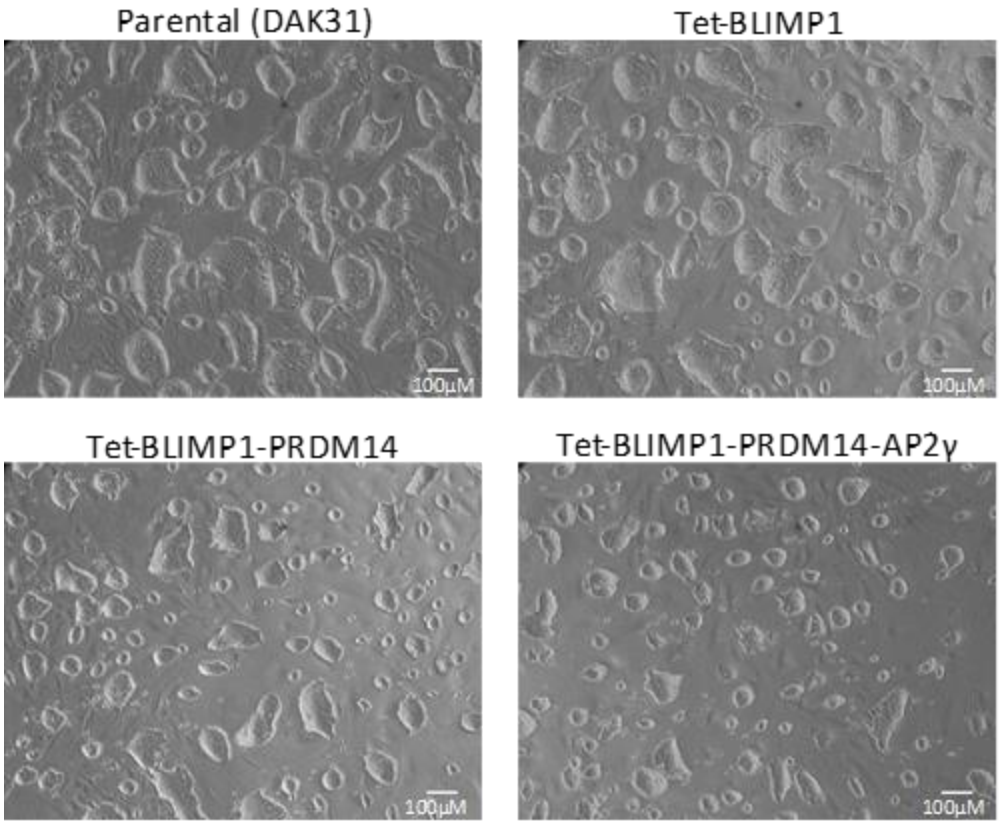

Figure 5.3.1 Stably transfected cells containing Tet-On vectors. *Bright field photographs of cell pools of DAK31 rat ESCs containing 3 of the Tet-On vectors compared to the parental when cultured in standard 2i+LIF conditions for 2 days. Each pool was seeded at 1.5 x 10^5 cells on MEF layers. Pools from all rat cell lines showed reduced growth rate and colony size when stably transfected with Tet-On vectors containing multiple PGC transcription factors.*

5.3.2 mCherry expression in transfected cells cultured with doxycycline

Expression of PGC transcription factor/mCherry gene cassettes was induced by culturing the transfected cell pools in medium containing 1µg/ml doxycycline for up to 48 hours. Expression of the mCherry fluorescent marker in the presence or absence of doxycycline was monitored using both fluorescent microscopy (Figure 5.3.2) and by flow cytometry (Figure 5.3.3). The gating strategy detailed in section 2.6.7 was used. The remaining cells were gated to isolate populations of mCherry^{+ve} cells by plotting mCherry (610/20A) versus cell counts. The gates were set against rat ESCs transfected with the Tet-Empty vector.

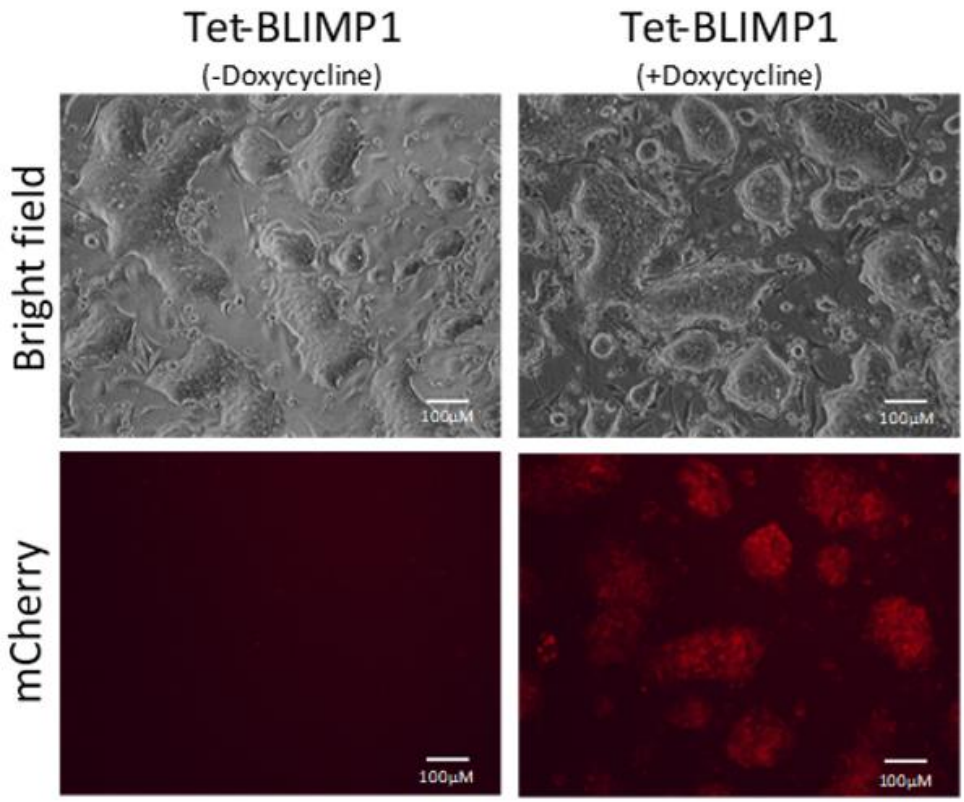

Figure 5.3.2. mCherry fluorescence from Tet-BLIMP1 vector DAK31 ESC pools cultured in the presence of doxycycline. *Photographs show Tet-BLIMP1 transfected cells cultured in 2i+LIF medium in the presence (+) or absence (-) of doxycycline for two days.*

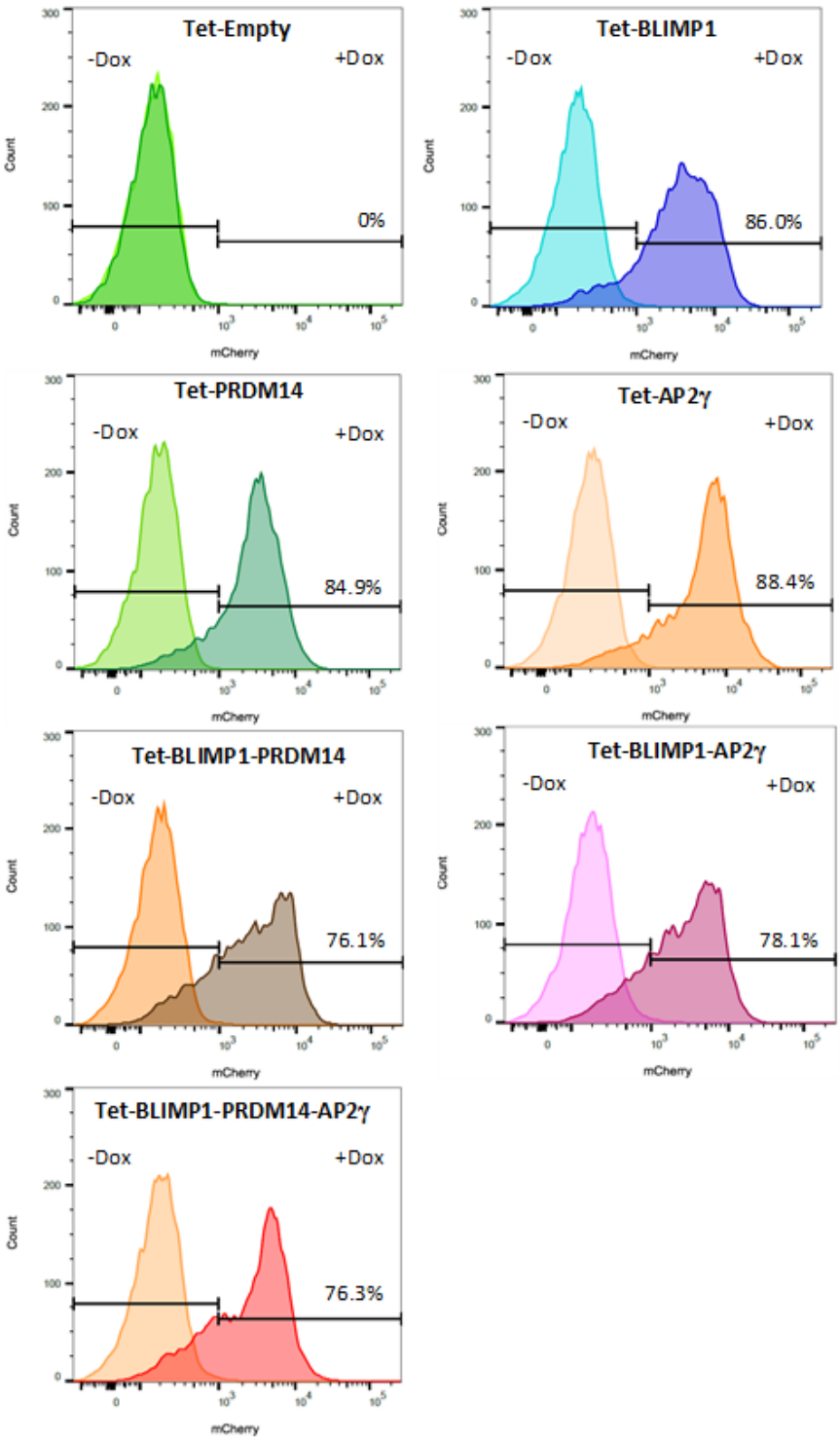

Figure 5.3.3. Flow cytometry plots showing mCherry expression from Tet-On vector cell pools. *Histograms represent the number cells expressing mCherry in the presence (+dox) and absence (-dox) of doxycycline. Paler peaks represent cells cultured in –dox conditions, while darker peaks represent those cultured +dox conditions. Percentages of cells which were mCherry^{+ve} in +dox conditions are highlighted.*

Both detection methods showed that transfected cells cultured in the presence of doxycycline were positive for mCherry expression. The expression profiles and intensity of mCherry expression from all three rat cell lines were similar, indicating that efficiency of doxycycline induced Tet-On vector activation was equally effective in all cell lines. The flow cytometry data presented in Figure 5.3.3 showed cells expressing multiple PGC transcription factor transgenes had more variable intensity of mCherry expression when compared to the distinct peaks seen from cells expressing a single transgene. Additionally, the flow cytometry data showed that even when stably transfected pools were cultured in the presence of 1µg/ml puromycin for an extended period, there were cells within that population which were mCherry negative in the presence of doxycycline (Figure 5.3.3).

5.3.3 qRT-PCR analysis of transfected cell pools cultured with doxycycline

The expression of mRNA transcripts from transfected cell pools was determined by performing qRT-PCR analysis on RNA processed from cells cultured in the presence and absence of doxycycline (Figure 5.3.4). The results represent the average transcript expression taken from the three independent rat ESCs. All cell lines transfected with a Tet-On vector containing at least a single cDNA copy of a PGC transcription factor saw significantly increased total mRNA transcript level of the PGC transcription factors they were expressing compared to the Tet-On Empty vector (Figure 5.3.4). Increased PGC transcription factor expression in the single, double and triple Tet-On vectors were very similar (Figure 5.3.4), indicating that the complexity of the larger vectors was not affecting the activation of the transgene cassettes in the presence of doxycycline.

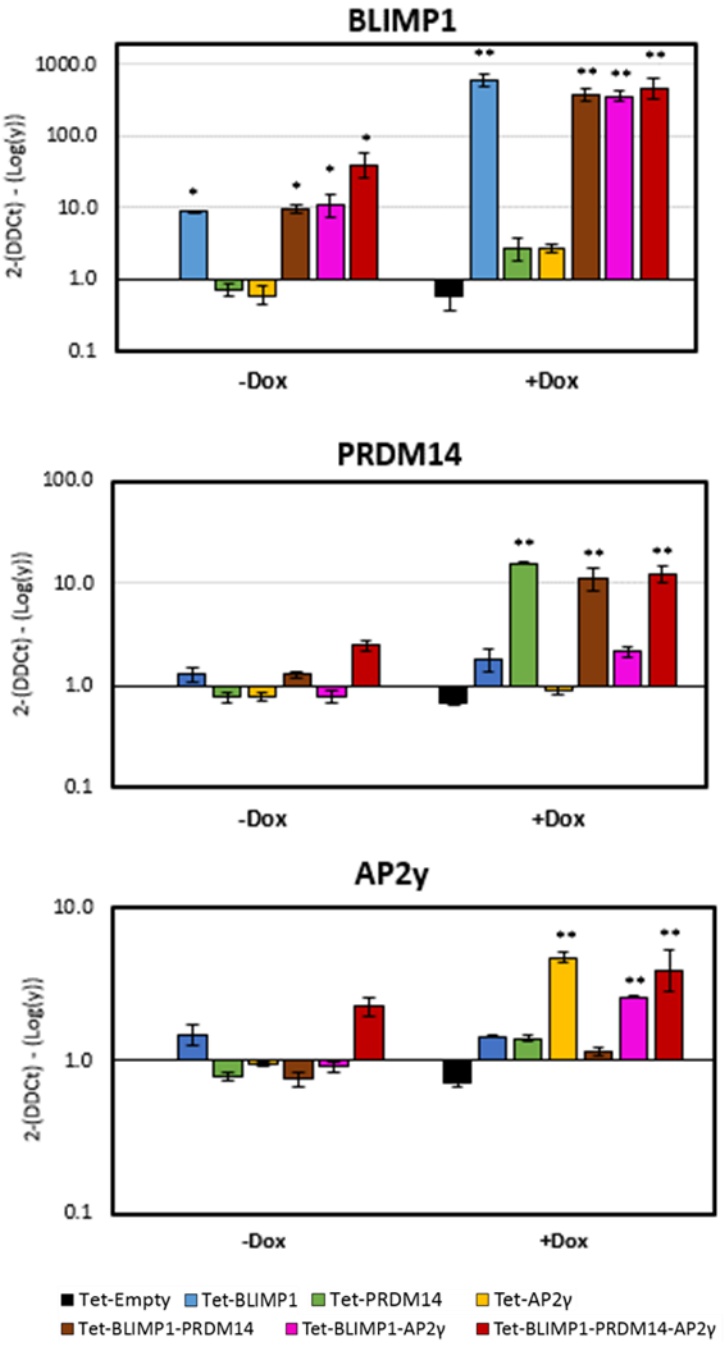

Figure 5.3.4. qRT-PCR analysis of Tet-On transfected ESC pools in presence and absence of doxycycline. *Average of three independent rat cell lines (two DA lines, one SD line). All data was normalised to the house keeping gene β-actin (dCT) and the fold change (2-DDCT) values (Log scale) generated by normalising gene expression to –Dox Tet-Empty transfected cell pools. Bars represent mean ± SD, *P<0.05, **P<0.01.*

5.4 Embryoid body (EB) differentiation of stably transfected rat ESCs

5.4.1 Activation of PGC transcription factor transgene expression during an undirected EB differentiation protocol

PGC transcription factor transgene expression was induced at different stages during an undirected embryoid body differentiation protocol in order to identify whether the PGC transcription factors could induce the expression of endogenous PGC markers, potentially directing a proportion of the cell population towards a germ cell-like fate. The three rat cell lines transfected with the Tet-On vectors were induced to differentiate via embryoid body (EB) differentiation for 6 days using EB differentiation protocol designed for rat ESCs (Figure 5.4.1).

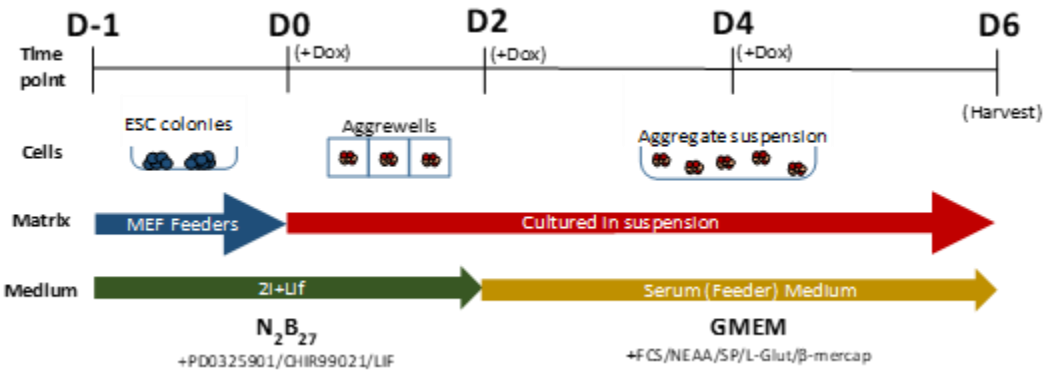

Figure 5.4.1: Schematic of the rat EB differentiation protocol. *Rat ESCs cultured in 2i+Lif conditions on a MEF layer were transferred to an aggrewell™ plate at a cellular density equivalent to 3,000 cells per microwell depression. After 2 days, the cell aggregates were transferred from the aggrewell™ plate to low adhesion plates with serum medium. These aggregates were retained in this condition for a further 4 days and then harvested at day 6. Doxycycline was introduced at Day 0, Day 2 and Day 4. Once introduced, doxycycline was maintained in the medium until the cells were harvested (day 6).*

In summary, the protocol involved culturing cells in suspension in 2i+LIF conditions for 2 days to allow for cellular aggregation. Moving rat ESCs directly into serum medium induced widespread cellular death, therefore, it was important to perform an intermediate aggregation step in 2i+LIF medium. These aggregates were then moved into serum medium for a further 4 days to induce transition out of the naïve state. This transition was monitored by the loss of Rex1-EGFP expression from the E3 rat cell line during the EB differentiation protocol (Figure 5.4.2).

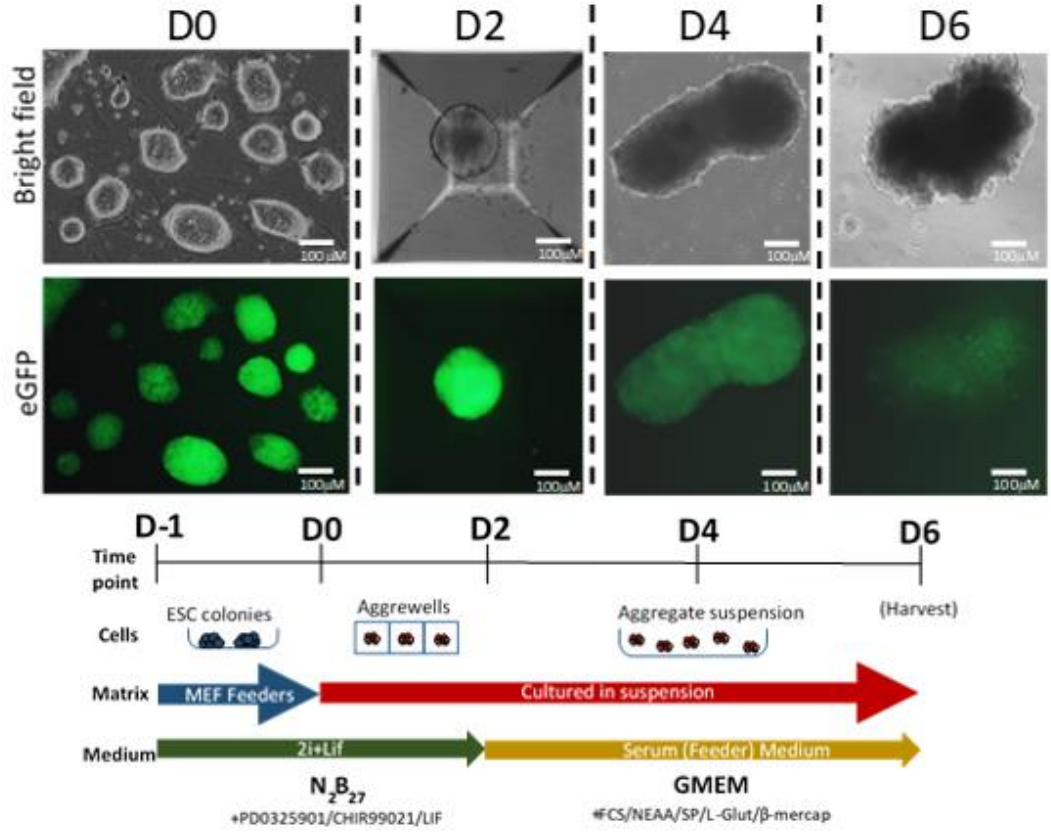

Figure 5.4.2. eGFP fluorescence from Tet-empty transfected cells undergoing an EB differentiation protocol. *Photographs depict Tet-empty cells at day 0, day 2, day 4 and day 6 of the EB differentiation protocol. The bottom panels show the reduction of eGFP expression as the cells differentiate out of the naïve ESC state (day 0).*

Doxycycline was introduced into the culture medium at different time points (Day 0, Day 2 or Day 4) to induce expression of the transgene cassettes within the incorporated Tet-On vectors. Transfected cells which were not exposed to doxycycline were used to monitor leakiness from the Tet-On vectors and whether this leakiness could influence gene expression.

Tet-On vector activation by doxycycline was determined by monitoring mCherry expression using fluorescent microscopy. In all cases, cells containing a mCherry expressing Tet-On vector cultured in the presence of doxycycline from Day 0, Day 2 (Figure 5.4.3A) or Day 4 (Figure 5.4.3B) showed mCherry expression. No mCherry was visible from cells cultured in the absence of doxycycline or transfected with the Tet-Empty vector (Figure 5.4.3A & B).

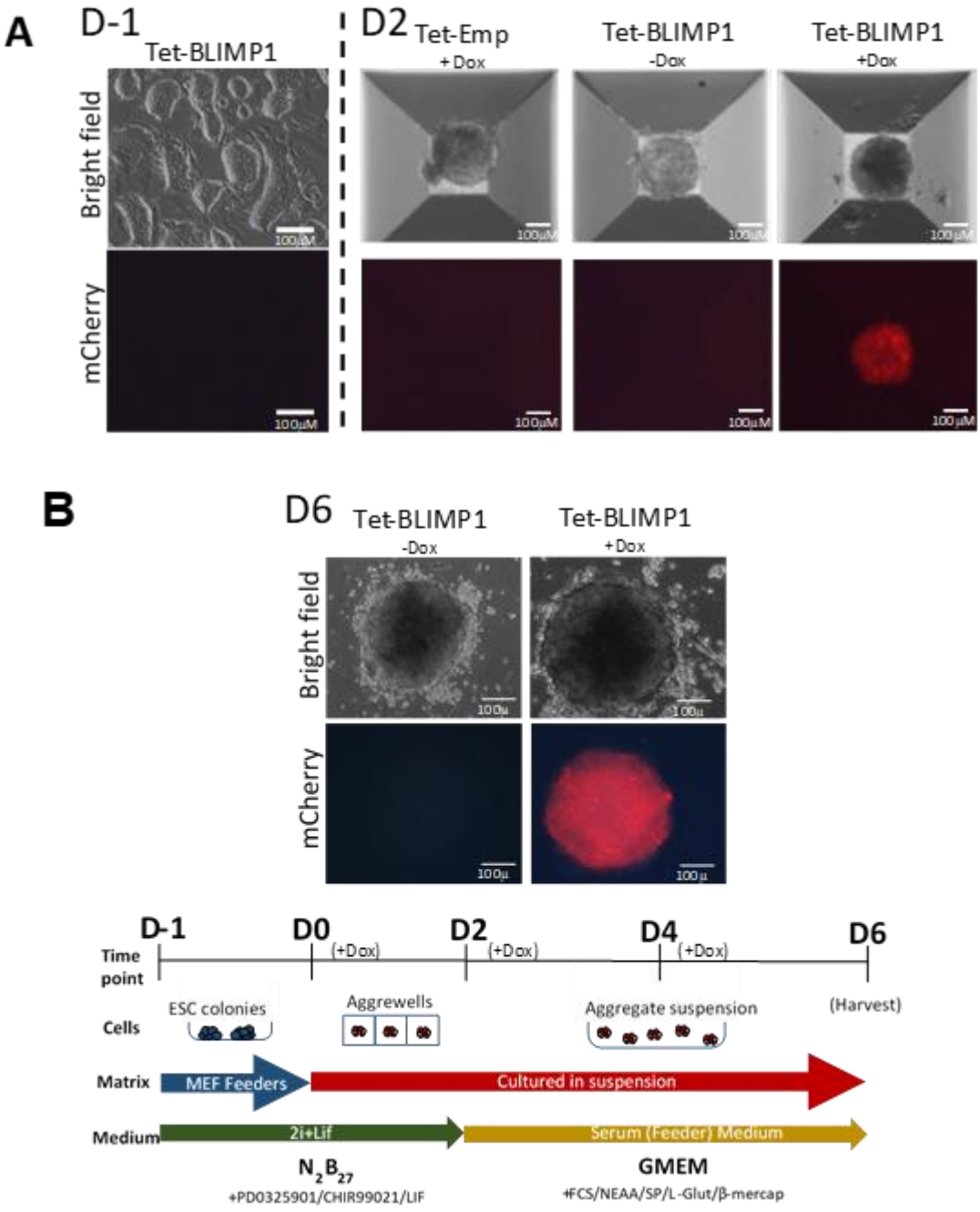

Figure 5.4.3 mCherry fluorescence from Tet-BLIMP1 transfected cells undergoing an EB differentiation protocol. *(A) Expression of mCherry in Tet-BLIMP1 transfected cells at day 0 and day 2 of the EB differentiation protocol in the presence and absence of doxycycline. Tet-Empty cells in the presence of doxycycline showed no mCherry expression. Tet-BLIMP1 cells cultured in the presence of doxycycline from day 0 showed mCherry expression, while those in its absence did not. (B) Expression of mCherry in Tet-BLIMP1 transfected cells at day 6 of the EB differentiation protocol. Cells cultured in the absence of doxycycline remained mCherry^{-ve} while those cultured in doxycycline were mCherry^{+ve}.*

To assess the effect of PGC transcription factors transgene expression on rat ESC differentiation, expression of pluripotency and PGC markers were analysed by qRT-PCR. Aggregates were pelleted after the 6-day EB differentiation protocol and RNA processed for qRT-PCR analysis. The results represent the average transcript expression taken from the three independent rat cell lines.

qRT-PCR analysis revealed that all Tet-On vector transfected cells showed a significant increase in transcript expression of their respective PGC transcription factors compared to Tet-Empty cells, regardless of which day doxycycline was introduced into the medium (Figure 5.4.4). Significant rises in *Blimp1* expression was seen from all Tet-On vectors compared to Tet-Empty transfected cells (Figure 5.4.4). Interestingly, increased expression of *Blimp1* was seen at day 0 within Tet-On transfected cells (Figure 5.4.4), when the cells were in an ESC state prior to the addition of doxycycline. This could be due to vector 'leakiness', where low level expression from the Tet-On vector is present even in the absence of doxycycline. The transcript expression of both *Prdm14* and *Ap2γ* exhibited similar significant rises in the presence of doxycycline (Figure 5.4.4). The Tet-On vectors which expressed two PGC transcription factors showed a smaller rise in transcript expression of the second gene in the cassette compared to vectors expressing only a single transgene (Figure 5.4.4). The Tet-On vector containing cDNA copies of all three genes had lower expression of all PGC transcription factors compared to the single vectors, with *Blimp1* showing the greatest reduction in total transcript level (Figure 5.4.4). This suggests that the mRNA transcript generated from the transgene cassette may have had compromised stability due to its complexity, reducing the total transcript expression level of these genes.

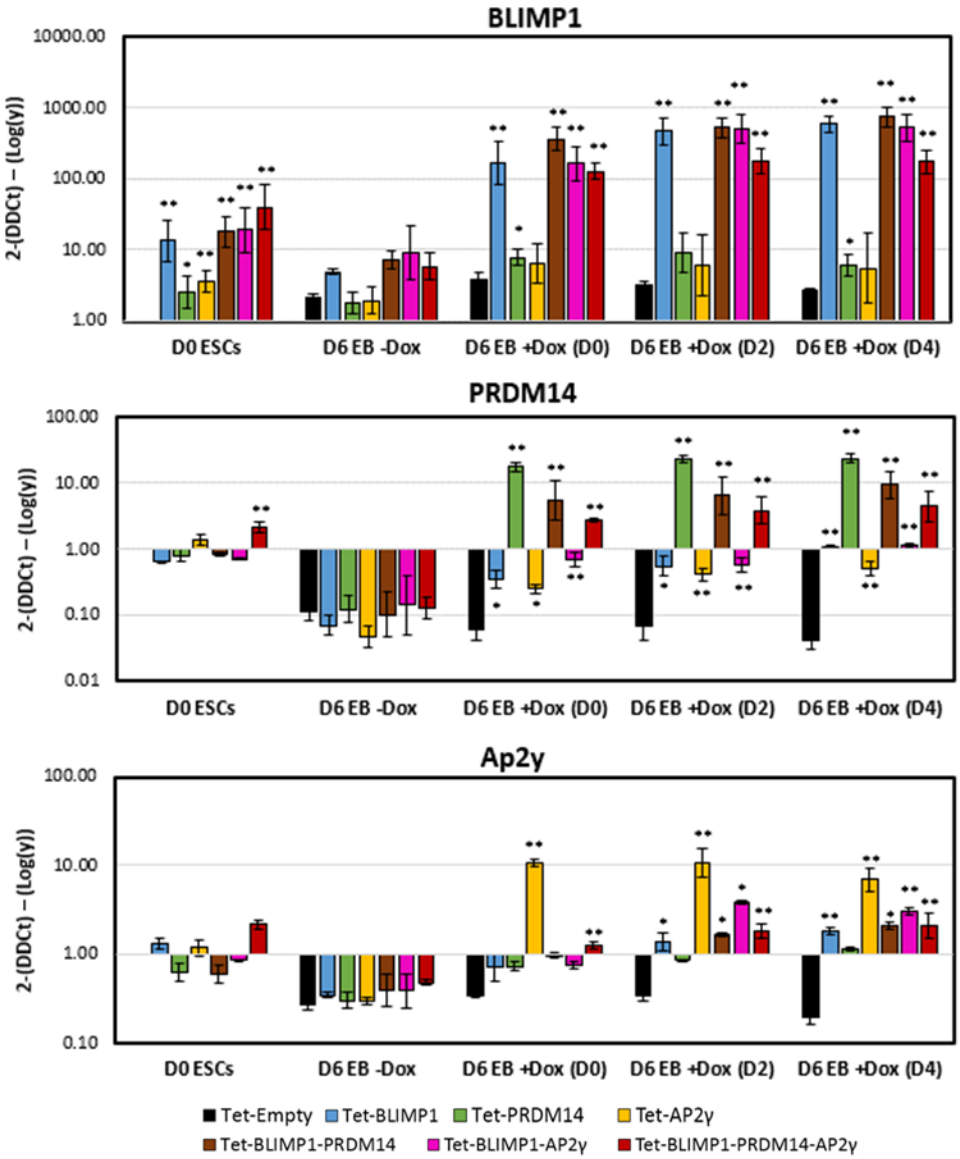

Figure 5.4.4. qRT-PCR analysis of PGC transcription factors within Tet-On transfected cells after a 6-day EB differentiation protocol. *Average of three independent rat cell lines (two DA lines, one SD line). All data was normalised to the house keeping gene β-actin (dCT) and the fold change (2-DDCT) values (Log scale) generated by normalising gene expression to day 0 Tet-Empty transfected cells. (D0), (D2), (D4) represent cells which were cultured in the presence of doxycycline from day 0, day 2 and day 4 of EB differentiation respectively. Bars represent mean ± SD, *P<0.05, **P<0.01.*

Expression of *Blimp1*, *Ap2γ* or any combination of two PGC transcription factors induced a significant increase in *Nanog* compared to the Tet-Empty transfected cells (Figure 5.4.5). This difference was most noticeable when doxycycline was introduced at day 4 of EB differentiation onwards (Figure 5.4.5). Interestingly, the expression levels of cells containing a Tet-On vector with either a combination of two PGC transcription factors or *Prdm14* alone showed a significant drop in *Nanog* expression at day 0, when cells are in an ESC state (Figure 5.4.5).

This may suggest that the leakiness of these Tet-On vectors was affecting the basal gene expression in ESCs. In all but one case, there was no significant difference in *Oct4* expression in the presence or absence of doxycycline (Figure 5.4.5). A significant drop in *Oct4* could be identified in cells expressing *Ap2γ* transgene alone when cultured in doxycycline at day 0 onwards, suggesting that *Ap2γ* may have a suppressive effect on *Oct4* expression within these cells (Figure 5.4.5).
The expression of *Stella*, both a marker of naïve ESCs and germ cells (Wongtrakoongate et al. 2013), was significantly increased when transgene copies of *Blimp1* or *Prdm14* or both were expressed from day 0 of the EB differentiation protocol (Figure 5.4.5).

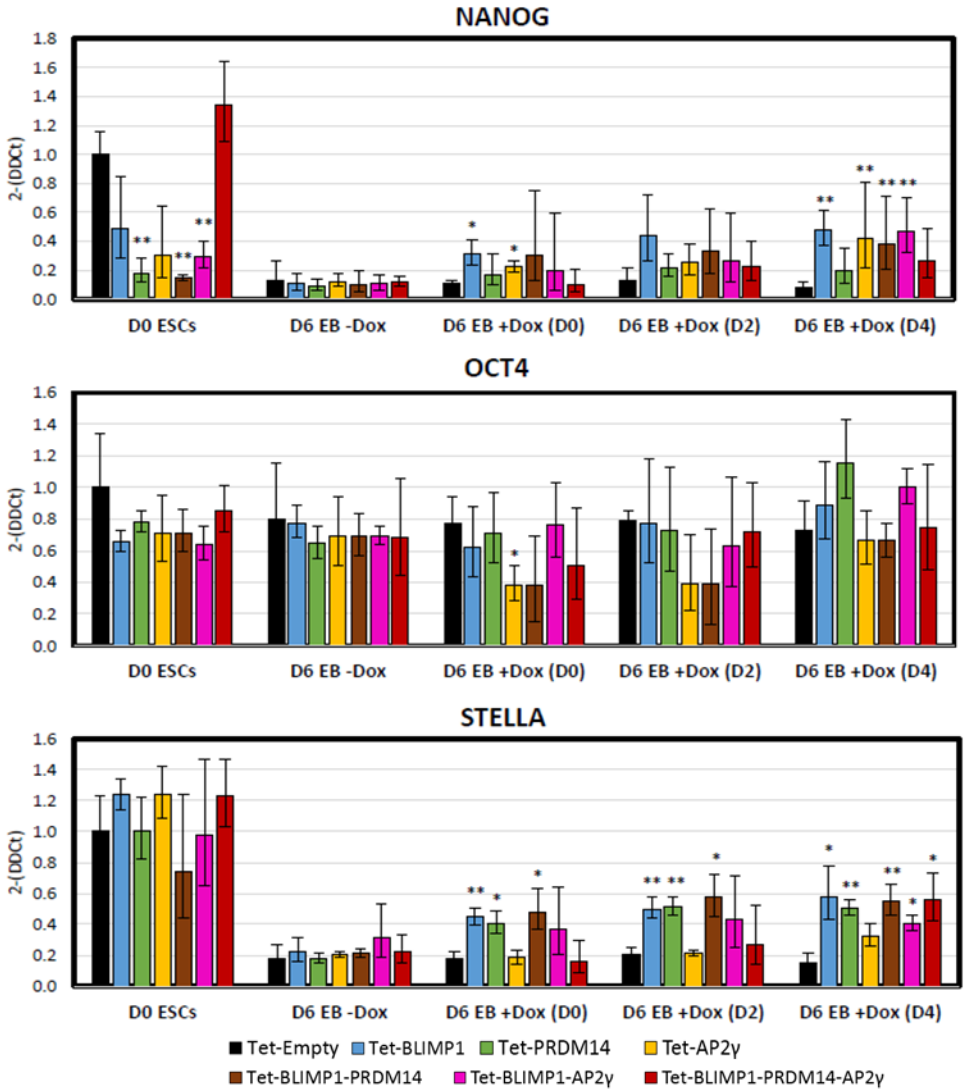

Figure 5.4.5. qRT-PCR analysis of pluripotency markers in Tet-On transfected cells after a 6-day EB differentiation protocol. *Average of three independent rat cell lines (two DA lines, one SD line). All data was normalised to the house keeping gene β-actin (dCT) and the fold change (2-DDCT) values generated by normalising gene expression to day 0 Tet-Empty transfected cell. (D0), (D2), (D4) represent cells which were cultured in the presence of doxycycline from day 0, day 2 and day 4 of EB differentiation respectively. Bars represent mean ± SD, *P<0.05, **P<0.01.*

Expression of PGC transcription factor transgenes induced a significant rise in both *Nanos3* and *Dazl* expression after the 6-day EB differentiation protocol, most notably when the transgenes were expressed from day 4 onwards (Figure 5.4.6). Tet-BLIMP1-PRDM14 transfected cells had the greatest increase in *Nanos3* transcript when cultured in the presence of doxycycline (Figure 5.4.6). Tet-BLIMP1-PRDM14 was the only vector to increase *Nanos3* expression in rat cells from day 0 of the EB differentiation protocol (Figure 5.4.6). Tet-BLIMP1, Tet-PRDM14 and Tet-BLIMP1-AP2γ transfected cells had a significant rise in *Nanos3* when cultured with doxycycline from day 2 (Figure 5.4.6). Cells transfected with Tet-BLIMP1-AP2γ had similar *Nanos3* transcript expression level to cells transfected with Tet-BLIMP1-PRDM14 when both were cultured in doxycycline from day 4 (Figure 5.4.6).
Tet-BLIMP1 and Tet-PRDM14 both induced a significant increase in *Dazl* expression when doxycycline was introduced to the medium from day 4 onwards (Figure 5.4.6). However, Tet-BLIMP1-PRDM14 and TET-BLIMP1-AP2γ both induced a significant rise in *Dazl* when activated from day 0 onwards, and prompted the greatest changes when induced from day 4 (Figure 5.4.6).
The transcript expression levels of *Vasa* showed no significant increase from any transfected cell line in the presence or absence of doxycycline (Figure 5.4.6). In Tet-AP2γ, Tet-BLIMP1-PRDM14 and Tet-BLIMP1-AP2γ transfected cells, there was a significant decrease in *Vasa* expression when the exogenous PGC transcription factors were expressed from day 2 of the EB differentiation protocol (Figure 5.4.6). The cells transfected with the Tet-BLIMP1-PRDM14-AP2γ vector showed no significant changes in the expression of any PGC gene marker when cultured in the presence of doxycycline (Figure 5.4.6). This result was most likely due to the reduced transcript expression of the three PGC transcription factors in cells transfected with the Tet-BLIMP1-PRDM14-AP2γ vector.

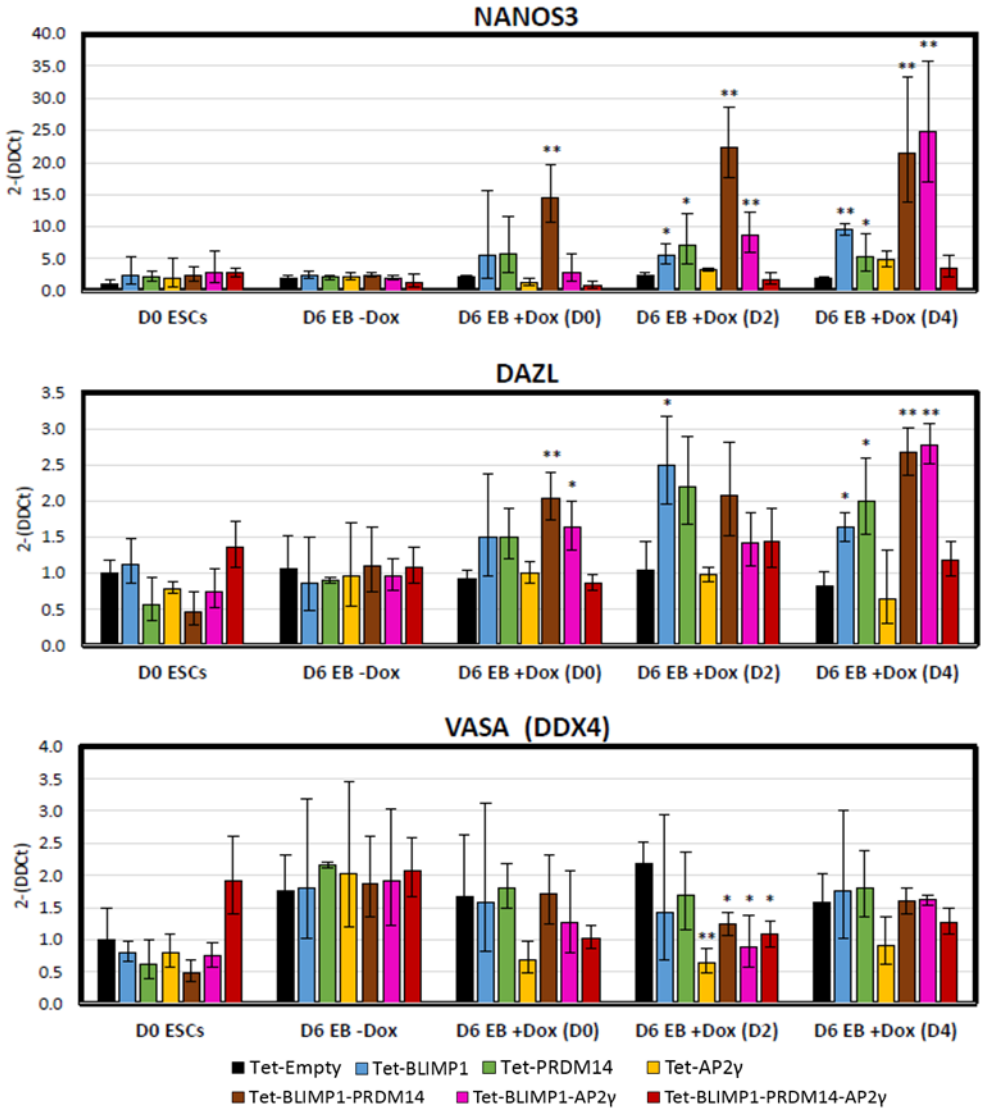

Figure 5.4.6. qRT-PCR analysis of PGC gene markers in Tet-On transfected cells after a 6-day EB differentiation protocol. *Average of three independent rat cell lines (two DA lines, one SD line). All data was normalised to the house keeping gene β-actin (dCT) and the fold change (2-DDCT) values generated by normalising gene expression to day 0 Tet-Empty transfected cells. (D0), (D2), (D4) represent cells which were cultured in the presence of doxycycline from day 0, day 2 and day 4 of EB differentiation respectively. Bars represent mean ± SD, *P<0.05, **P<0.01.*

In summary, the qRT-PCR data generated suggested that expression of PGC transcription factor transgenes could induce a significant rise in PGC gene markers during an undirected EB differentiation protocol. The greatest induction of endogenous PGC markers was achieved by co-expressing a combination of two PGC transcription factor transgenes, *Blimp1* in combination with either *Prdm14* or *Ap2γ*. Although the formation of functional PGC transcription factor protein has not been proven from transgene vectors, increased gene expression from cells transfected with the transgene vectors compared to the control cells suggests these transgene factors are the cause of increased PGC marker expression.

5.4.2 Changes in PGC marker expression were the result of transgene expression, not the presence of doxycycline

As previously shown (section 5.3.2), mCherry expression can be used as a marker the activation of Tet-On vectors when cultured in the presence of doxycycline. To examine whether the changes in PGC marker gene expression were exclusively inherent to the mCherry positive cells and not to non-cell autonomous effects, cells which had been transfected with the Tet-BLIMP1-PRDM14 and Tet-BLIMP1-AP2γ vectors were subjected to the EB differentiation protocol alongside Tet-Empty transfected cells. Expression of the transgene cassettes was induced at day 4 of the EB differentiation protocol by introducing doxycycline into the serum medium during the suspension culture phase. These conditions were chosen as they showed the greatest difference in expression of the PGC marker genes *Nanos3* and *Dazl*. At day 6, cells were sorted into mCherry positive (mCherry^{+ve}) and negative (mCherry^{-ve}) populations by fluorescence activated cell sorting (FACs) (Figure 5.4.7A). The gating strategy detailed in section 2.6.7 was used. The remaining cells were gated to isolate populations of mCherry^{+ve} cells by plotting mCherry (610/20A) versus cell counts. The gates were set against rat ESCs transfected with the Tet-Empty vector. The sorted populations were then analysed by qRT-PCR to determine which population had the greatest changes in gene expression (Figure 5.4.7B).

Flow data generated during FACs determined that only ~50% of the cells were mCherry^{+ve} (Figure 5.4.7A). Since the Tet-On transposons are randomly integrated into the genome of ESCs, this result may have arisen through Tet-On vector silencing, where copies of the transposon cassette have been inserted into genomic regions which become inactive during cell differentiation.

Of those cells which were mCherry^{+ve}, there was a substantial increase in almost all PGC transcription factors and PGC gene markers compared to the mCherry^{-ve} population and Tet-Empty transfected cells (Figure 5.4.7B). As all populations were cultured in the presence of doxycycline, changes in transcript expression were in response to PGC transcription factor transgene expression rather than a response to doxycycline. Therefore, it appears that expression of PGC transcription factor transgenes during an EB differentiation protocol does induce expression of PGC markers and may potentially guide a greater proportion of differentiating cells towards a PGC-like state.

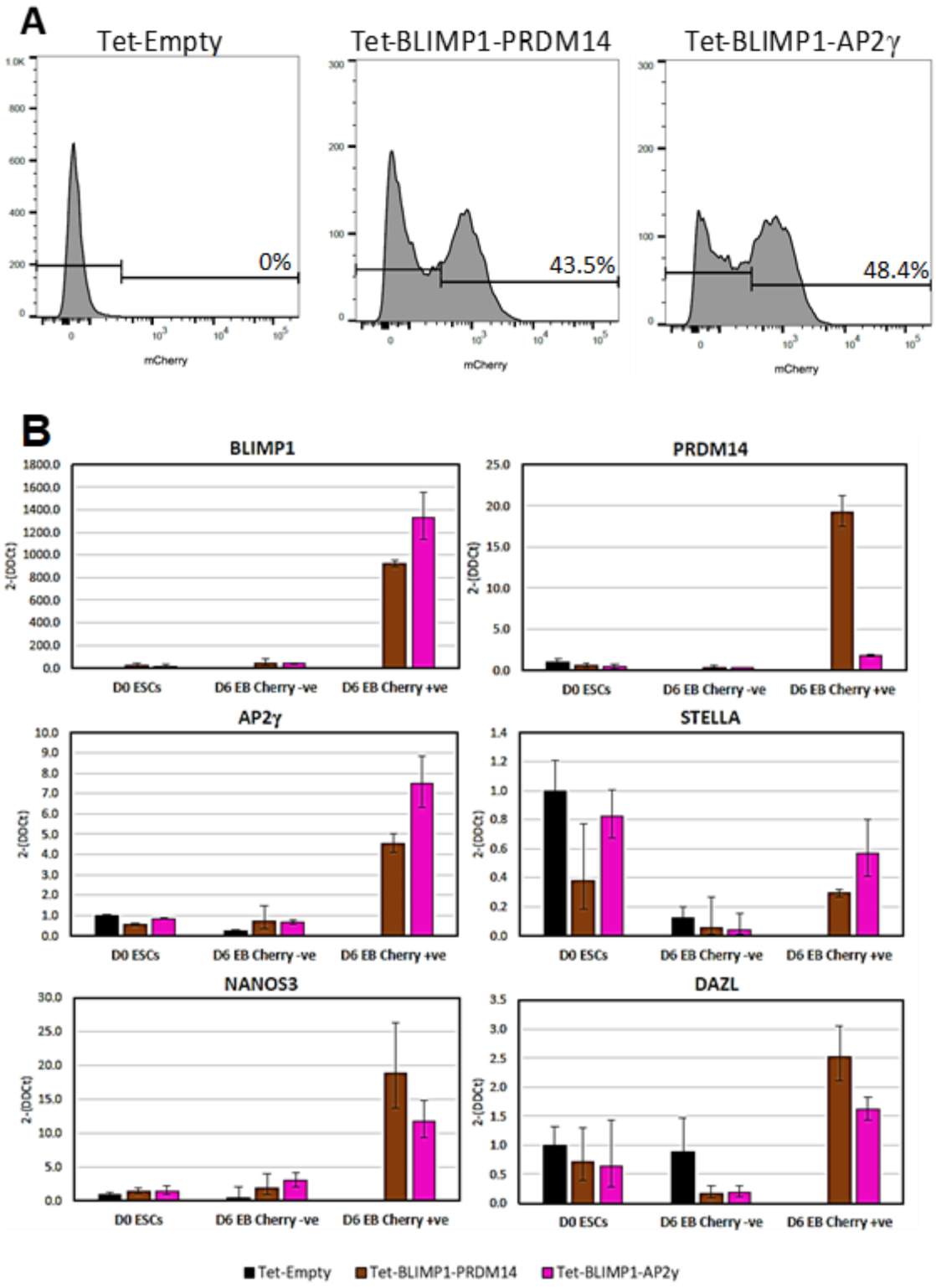

Figure 5.4.7: Sorting mCherry^{+ve} and mCherry^{-ve} populations of Tet-On transfected cells after undergoing an EB differentiation protocol. (*A) FACs plots of D6 EBs separating mCherry positive and negative populations. (B) qRT-PCR data generated from Tet-BLIMP1-PRDM14 and Tet-BLIMP1-APy mCherry positive and negative populations. The data presented was an average of two experiments performed with Tet-On vector transfected DAK31 cells. All data was normalised to the house keeping gene β-actin (dCT) and the fold change (2-DDCT) values generated by normalising gene expression to day 0 Tet-Empty transfected cells. Bars represent mean ± SD.*

5.4.3 Exogenous expression of all three PGC transcription factors from multiple Tet-vectors

ESCs containing the Tet-On vector designed to express transgene copies of all three PGC transcription factors (Tet-BLIMP1-PRDM14-AP2γ) did show strong induction of the PGC transcription factor cassette in the presence of doxycycline (sections 5.3.2 & 5.3.3). However, during the EB differentiation protocol, the total transcript expression of the PGC transcription factors and the mCherry fluorescent marker was much lower than vectors containing one or two PGC transcription factor transgenes (section 5.4.1). This was seen in all three cell lines, suggesting that the design or construction of the Tet-BLIMP1-PRDM14-AP2γ expression vector was suboptimal.

A second attempt was made to construct a vector co-expressing all three PGC transcription factors by introducing a transgene copy of *Ap2γ* downstream of the Blimp1-2A-Prdm14 cassette present in the Tet-BLIMP1-PRDM14 vector. This *Ap2y* transgene had a different 2A peptide attached to the 5' end as it is reported that vectors comprising of multiples of the same 2A peptide are less efficient than those using different 2A peptides (Liu et al. 2017). The newly constructed vector however did not show improved transcript expression compared to the first constructed vector.

As co-expression of all genes from a single expression vector was proving difficult, an alternative strategy was implemented to co-transfect three independent Tet-On vectors, each expressing a single PGC transcription factor transgene into the same population of cells. Addition of doxycycline to the culture medium would then drive each Tet-On vector separately to induce the co-expression of all three PGC transcription factors. Two additional Tet-On vectors were constructed, the first was a *Blimp1* expressing Tet-On vector without a fluorescent marker, the second an *Ap2γ* expressing Tet-On vector with a blue fluorescent protein (BFP) instead of mCherry (Table 5.4.1). The reason for the lack of a fluorescence marker on one vector was to reduce the need for compensation if these cells were to be stained for any other marker.

Table 5.4.1. Newly designed vectors for expressing all three PGC transcription factors within the same cell population

Vector name	Purpose	Fluorescence marker
Tet-BLIMP1-NO	Express rat BLIMP1	None
Tet-AP2γ-BF	Express rat AP2γ with a blue fluorescent marker	BFP

A wild-type DAK31 cell line was transfected with the Tet-On BLIMP1-NO vector and placed into puromycin selection to remove un-transfected cells. This resulted in a population of cells which would express *Blimp1* transgene in the presence of doxycycline without fluorescence. The Tet-BLIMP1-NO cells were co-transfected with the Tet-On PRDM14 vector with mCherry (described previously) and the newly constructed Tet-AP2γ-BF vector. After two days recovery, the cells were cultured with doxycycline for 12 hours to induce the expression of the fluorescent markers. These cells were then sorted via FACs, plating cells expressing both mCherry and BFP into 24-well plates to recover and grow. The gating strategy detailed in section 2.6.7 was used. However, the live cells were not gated due to the overlap of blue fluorescent staining with the DAPI antibody. The remaining cells were gated to isolate populations of double positive cells by plotting mCherry (610/20A) versus blue fluorescence (450/50). The gates were set against rat ESCs transfected with the Tet-Empty vector. Plated cells were cultured in the presence of puromycin and the absence of doxycycline to allow the cells to recover from sorting. To distinguish these cells from those transfected with the Tet-BLIMP1-PRDM14-AP2γ vector, this cell line was referred to as being transfected with Tet-B1-P14-Aγ. Once the cells had recovered from sorting, Tet-B1-P14-Aγ transfected cells were cultured in the presence and absence of doxycycline for two days and flow cytometry used to characterise the expression of both mCherry and BFP markers (Figure 5.4.8).

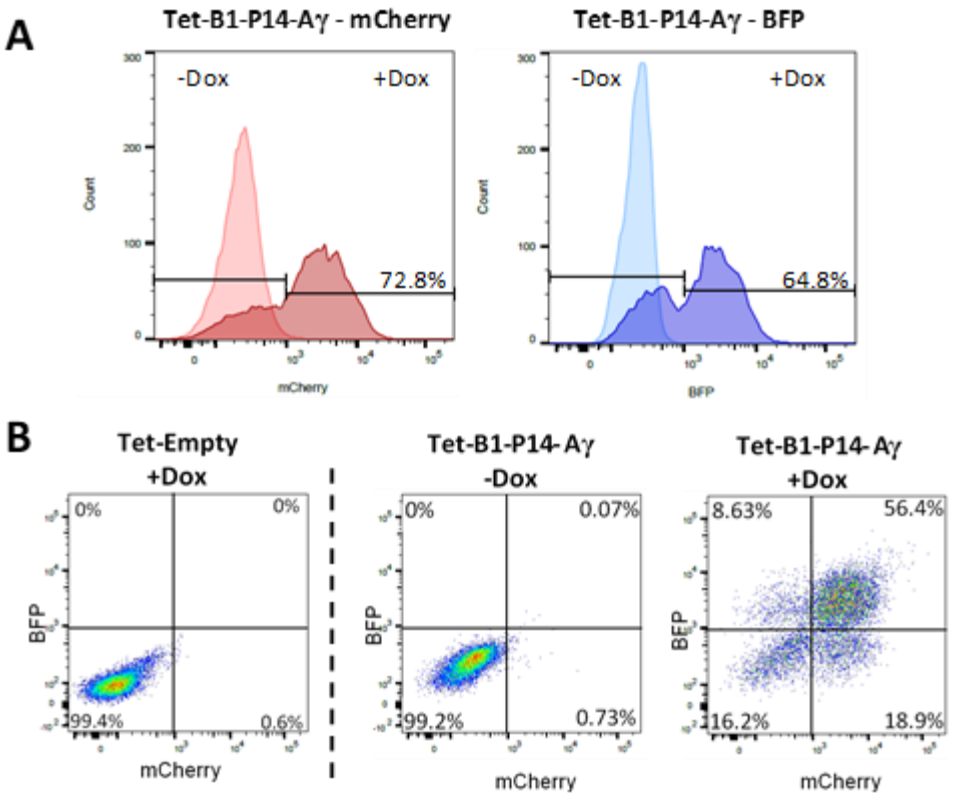

Figure 5.4.8 Flow cytometry data of DAK31 cells transfected with Tet-B1-P14-AP2γ. *(A) Flow cytometry histograms displaying cells cultured in either the presence or absence of doxycycline for 2 days. The pale peaks represent cells cultures in the absence of doxycycline, while darker peaks represent populations cultured in the presence of doxycycline. Percentages shown are the percentage of positive cells in the presence of doxycycline. (B)Flow cytometry plots, mCherry vs BFP. Percentages represent proportion of the population present within that gate.*

Unfortunately, even after sorting for cells positive for both mCherry and BFP, the resulting population was heterogeneous, comprised of distinct populations of double negative, mCherry only and BFP only positive cells (Figure 5.4.8B). Nevertheless, it was decided that these cells had been sufficiently enriched to be of use and analysed further. ESCs which had been cultured in the presence and absence of doxycycline for two days were harvested and RNA prepared for use in qRT-PCR analysis. This was to ensure an increase in transcript level of the three PGC transcription factors in the presence of doxycycline could be observed. The data gathered was then compared to the qRT-PCR data generated from cells expressing each of the PGC transcription factors separately and Tet-BLIMP1-PRDM14-AP2γ cells (Figure 5.4.9).

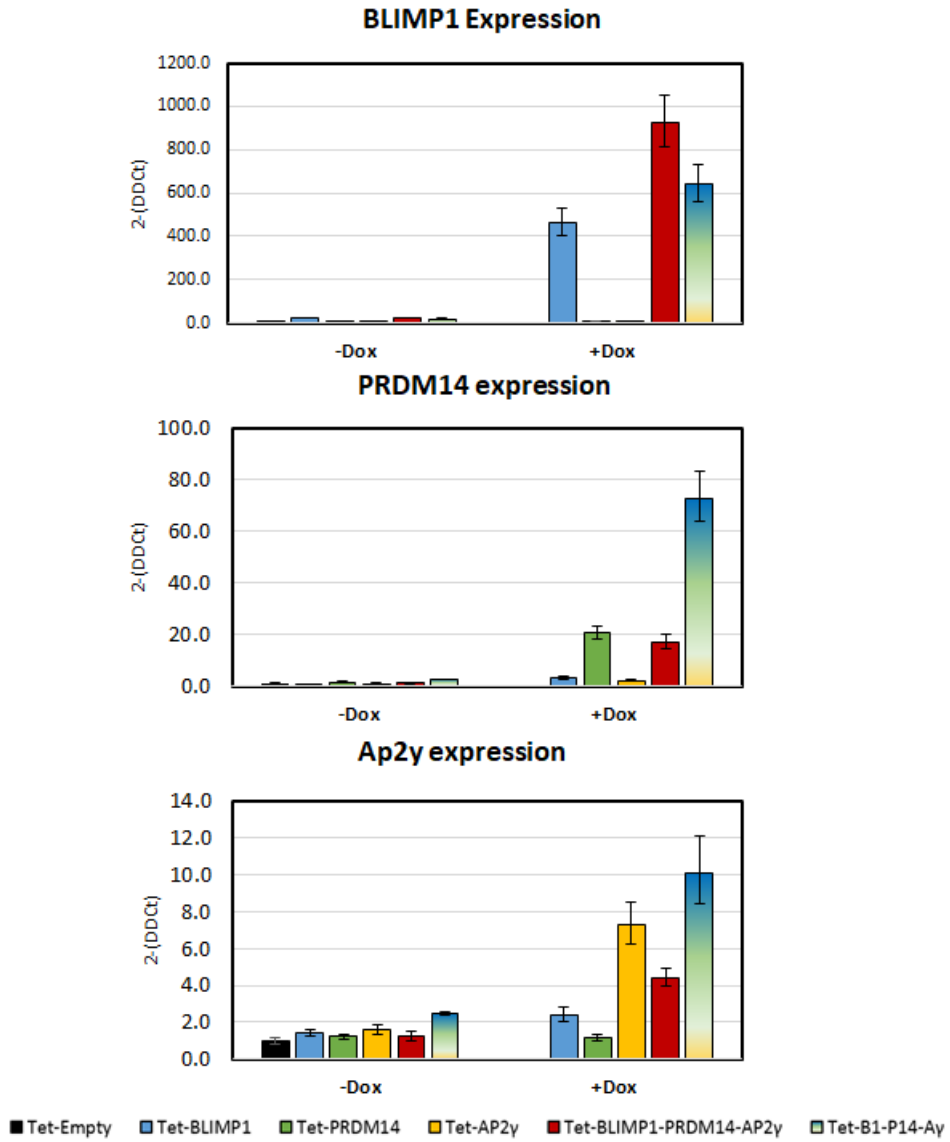

Figure 5.4.9. qRT-PCR analysis of Tet-B1-P14-Ay transfected ESCs. *The data presented was an average of two experiments performed with Tet-On vector transfected DAK31 cells. All data was normalised to the house keeping gene β-actin (dCT) and the fold change (2-DDCT) values generated by normalising gene expression to –dox Tet-Empty transfected cells. Bars represent mean ± SD.*

Cells which had been co-transfected to form the Tet-B1-P14-Aγ cells showed an increased transcript expression of all PGC transcription factors. Additionally, the expression of *Prdm14* and *Ap2γ* was elevated in Tet-B1-P14-Ay cells compared to the cells transfected with the previously designed Tet-BLIMP1-PRDM14-AP2γ. Tet-B1-P14-Aγ cells were then induced to differentiate via an undirected EB differentiation as discussed previously. Doxycycline was introduced at day 0, day 2, day 4, or not at all. Expression from the Tet-On vectors was monitored by fluorescent microscopy throughout the protocol.

Cells transfected with Tet-B1-P14-Aγ and cultured in the presence of doxycycline showed co-expression of both mCherry and BFP fluorescent proteins (Figure 5.4.10B).

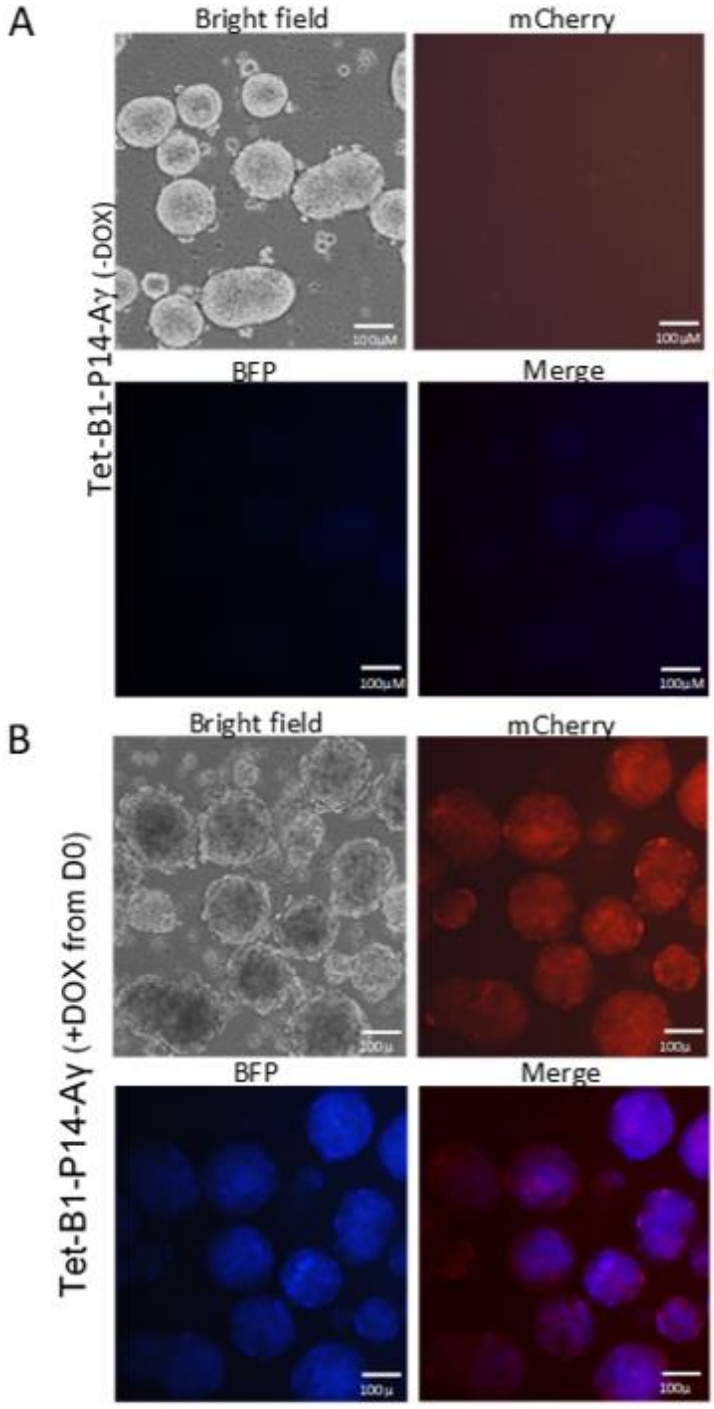

Figure 5.4.10. Fluorescence photographs of Tet-B1-P14-Ay transfected cells. *All photographs were taken at day 6 of the EB differentiation protocol. (A) Panels show EBs cultured in the absence of doxycycline. (B) Panels show EBs cultured in the presence of doxycycline from day 0 of the EB differentiation protocol.*

qRT-PCR data generated for cells transfected with Tet-B1-P14-Aγ were compared against the data obtained with Tet-Empty cells and from Tet-BLIMP1-PRDM14-AP2γ cells. Transcript expression of all three PGC transcription factors from the Tet-B1-P14-Aγ transfected cells were greater than that in Tet-BLIMP1-PRDM14-AP2γ cells when both were cultured in doxycycline from day 0 of EB differentiation onwards (Figure 5.4.11). However, when doxycycline was introduced to the cells later during the EB differentiation protocol, the expression of PGC transcription factors decreased, with cells induced from day 4 onwards having lower transcript expression than the Tet-BLIMP1-PRDM14-AP2γ cells.

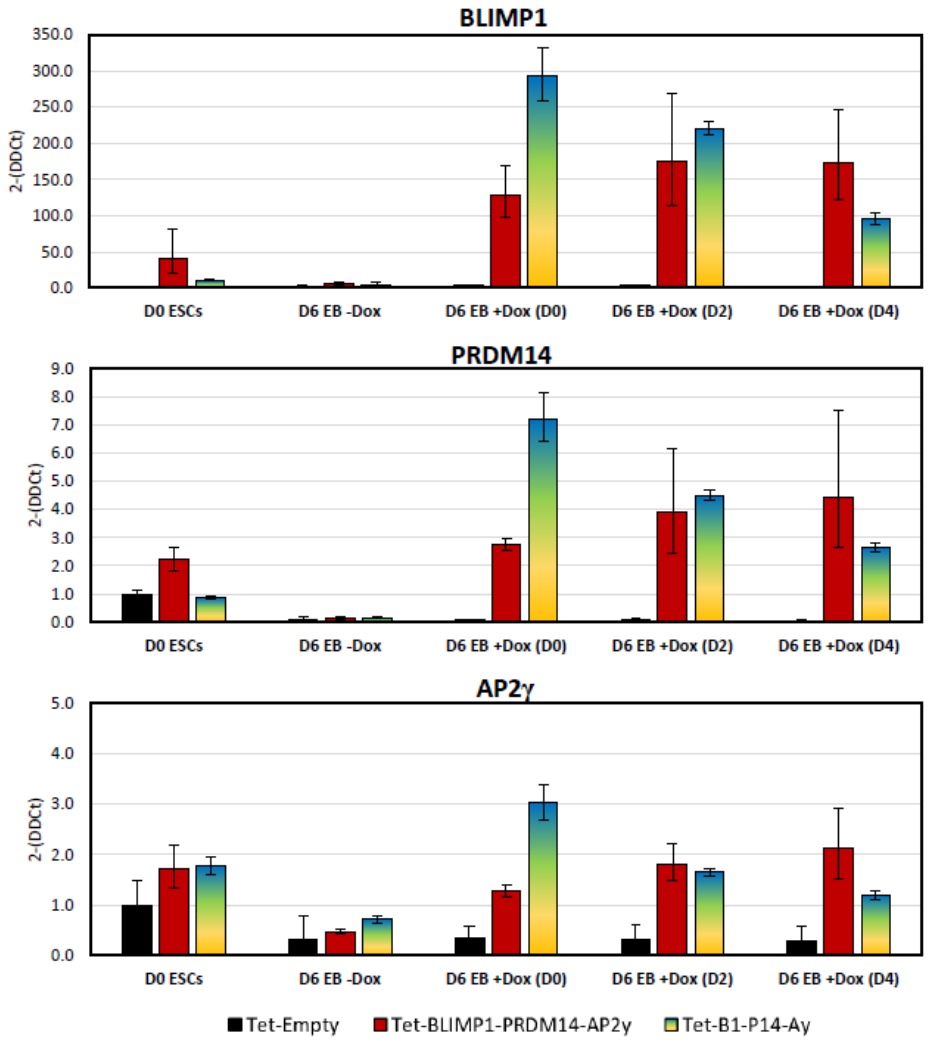

Figure 5.4.11. qRT-PCR analysis of PGC transcription factors from Tet-B1-P14-Aγ transfected cells undergoing an EB differentiation protocol. *The data presented was an average of two experiments performed with Tet-On vector transfected DAK31 cells. All data was normalised to the house keeping gene β-actin (dCT) and the fold change (2-DDCT) values generated by normalising gene expression to –dox Tet-Empty transfected cells. (D0), (D2), (D4) represent cells which were cultured in the presence of doxycycline from day 0, day 2 and day 4 of EB differentiation respectively. Bars represent mean ± SD.*

Transcript expression of both *Nanog* and *Oct4* in Tet-B1-P14-AP2γ cells was lower than the expression seen in the Tet-Empty and Tet-BLIMP1-PRDM14-AP2γ transfected cells (Figure 5.4.12). This suggested that the Tet-B1-P14-AP2γ cells were being driven out of the naïve cell fate more efficiently than the Tet-BLIMP1-PRDM14-AP2γ cells. The transcript expression of *Stella* from both Tet-B1-P14-AP2γ and Tet-BLIMP1-PRDM14-AP2γ was similar in almost all conditions (Figure 5.4.12). There was however a lower expression of *Stella* in Tet-B1-P14-AP2γ transfected cells when cultured in the presence of doxycycline from day 4 onwards (Figure 5.4.12).

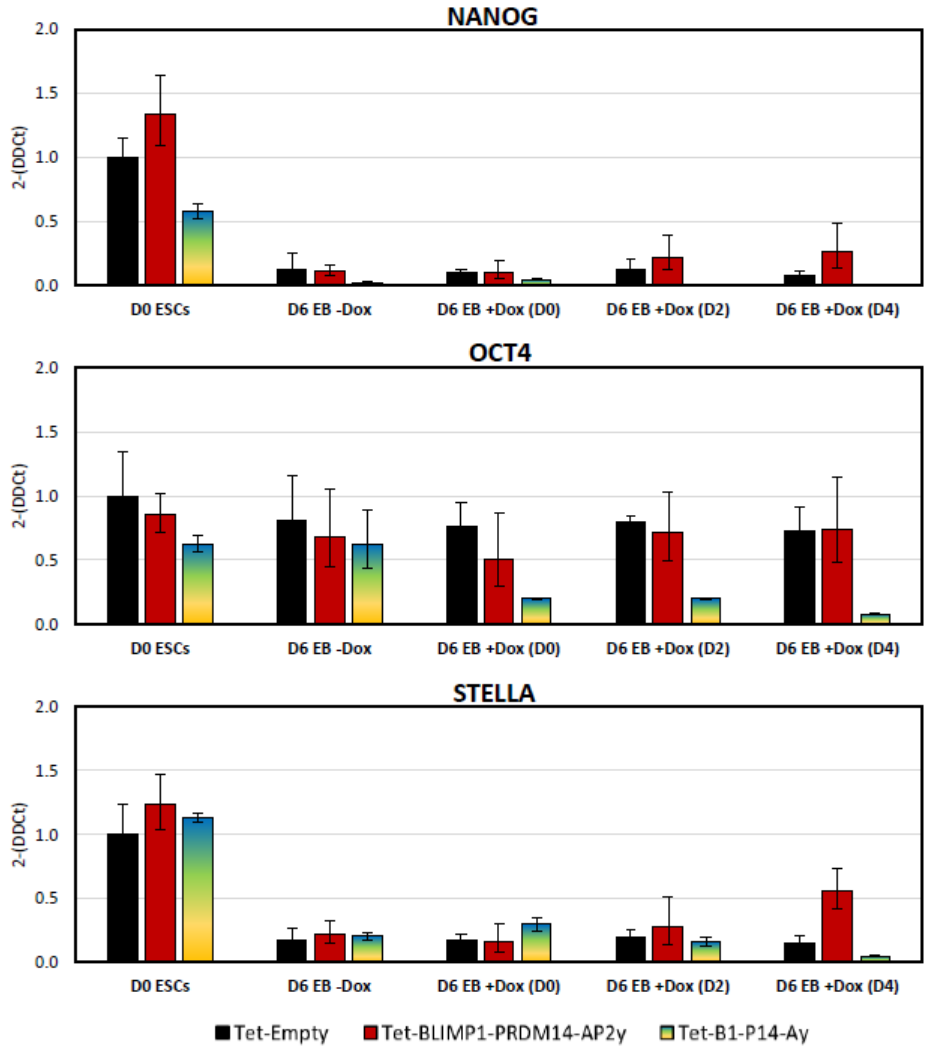

Figure 5.4.12. qRT-PCR analysis of pluripotency genes from Tet-B1-P14-Ay transfected cells undergoing an EB differentiation protocol. *The data presented was an average of two experiments performed with Tet-On vector transfected DAK31 cells. All data was normalised to the house keeping gene β-actin (dCT) and the fold change (2-DDCT) values generated by normalising gene expression to –dox Tet-Empty transfected cells. (D0), (D2), (D4) represent cells which were cultured in the presence of doxycycline from day 0, day 2 and day 4 of EB differentiation respectively. Bars represent mean ± SD.*

Expression of the PGC marker genes *Nanos3, DazL and Vasa* within the Tet-B1-P14-Aγ cells were on average lower than Tet-BLIMP1-PRDM14-AP2γ cells when cultured in the presence of doxycycline (Figure 5.4.13).

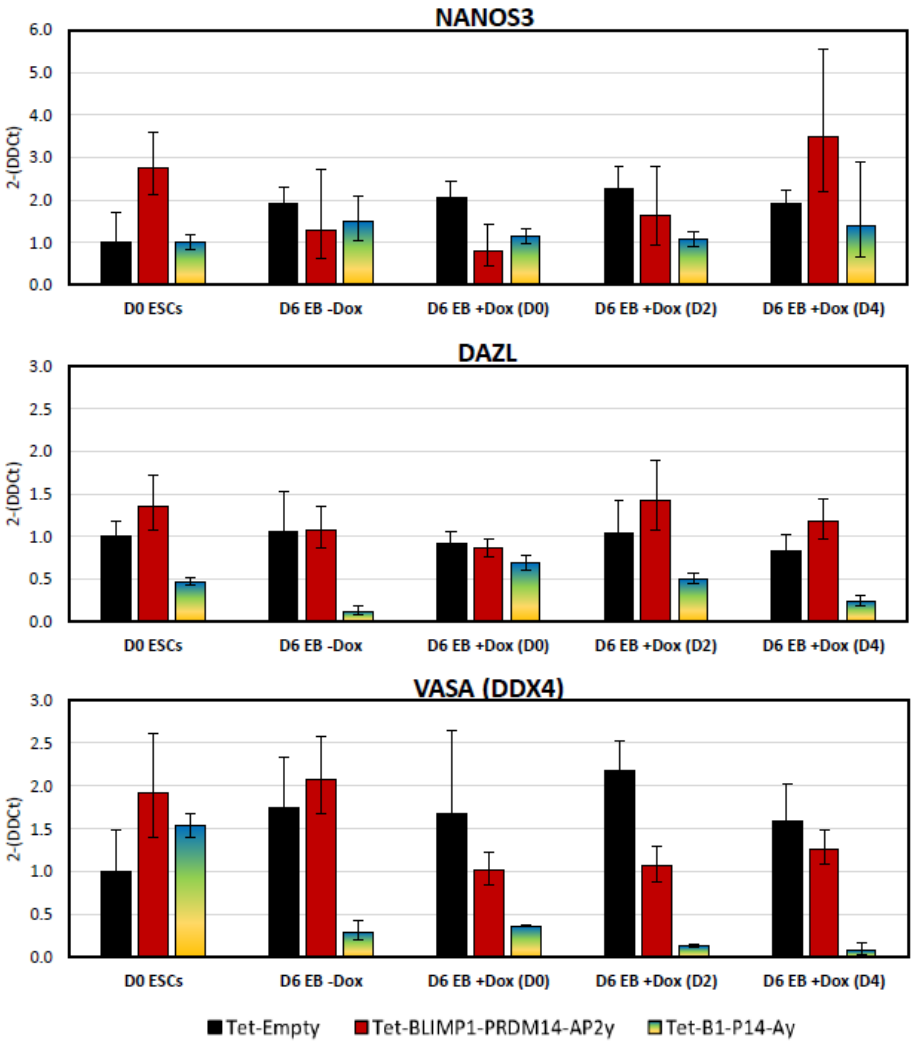

Figure 5.4.13. qRT-PCR analysis of PGC gene markers from Tet-B1-P14-Ay transfected cells undergoing an EB differentiation protocol. *The data presented was an average of two experiments performed with Tet-On vector transfected DAK31 cells. All data was normalised to the house keeping gene β-actin (dCT) and the fold change (2-DDCT) values generated by normalising gene expression to –dox Tet-Empty transfected cells. (D0), (D2), (D4) represent cells which were cultured in the presence of doxycycline from day 0, day 2 and day 4 of EB differentiation respectively. Bars represent mean ± SD*

Both the three individual vector and 2A polycistronic approaches to express transgene copies of all three PGC transcription factors simultaneously did not improve PGC marker gene expression during an undirected EB differentiation protocol when compared to the cells expressing the combination of just two PGC transcription factors. This suggests that in rat ESCs, the expression of all three PGC transcription factors may impair differentiation of rat ESCs towards the germline when exposed to an undirected EB differentiation protocol.

5.5 Primordial germ cell-like (PGCLC) differentiation of stably transfected rat ESC pools

5.5.1 Expression of PGC transcription factors during PGCLC differentiation

Tet-Empty, Tet-BLIMP1, Tet-BLIMP1-PRDM14 and Tet-BLIMP1-AP2γ transfected cells were induced to differentiate by following the rat PGCLC differentiation protocol with minor modifications (Figure 4.5.9). These Tet-On transfected cells were chosen as they had shown induction of PGC marker genes during the undirected EB differentiation protocol. Therefore, it was reasonable to assume that these cells were more likely to be driven towards the PGC lineage during the PGCLC differentiation protocol.

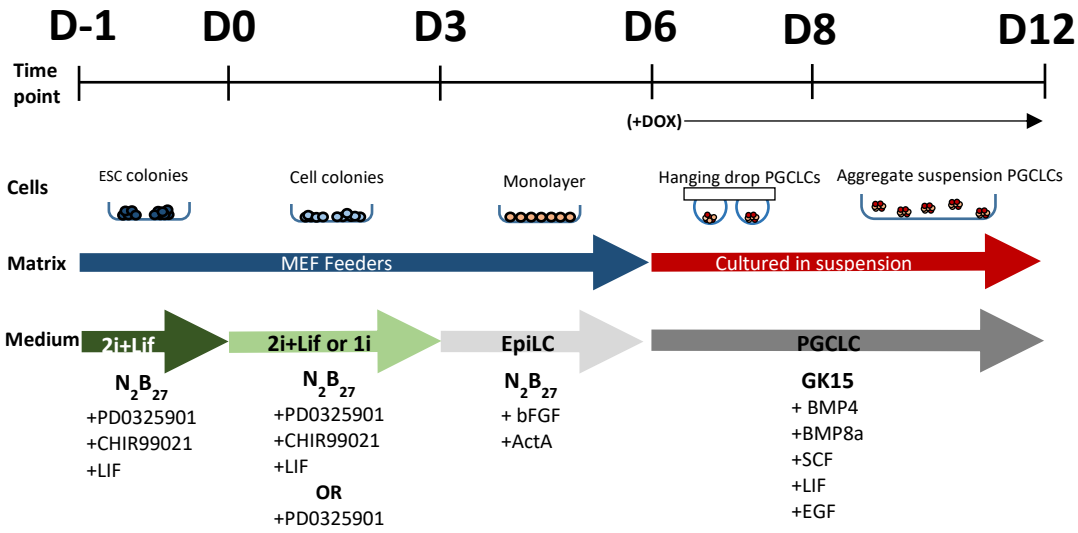

Figure 5.5.1 Schematic of the rat PGCLC differentiation protocol used for differentiation of Tet-On transfected cells. *Rat ESCs pre-cultured in 2i+Lif or 1i culture medium on a MEF layer were transferred onto a fresh MEF feeder layer with EpiLC differentiation medium for 3 days. These cells where then pipetted into hanging drops containing 2,000 cells in PGCLC culture medium supplemented with doxycycline (1ug/ml). After 2 days of culture, aggregates were collected and cultured fresh PGCLC + doxycycline culture medium in low adhesion plate for 4 days.*

Tet-Empty, Tet-BLIMP1, Tet-BLIMP1-PRDM14 and Tet-BLIMP1-AP2γ DAK31 cells were pre-cultured in 2i+LIF and 1i culture mediums on MEF feeder layers for 3 days. After pre-culture, cells were passaged onto 12-well plates coated with MEFs and cultured for 3 days in EpiLC culture medium. EpiLC medium was exchanged every 24 hours to replenish active bFGF. When observed under a brightfield microscope, it was determined that cells which had been pre-cultured in 1i culture medium had less evidence of cellular debris compared to those pre-cultured in 2i+LIF, suggesting that 1i pre-culture had improved the survival of these cells when cultured in EpiLC medium (Figure 5.5.2).

Apart from decreased cellular debris, there appeared to be no obvious differences in morphology or the growth rate of cells cultured in either pre-culture medium.

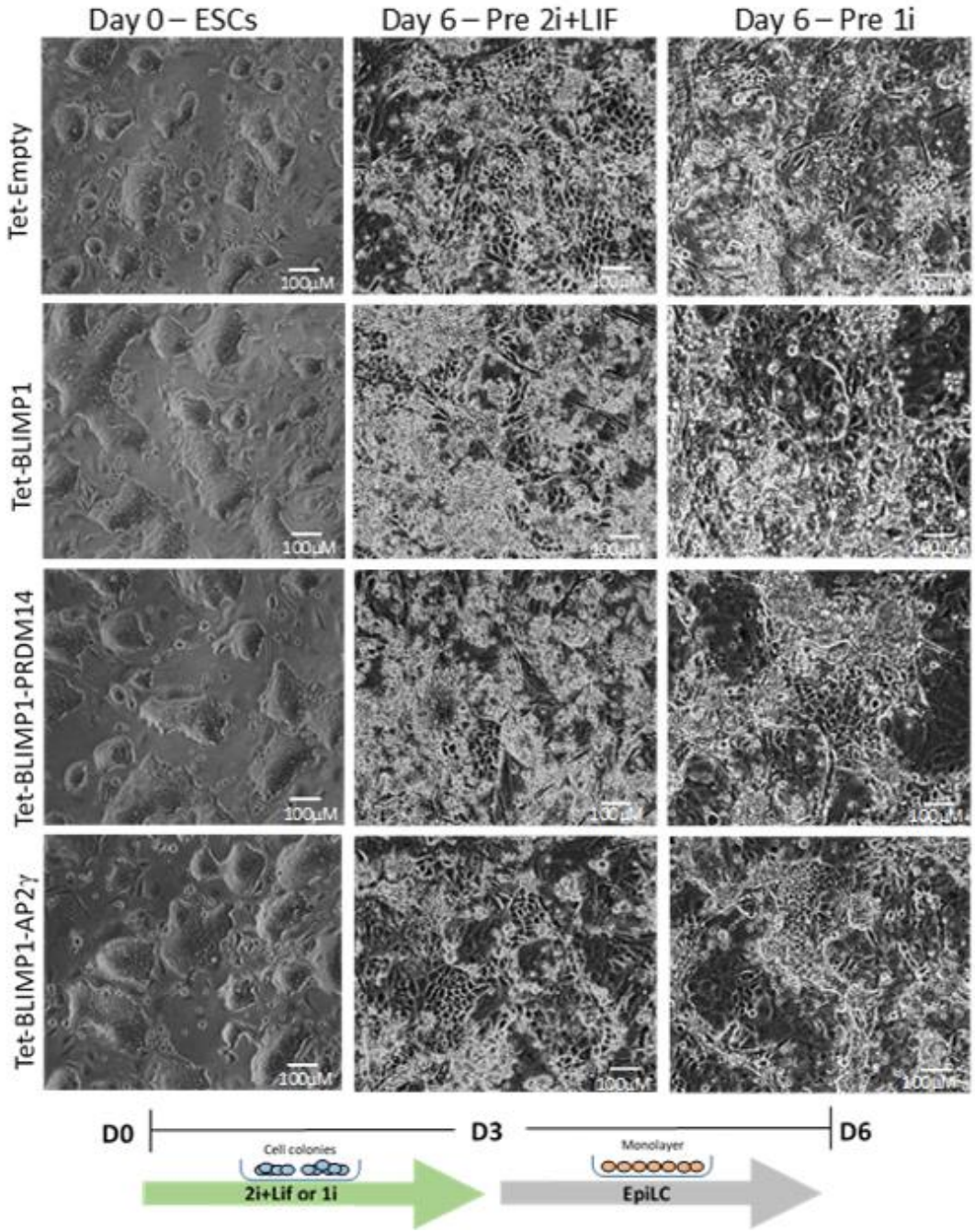

Figure 5.5.2. Bright field microscopy photographs of DAK31 Tet-On transfected cell pools during EpiLC differentiation. *Photographs taken from cell pools of Tet-Empty, Tet-BLIMP1, Tet-BLIMP1-PRDM14 and Tet-BLIMP1-AP2γ transfected cell pools. After 3 days of culture in EpiLC medium (day 6), increased cellular death was present in all cell pools pre-cultured in 2i+LIF medium (Pre 2i+LIF) compared to pools pre-cultured in 1i medium (Pre 1i).*

After the 3-day EpiLC medium culture, cells were collected and suspended in hanging drops of PGCLC medium supplemented with doxycycline (1μg/ml). Doxycycline was introduced at day 6 of the PGCLC differentiation protocol, mimicking the induction of PGC transcription factor transgenes in mouse ESCs after EpiLC differentiation (Nakaki et al. 2013). Each hanging drop consisted of 2,000 EpiLCs contained within 30μl PGCLC culture medium 'drops'. Dishes containing the suspended hanging drops were incubated for 2 days to allow aggregation of the cells. After 2 days, aggregates were transferred into 6-well low adhesion plates with fresh PGCLC culture medium and incubated in suspension for a further 4 days. mCherry fluorescent protein was detected in Tet-On cells cultured in the presence of doxycycline (1μg/ml) by fluorescent microscopy (Figure 5.5.3). Bright field microscopy revealed cell pools expressing *Blimp1* cDNA alone during the PGCLC differentiation protocol produced fewer cellular aggregates than the other cell pools (Figure 5.5.3). However, the remaining *Blimp1* aggregates were larger than those observed in other cell pools, suggesting aggregates were made up of multiple smaller aggregates bound together.

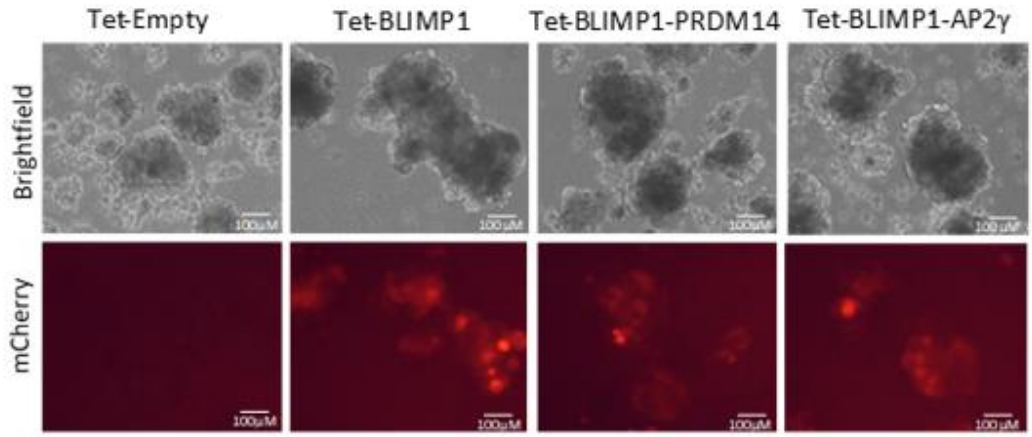

Figure 5.5.3. Wide field fluorescence imaging of Tet-On vector transfected cell pools after PGCLC differentiation. *D12 Aggregates shown were cultured in PGCLC medium supplemented with doxycycline (1μg/ml). mCherry fluorescence was detected in cells harbouring a Tet-On vector containing a PGC transcription factor cassette. Cells transfected with the Tet-Empty vector had no detectable mCherry fluorescence.*

Aggregates were broken apart by gentle pipetting (trituration) and the cell suspensions sorted into mCherry^{+ve} and mCherry^{-ve} populations by FACs (Figure 5.5.4). By separating these populations, it could be determined whether cells with activate Tet-On vector transgene expression (mCherry^{+ve}) had elevated expression of PGC markers compared inactive Tet-On vector transgene expression (mCherry^{-ve}).

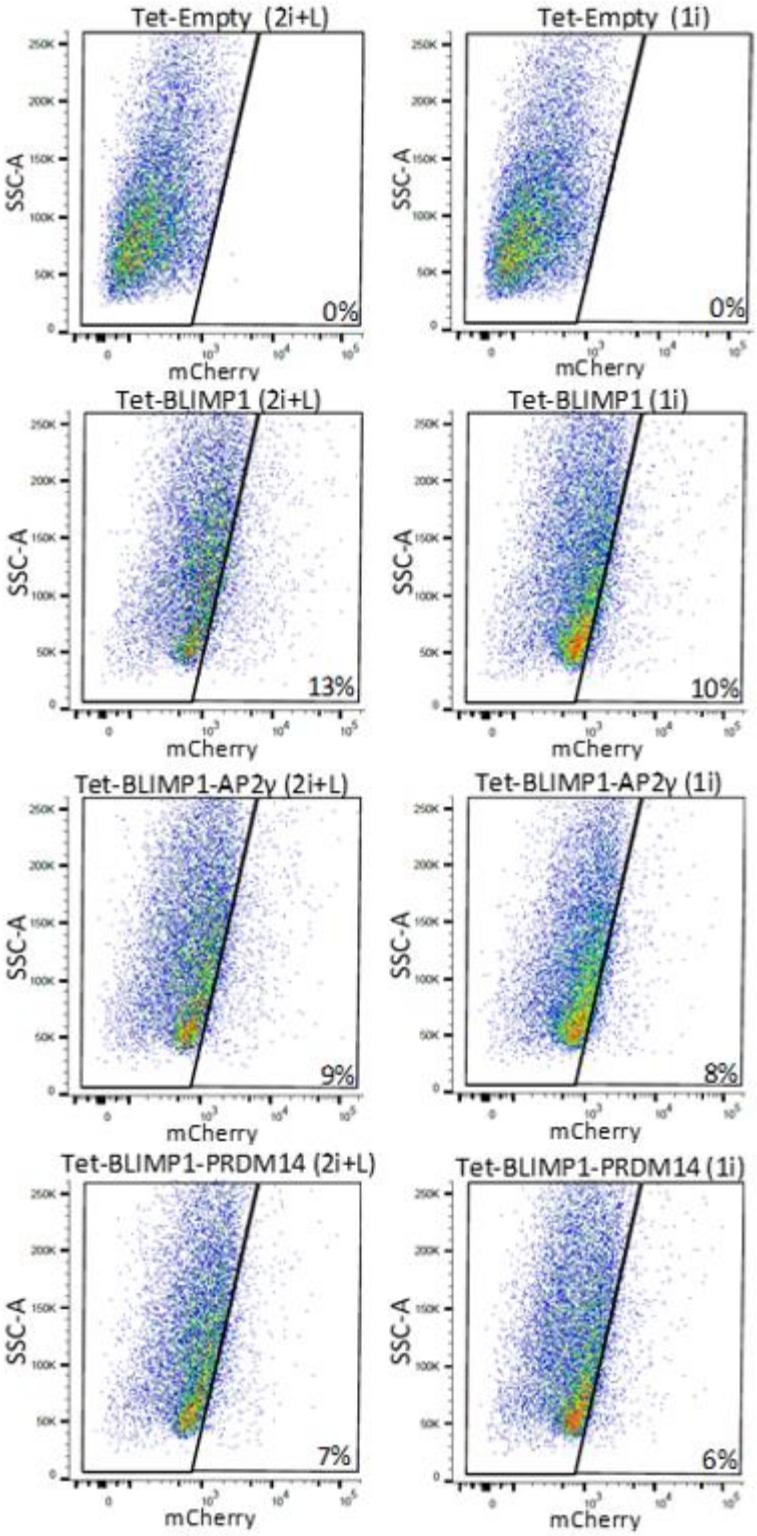

Figure 5.5.4. FACs plots of Tet-On vectors undergoing a PGCLC differentiation protocol. *Percentages shown display the proportion of the population that was mCherry positive at day 12 of the PGCLC differentiation protocol.*

qRT-PCR analysis showed elevated expression of *Blimp1* and *Prdm14* transcripts within mCherry^{+ve} Tet-BLIMP1, Tet-BLIMP1-PRDM14 and Tet- BLIMP1-AP2γ cells compared to Tet-Empty cells (Figure 5.5.5). However, there was no substantial difference in *Blimp1* or *Prdm14* expression between the 2i+Lif or 1i pre-treated conditions (Figure 5.5.5). Expression of *Ap2*γ in all Tet-On PGC transcription factor cells pre-cultured in either condition was similar to that in the Tet-Empty cells (Figure 5.5.5).

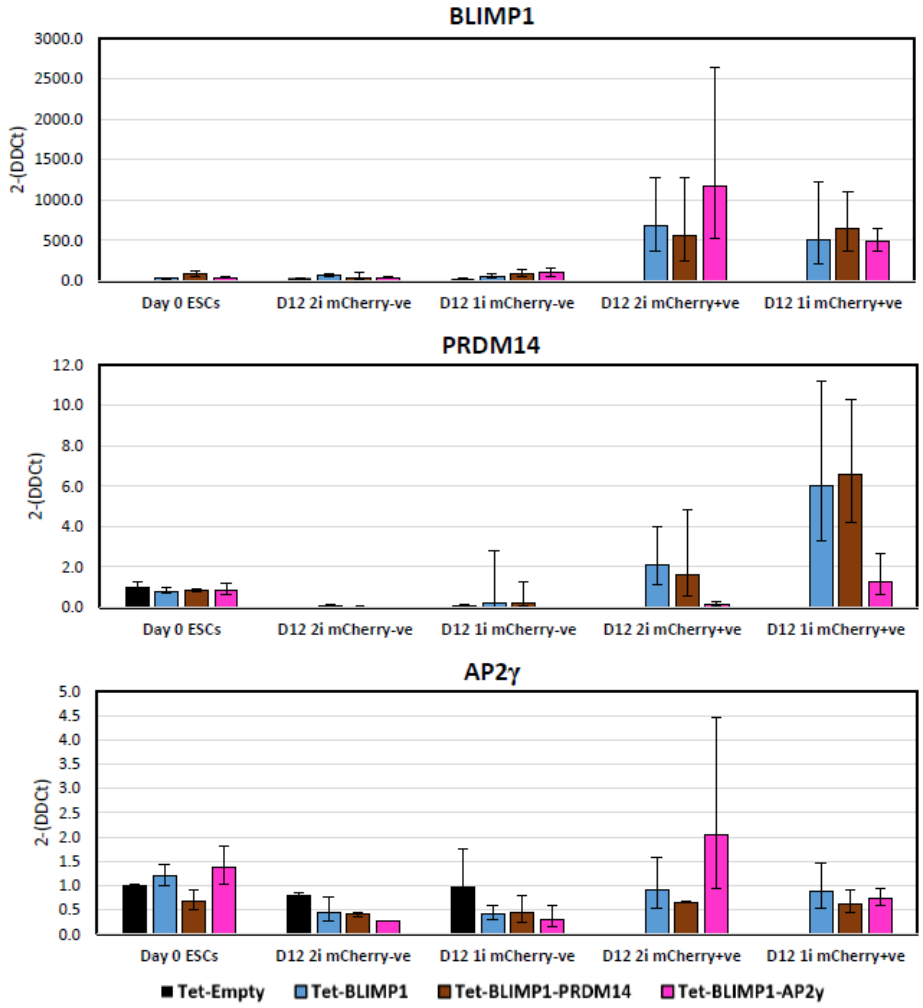

Figure 5.5.5. qRT-PCR analysis of PGC transcription factors in Tet-On transfected cell pools undergoing a PGCLC differentiation protocol. *The data presented was an average of two experiments performed with Tet-On vector transfected DAK31 cells. All data was normalised to the house keeping gene β-actin (dCT) and fold change was calculated by normalising gene expression to Day 0 Tet-Empty ESCs (2-DDCT). 2i = Pre-cultured in 2i +LIF medium, 1i = Pre-cultured in 1i medium. Bars represent mean ± SD.*

Nanog expression was increased in mCherry^{+ve} cells of all Tet-On PGC vector transfected cells, particularly those which had been pre-cultured in 1i medium (Figure 5.5.6). However, this expression level was far lower than that seen in any population of ESCs (Figure 5.5.6). On average, *Oct4* expression in mCherry^{+ve} cells expressing transgene copies of any of the PGC transcription factors was lower than the expression in the Tet-Empty cell pools (Figure 5.5.6). Only Tet-AP2γ 1i pre-cultured cells had similar *Oct4* expression to the Tet-Empty cells (Figure 5.5.6). Tet-On cells pre-cultured in 2i+LIF medium had reduced *Stella* expression compared to Tet-Empty cells (Figure 5.5.6). *Stella* expression from the mCherry^{+ve} cells of Tet-BLIMP1-PRDM14 and Tet-BLIMP1-AP2γ pre-cultured in 1i medium was similar to that in the Tet-Empty transfected cells (Figure 5.5.6). However, there was large variability between the two experiments, generating large error bars for *Stella* expression in 1i mCherry positive cells.

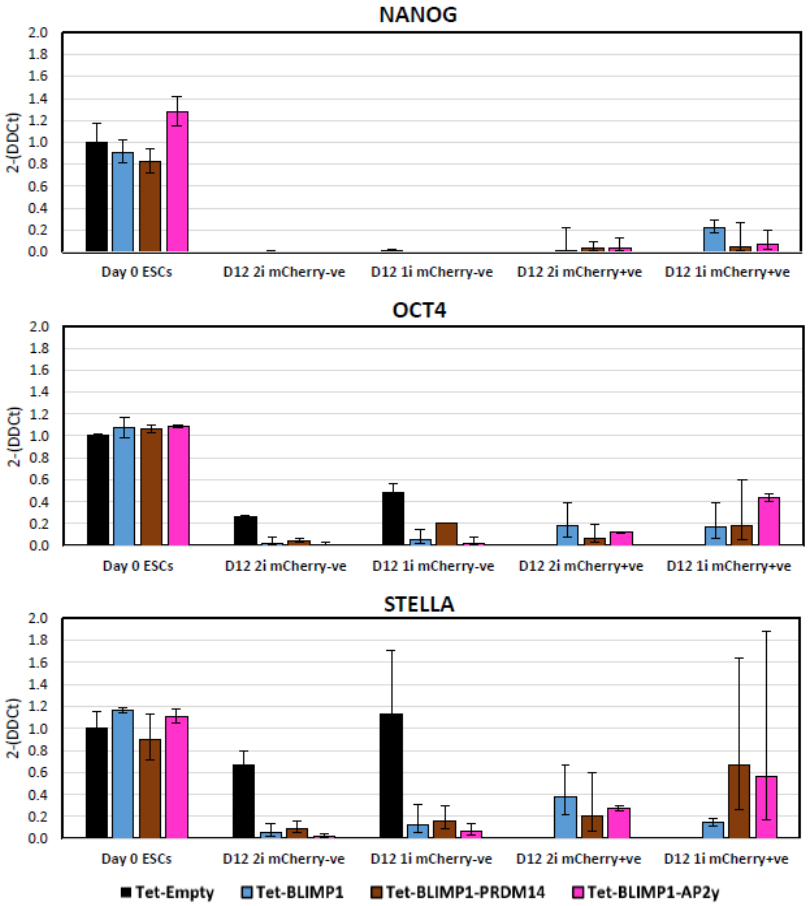

Figure 5.5.6. qRT-PCR analysis of pluripotency markers in Tet-On transfected cell pools undergoing a PGCLC differentiation protocol. *The data presented was an average of two experiments performed with Tet-On vector transfected DAK31 cells. All data was normalised to the house keeping gene β-actin (dCT) and fold change was calculated by normalising gene expression to Day 0 Tet-Empty ESCs (2-DDCT). 2i = Pre-cultured in 2i +LIF medium, 1i = Pre-cultured in 1i medium. Bars represent mean ± SD.*

Expression of the PGC marker *Nanos3* was increased in mCherry^{+ve} Tet-BLIMP1-PRDM14 and Tet-BLIMP1-AP2γ cells which had been pre-cultured in 1i medium (Figure 5.5.7). Interestingly, expression of *Blimp1* cDNA alone did induce a small increase in *Nanos3* transcript in 2i+LIF pre-cultured mCherry^{+ve} cells, but not after 1i medium pre-culture (Figure 5.5.7).

Due to large variations between the experimental replicates, the expression of *DazL* transcript proved difficult to interpret from the mCherry^{+ve} cells (Figure 5.5.7). There may have been increased *Dazl* transcript expression in 1i pre-cultured mCherry^{+ve} Tet-BLIMP1-PRDM14 and Tet-BLIMP1-AP2γ cells, but this could not be accurately determined due to the large variation between the two experiments (Figure 5.5.7). All mCherry^{+ve} Tet-On cells expressing at least one PGC transcription factor had increased *Vasa* expression compared to Tet-Empty cells (Figure 5.5.7).

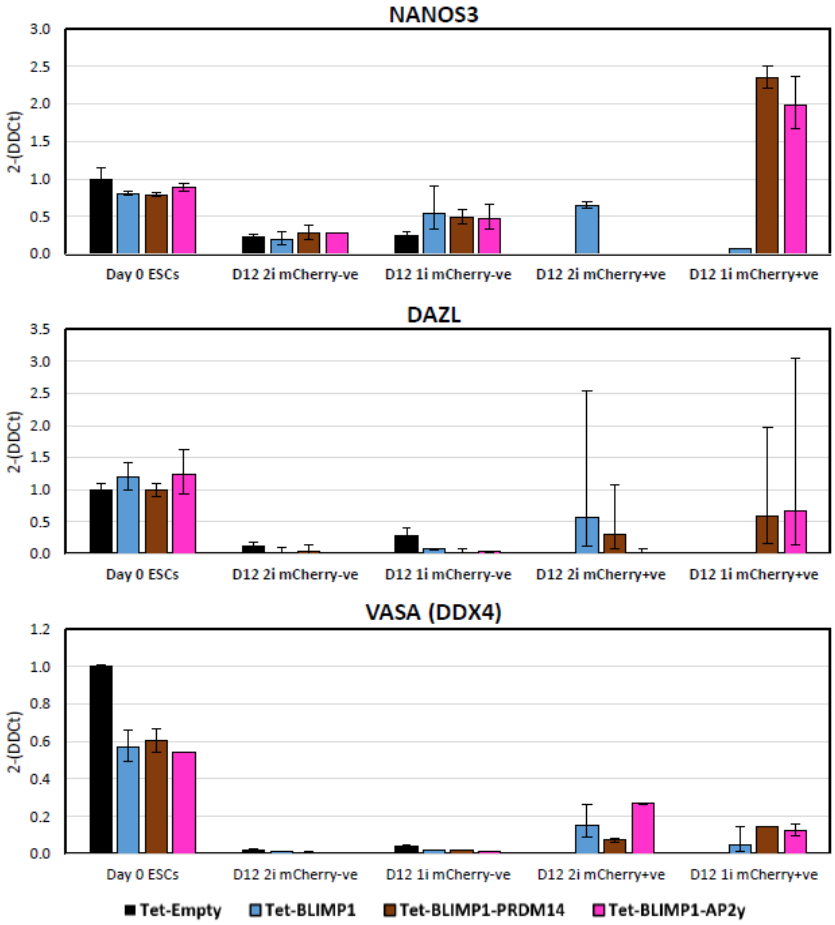

Figure 5.5.7 qRT-PCR analysis of PGC gene markers in Tet-On transfected cell pools undergoing a PGCLC differentiation protocol. *The data presented was an average of two experiments performed with Tet-On vector transfected DAK31 cells. All data was normalised to the house keeping gene β-actin (dCT) and fold change was calculated by normalising gene expression to Day 0 Tet-Empty ESCs (2-DDCT). 2i = Pre-cultured in 2i +LIF medium, 1i = Pre-cultured in 1i medium. Bars represent mean ± SD.*

Transcript expression of markers of endoderm (*Gata4*, *Gata6*) and trophectoderm (*Gata3*) were also analysed to determine whether the expression of PGC transcription factor cDNA influenced the proportion of the Tet-On cells differentiating towards these lineages. *Gata4* expression was reduced in mCherry^{+ve} cells of all Tet-On PGC transcription factor expressing cells compared to Tet-Empty cells (Figure 5.5.8). Interestingly, mCherry^{-ve} cells which had been pre-cultured in 1i medium also had reduced *Gata4* expression compared to Tet-Empty cells (Figure 5.5.8). However, Tet-BLIMP1-PRDM14 cells pre-cultured in 2i+LIF medium had similar *Gata4* expression to Tet-Empty cells (Figure 5.5.8).

Gata6 expression was considerably higher in the mCherry^{+ve} cells of all Tet-On PGC transcription factor expressing cells pre-cultured in 1i medium compared to Tet-Empty cells. In 2i+LIF pre-cultured mCherry^{+ve} cells, Tet-BLIMP1-AP2γ cells had greater expression of *Gata6* than either Tet-BLIMP1 or Tet-BLIMP1-PRDM14 cells. However, when pre-cultured in 1i medium, the mCherry^{+ve} populations of both Tet-BLIMP1 and Tet-BLIMP1-PRDM14 had far greater expression of *Gata6* than the mCherry^{+ve} population of Tet-BLIMP1-AP2γ cells.

The mCherry^{+ve} population of Tet-BLIMP1-PRDM14 cells pre-cultured in 2i+LIF had a similar *Gata3* expression to the Tet-Empty cells. However, mCherry^{+ve} Tet-BLIMP1-PRDM14 cells pre-cultured in 1i medium, alongside both the Tet-BLIMP1 and Tet-BLIMP1-AP2γ cells had a greatly reduced expression of *Gata3* compared to the Tet-Empty cells. The reduction of *Gata3* after 1i medium pre-culture in the mCherry^{+ve} populations suggested that expression of these PGC transcription factors decreased the proportion of differentiating cells being driven towards *Gata3*$^{+ve}$ lineages such as trophectoderm. However, expression of both *Blimp1* and *Prdm14* cDNA in cells pre-cultured in 2i+LIF was able to retain the proportion of cells entering *Gata3*$^{+ve}$ lineages.

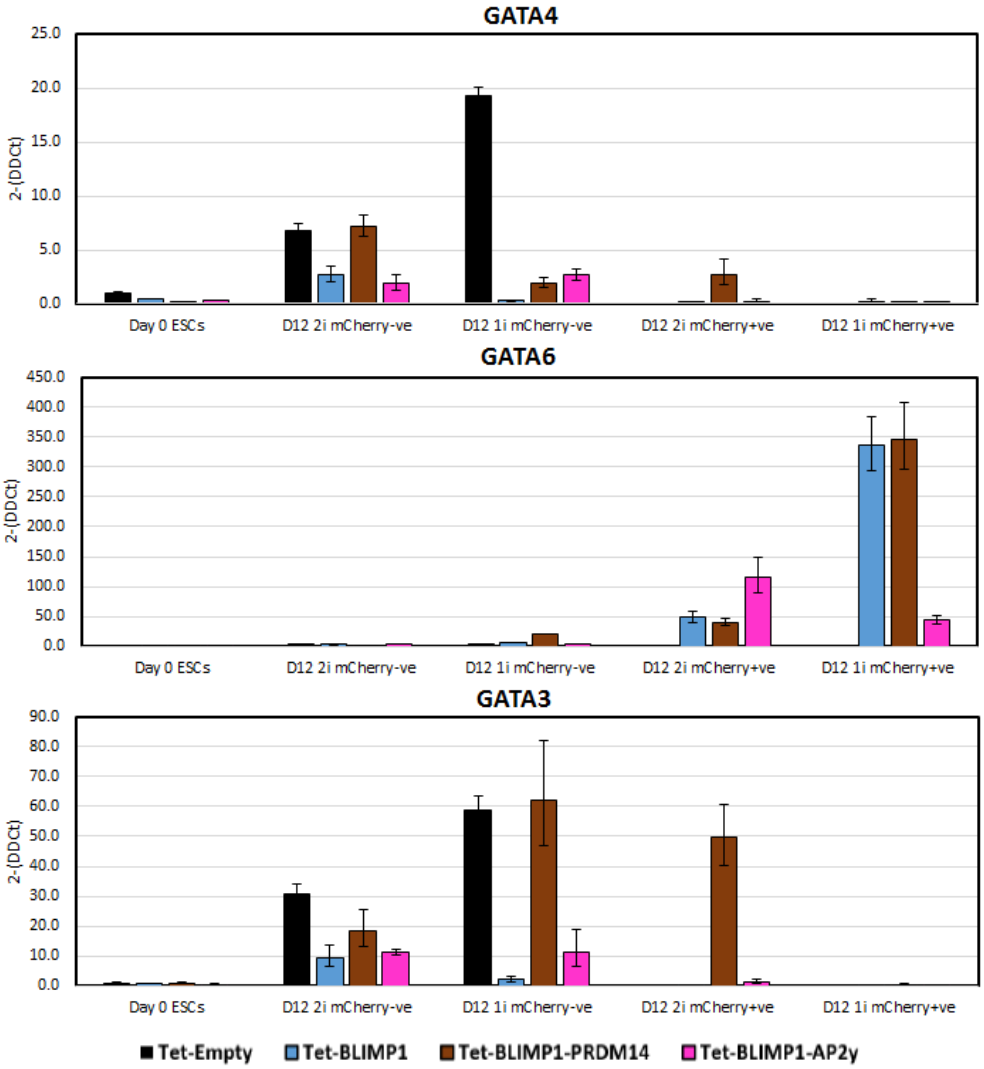

Figure 5.5.8. qRT-PCR analysis of PGC gene markers in Tet-On transfected cell pools undergoing a PGCLC differentiation protocol. *The data presented was an average of two experiments performed with Tet-On vector transfected DAK31 cells. All data was normalised to the house keeping gene β-actin (dCT) and fold change was calculated by normalising gene expression to Day 0 Tet-Empty ESCs (2-DDCT). 2i = Pre-cultured in 2i +LIF medium, 1i = Pre-cultured in 1i medium. Bars represent mean ± SD.*

Overall, mCherry^{+ve} cells which had undergone the PGCLC differentiation protocol had a different gene expression profile to the mCherry^{-ve} cells within the same culture wells, suggesting these results were due to the expression of PGC transcription factor transgenes rather than the presence of doxycycline. Additionally, co-expression of *Blimp1* and either *Prdm14* or *Ap2γ* within the mCherry^{+ve} cells induced the greatest increased expression of the PGC marker *Nanos3*, suggesting that expression of these transgene factors can positively influence the differentiation of cells towards the germ cell lineage during a PGCLC differentiation protocol.

5.6 Expression of exogenous NANOG transcription factor using the Tet-On vector system

5.6.1 Exogenous Nanog expression alone can induce PGCLC formation

NANOG is a transcription factor that forms part of the core network maintaining ESC self-renewal (Chambers et al. 2003, Chambers et al. 2007, Murakami et al. 2016). Loss of *Nanog* expression can predispose ESCs to differentiation (Chambers et al. 2007), while its overexpression can supress differentiation and promote ESC self-renewal (Chambers et al. 2003, Murakami et al. 2016). A study performed in mouse ESCs determined that the expression of *Nanog* transgene within EpiLCs generated cells with a similar epigenetic pattern to *in vivo* early germline cells, as well as increased expression of PGC transcription factors and PGC markers (e.g. *Nanos3*) (Murakami et al. 2016). This was thought to be due to NANOG assisting the recruitment of histone modifying enzymes to the promotor regions of PGC promoting factors (e.g. *Blimp1*, *Prdm14* and *Ap2γ*), activing their expression and thereby directing differentiation towards the PGC fate (Murakami et al. 2016). Could the proportion of rat cells entering the germ cell lineage be improved by combining ESC differentiation with overexpression of *Nanog*?

5.6.2 Cloning rat Nanog into the Tet-On transposon and production of stably transfected cell pools

Rat *Nanog* cDNA was generated by PCR amplification with oligonucleotides designed to bind to the NANOG mRNA sequence on the Ensembl database (ENSRNOT00000060937.3). Homology to the Tet-On vector and to the 2A-mCherry of the linearised Tet-On vector (Figure 5.2.3) were introduced to the amplified *Nanog* cDNA by a second round of PCR amplification. Ligation of the amplified *Nanog* cDNA into the linearised 2A-mCherry vector was performed by Gibson cloning, followed by Sanger sequencing to confirm the proper insertion of the *Nanog* ORF cDNA into the Tet-On vector. Similar to the previously generated Tet-On vectors, a confirmed Tet-NANOG vector was transfected into two dark agouti (DAK31 and E3) and one Sprague-Dawley (A4) derived rat ESC lines using Lipofectamine LTX and subjected to puromycin selection to remove any un-transfected cells. Cell pools containing Tet-NANOG transfected ESC were then cultured in the presence and absence of 1µg/ml doxycycline for 2 days to induce the expression of the *Nanog* and mCherry fluorescent protein.

Expression of the mCherry marker was monitored by fluorescence microscopy (Figure 5.6.1A) and by flow cytometry (Figure 5.6.1B). The gating strategy detailed in section 2.6.7 was used. The remaining cells were gated to isolate populations of mCherry^{+ve} cells by plotting mCherry (610/20A) versus cell counts. The gates were set against rat ESCs transfected with the Tet-Empty vector.

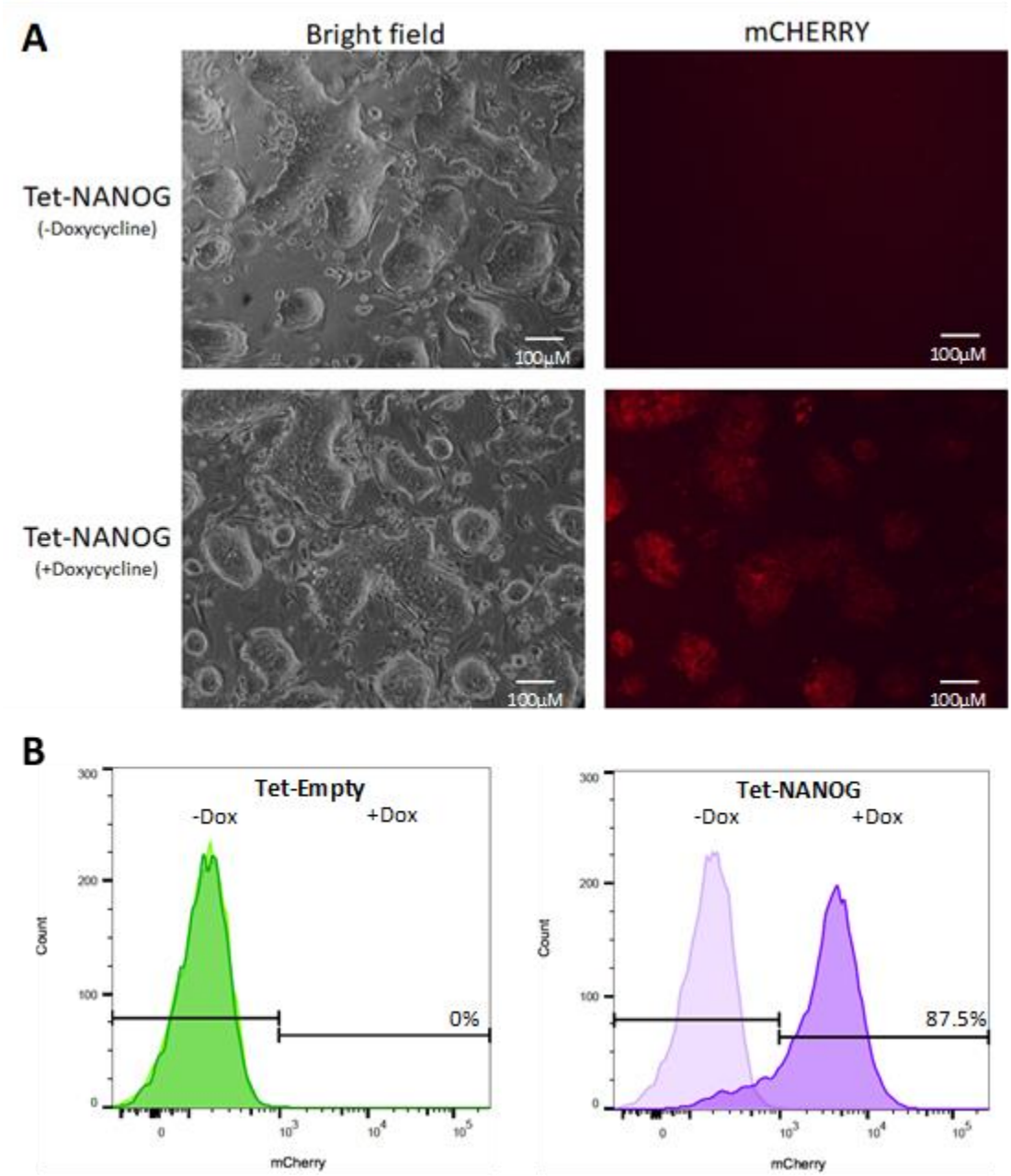

Figure 5.6.1. mCherry fluorescence and flow cytometry data produced from DAK31 cells transfected with Tet-NANOG. *(A) Bright field and fluorescence photographs of DAK31 cell pools stably transfected with the Tet-NANOG vector. 1.5x10^5 rat ESCs were cultured in 2i+LIF medium in the absence (top panels) or presence (bottom panels) of doxycycline (1µg/ml) for 2 days. (B) Flow cytometry histograms displaying cells cultured in either the presence (dark peak) or absence (pale peak) of doxycycline for 2 days. Percentages shown are the percentage of mCherry positive cells in the presence of doxycycline.*

5.6.3 Functional *Nanog* transgene expression from the Tet-NANOG vector

Rat ESCs cultured in culture medium containing high concentrations of CHIR99021 are driven to differentiate due to the inhibition of GSK3 activity, which leads to stabilisation of β-catenin and therefore increases β-catenin activity (Meek et al. 2013). A *Rex1*-EGFP reporter cell line was transfected with the Tet-NANOG vector and cultured for two days in medium containing 4 different concentrations of CHIR99021 (0, 1, 4, and 8μM) in the presence and absence of doxycycline (1μg/ml). Differentiation of the reporter cell line was monitored by observing the loss of EGFP expression. Cells cultured in standard 2i+LIF conditions (2μM) were used as a titration control. It was hypothesised that functional expression of the *Nanog* transgene from the Tet-On vector would increase the number of $EGFP^{+ve}$ present after the cells had been subjected to the CHIR99021 titration. Flow cytometry was performed to ascertain the effect *Nanog* transgene expression had on the expression of EGFP in the *Rex1*-EGFP reporter cell line (Figure 5.6.2).
Increased EGFP expression was seen in cells cultured in medium containing doxycycline (red) compared to those cultured in the absence of doxycycline (green) (Figure 5.6.2). This showed that functional *Nanog* transgene was being expressed from the Tet-NANOG vector, reducing the number of cells differentiating in the presence of high concentrations of CHIR99021.

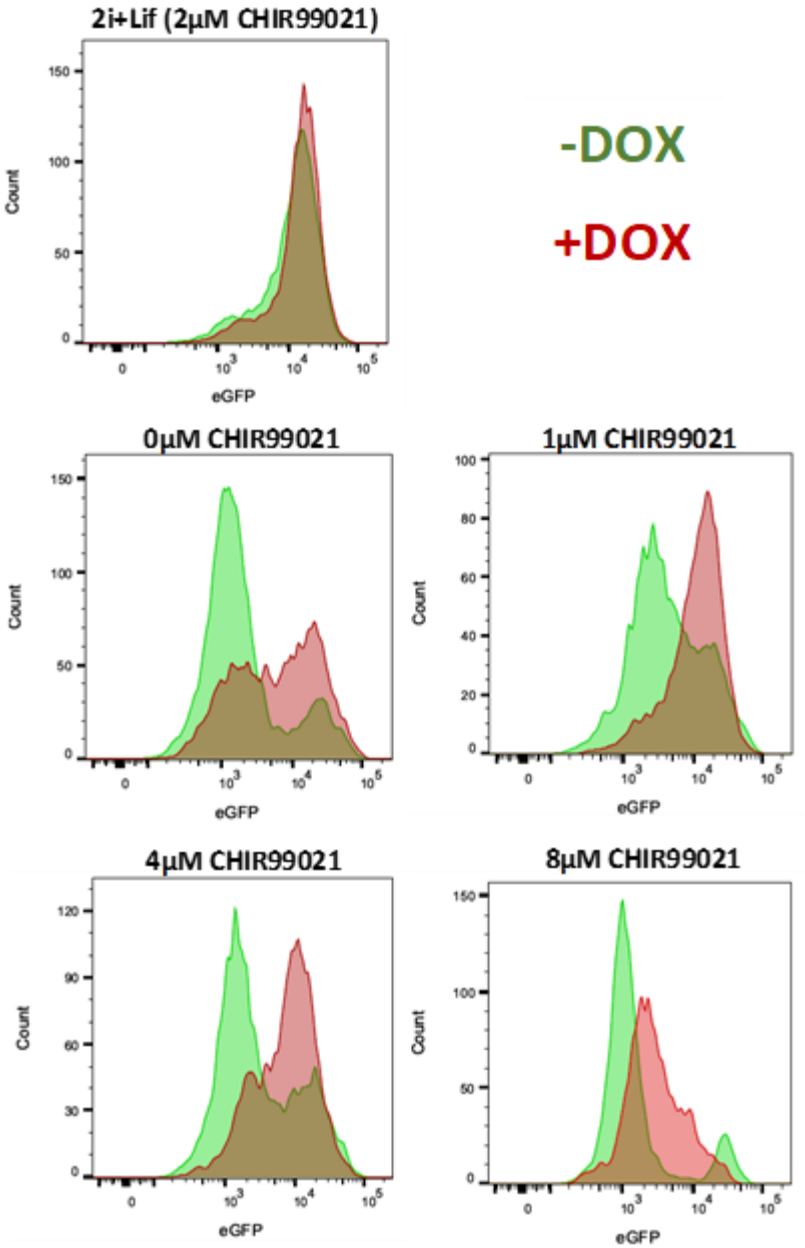

Figure 5.6.2 Flow cytometry of Tet-NANOG transfected Rex1-EGFP cell pools undergoing CHIR99021 titration. *Flow cytometry histograms displaying cell pools cultured in increasing concentrations of CHIR99021 in the presence or absence of doxycycline for 2 days. Green peaks represent pools cultures in the absence of doxycycline, while red peaks represent populations cultured in the presence of doxycycline.*

5.6.4 Expression of Nanog cDNA during an EB differentiation protocol

Tet-NANOG transfected cells generated from three different rat ESC lines were induced to differentiate for 6 days via the undirected EB differentiation protocol. This was to assess the effect *Nanog* transgene expression had on rat ESC differentiation, and to determine whether there was any increase in the expression of PGC markers during undirected differentiation of these cells.

qRT-PCR analysis performed on cells after the 6-day protocol revealed that *Nanog* transcript levels were significantly increased when doxycycline was introduced to the culture medium of Tet-NANOG cells when compared to the Tet-Empty cells (Figure 5.6.3). However, there was no significant difference in *Oct4* or *Stella* expression in the presence or absence of doxycycline (Figure 5.6.3).

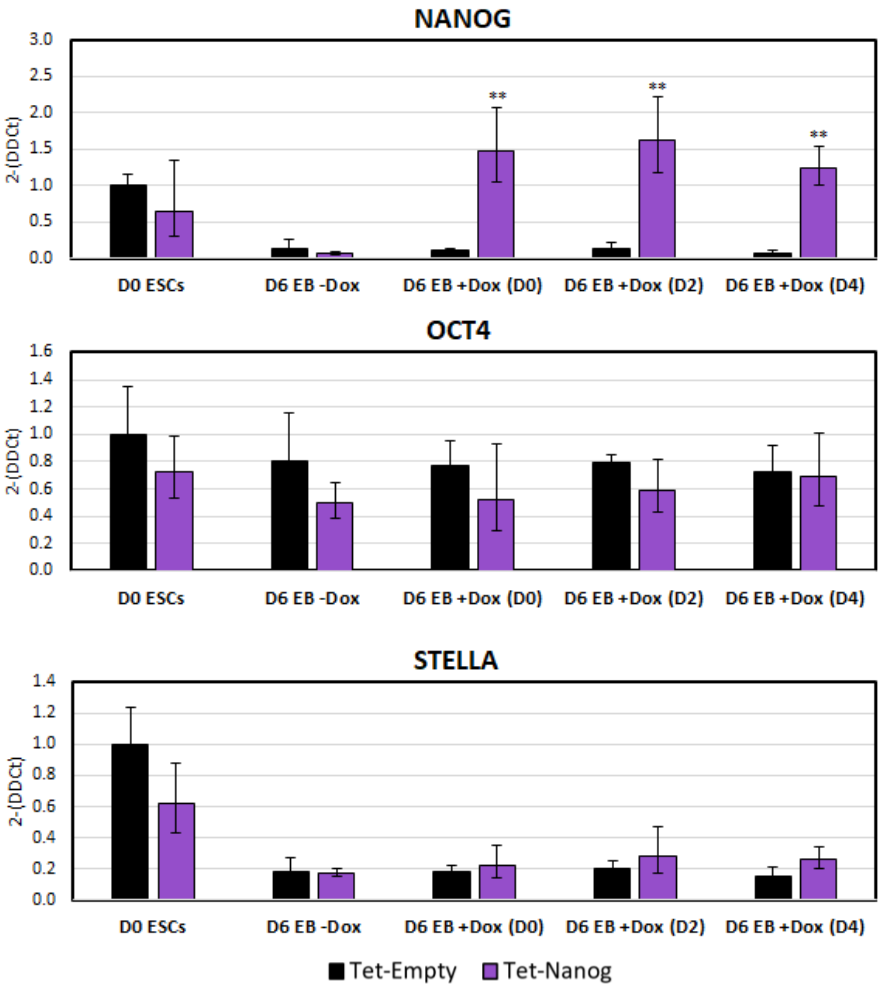

Figure 5.6.3 qRT-PCR analysis of pluripotency markers in Tet-NANOG transfected cells. *Average of three independent rat cell lines (two DA lines, one SD line). All data was normalised to the house keeping gene β-actin (dCT) and the fold change was calculated by normalising expression to the basal transcript level seen in ESCs harvested from Tet-Empty ESCs (D0 ESCs) (2-DDCT). (D0), (D2), (D4) represent cell pools which were cultured in the presence of doxycycline from day 0, day 2 and day 4 of EB differentiation respectively. Bars represent mean ± SD, *P<0.05, **P<0.01.*

The expression of *Nanog* cDNA had no significant effect on *Blimp1* or *Ap2γ* transcript expression within the Tet-NANOG cells (Figure 5.6.4). However, when *Nanog* cDNA was expressed from day 4 of the EB differentiation protocol, there was a significant increase in *Prdm14* expression compared to the Tet-Empty cells (Figure 5.6.4).

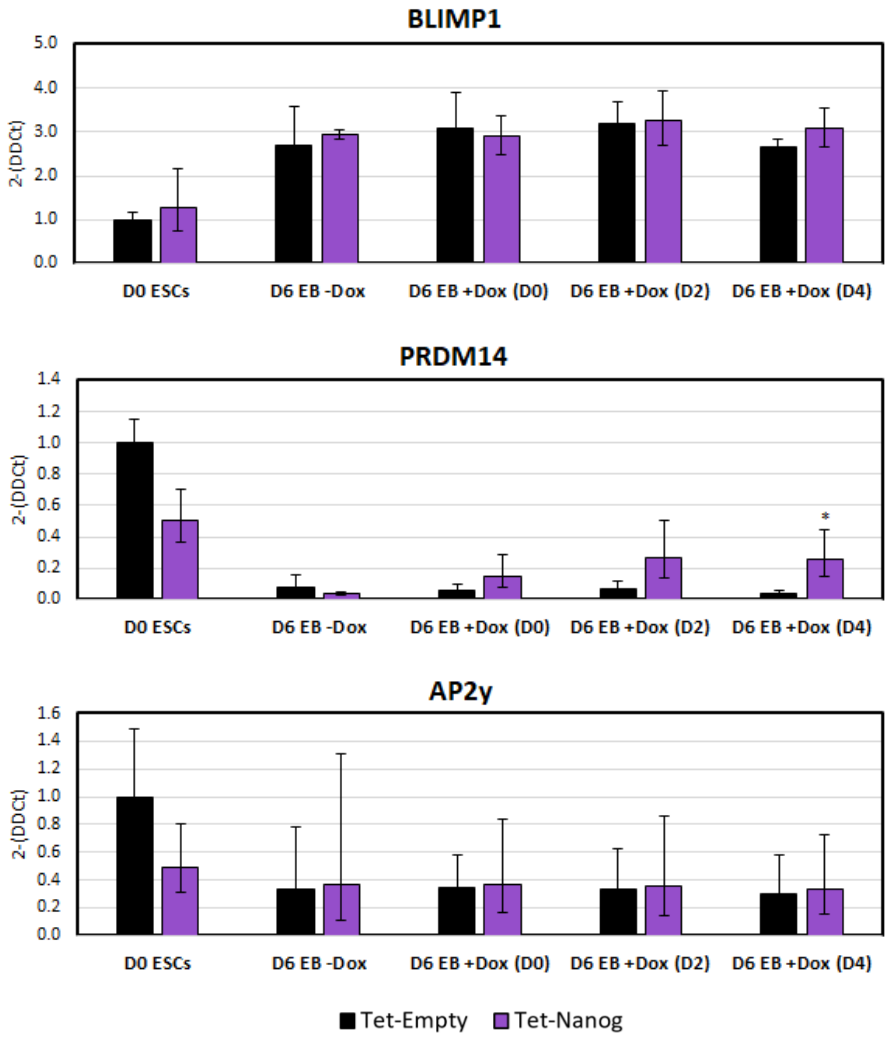

Figure 5.6.4 qRT-PCR analysis of PGC transcription factors in Tet-NANOG transfected cells. *Average of three independent rat cell lines (two DA lines, one SD line). All data was normalised to the house keeping gene β-actin (dCT) and the fold change was calculated by normalising expression to the basal transcript level seen in ESCs harvested from Tet-Empty ESCs (D0 ESCs) (2-DDCT). (D0), (D2), (D4) represent cell pools which were cultured in the presence of doxycycline from day 0, day 2 and day 4 of EB differentiation respectively. Bars represent mean ± SD, *P<0.05, **P<0.01.*

Expression of the PGC markers *Nanos3* and *Dazl* were also largely unaffected by the expression of *Nanog* cDNA during the EB differentiation protocol. However, there was a statistically significant drop in *Nanos3* transcript expression within Tet-NANOG cells cultured in the presence of doxycycline from day 2 of the protocol, but not from day 4 onwards (Figure 5.6.5).

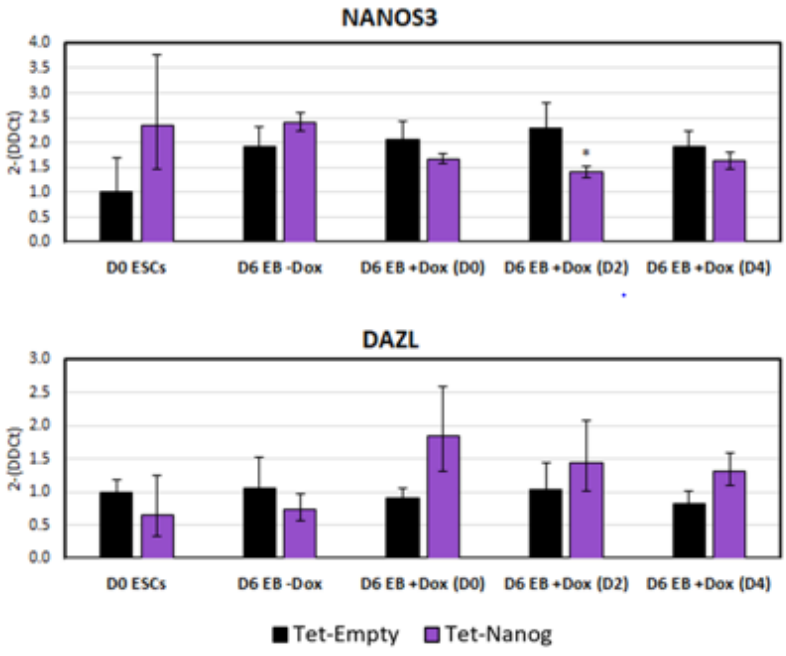

Figure 5.6.5 qRT-PCR analysis of PGC marker genes in Tet-NANOG transfected cells. *Average of three independent rat cell lines (two DA lines, one SD line). All data was normalised to the house keeping gene β-actin (dCT) and the fold change was calculated by normalising expression to the basal transcript level seen in ESCs harvested from Tet-Empty ESCs (D0 ESCs) (2-DDCT). (D0), (D2), (D4) represent cell pools which were cultured in the presence of doxycycline from day 0, day 2 and day 4 of EB differentiation respectively. Bars represent mean ± SD, *P<0.05, **P<0.01.*

Overall, these results suggested although functional expression of *Nanog* cDNA was demonstrated in the Tet-NANOG transfected cells, unlike the PGC transcription factors, *Nanog* alone could not induce expression of PGC markers in cells undergoing an undirected EB differentiation protocol. Interestingly, the expression of *Nanog* cDNA during EB differentiation did not appear to halt EB differentiation either as markers commonly associated with the pluripotent state remained low (e.g. *Stella* and *Prdm14*).

5.6.5 Expression of Nanog cDNA during a PGCLC differentiation protocol

DAK31 Tet-NANOG cells were subjected to the rat PGCLC differentiation protocol as described previously (Section 5.5), introducing 1μg/ml doxycycline after day 6 of the protocol. Aggregates formed from Tet-NANOG transfected cell pools at day 12 of the PGCLC differentiation protocol were imaged for mCherry fluorescent protein (Figure 5.6.6A), broken apart by gentle pipetting (trituration) and sorted into $mCherry^{+ve}$ and $mCherry^{-ve}$ populations by FACs (Figure 5.6.6B). By sorting Tet-NANOG cells into these two populations, it could be determined whether the expression of *Nanog* cDNA influenced the expression of PGC gene markers.

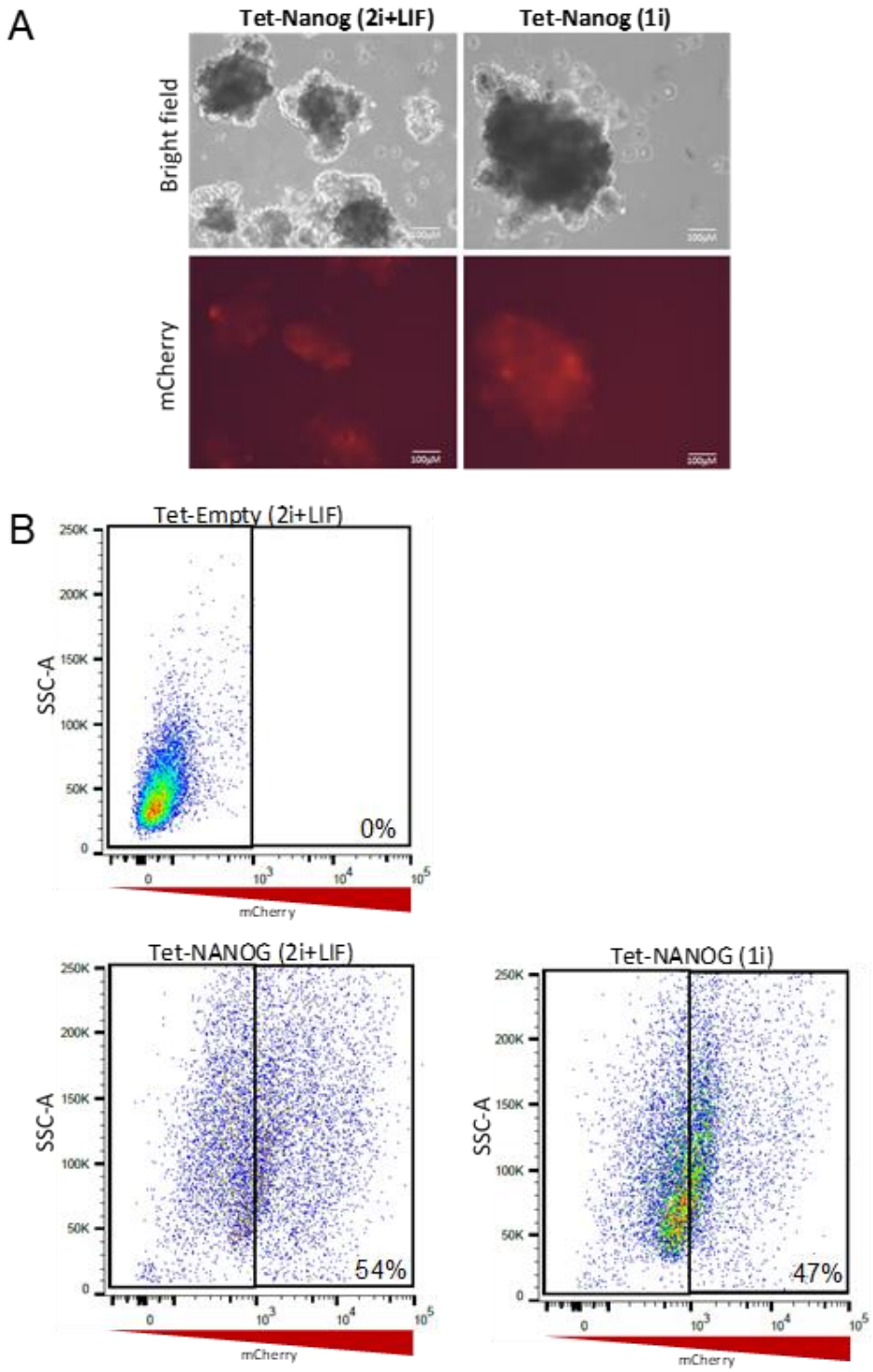

Figure 5.6.6. Tet-NANOG transfected cell pools undergoing PGCLC differentiation in the presence of doxycycline. *(A) DAK31 Tet-Nanog aggregates formed after D12 of PGCLC differentiation protocol. Aggregates cultured in the presence of doxycycline from Day 6 onwards. 2i+LIF = Pre-cultured in 2i+LIF prior to EpiLC differentiation, 1i = Pre-cultured in 1i medium prior to EpiLC differentiation. (B) FACs plots of D12 aggregates. Percentages represent population of mCherry^{+ve} cells.*

The separated populations were processed for RNA and used for qRT-PCR analysis. qRT-PCR analysis revealed there was a substantial increase in the expression of *Nanog* transcript in the mCherry^{+ve} population of the Tet-NANOG cells compared to the Tet-Empty cells (Figure 5.6.7). The expression level of *Nanog* did not differ between either pre-culture conditions (Figure 5.6.7). Both *Oct4* and *Stella* expression were greatly reduced in both populations of Tet-NANOG cells when compared to Tet-Empty cells (Figure 5.6.7).

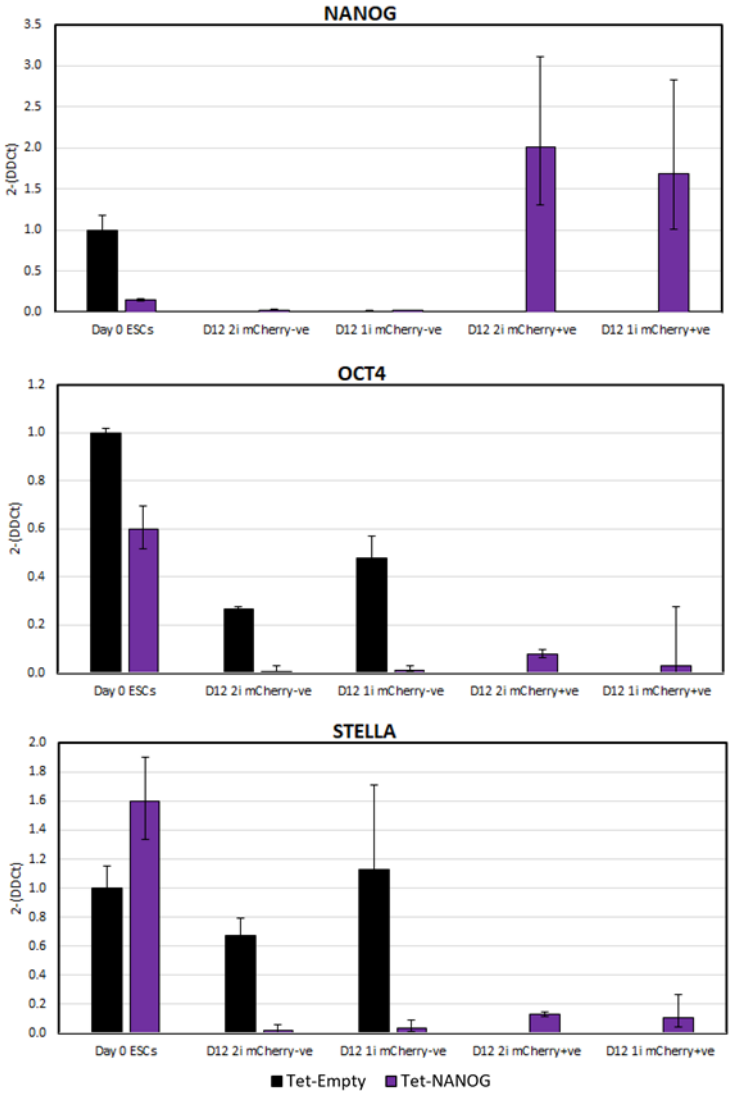

Figure 5.6.7. qRT-PCR analysis of pluripotency markers in Tet-NANOG cells undergoing a PGCLC differentiation protocol. *The data presented was an average of two experiments performed with Tet-Empty and Tet-Nanog transfected DAK31 cells. All data was normalised to the house keeping gene β-actin (dCT) and fold change was calculated by normalising gene expression to Day 0 Tet-Empty ESCs (2-DDCT). Bars represent mean ± SD.*

Tet-NANOG mCherry^{+ve} cells which had been pre-cultured in 1i medium had increased expression of all PGC transcription factors compared to the Tet-Empty cells (Figure 5.6.8). Expression of the *Blimp1* was over 8-fold greater in the Tet-NANOG mCherry^{+ve} cells compared to the Tet-Empty, while expression of *Prdm14* transcript was nearly 10-fold greater (Figure 5.6.8). Expression of *Blimp1* and *Prdm14* were also elevated in the Tet-NANOG mCherry^{+ve} cells which had been pre-cultured in 2i+LIF conditions, however, these levels were far lower than those achieved after the 1i pre-culture condition (Figure 5.6.8).

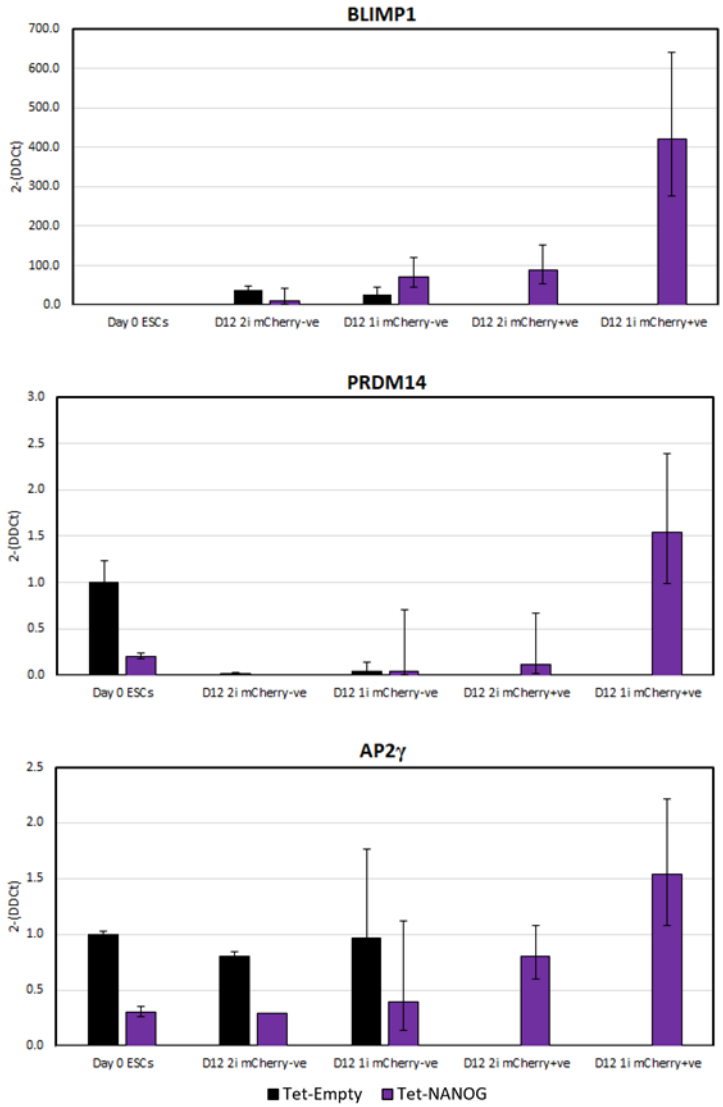

Figure 5.6.8. qRT-PCR analysis of PGC transcription factors in Tet-NANOG cells undergoing a PGCLC differentiation protocol. *The data presented was an average of two experiments performed with Tet-Empty and Tet-Nanog transfected DAK31 cells. All data was normalised to the house keeping gene β-actin (dCT) and fold change was calculated by normalising gene expression to Day 0 Tet-Empty ESCs (2-DDCT). Bars represent mean ± SD.*

Expression of the PGC gene markers *Nanos3* and *Dazl* were slightly elevated in Tet-NANOG mCherry^{+ve} cells which had been pre-cultured in 1i medium when compared to the Tet-Empty cells (Figure 5.6.9). However, no substantial change in *Vasa* expression could be identified in any population of Tet-NANOG cell compared to the Tet-Empty cells (Figure 5.6.9).

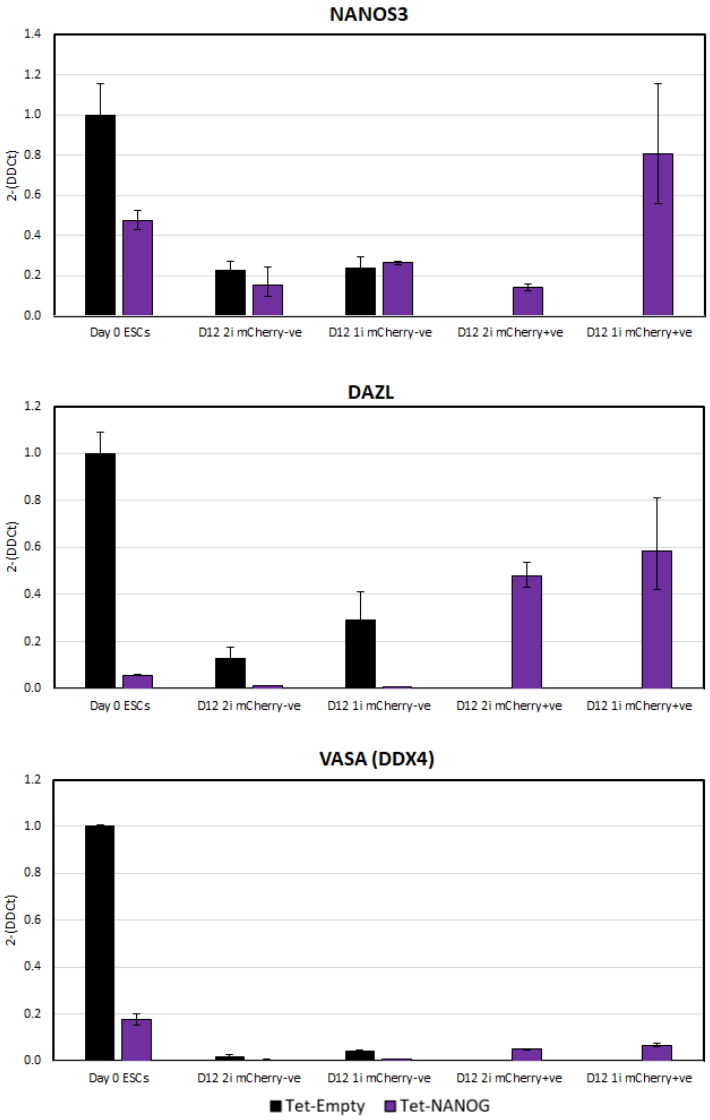

Figure 5.6.9. qRT-PCR analysis of PGC gene markers in Tet-NANOG cells undergoing a PGCLC differentiation protocol. *The data presented was an average of two experiments performed with Tet-Empty and Tet-Nanog transfected DAK31 cells. All data was normalised to the house keeping gene β-actin (dCT) and fold change was calculated by normalising gene expression to Day 0 Tet-Empty ESCs (2-DDCT). Bars represent mean ± SD.*

Transcript expression of markers of endoderm (*Gata4*, *Gata6*) and trophectoderm (*Gata3*) were also analysed to determine whether the expression of *Nanog* cDNA influenced the proportion of the Tet-On cells differentiating towards these lineages. *Gata4* expression was increased in the Tet-NANOG mCherry^{-ve} cells when compared to the Tet-Empty pools (Figure 5.6.10). However, Tet-NANOG mCherry^{+ve} cells had similar *Gata4* expression to the Tet-Empty pools (Figure 5.6.10).
The expression of *Gata6* in Tet-NANOG cells was on average lower than the expression level in Tet-Empty cell pools, with only the mCherry^{-ve} population of Tet-NANOG cells pre-cultured in 1i medium showing a similar expression to Tet-Empty cells cultured in the same conditions (Figure 5.6.10).
Gata3 expression in Tet-NANOG mCherry^{-ve} cells which had been pre-cultured in 2i+LIF medium was elevated compared to the Tet-NANOG mCherry^{+ve} cells and the Tet-Empty cell pools pre-cultured in the same conditions (Figure 5.6.10). However, Tet-NANOG mCherry^{+ve} cells pre-cultured in 1i medium had a greater *Gata3* expression compared to the Tet-NANOG mCherry^{-ve} cells and the Tet-Empty cell pools pre-cultured in the same conditions (Figure 5.6.10).
This increase in *Gata3* after 1i medium pre-culture in the mCherry^{+ve} population could highlight that *Nanog* cDNA expression increased the potential of differentiating cells differentiating into a *Gata3*$^{+ve}$ lineage *(*e.g. trophectoderm).

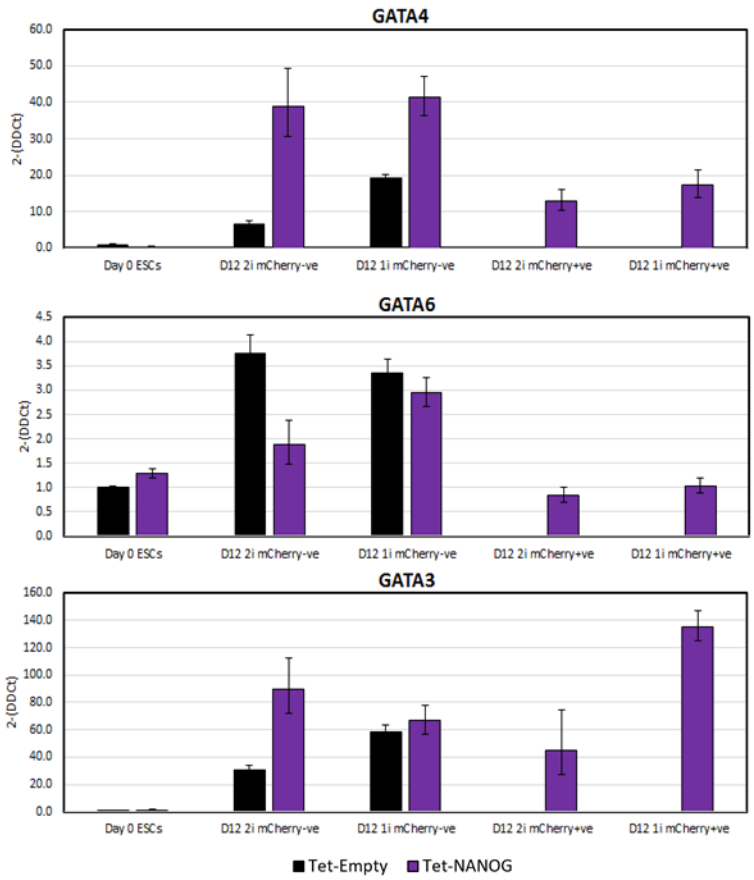

Figure 5.6.10. qRT-PCR analysis of the expression of endoderm (Gata4 and Gata6) and trophectoderm (Gata3) marker genes in Tet-NANOG cells undergoing a PGCLC differentiation protocol. *The data presented was an average of two experiments performed with Tet-Empty and Tet-Nanog transfected DAK31 cells. All data was normalised to the house keeping gene β-actin (dCT) and fold change was calculated by normalising gene expression to Day 0 Tet-Empty ESCs (2-DDCT). Bars represent mean ± SD.*

Expression of *Nanog* transgene during the PGCLC differentiation protocol increased the expression of the PGC transcription factors *Blimp1* and *Prdm14*, similar to that reported in mouse cells (Murakami et al. 2016). Slight increases in both *Nanos3* and *Dazl* expression could be identified in cells expressing *Nanog* transgene compared to the Tet-Empty cells after being subjected to the PGCLC differentiation protocol. However, these expression levels did not surpass those detected in rat ESCs, suggesting *Nanog* alone is not strong enough to efficiently direct rat ESCs towards the germline.

5.7 Chapter 5 discussion

Overexpression of the PGC transcription factors *Blimp1*, *Prdm14* and *Ap2γ* in mouse EpiLCs has been shown to generate a distinct population of PGCLCs without the need for PGC cytokine inducers (e.g. BMP4) in the culture medium (Nakaki et al. 2013). The efficiency of PGCLC determination was increased by inducing transgene expression of the PGC transcription factors in cells subjected to the PGCLC differentiation protocol described by Hayashi et al (Hayashi & Saitou 2013, Nakaki et al. 2013). Additionally, it has been reported that overexpression of pluripotency transcription factor *Nanog* in mouse cells which have transitioned irreversibly into the EpiLC fate directs cell differentiation towards the germ cell lineage (Murakami et al. 2016). The aim of this chapter was to determine whether the overexpression of the PGC transcription factors or *Nanog* via doxycycline-inducible Tet-On piggyBac transposon vectors could improve the proportion of rat cells directed towards the germ cell lineage.

5.7.1 Co-expression of *Blimp1* and *Prdm14* or *Blimp1* and *Ap2γ* transgenes increased PGC gene marker expression during rat ESC differentiation

Rat cells induced to overexpress a combination of *Blimp1* & *Prdm14*, or *Blimp1* & *Ap2γ* during an undirected EB differentiation protocol had significantly increased expression of endogenous PGC gene markers compared to control cells. A similar increase in PGC marker gene expression was also obtained in cells overexpressing either *Blimp1* and *Prdm14* or *Blimp1* and *Ap2γ* whilst undergoing the directed PGCLC differentiation protocol. By separating cells which were actively expressing the PGC transgenes (mCherry^{+ve}) from the inactive cells (mCherry^{-ve}), it was evident that increased PGC marker gene expression was only present in the mCherry^{+ve} population after being induced to differentiate. This suggested that increased PGC gene marker expression was in response to PGC transcription factor overexpression and not non-cell autonomous effects (e.g. the presence of doxycycline in the culture medium). A similar increase in PGC gene marker expression was reported in mouse ESCs, where co-expression of the PGC transcription factors directed a greater proportion of differentiating mouse cells towards the germ cell lineage (Nakaki et al. 2013).

Interestingly, the fold change increase of PGC gene marker expression was far greater in cells subjected to the EB differentiation protocol than those subjected to the PGCLC differentiation protocol when compared to control ESCs and differentiated cells. This suggests that the cells generated after the EB differentiation protocol were more responsive to the signals directing differentiation towards the germline than cells cultured in the rat EpiLC differentiation conditions.

Perhaps forming cell aggregates generated by the undirected EB differentiation protocol and then applying the PGCLC differentiation protocol might improve cell differentiation towards the germline, especially when inducing the overexpression of PGC transcription factors.

Nakaki et al previously concluded that the expression of all three PGC transcription factors was most beneficial for directing mouse cell differentiation to PGCLCs (Nakaki et al. 2013). However, expression of all three PGC transcription factors in rat cells from either a single vector or multiple transposon vectors had a negative effect on PGC marker gene expression. Elevated basal levels of lineage specific genes are evident in rat ESCs compared with mouse ESCs, suggesting that the initial pluripotency state of rat ESCs might be more “primed” than their mouse counterparts (Blair et al. 2011, Hong et al. 2013). Therefore, the overexpression of all three PGC transcription factors may have directed primed rat ESCs within the population towards alternative lineages instead of the germline. This result may also suggest that not all of these three PGC transcription factors are required for rat PGC specification. In porcine and human cells, *Sox17* and *Blimp1* are required for generating PGCLCs, with *Prdm14* and *Ap2γ* appearing to have little influence (Irie et al. 2015, Wang et al. 2016). It would be of interest to further explore the role of the three key PGC transcription factors, and whether *Sox17* is also involved in rat PGC specification.

5.7.2 Expression of *Nanog* transgene alone increased PGC transcription factor expression during rat ESC differentiation

In mouse ESCs, overexpression of *Nanog* in EpiLCs during a PGCLC differentiation protocol induced the expression of all three PGC transcription factors, driving cell differentiation towards the germ cell lineage (Murakami et al. 2016). Overexpression of *Nanog* in rat cells subjected to an undirected EB differentiation protocol showed no induction of PGC specific gene markers.

This result suggests that unlike the co-expression of *Blimp1* with either *Prdm14* or *Ap2γ, Nanog* alone is not able to drive the differentiation of cells undergoing the EB differentiation protocol towards the germline. Unlike mouse cells, where expression of *Nanog* within the first few days of cell differentiation was able to revert cells back into an ESC state (Murakami et al. 2016), overexpression of *Nanog* at any stage during the EB differentiation protocol did not appear to retain rat cells in an ESC state or revert them back into the ESC state. As rat ESC cultures have higher expression of lineage specific genes despite their overall pluripotent state (Blair et al. 2011, Hong et al. 2013), this suggests that within the heterogeneous pool, the more 'primed' rat cells cannot be directed back to a pluripotent state by the expression of *Nanog* once they are stimulated to differentiate.

Nanog overexpressing cells pre-cultured in 1i medium and subjected to the PGCLC differentiation protocol had increased expression of all three PGC transcription factors (*Blimp1, Prdm14, Ap2γ*) compared to control cells, similar to what has been reported in mouse cells (Murakami et al. 2016). *Nanog* overexpressing cells also had increased expression of PGC specific marker genes compared to control cells. However, this induction did not appear to be of the magnitude determined in mouse ESCs (Murakami et al. 2016). NANOG is reported to bind to enhancer regions of *Blimp1* and *Prdm14* in differentiating cells, activing their expression independently of BMP4 and WNT signalling (Murakami et al. 2016). As *Nanog* transgene expression increased the expression of PGC transcription factors, perhaps this increase in PGC specific gene markers is the result of increased *Blimp1*, *Prdm14* and/or *Ap2γ* expression, rather than the direct involvement of *Nanog* on specific marker gene expression. Therefore, there could be a potential benefit in co-expressing *Nanog* with *Blimp1*, *Prdm14* and/or *Ap2γ* during directed differentiation of rat cells towards PGCs.

Chapter 6 Directing differentiation away from the somatic lineage via the deletion of the OTX2 transcription factor

6.1 Introduction

Otx2 is a homeobox gene expressed in the epiblast compartment during embryogenesis (Kurokawa et al. 2004). In mouse, the OTX2 transcription factor targets OCT4 to alternative enhancer elements during epiblast differentiation, activating the expression of transcription factors which drive the cells out of the naïve stem cell fate (Buecker et al. 2014, Yang et al. 2014). In a recent study, it was shown that mouse *Otx2*-deficient ESCs generated a greater number of PGCLCs during cytokine induced PGCLC differentiation compared to their *Otx2* wild-type counterparts (Zhang et al. 2018). Also, the overexpression of *Otx2* blocked the expression of the PGC transcription factors *Blimp1*, *Prdm14*, and *Ap2γ*, preventing mouse ESCs entering the PGC lineage and directed the cells towards the somatic cell fate (Zhang et al. 2018). *Otx2*$^{-/-}$ EpiLCs cultured in PGCLC medium as described by Hayashi et al (2011, 2013), induced more rapid expression of all three key PGC transcription factors (*Blimp1*, *Prdm14*, and *Ap2γ*) and *Nanog* (Zhang et al. 2018). The elevated expression of these factors increased the proportion of mouse ESCs being driven towards the PGCLC fate (Zhang et al. 2018). The rat *Otx2* locus is roughly half the size of the *Otx2* locus found within mice, however, the coding sequence structure of both rat and mouse OTX2 are well conserved (Figure 6.1.1).

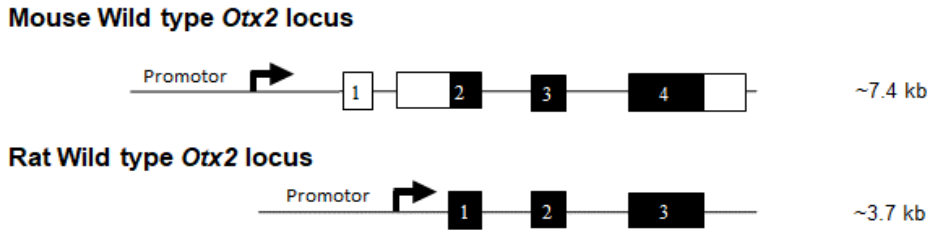

Figure 6.1.1. Schematic of the OTX2 locus of rat and mice. Black bars indicate the translated exons, while white bars represent the untranslated region.

The aim of this chapter was to determine if the loss of *Otx2* expression in rat ESCs could increase the proportion of differentiating cells that enter the PGC lineage. A CRISPR/Cas9 gene editing strategy was used to create a deletion within the *Otx2* locus, disrupting OTX2 protein expression. The aim of this chapter was to generate rat ESC clones carrying a homozygous deletion within in the *Otx2* locus, thereby generating *Otx2*$^{-/-}$ knock-out cells.

6.2 Generating rat *Otx2*$^{-/-}$ knock-out cell lines via CRISPR/Cas9 gene-editing

6.2.1 CRISPR/Cas9 gene editing strategy for inducing a deletion within the *Otx2* locus

A CRISPR gene-editing strategy was used to generate two separate double strand breaks (DSBs) within the *Otx2* gene. These DSBs induced the removal of a 1.4kb region of the *Otx2* locus, spanning the first two exons of the *Otx2* gene. The deletion removed the start codon of *Otx2*, resulting in a frameshift mutation and loss of functional OTX2 production (Figure 6.2.1).

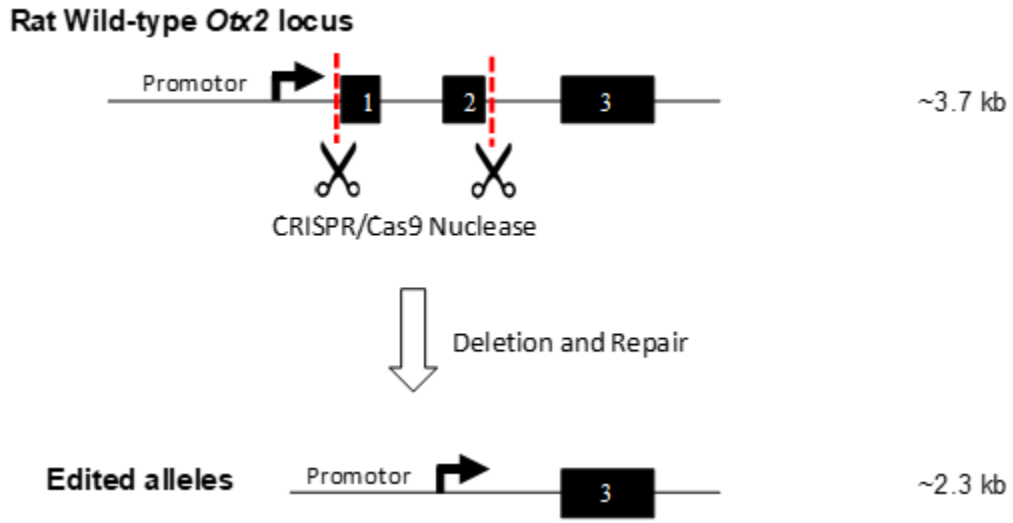

Figure 6.2.1. Strategy for generating rat Otx2$^{-/-}$ knock-out cell lines. *Two separate gRNAs were designed to target Cas9 nuclease to separate sites in the OTX2 locus. DSBs would be introduced at these separate sites, inducing the deletion of a 1.4kb region of the Otx2 locus, including exon 1 and exon 2. Non-homologous end joining (NHEJ) would induce reattachment of the broken strands, forming a genome lacking the full Otx2 gene sequence.*

Multiple gRNA sequences were designed which would target the Cas9 nuclease to PAM sites upstream of exon 1 and downstream of exon 2 of the *Otx2* gene. Using the CRISPR Design tool produced by the Zhang Lab (crispr.mit.edu), six gRNA oligonucleotides with PAM sites within 50 base pairs of the intended cut sites of the *Otx2* locus were generated (*Figure 6.2.2*). These gRNAs were designed to target the rat *Otx2* gene sequence presented on the ensembl database (ENSRNOT00000074488.2). The gRNA oligonucleotides were ligated into the PX458 Cas9 nuclease vector as described in Chapter 4.

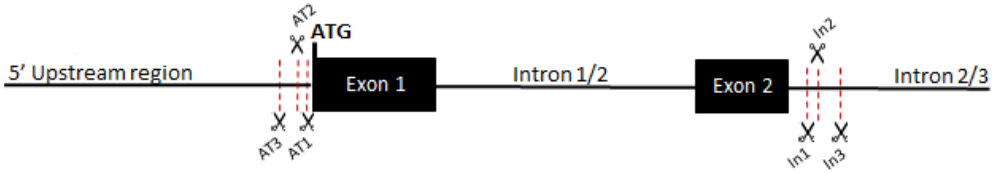

gRNA Name	Sequence (-PAM, 20bp + G)	PAM	Direction	DSB location (From ATG site)
AT1	(G)TTAGATAAGACATCATGCTA	AGG	3' to 5'	-4bp
AT2	GACATCATGCTAAGGTTGTT	TGG	3' to 5'	-12bp
AT3	(G)CCGGCTGGGTCCCCCCAATT	TGG	5' to 3'	-33bp
In1	(G)tcagtataatccacgattca	agg	3' to 5'	+1262bp
In2	ggtttcttgaccttgaatcg	tgg	5' to 3'	+1269bp
In3	gattatactgacgacccaat	agg	5' to 3'	+1286bp

Figure 6.2.2. ***gRNA sequences for inducing OTX2 deletion.*** *Each gRNA would target the Cas9 nuclease to the Otx2 gene, inducing the formation of a DSB either upstream of the ATG site or within intron 2/3. "5' to 3'" gRNA would target Cas9 nuclease to the sense (5' to 3') strand, "3' to 5'" gRNA would target Cas9 nuclease to the anti-sense (3' to 5') strand.*

6.2.2 Determining efficiency of Cas9 induced DSBs within the *Otx2* locus

To readily assess the efficiency of CRISPR/Cas9 induced DSBs within the *Otx2* locus, rat DAK31 cells were co-transfected with varying combinations of the gRNA containing PX458 Cas9 nuclease vectors (*Figure 6.2.2*). Vectors containing either AT1, AT2 or AT3 were co-transfected with vectors containing either In1, In2 or In3 to induce DSBs upstream of the ATG start codon and downstream of exon 2 within the *Otx2* locus. Successful transfection was determined by the detection of mCherry fluorescent protein 24 hours post transfection. DAK31 ESCs were chosen as they contained no fluorescent marker which could interfere with mCherry immunofluorescence screening of the transfected cell pools. PCR amplification of gDNA isolated from transfected DAK31 cells was performed with oligonucleotides spanning a region of ~1775bp of the *Otx2* locus, encompassing both exon 1 and 2 (Figure 6.2.3A). Gel electrophoresis was performed to confirm that Cas9-induced DSBs had occurred within the *Otx2* locus (Figure 6.2.3B). Evidence of a deletion within the *Otx2* gene would result in a band of ~490bp.

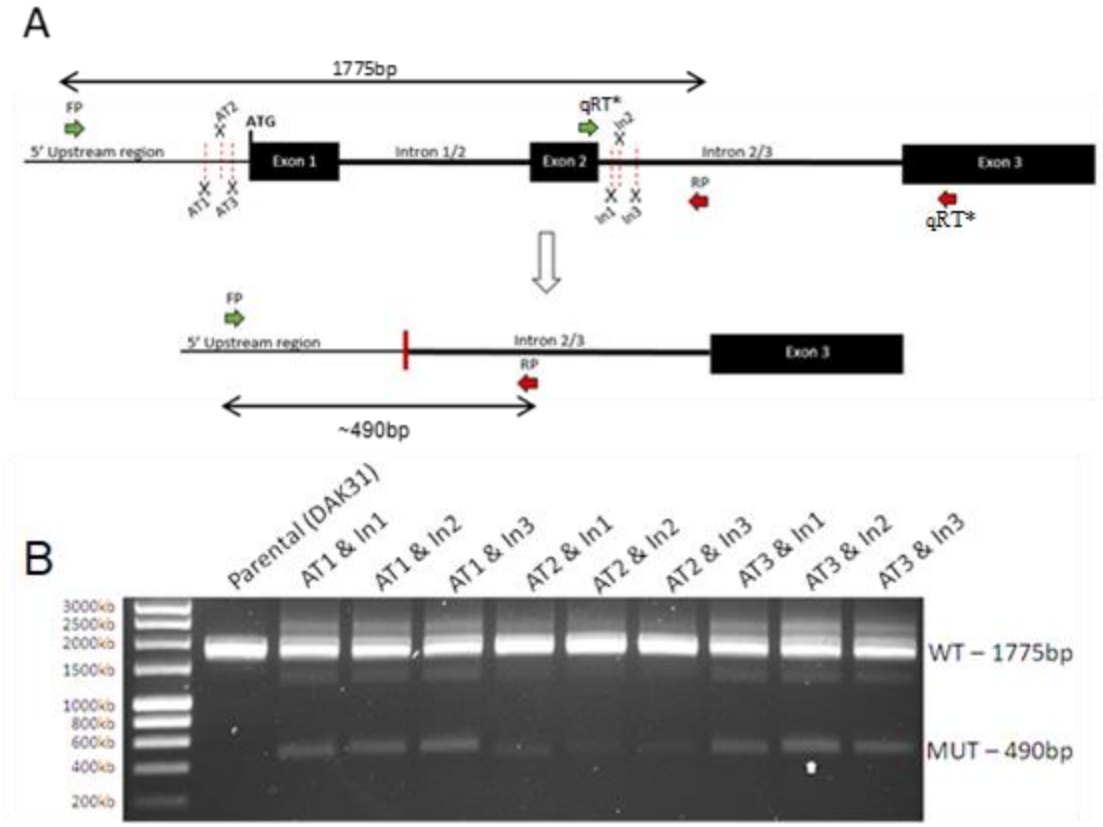

Figure 6.2.3. Validation of CRISPR cas9 induced deletion in the OTX2 locus. *(A) Schematic showing the amplified regions of wild-type and edited Otx2 locus. 'qRT' indicates the building sites of the Otx2 qRT-PCR primers (B) Gel electrophoresis of PCR bands from DAK31 cells transfected with Otx2 targeting gRNA. White arrow indicates the chosen pair of gRNAs to be used to induce the knock-out of the rat Otx2 gene.*

Every combination of AT-PX458 and IN-PX458 vector showed a faint band matching the size of a DSB-mediated deletion within the *Otx2* gene (~490bp) and an intense wild-type band (~1775bp) (Figure 6.2.3B). DAK31 cells transfected with AT3-PX458 and In2-PX458 vectors (Figure 6.2.3B - white arrow) resulted in the most intense deleted band of all combinations (Figure 6.2.3B). Therefore, it was decided that the AT3-PX458 and In2-PX458 vectors would be used to generate the *Otx2*$^{-/-}$ knock-out cell lines.

6.2.3 Generation of rat DAK31 *Otx2*$^{-/-}$ clones

DAK31 ESCs were co-transfected with the AT3-PX458 and In2-PX458 vectors (Figure 6.2.4). 48 hours after transfection, ~200 mCherry^{+ve} transfected cells were single cell sorted into 96 well plates. The gating strategy detailed in section 2.6.7 was used. The remaining cells were gated to isolate populations of mCherry^{+ve} cells by plotting mCherry (610/20A) versus side scatter area (SSC-A). The gates were set against untransfected rat ESCs. The flow cytometry plots generated during the FACs of these mCherry^{+ve} are shown in Figure 6.2.4. These single cells were cultured in 2i+LIF medium and allowed to recover for 7 days. Of these sorted mCherry^{+ve} cells, 85 cell clones survived the single cell plating procedure and generated large enough colonies to propagate further. After a further 2 weeks, 30 clones had generated colonies that could be passaged into 24-well plates. Aliquots of the 30 clones were frozen and screened for a deletion within the *Otx2* gene by PCR amplification of purified gDNA. Of the 30 clones screened, 20 produced at least a single band which was substantially smaller than a wild-type *Otx2* band. 9 clones lacked a PCR band matching the wild-type *Otx2* gene (an example is marked in Figure 6.2.4). Of these 9 clones, only 3 were determined to be largely karyotypically normal, DA15, DA16 and DA28.

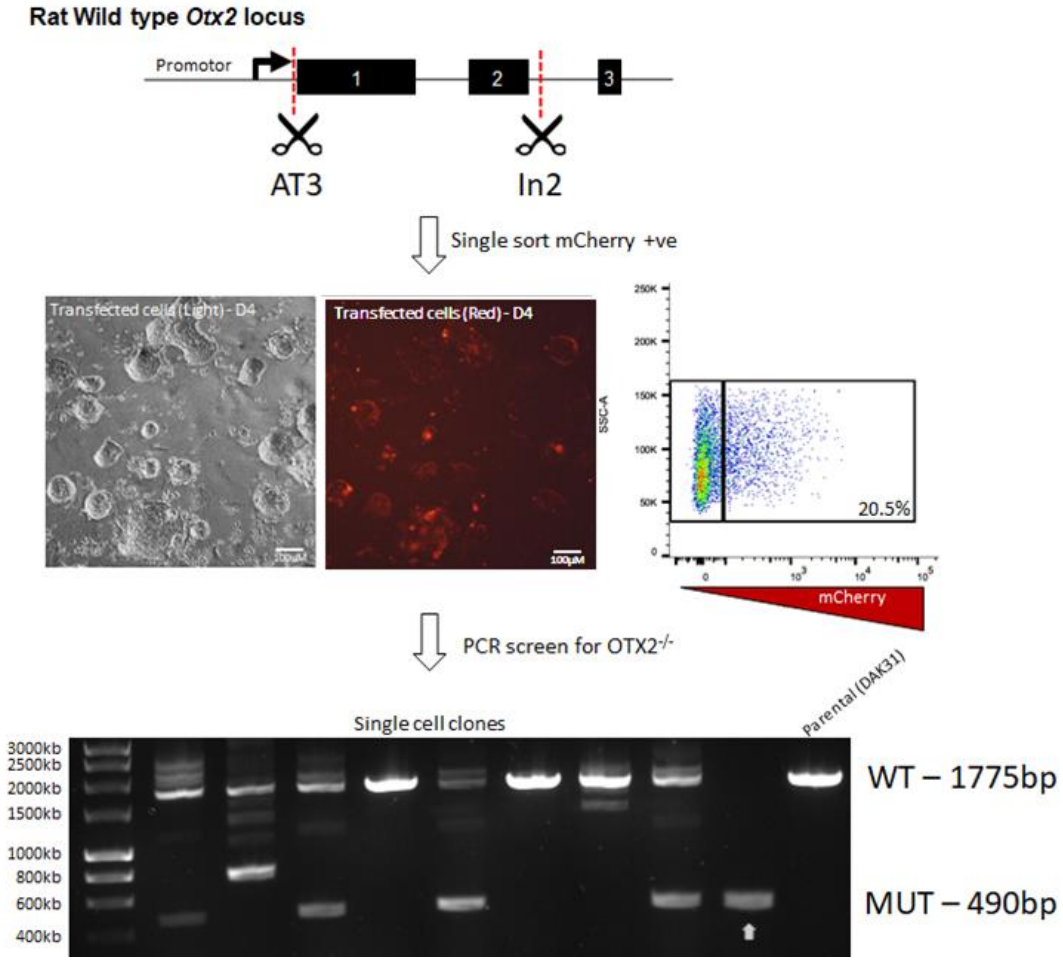

Figure 6.2.4. Transfection of DAK31 and validation of cell clones. *Transfected cells underwent FACs sorting, sorting single cell clones of mCherry positive cells. ~20% of the transfected cells were mCherry positive. Single cells were bulked up and then harvested for genomic DNA. The region to be edited was PCR amplified and gel electrophoresis used to determine any clones which lacked a wild-type (WT) copy of the Otx2 gene.*

Sanger sequencing of DA15, DA16 and DA28 cell clones determined that the region encompassing exon 1 and 2 of the *Otx2* gene had been successfully deleted (Figure 6.2.5). Additionally, Sanger sequencing performed on another clone (DA13) was identified as having a wild-type copy of the *Otx2* gene (Figure 6.2.5A), as well as multiple larger fragments which may have been the result of insertions into the locus via NHEJ repair of the region. Due to these larger bands, this clone was potentially a heterozygous *Otx2*$^{+/-}$ cell line and so would be analysed further to observe any potential effects caused by heterozygous expression of the *Otx2* gene.

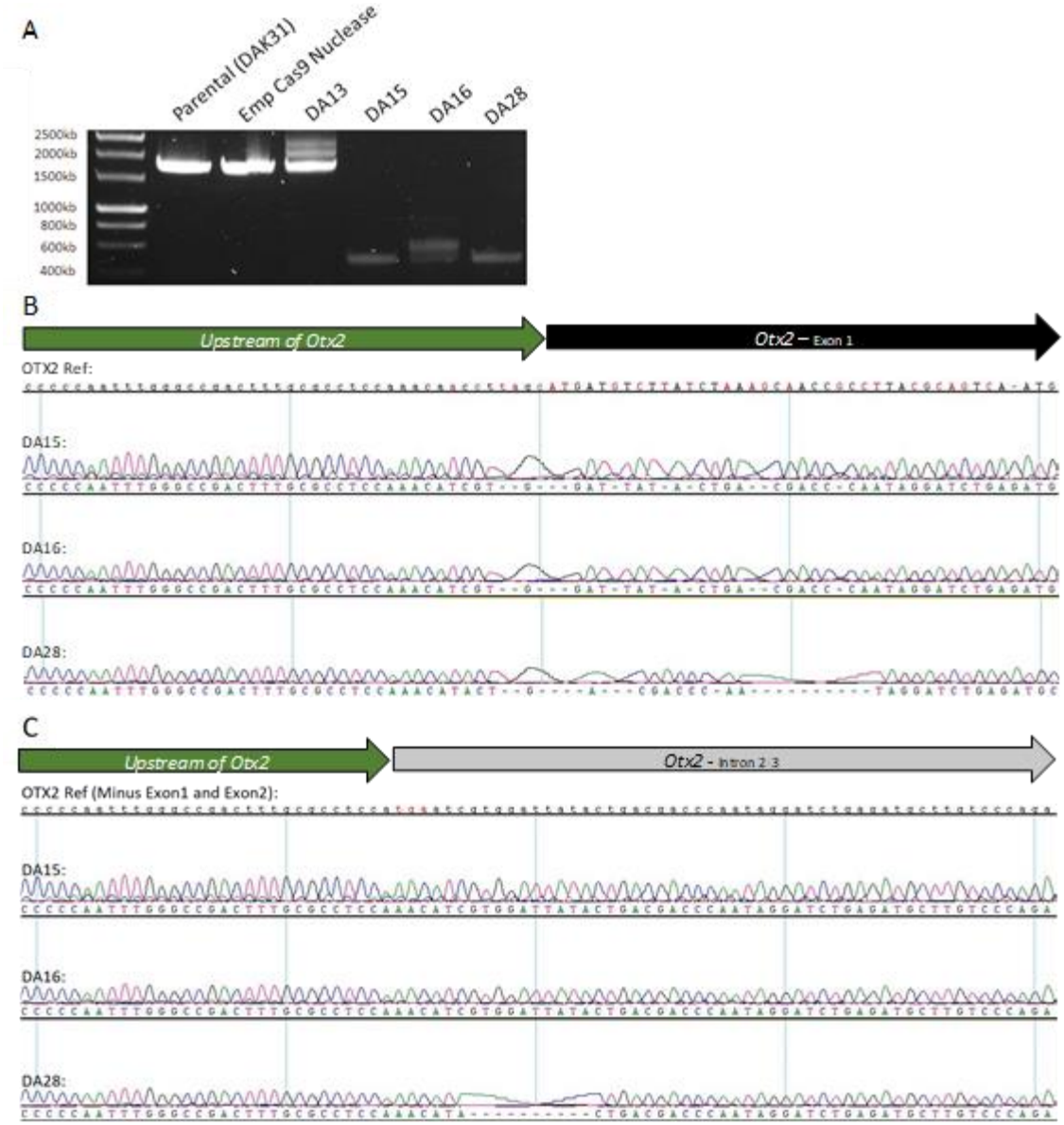

Figure 6.2.5. Validated Otx2$^{-/-}$ knock-out clones. *(A) Gel electrophoresis of PCR fragments amplified from genomic DNA. The parental DAK31 line and cells transfected with a PX458 vector containing no gRNA were used as a deletion control. (B) Sanger sequencing of OTX2$^{-/-}$ clones compared to full Otx2 reference sequence. (C) Sanger sequencing of OTX2$^{-/-}$ clones compared to an Otx2 reference sequence missing exon 1 and 2. Both B&C show deletions within clones DA15, DA16, and DA28 spanning from the ATG start codon up to Intron 2 of the Otx2 gene.*

All *Otx2*$^{-/-}$ clones grew noticeably slower than the parental DAK31 cell line when cultured in 2i+LIF conditions (Figure 6.2.6). Colonies produced from DA13, DA16 and DA28 clones were on average smaller and more spherical than the parental DAK31 cell line (Figure 6.2.6). However, this could be the result of sub-clonal variation due to the single cell sorting procedure.

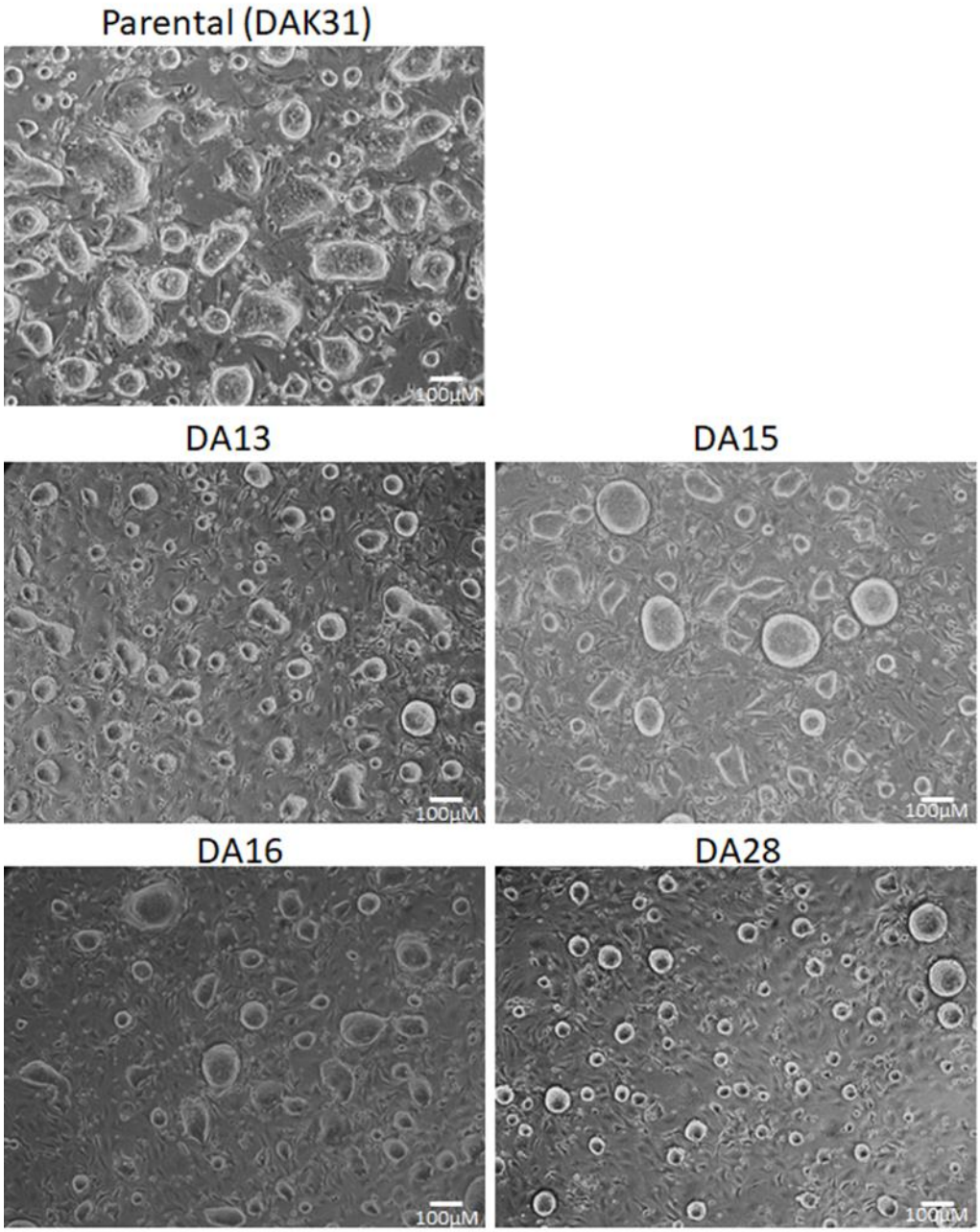

Figure 6.2.6. Bright field microscopy photographs of Otx2$^{-/-}$ clones (DA15, DA16 and DA28) and the DA13 clone. *Photographs were taken of the remaining clones after single cell sorting and screening for Otx2 knock-outs. The top panel shows the parental WT cell line (DAK31). All cells were seeded at 1.5 x 10^5 cells and cultured for 2 days in 2i+LIF culture medium.*

6.3 Confirming loss of OTX2 protein within *Otx2*$^{-/-}$ clones

6.3.1 Immunostaining clones for OTX2 protein

Published data has shown that *Otx2* gene expression increases in rat ESCs when cultured in a base culture medium (N_2B_{27}) containing only PD0325091 without CHIR99021 and LIF, referred to as 1i medium (Meek et al. 2013). To confirm that *Otx2*$^{-/-}$ knock-out clones did not produce OTX2 protein, cells were cultured in 1i medium conditions for 3 days and immunostained for OTX2 protein.

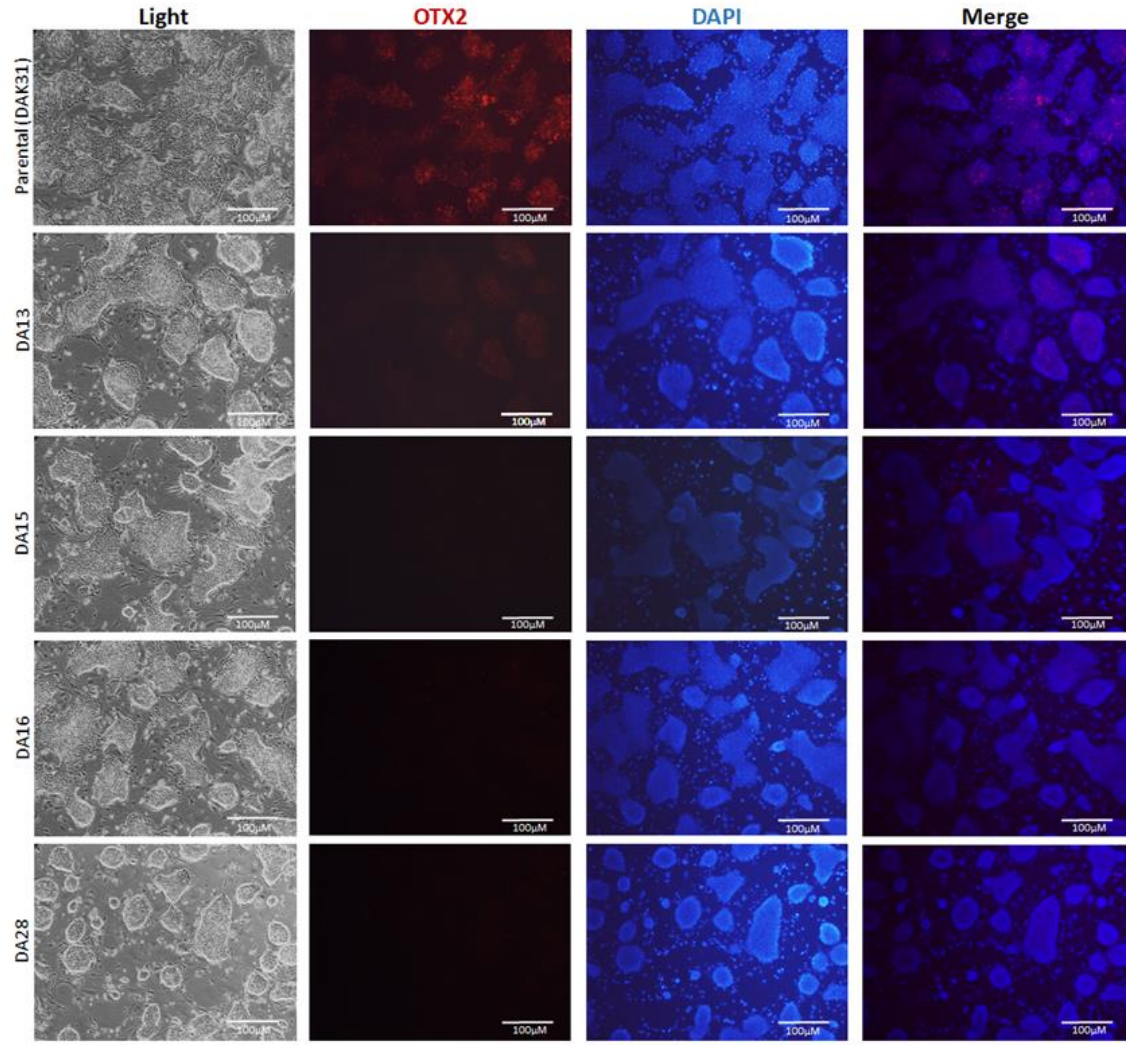

Figure 6.3.1. Immunostaining Otx2$^{-/-}$ knock-out clones for the presence of OTX2 protein. *OTX2 protein (Red), DAPI nuclear stain (Blue).*

The parental DAK31 cell line cultured in 1i culture medium showed positive OTX2 protein staining (red) (Figure 6.3.1). DA13 showed faint OTX2 fluorescent staining, but no OTX2 fluorescent staining was observed for DA15, DA16 or DA28 *Otx2*$^{-/-}$ knock-out clones (Figure 6.3.1). This meant that either the deletions induced by CRISPR/Cas9 gene editing had induced loss of function mutations in the *Otx2* locus or that these *Otx2*$^{-/-}$ clones were less responsive to 1i medium culture.

6.4 Differentiation potential of *Otx2*$^{-/-}$ knock-out clones

6.4.1 *Otx2*$^{-/-}$ clones undergoing an Embryoid body (EB) differentiation protocol

The *Otx2*$^{-/-}$ clones, alongside the parental and DA13 clone, underwent a 6-day rat Embryoid body (EB) differentiation protocol to observe whether the loss *Otx2* impacted the differentiation potential of these cells. Cellular aggregates produced after the 6-day protocol were harvested and RNA processed for qRT-PCR analysis. All *Otx2*$^{-/-}$ clones had reduced *Blimp1* transcript expression compared to the parental in the ESC state (Day 0 ESCs) and after the 6-day EB differentiation protocol (Figure 6.4.1). However, the significance of this reduced *Blimp1* is questionable due to the low basal expression in rat ESCs. The expression of the other PGC TFs (*Prdm14* and *Ap2γ*) were elevated in *Otx2*$^{-/-}$ clones compared to the parental line after the 6-day protocol (Figure 6.4.1). As expected, no *Otx2* transcript expression was detected in the *Otx2*$^{-/-}$ clones DA15, DA16 and DA28 (Figure 6.4.1). DA13 did show expression of *Otx2*, but this was lower than the *Otx2* expression identified in the parental DAK31 cell line (Figure 6.4.1).

Nanog transcript expression in the parental DAK31 cell line was dramatically decreased after cells had been subjected to the EB differentiation protocol (Figure 6.4.1). However, *Nanog* expression in all O*tx2*$^{-/-}$ clones (including DA13) after the 6-day differentiation protocol remained relatively unchanged when compared to the expression level in *Otx2*$^{-/-}$ ESCs (Figure 6.4.1).

Otx2$^{-/-}$ clones had reduced expression of the epiblast markers *Brachyury* and *Fgf5* compared to the parental cell line after the 6-day differentiation protocol (Figure 6.4.1). Additionally, DA16 and DA28 both had elevated expression of the endoderm marker *Gata6* compared to the parental line after undergoing the EB differentiation protocol (Figure 6.4.1).

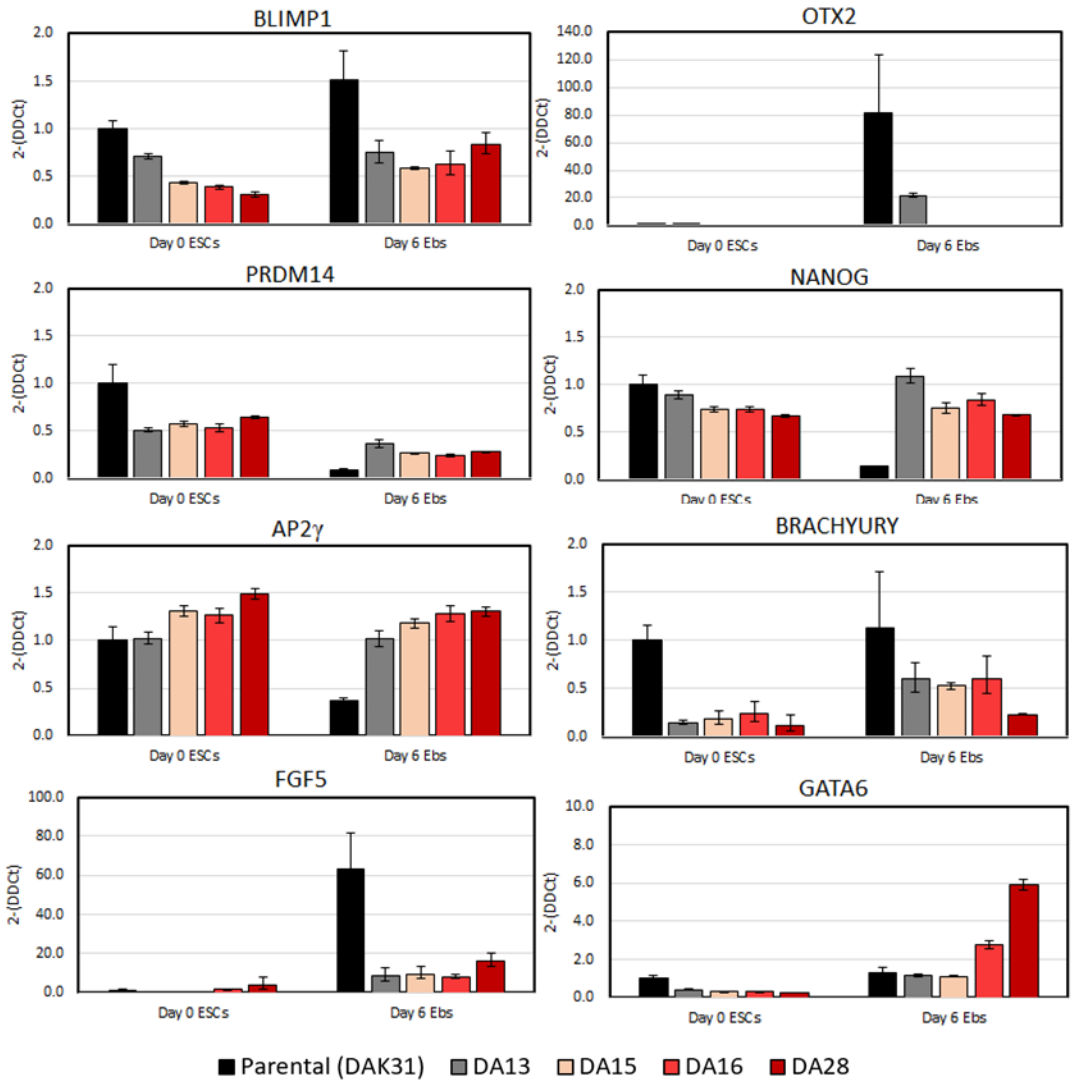

Figure 6.4.1. qRT-PCR analysis of OTX$^{-/-}$ clones before and after EB differentiation. *Average of three technical replicates generated from 1 experimental repeat. Expression was normalised to the house keeping gene β-actin (dCT) and fold change (2-DDCT) values generated by normalising gene expression to day 0 DAK31 ESCs. Bars represent mean ± SD.*

Overall, the qRT-PCR data generated from cells undergoing an EB differentiation protocol produced a similar pattern to what had been determined in the mouse *In vitro* system (Hayashi et al. 2011, Zhang et al. 2018), loss of *Otx2* expression prevented the inactivation of the *Nanog* gene and reduced the activation of *Fgf5* expression during cellular differentiation. Interestingly, the DA13 clone also showed a similar result to the *Otx2*$^{-/-}$ cell lines. This result could be the result of haploinsufficiency, that the loss of single copy of the *Otx2* gene generates a similar phenotype to the homozygous knock-out of *Otx2*. However, the similar gene expression from DA13 could also suggest that the response seen in the the *Otx2*$^{-/-}$ clones are the result of sub-clonal variation rather than the loss of *Otx2* expression.

6.4.2 *Otx2*$^{-/-}$ clones undergoing a PGCLC differentiation protocol

The *Otx2*$^{-/-}$ clones underwent the PGCLC differentiation protocol (Figure 4.5.9) as described previously, to determine whether the loss of *Otx2* expression helped to direct differentiating rat ESCs towards the PGCLC fate.

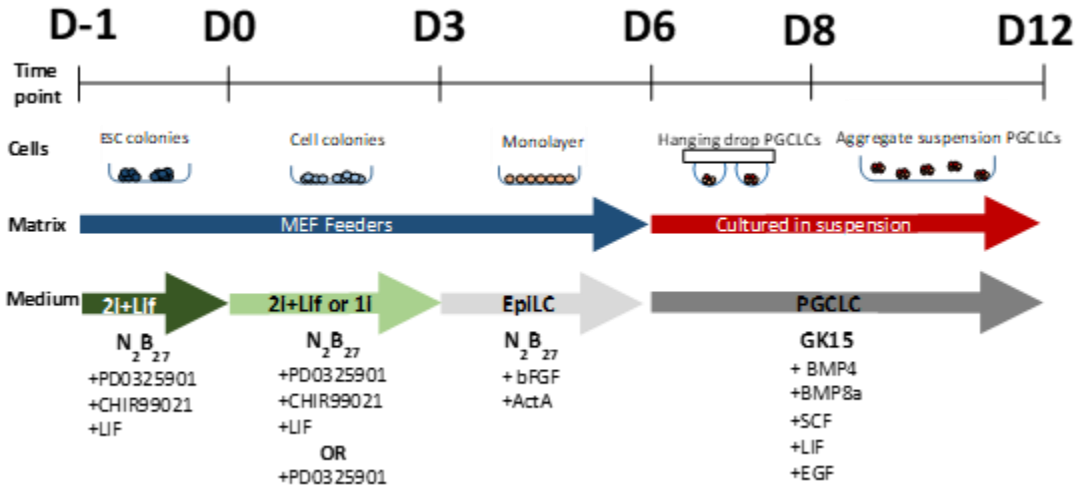

Figure 6.4.2 Schematic of the rat PGCLC differentiation protocol used for differentiation of Otx2$^{-/-}$ clones. *Rat ESCs cultured in 2i+Lif or 1i medium conditions on a MEF layer were transferred onto a fresh MEF feeder layer with EpiLC differentiation medium for 3 days. These cells where then pipetted into hanging drops containing ~2,000 cells in PGCLC medium. After 2 days the hanging drops were collected and placed into fresh PGCLC medium in 6 well low adhesion plates for a further 4 days.*

6.4.2.1 EpiLC differentiation protocol

The *Otx2*$^{-/-}$ clones (DA15, DA16 & DA28), DA13 and the parental DAK31 cell line were pre-cultured for 3 days in 2i+LIF and 1i culture medium on MEF feeder layers. After the 3-day culture, 1 x 10^5 of each cell line were passaged into multiple wells of 12-well plates coated with fresh MEF layers in EpiLC medium. Cells were incubated for a further 3 days, with the EpiLC medium being replaced with fresh medium every 24 hours to replenish the bFGF and activin A. Cell pools were photographed after 3 days culture in EpiLC culture medium (Figure 6.4.3). Both 2i+LIF and 1i medium pre-cultured cells (Figure 6.4.3) showed a flattened morphology compared to the domed ESCs (Figure 6.2.6). However, *Otx2*$^{-/-}$ knock-out cell lines showed more evidence of cellular debris compared to the parental DAK31 wells.

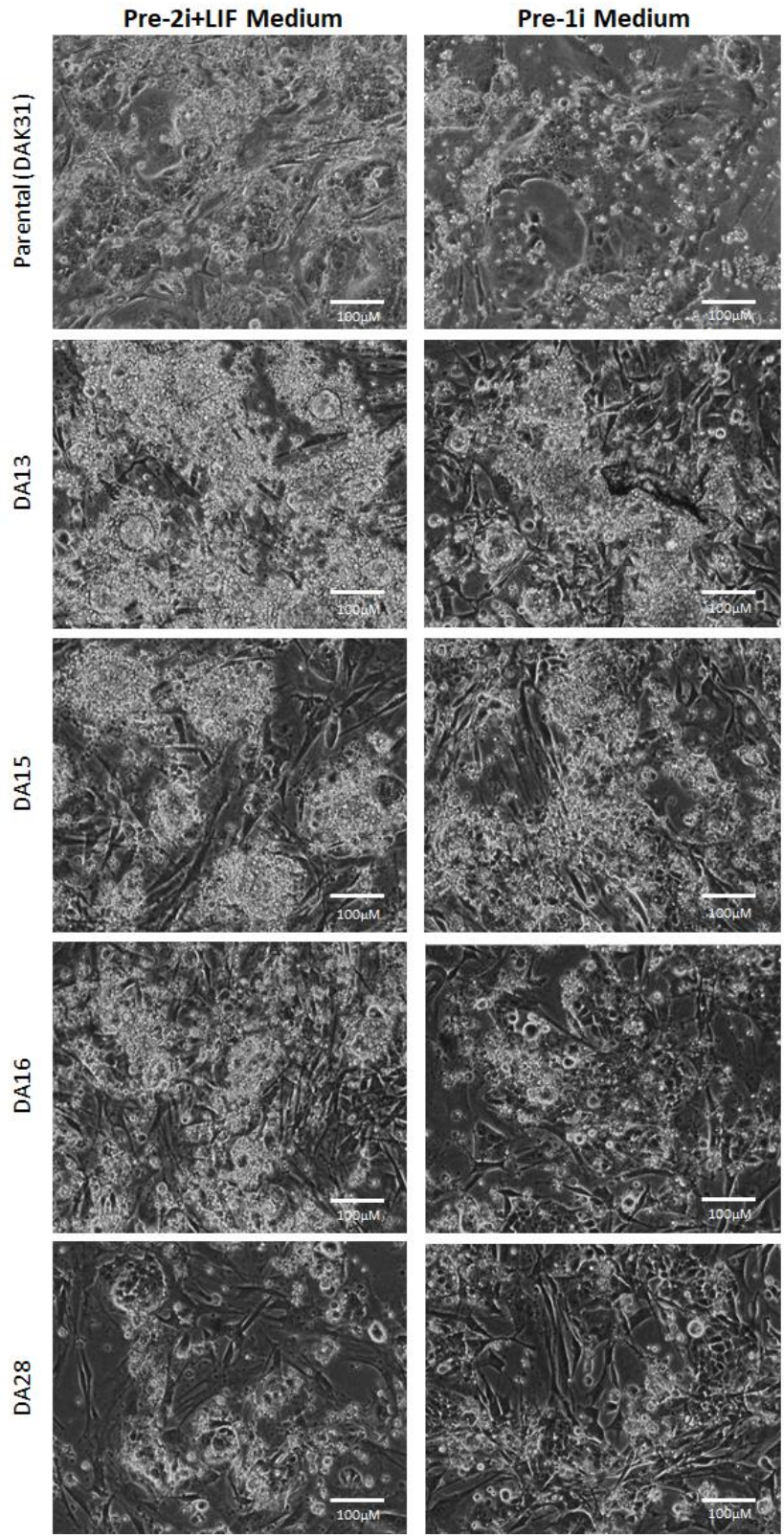

Figure 6.4.3. Bright field microscopy photographs of Otx2$^{-/-}$ cells undergoing EpiLC differentiation. Parental DAK31, DA13 and Otx2$^{-/-}$ clone undergoing EpiLC differentiation. *Photographs taken at day 3 of EpiLC culture (day 6 EpiLC differentiation). Left panels are cells pre-cultured with 2i+LIF, right panels are cells pre-cultured with 1i medium.*

Cells which had been cultured in EpiLC medium for 3 days were harvested and used for qRT-PCR analysis to quantify the expression of markers commonly associated with EpiLC differentiation. After the 3-day culture in EpiLC medium, all cell lines showed a substantial reduction in *Nanog* transcript expression (Figure 6.4.4). There was no substantial difference in *Tcf15* expression within any *Otx2*$^{-/-}$ clones compared to the parental cell line after 3-day culture in EpiLC medium (Figure 6.4.4). *Fgf5* was very weakly expressed in all three *Otx2*$^{-/-}$ clones (DA15, DA16 & DA28) and DA13 compared to the parental DAK31 cell line after the 3-day culture in EpiLC medium (Figure 6.4.4).

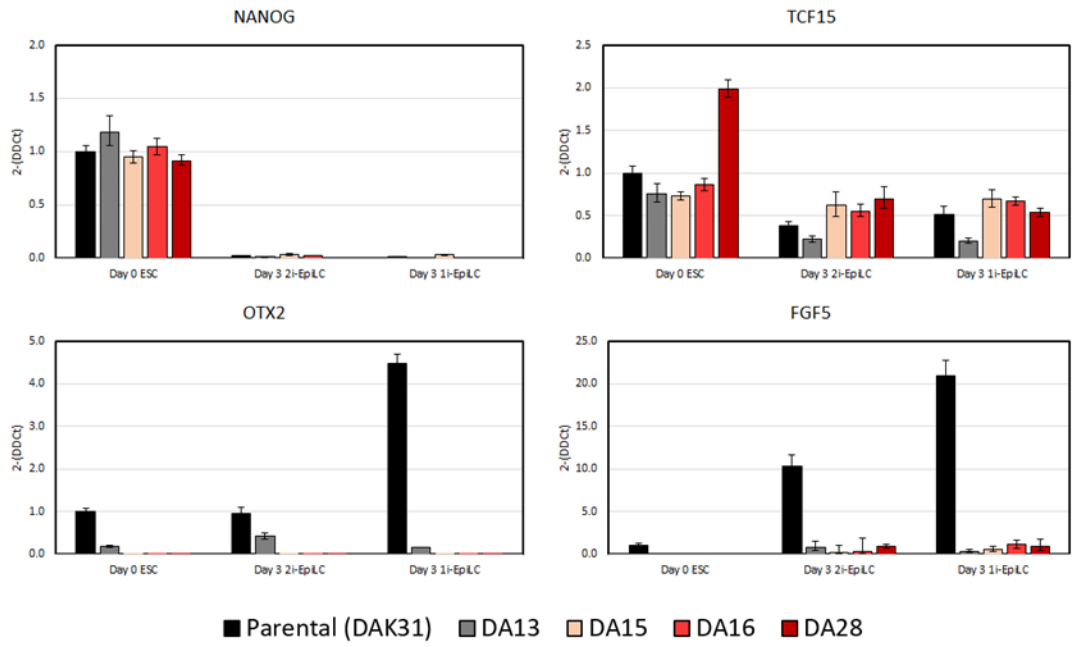

Figure 6.4.4. qRT-PCR analysis of Otx2$^{-/-}$ clones after 3-day culture in EpiLC medium. *Average of three technical replicates generated during 1 experimental repeat. Expression was normalised to the house keeping gene β-actin (dCT) and fold change (2-DDCT) values generated by normalising gene expression to day 0 DAK31 ESCs. Day 3 represents the 3rd day of cells being cultured in EpiLC medium, which translates to day 6 of the PGCLC differentiation protocol. Bars represent mean ± SD.*

This proposed that the loss of *Otx2* expression in rat ESCs was negatively impacting the cells ability to enter an epiblast fate. However, as DA13 also showed a similar result to the *Otx2*$^{-/-}$ cells, it is still questionable whether these results are genuine and that DA13 is influenced by haploinsufficiency, or that the results are related to sub-clonal variation.

6.4.2.2 PGCLC differentiation protocol

Cells subjected to the EpiLC differentiation protocol were transferred into hanging drops of PGCLC culture medium. Each hanging drop consisted of ~2,000 cells contained within 30µl PGCLC culture medium. Dishes containing the suspended hanging drops were incubated for 2 days to promote aggregation of the cells. After 2 days, the aggregates were transferred into 6-well low adhesion plates and remained in suspension for a further 4 days. After the 12 day differentiation protocol, the aggregates were carefully broken apart by gentle pipetting (trituration) and the cell suspensions were stained with fluorescent antibodies for SSEA-1 and CD61. These surface markers were used to monitor the differentiation status of the cells and sort them into populations which were either unstained, single stained, or double stained for both surface markers by fluorescent activated cell-sorting (FACs). The gating strategy detailed in section 2.6.7 was used. The remaining cells were gated to isolate populations of double negative, single stained and double stained populations by plotting CD61 (586/15A) versus SSEA-1 (670/14A) using fluorescent activated cell-sorting (FACs). The gates were set against unstained DAK31 ESCs.
Rat ESC cultures maintained in 2i+LIF on MEFs possessed both SSEA-1^{+ve} and SSEA-1^{-ve} cells (Figure 6.4.5). The parental cells which had been subjected to the PGCLC differentiation protocol showed a general loss of SSEA-1^{+ve} cells within the whole population, but very few $CD61^{+ve}$ cells (Figure 6.4.5).
After being subjected to the PGCLC differentiation protocol, the *Otx2*$^{-/-}$ clones (DA15, DA16 & DA28) and DA13 clone were found to have a greater proportion of $CD61^{+ve}$ cells compared to the parental DAK31 cell line (Figure 6.4.5).
DA13, DA15 and DA16 clones pre-cultured in 2i+LIF medium retained a distinct population of SSEA-1^{+ve}/$CD61^{-ve}$ cells, proposing that some cells from these clonal populations retained a stem cell characteristic despite being subjected to a PGCLC differentiation protocol (Figure 6.4.5). When pre-cultured in 1i medium, these same clones had smaller proportions of SSEA-1^{+ve}/$CD61^{-ve}$ cells and a greater proportion of SSEA-1^{-ve}/$CD61^{+ve}$ cells compared to the 2i+LIF pre-cultured cells (Figure 6.4.5). The 1i medium pre-culture appeared to be better suited to drive these clonal populations out of the stem cell fate.
DA28 cells pre-cultured in 2i+LIF medium had a similar reduction in the number of SSEA-1^{+ve}/$CD61^{-ve}$ cells to the parental DAK31 cell line after being subjected to the PGCLC differentiation protocol.

Pre-culturing DA28 cells in 1i medium improved the proportion of SSEA-1^{-ve}/CD61^{+ve} cells present after undergoing the PGCLC differentiation protocol, but did not promote a further reduction in the proportion of cells retaining the SSEA-1^{+ve}/CD61^{-ve} profile.

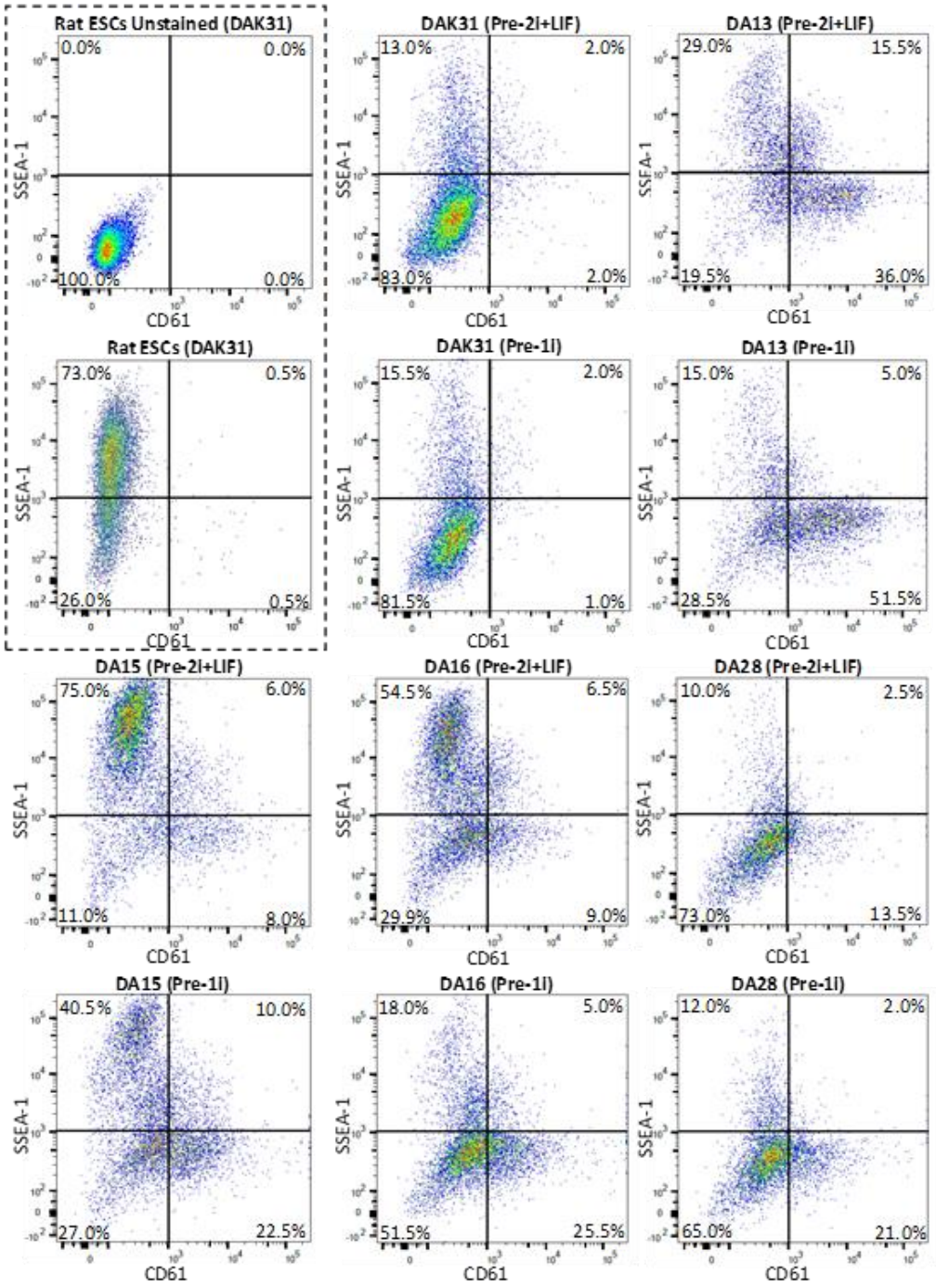

Figure 6.4.5. Flow cytometry plots for Otx2$^{-/-}$ clones undergoing the PGCLC differentiation protocol. *Each flow cytometry plot displays percentage of population which stained positively for CD61 and SSEA-1. Rat ESCs (DAK31) = ESCs stained for SSEA-1 and CD61. Pre-2i+LIF = pre-cultured in 2i+LIF medium for 3 days prior to EpiLC differentiation. Pre-1i = pre-cultured in 1i medium for 3 days prior to EpiLC differentiation.*

These individual populations were analysed for expression of PGC related transcripts. It was hypothesised that there would be an increased expression of PGC markers within differentiated *Otx2*$^{-/-}$ clones compared to the parental line. The qRT-PCR data represents a single experimental replicate, with the average transcript expression being calculated from 3 technical replicates. Data from DA13 cells pre-cultured in 1i medium was omitted due to an operator fault during the sorting of this clone.

Blimp1 expression from the SSEA-1^{-ve}/CD61^{-ve} population was elevated in DA15 and DA16 cells which had been pre-cultured in 1i medium (Figure 6.4.6). However, SSEA-1^{+ve}/CD61^{-ve} and SSEA-1^{-ve}/CD61^{+ve} cells from all cell lines either showed similar or reduced *Blimp1* expression compared to the parental DAK31 cell line (Figure 6.4.6). *Prdm14* transcript expression was elevated in the SSEA-1^{-ve}/CD61^{-ve} and SSEA-1^{+ve}/CD61^{-ve} populations of DA15 and DA16 cells previously pre-cultured in 1i medium, as well as DA13 cells which had been pre-cultured in 2i+LIF medium (Figure 6.4.6). Both DA15 and DA16 cells had elevated *Ap2γ* expression in the SSEA-1^{-ve}/CD61^{-ve} and CD61^{+ve} populations compared to the parental DAK31 cell line (Figure 6.4.6). However, DA28 cells had raised *Ap2γ* expression in all stained populations when compared to the parental cell line (Figure 6.4.6).

The expression of all three PGC transcription factors *Blimp1*, *Prdm14* and *Ap2γ* were elevated in the SSEA-1^{+ve}/CD61^{+ve} population of DA15, DA16, and DA28 clones pre-cultured in 1i medium when compared to the parental DAK31 cell line (Figure 6.4.6).

The qRT-PCR data showed that the loss of *Otx2* in the *Otx2*$^{-/-}$ clones DA15 and DA16 had a positive influence on the expression of all PGC transcription factors expression during the PGCLC differentiation protocol, but there was considerable variability in PGC transcription factor expression between the different *Otx2*$^{-/-}$ clones.

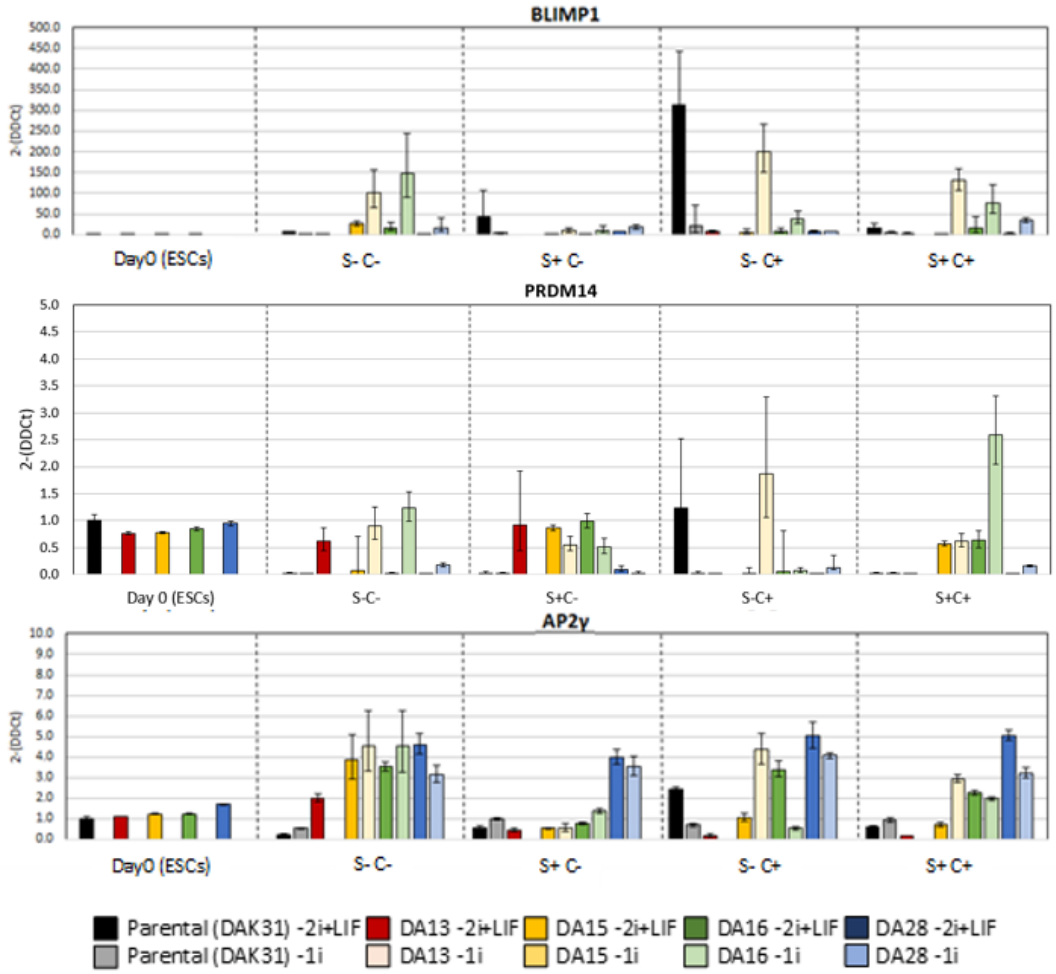

Figure 6.4.6 qRT-PCR analysis of the expression of PGC transcription factors in SSEA1/CD61 stained populations of Otx2$^{-/-}$ clones subjected to a PGCLC differentiation protocol. *Cells were harvested after 12 days of PGCLC differentiation and separated into SSEA-1 (S) and CD61 (C) stained populations. (+) = Positive for stain, (-) = Negative for stain. Expression was normalised to the house keeping gene β-actin (dCT) and fold change (2-DDCT) values generated by normalising gene expression to day 0 DAK31 ESCs. Data shown is the mean of technical triplicates generated from one experiment ± SD.*

Nanog and *Stella* gene expression were substantially increased in SSEA-1^{+ve}/CD61^{-ve} and SSEA-1^{+ve}/CD61^{+ve} cells of both DA15 and DA16 clones compared to the parental cell line (Figure 6.4.7). *Oct4* expression in the SSEA-1^{+ve}/CD61^{-ve} and the SSEA-1^{+ve}/CD61^{+ve} populations of DA15 and DA16 was similar to that of the parental (Figure 6.4.7). However, *Oct4* expression in the SSEA-1^{-ve}/CD61^{-ve} and SSEA-1^{-ve}/CD61^{+ve} cells of *Otx2*$^{-/-}$ clones was reduced compared to the parental (Figure 6.4.7). Pluripotency gene expression of DA28 cells was far lower than that in the parental DAK31 cell line (Figure 6.4.7).

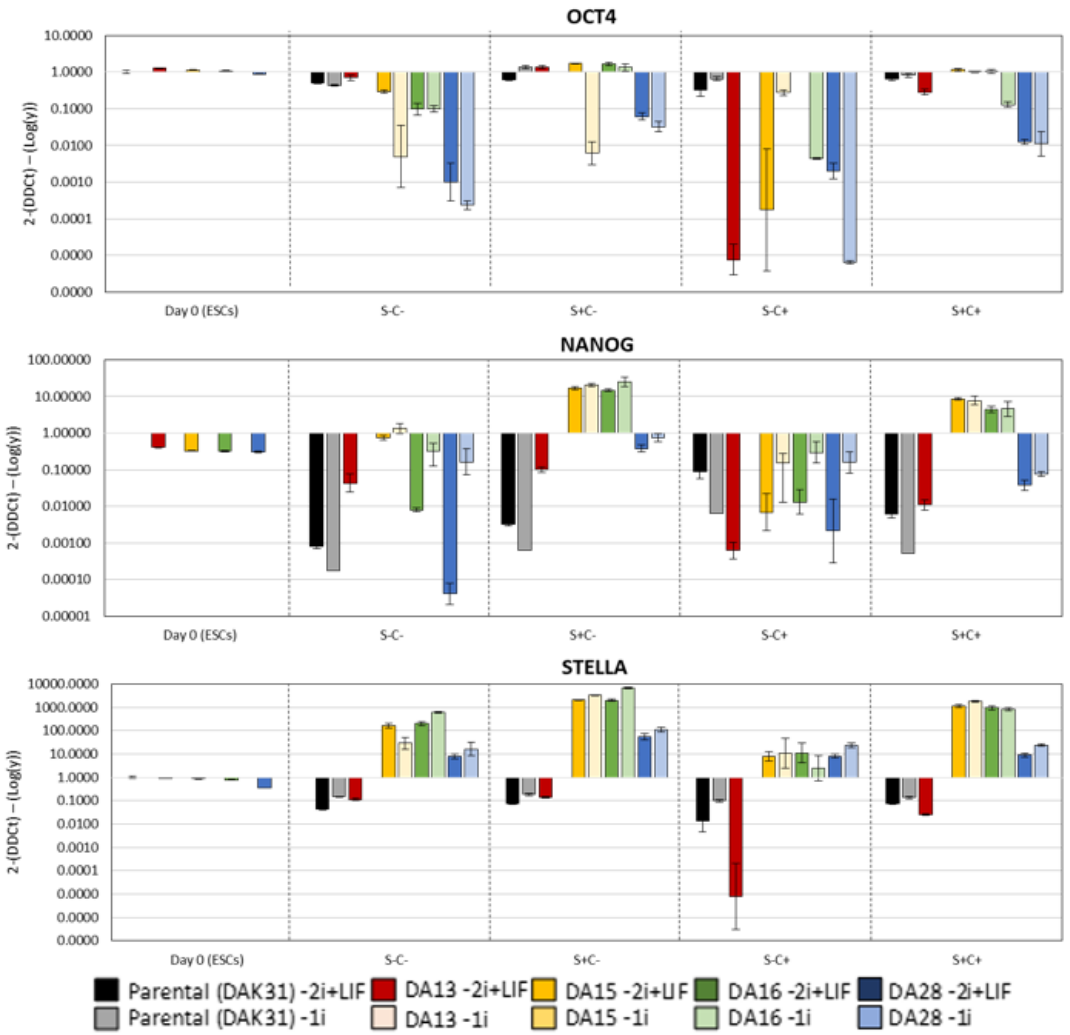

Figure 6.4.7. qRT-PCR analysis of the expression of pluripotency genes in SSEA1/CD61 stained populations of Otx2$^{-/-}$ clones subjected to a PGCLC differentiation protocol. *Cells were harvested after 12 days of PGCLC differentiation and separated into SSEA-1 (S) and CD61 (C) stained populations. (+) = Positive for stain, (-) = Negative for stain. Expression was normalised to the house keeping gene β-actin (dCT) and fold change (log scale) (2-DDCT-Log(y)) values generated by normalising gene expression to day 0 DAK31 ESCs. Data shown is the mean of technical triplicates generated from one experiment ± SD.*

DA15 was the only *Otx2*$^{-/-}$ clone to have a substantial increase in PGC marker expression within CD61^{+ve} cells compared to the parental DAK31 cell line (Figure 6.4.8). qRT-PCR analysis determined that *Nanos3* and *Dazl* expression were both elevated in SSEA-1^{+ve}/CD61^{-ve} and SSEA-1^{+ve}/CD61^{+ve} DA15 cells pre-cultured in 2i+LIF medium, whereas increased *Vasa* was detected in CD61^{+ve} DA15 cells pre-cultured in 1i medium (Figure 6.4.8).

Increased *Nanos3* expression was also present in SSEA-1^{-ve}/CD61^{-ve} DA16 and DA28 cells pre-cultured in 1i medium, as well as in SSEA-1^{+ve}/CD61^{-ve} DA13 and DA16 cells pre-cultured in 2i+LIF medium (Figure 6.4.8).

All other *Otx2*$^{-/-}$ clones had similar or reduced expression of *Dazl* or *Vasa* compared to the parental after undergoing the PGCLC differentiation protocol (Figure 6.4.8).

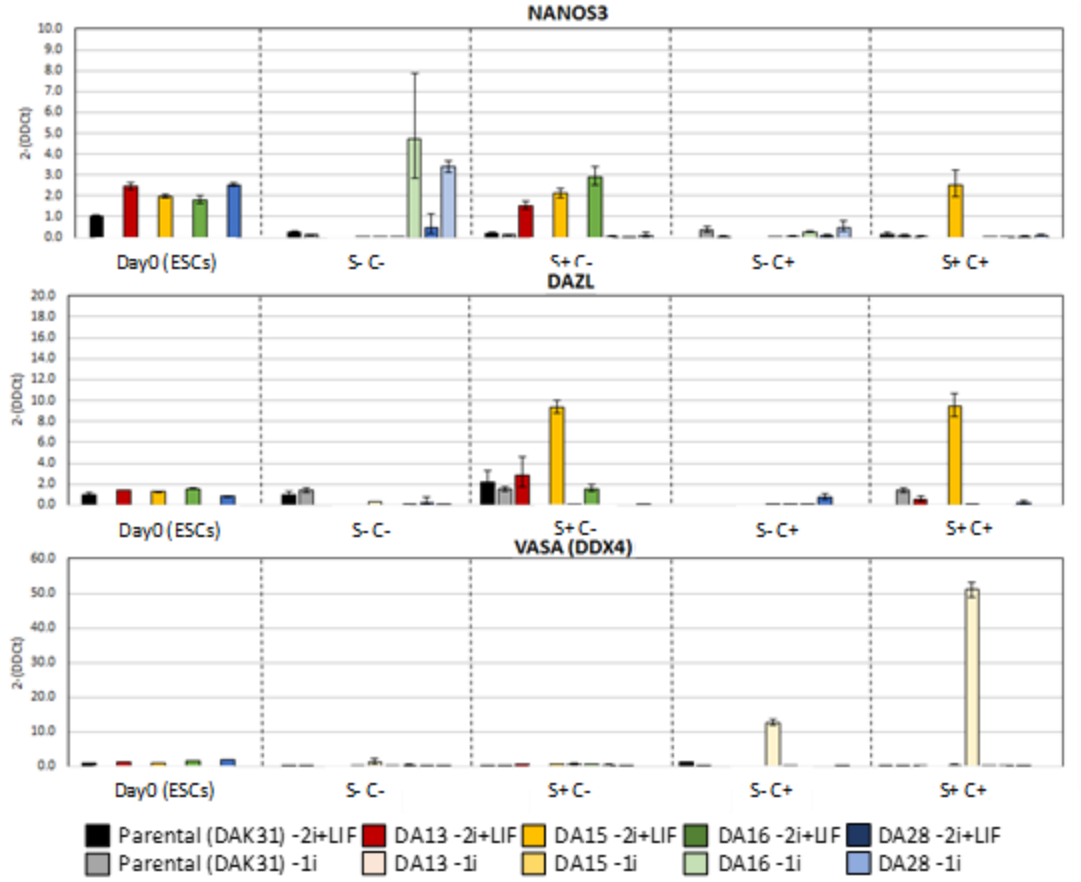

Figure 6.4.8. qRT-PCR analysis of the expression of PGC marker genes in SSEA1/CD61 stained populations of Otx2$^{-/-}$ clones subjected to a PGCLC differentiation protocol. *Cells were harvested after 12 days of PGCLC differentiation and separated into SSEA-1 (S) and CD61 (C) stained populations. (+) = Positive for stain, (-) = Negative for stain. Expression was normalised to the house keeping gene β-actin (dCT) and fold change (2-DDCT) values generated by normalising gene expression to day 0 DAK31 ESCs. Data shown is the mean of technical triplicates generated from one experiment ± SD.*

Transcript expression of markers of endoderm (*Gata4*, *Gata6*) and trophectoderm (*Gata3*) were also analysed to determine whether the loss of *Otx2* expression influenced the proportion of the cells differentiating into these lineages during the PGCLC differentiation protocol. DA13, DA15, DA16 and (almost all) DA28 populations had reduced *Gata4* and *Gata6* expression compared to the parental cell line (Figure 6.4.9). However, the SSEA-1^{+ve}/CD61^{-ve} DA28 cells did have similar *Gata4* expression to the parental when pre-cultured in 1i medium (Figure 6.4.9). *Gata3* expression was higher in SSEA-1^{-ve}/CD61^{-ve} and SSEA-1^{-ve} / CD61^{+ve} cells of all *Otx2*$^{-/-}$ knock-out cell lines when compared to the parental cell line (Figure 6.4.9). However, only DA28 showed increased *Gata3* expression in SSEA-1^{+ve}/CD61^{-ve} and SSEA-1^{+ve} / CD61^{+ve} cells when compared to the parental (Figure 6.4.9).

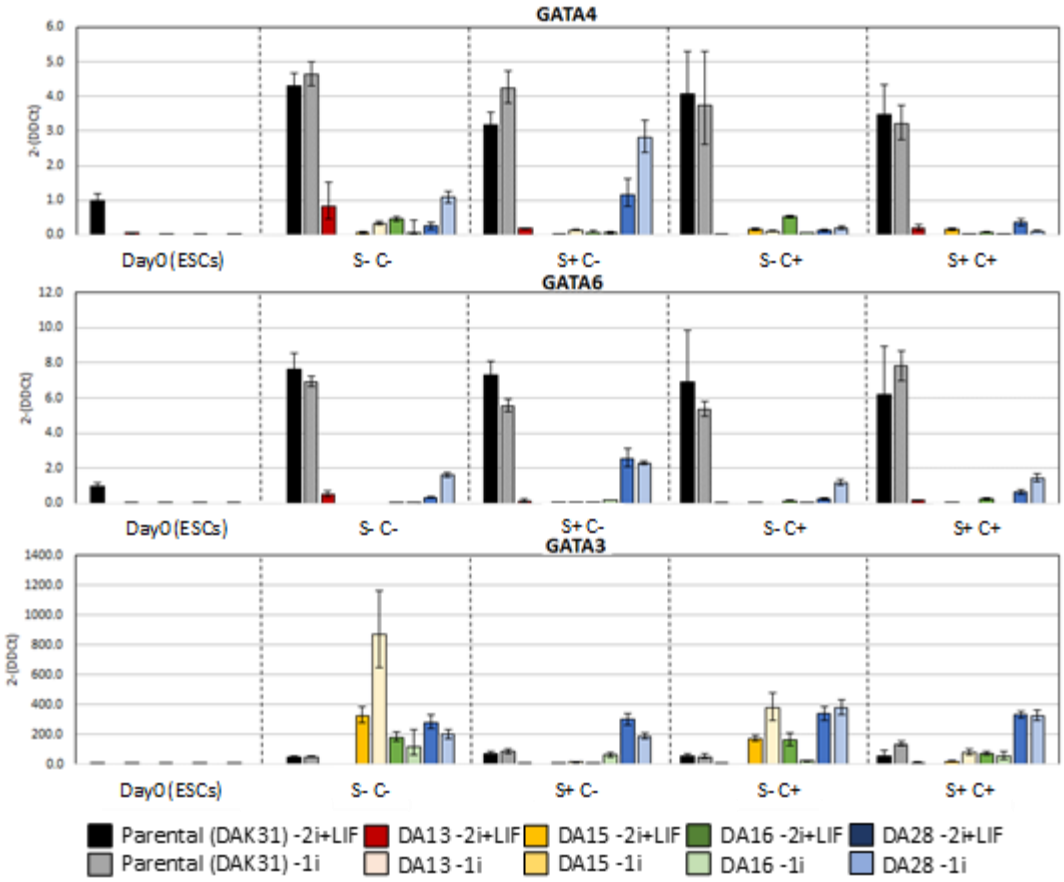

Figure 6.4.9. qRT-PCR analysis of the expression of Endoderm (Gata4, Gata6) and Trophectoderm (Gata3) genes in SSEA1/CD61 stained populations of Otx2$^{-/-}$ clones subjected to a PGCLC differentiation protocol. *Cells were harvested after 12 days of PGCLC differentiation and separated into SSEA-1 (S) and CD61 (C) stained populations. (+) = Positive for stain, (-) = Negative for stain. Expression was normalised to the house keeping gene β-actin (dCT) and fold change (2-DDCT) values generated by normalising gene expression to day 0 DAK31 ESCs. Data shown is the mean of technical triplicates generated from one experiment ± SD.*

6.5 Chapter 6 discussion

OTX2 assists the transition of mouse ESCs out of naïve pluripotency, and is involved in the stabilisation of the primed epiblast-like state (Yang et al. 2014, Buecker et al. 2014). This is accomplished by redirecting transcription factors such as OCT4 to alternative enhancer elements, driving the expression of genes involved in Epiblast fate determination (Yang et al. 2014, Buecker et al. 2014). Loss of *Otx2* expression in *Nanog* expressing mouse ESCs reduces the proportion of cells within an FGF-induced early primed state, suggesting that *Otx2*$^{-/-}$ ESCs are more resistant to differentiation into the Epiblast fate (Acampora et al. 2017). However, it has also been shown that mouse *Otx2*$^{-/-}$ knock-out cell lines generate a greater proportion of PGCLCs compared to wild-type cells when induced to differentiate via a PGCLC differentiation protocol (Zhang et al. 2018). It has been proposed that the loss of *Otx2* extends the time that mouse cells are in a competent state to enter the PGCLC lineage, before the cells become committed to differentiate into other cell fates (Zhang et al. 2018). During the course of this project, it has been shown that although basal expression of *Otx2* in rat ESCs is lower than mouse ESCs, *Otx2* is induced in rat cells cultured in EpiLC medium. Based on the work in mouse ESCs, it was hypothesised that loss of *Otx2* expression in rat ESCs would improve the proportion of cells being directed towards the germ cell lineage during a PGCLC differentiation protocol.

6.5.1 *Otx2* expression is not required for maintaining rat ESCs *in vitro*

A CRISPR/Cas9 gene-editing strategy was used to generate rat ESCs clones lacking a functional copy of the *Otx2* gene. Approximately 70% of rat ESC clones post cell-sorting had the intended deletion within one or both alleles of the *Otx2* gene. Of these edited clones, 45% had evidence of a deletion within both alleles of *Otx2* gene. Due to the generally high efficiency of CRISPR/Cas9 induced edits in rodent cell lines (Jin & Li 2016), it was anticipated that the majority of the clones would have indels introduced at either or both CRISPR cut sites if all clones had been analysed. Three *Otx2*-deficient rat ESC clones were selected based on their normal karyotype, and were shown to lack detectable OTX2 protein by immunostaining. These results demonstrate that OTX2 is not required for the self-renewal of rat ESCs.

6.5.2 *Otx2* knock-out impairs the differentiation of rat cells into an epiblast state

Rat *Otx2*$^{-/-}$ clones were subjected to two independent differentiation protocols to determine whether the loss of *Otx2* affected the differentiation of rat ESCs into an Epiblast-like state. When induced to differentiate during the undirected EB differentiation protocol, rat *Otx2*$^{-/-}$ clones had reduced expression of the epiblast markers *Fgf5* and *Brachyury* compared to the parental cell lines. Additionally, rat *Otx2*$^{-/-}$ clones retained similar *Nanog* expression to clones in the ESC state, while *Nanog* expression was lost in the rat ESC parental cell line. OTX2 and NANOG are reported to have antagonistic functions in mouse ESCs, *Nanog*$^{+ve}$/*Otx2*$^{-ve}$ cells are considered to be naïve stem cells while *Nanog*$^{-ve}$/*Otx2*$^{+ve}$ cells have primed stem cell characteristics (Acampora et al. 2017). In the mouse, OTX2 helps stabilise the more primed epiblast-like state by targeting OCT4 to alternative enhancer elements of genes associated with epiblast differentiation (Yang et al. 2014, Buecker et al. 2014). Therefore, as hypothesised, the loss of functional OTX2 protein expression within rat ESCs may have reduced the capacity of these cells to differentiate out of the naïve state and into the epiblast fate. Finally, *Otx2*$^{-/-}$ clones had increased expression of the PGC transcription factors *Prdm14* and *Ap2γ*. In mice, NANOG can induce the expression of *Prdm14* independently of the BMP4 signalling pathway within EpiLCs (Murakami et al. 2016). This may suggest that the increased *Prdm14* expression observed in *Otx2* null rat ESCs could be related to the sustained expression of *Nanog* within the *Otx2*$^{-/-}$ cells. *Ap2γ* expression has been detected in the trophectoderm lineage during embryogenesis (**Chazaud et al. 1996,** Auman et al. 2002), suggesting that some ESCs may have been directed towards the trophectoderm lineage in the absence of OTX2 rather than the epiblast.

Rat *Otx2*$^{-/-}$ clones subjected to the more directed EpiLC differentiation protocol had reduced *Fgf5* expression compared to the parental cell line. This result was similar to that generated by mouse *Otx2*$^{-/-}$ knock-out cell lines (Zhang et al. 2018), supporting the suggestion that loss of OTX2 protein impairs the ability of rat cells to differentiate efficiently into the epiblast fate. However, unlike the cells which had been subjected to the EB differentiation protocol*, Nanog* expression was almost undetectable in *Otx2*$^{-/-}$ cells cultured in EpiLC medium. A small decrease in *Nanog* expression has been shown in mouse *Otx2*$^{-/-}$ cells during EpiLC differentiation (Zhang et al. 2018), but is not as dramatic as that seen in the rat *Otx2*$^{-/-}$ cells.

This suggests that the EpiLC differentiation conditions used were still capable of driving *Otx2*$^{-/-}$ rat ESC differentiation out of naïve state. Activin A (a key component of the EpiLC medium) can be used to direct the differentiation of mouse (Tada et al. 2005, Yasunaga et al. 2005) and human (D'Amour et al. 2005) ESCs to produce endoderm. Rat ESCs have been previously reported to have a pre-disposition for differentiating into the endoderm lineage (Nichols et al. 1998). Therefore, when epiblast differentiation via the loss of *Otx2* expression is suppressed, perhaps Activin A drives a greater proportion of rat ESCs towards the endoderm lineage. The concentrations of cytokines within the EpiLC medium used to induce mouse EpiLC differentiation are perhaps more suited for driving rat ESCs towards the endoderm lineage rather than the epiblast. Future investigations should determine whether accurate titration of factors such as Activin A can identify a suitable concentration of cytokines that effectively stimulates rat EpiLC differentiation. In summary, loss of *Otx2* expression impaired the ability of rat ESCs to transition into the Epiblast fate, but did not prevent cellular differentiation into other lineages.

6.5.3 *Otx2* knock-out does not reliably improve rat PGCLC determination when cells are subjected to the PGCLC differentiation

Rat *Otx2*$^{-/-}$ clones subjected to the PGCLC differentiation protocol had an increased proportion of CD61^{+ve} cells (14% - 32.5%) compared to the parental cell line (3% - 4%), especially after pre-treatment in 1i medium. This is similar to what has been shown in the mouse ESC, where a greater proportion of CD61^{+ve} cells are present from *Otx2*$^{-/-}$ cells (~80%) compared to the control (~10%) after PGCLC differentiation (Zhang et al. 2018). *Otx2*$^{-/-}$ mouse cells are also reported to have increased PGC transcription factor and *Nanog* expression within the PGCLC population compared to control cells (Zhang et al. 2018). Two *Otx2*$^{-/-}$ clones had increased expression of PGC transcription factors and pluripotency genes within the CD61^{+ve} population. However, only one of these two clones had increased expression of PGC specific marker genes. This suggests that the loss of *Otx2* in rat cells may not have the same effect on PGCLC determination as it does in the mouse. However, as there appeared to be some increase in PGC transcription factor expression, there could be a benefit in combining *Otx2* knock-out with overexpression of the PGC transcription factors. Using a CRISPR/Cas9 strategy similar to that used in Chapter 4, PGC transcription factor transgene cassettes could be inserted downstream of the *Otx2* promotor.

The loss of *Otx2* expression coupled with increased PGC transcription factor expression might increase the efficiency of directing rat ESC differentiation towards the PGC lineage.

6.5.4 *Otx2* knockout reduces the expression of endoderm markers and increases *Gata3* expression when cells are subjected to the PGCLC differentiation protocol

All *Otx2*$^{-/-}$ CD61^{+ve} rat cells had reduced expression of endoderm markers *Gata4* and *Gata6* when compared to the parental cell line. The loss of *Otx2*$^{-/-}$ expression in mouse embryos leads to defects in the endoderm of the developing mouse embryo (Rinn et al. 1998, Acampora et al. 1998, 2009), regions which are positive for *Gata4* and *Gata6* expression (Cai et al. 2008). In zebrafish both *Gata4* and *Gata6* are noted to be reduced in the absence of *Otx2* expression during endoderm specification in early development (Tseng et al. 2011). Therefore, *Otx2*$^{-/-}$ rat cells may require stronger differentiation cues to direct cellular differentiation towards the endoderm lineage, e.g. the presence of Activin A within the medium (Tada et al. 2005, Yasunaga et al. 2005, D'Amour et al. 2005).

Sub-populations of *Otx2*$^{-/-}$ cells also had increased *Gata3* expression when compared to the parental cell line. In mouse ESCs, loss of *Nanog* and *Otx2* expression induced an increase in trophectoderm markers such as *Gata3* (Acampora et al. 2017). Increased *Gata3* expression in the rat *Otx2*$^{-/-}$ cells was also detected in populations with low expression of *Nanog*. Therefore, the combined loss of *Otx2* expression and *Nanog* in differentiating rat cells may also direct differentiation towards the *Gata3*$^{+ve}$ cell lineages (e.g. trophectoderm) rather than the PGC lineage. In conclusion, knockout of the *Otx2* gene could potentially allow cells to differentiate into other cellular lineages such as the trophectoderm, even when put through a directed differentiation protocol.

Chapter 7 Concluding remarks

7.1 Rat ESCs & PGCLC differentiation

During mammalian embryogenesis, a small proportion of cells within the proximal posterior region of the post-implantation epiblast adopt a germ cell fate (Ohinata et al. 2005, Dudley et al. 2007, Rao et al. 2010, Welling & Geijsen 2013, Günesdogan et al. 2014, Irie et al. 2014). This differentiation event is initiated by BMP4 and WNT3 signals generated by the adjacent extraembryonic ectoderm and visceral endoderm (Ohinata et al. 2005, Dudley et al. 2007, Rao et al. 2010, Welling & Geijsen 2013, Günesdogan et al. 2014). It is thought that the appropriate concentration of these signalling molecules, their location and the developmental timing of their actions (~E5.5 - E6.5 in mice) are crucial to ensure successful establishment of the germline (Tam & Zhou 1996, Ohinata et al. 2009). Transplantation experiments have shown that uncommitted "developmentally competent" post-implantation epiblast cells can be directed into the PGC fate if introduced into this "germ cell" inductive environment (Tam & Zhou 1996, Ohinata et al. 2009).

ESCs derived from rats will successfully colonise the somatic tissue of chimaeric animals (Buehr et al. 2008, Li et al. 2008), however, the efficiency of germline contribution of rat ESCs has been noted in our laboratory as being more variable than that observed from mouse ESCs (data not shown). This variability in germline transmission is likely to be influenced by two factors, the genetic integrity or the developmental competence of the ESCs. Cultured cell lines, including ESCs, are prone to aneuploidy (Liu et al. 1997, Sugawara et al. 2006) and genetic mutations/variations (Kim et al. 2017) during extended culture and passaging. ESCs carrying such genetic abnormalities are normally prevented from contributing to the germline and developing into functional gametes (Liu et al. 1997, Longo et al. 1997). Genetic damage can also impair differentiation potential, disrupting appropriate regulation of key developmental genes involved in pluripotency, self-renewal and/or fate determination (Mikkola et al. 2006, Imreh et al. 2006). Accumulation of these genetic abnormalities during the culture of rat ESCs may restrict their differentiation potential, reducing the efficiency of rat ESC transmission into the germline. However, this issue can be minimised by using rat ESCs with a lower passage number, reducing the impact of genetic damage to the variability in germline transmission (Li et al. 2017).

Reduced germline transmission could also be the result of rat ESCs in 2i+LIF culture being in state that has less potential than the authentic *in vivo* rat epiblast. Rat ESCs display increased expression of lineage specific genes compared to mouse ESCs (Blair et al. 2011, Hong et al. 2013), suggesting that established rat ESCs might exist in a primed, peri-naïve state compared to the naïve mouse ESCs. This state could be a key feature of rat ESCs in culture or be a by-product of maintaining rat ESCs in 2i+LIF culture conditions. Indeed, in common with mouse and human epiblast stem cells, rat ESCs are sensitive to the level of WNT/β-catenin signalling, where too little or too much β-catenin signalling in rat ESCs can induce differentiation (Buehr et al. 2008, Ying et al. 2008, Meek et al. 2013). This peri-naive state of rat ESCs may compromise their response to the pro-germline differentiation signals within the PGC-niche environment of the developing embryo, thereby effectively reducing the efficiency of the germline transmission of rat ESCs compared to the mouse. To mimic the naïve state of *in vitro* mouse ESCs, human pluripotent stem cells have been cultured in medium containing histone deacetylase (HDAC) inhibitors (Guo et al. 2017). HDAC-treated human cells expressed pluripotency markers which were only present in unprimed pluripotent cells but could not be efficiently differentiated into certain lineages such as definitive endoderm and neuroectoderm without first being pre-primed for differentiation (Guo et al. 2017). As the expression of epiblast markers in rat cells was improved when cells were pre-cultured in medium lacking CHIR99021 and LIF, perhaps a similar issue is present in our rat ESCs; efficient directed differentiation requires rat cells to be primed prior to exit out of the naïve state, ensuring the cells are susceptible to the differentiation cues in the directed differentiation medium.

The poor response of rat ESCs to the directed “Hayashi” PGCLC differentiation protocol, indicated that reduced PGC specification might directly contribute to the limited germline transmission of rat ESCs *in vivo*. Low level expression of PGC genes in the differentiated rat ESC cultures could indicate that either very few cells adopt a PGCLC fate or that the cells are unresponsive to the PGC inductive signals. Efficient induction of mouse ESCs into PGCLCs is thought to require transition through an EpiLC phase, where cells will respond to the PGCLC induction signals (Hayashi et al. 2011, 2013). However, differentiating rat cells had low expression levels of markers associated with EpiLC differentiation, indicating a failure to generate a suitable population of responsive cells.

Pre-treating rat cells in conditions that reduced β-catenin signalling increased the expression of epiblast markers including *Fgf5*, but this did not translate to increased expression of PGC-specific marker genes when the PGCLC differentiation protocol was applied. Inefficient activation of the PGCLC programme suggested that the differentiation of rat ESCs might be compromised by both reduced formation of the EpiLC state and by sub-optimal PGCLC differentiation signals in the ESC culture medium.

7.2 Manipulation of the epiblast network to improve germ cell fate

Two directed differentiation approaches were applied to improve the efficiency of rat PGCLC differentiation *in vitro*. These experimental approaches both involved the manipulation of the epiblast transcriptional network, either through the overexpression of PGC regulatory factors or the removal of a potentially antagonistic somatic differentiation factor. As well as the difference in sensitivity to β-catenin signalling (Buehr et al. 2008, Ying et al. 2008, Meek et al. 2013) and elevated expression of differentiation markers (Blair et al. 2011, Hong et al. 2013), a striking difference between rat and mouse ESCs is the negligible levels of *Blimp1* expression in rat ESCs. Downregulation of *Blimp1* expression reduces the efficiency of PGC specification in mice, due to the cells being unable to downregulate pro-somatic differentiation genes and reactivate the pluripotency gene network required for PGCs (Bikoff et al. 2009, John & Garrett-Sinha 2009, Schäfer et al. 2011). Rat cells expressing *Blimp1* transgene had increased expression of *Nanog* and the early PGC-specific marker *Nanos3* compared to parental controls when subjected to the "Hayashi" PGCLC differentiation protocol. However, expression of other commonly associated PGC markers such as the late stage PGC-specific markers *Vasa* and *DazL* or the *Oct4* transcription factor remained relatively unchanged or were reduced. Therefore elevated expression of *Blimp1* in rat ESCs might help to suppress unscheduled ESC differentiation or sporadic expression of somatic markers but requires increased expression of other PGC regulators to activate the full complement of PGC markers.

Overexpression of multiple PGC related factors did increase the expression of PGC-markers in differentiating rat ESCs. However, in contrast to mouse ESCs (Nakaki et al. 2013), the most effective combination was not the expression of all three factors but was BLIMP1 combined with either PRDM14 or AP2γ.

Over-expression of all three factors in rat ESCs was less effective, reducing the induction of PGC markers, even when the three factors were expressed from independent expression vectors. This indicated that expression levels of the PGC regulators was probably not a limiting factor. It also indicated that high level expression of PRDM14 and AP2γ together during rat ESC differentiation was potentially counterproductive in rat cells. In the mouse, PRDM14 and AP2γ have been noted to associate at similar enhancer regions (Günesdogan et al. 2014), resulting in the net upregulation of germ cell and pluripotency markers while also downregulating FGF signalling and somatic differentiation (Auman et al. 2002, Yamaji et al. 2013, Nakaki & Saitou 2014). At this time, there does not seem to be any reported evidence of *Prdm14* and *Ap2γ* working as direct antagonists to one another in the literature.

However, reduced germ cell marker expression in cells co-expressing both factors alongside *Blimp1* may be related to the timing of gene expression. Interestingly, it is known that expression of BLIMP1, PRDM14 and AP2γ occurs in temporal order during *in vivo* PGC specification in the mouse. *Blimp1* expression is first detected in PGC precursor cells at ~E6.25 dpc, closely followed by *Prdm14* expression at ~E6.75 dpc and finally *Ap2γ* at ~E7.25 dpc (Ohinata et al. 2005, 2009, Schäfer et al. 2011). Presumably the successive and overlapping actions of these factors ensure that the development of the epiblast cells advances appropriately to promote differentiation toward a germ cell fate (Ohinata et al. 2005, 2009, Schäfer et al. 2011). Overexpression of *Ap2γ* in mouse ESCs can promote their differentiation into a trophoblast stem cell (TSC) fate, increasing the expression of the pro-TSC transcription factor *Elf5* (Kuckenberg et al. 2010). Preliminary data generated from rat ESCs showed that cells overexpressing *Ap2γ* alone had increased expression of *Elf5* and other markers associated with trophoblast such as *Gata3*. However, large variation in trophoblast marker expression between the different rat ESC lines made it difficult to definitively consolidate the data. Simultaneous expression of *Ap2γ* and *Prdm14* (a known FGF signalling inhibitor (Yamaji et al. 2013, Nakaki & Saitou 2014)) in peri-naïve rat ESCs may interfere with PGC differentiation, diverting cell differentiation into other cell lineages such as trophoblast. It would be of interest to observe whether inducing the overexpression of the PGC transcription factor transgenes at comparative time points to the *in vivo* system would improve the efficiency of rat germ cell fate determination.

Given that expression of PGC regulators appears to be temporally controlled during the early phase of PGC differentiation (Ohinata et al. 2005, 2009, Schäfer et al. 2011), experimental systems where these transcription factors can be expressed at an appropriate time might provide a way to avoid potential conflict between differentiation signals and boost PGC differentiation. The insertion of *Blimp1* downstream of the *Brachyury* promoter was an attempt to target expression of *Blimp1* transgene to the post-implantation epiblast, thereby shifting differentiation away from the formation of the somatic lineages and enhance formation of PGCLCs. Key aspects of this approach were that the knock-in transgene did not require any external intervention, would only be expressed in differentiating ESCs, and could be executed *in vivo* when ESCs are injected into blastocysts. However, the results of the *in vitro* experiments suggest that although this approach could be achieved technically, cell clones had low level expression of early PGC markers, making this technique less efficient than the doxycycline-induced expression of PGC regulator cassettes.

In view of the results obtained with the doxycycline-inducible vectors, a more effective construct would combine BLIMP1 with either AP2γ or PRDM14.

An issue with this approach is that it relies on sufficient cells differentiating into a suitably receptive EpiLC/Epiblast state. Therefore, it would be necessary to ensure these rat cells are capable of entering this cell fate, either by modification of the differentiation protocol or the pre-treatment of cells prior to differentiation.

Another approach to controlling rat ESC differentiation was through overexpression of the pluripotency regulator *Nanog*. Overexpression of the NANOG transcription factor in mouse EpiLCs directs their differentiation towards the germ cell fate (Murakami et al. 2016). Expression of a *Nanog* transgene during rat cell differentiation increased the expression of *Blimp1, Prdm14* and *Ap2γ*, which was consistent with what was reported for mouse EpiLC differentiation (Murakami et al. 2016). Although this suggests that *Nanog* is involved in the activation of PGC transcription factor expression in rats, the increase in PGC-specific marker gene expression in *Nanog* overexpressing cells was not as substantial as that seen in rat cells expressing *Blimp1* in combination with *Prdm14* or *Ap2γ*. Perhaps co-expression of *Nanog* transgene with the PGC transcription factors during directed differentiation would further enhance the efficiency of rat cell differentiation into the germ cell fate?

It has been observed in mice that entry into the EpiLC state is accompanied by downregulation of the pluripotency related genes, including *Nanog* (Hayashi et al. 2011). This implies that loss of *Nanog* function might be critical for allowing ESCs to exit pluripotency, creating a developmental window when epiblast cells can respond to differentiation signals. It would be interesting to see if this pattern of expression could be simulated in the rat ESCs carrying the doxycycline-inducible *Nanog* transgene. Over-expression of *Nanog* in the undifferentiated rat ESCs prior to differentiation could reinforce and promote the naïve phenotype (reducing non-scheduled differentiation). This would be followed by downregulation of *Nanog* by withdrawal of doxycycline when the cells are exposed to EpiLC conditions, inducing a germ cell fate receptive state. Finally, re-expression of the *Nanog* transgene could be induced when cells are cultured in PGCLC conditions, potentially assisting PGC differentiation.

An important assumption that underpinned the experimental approaches in this project was that the functions of the key PGC regulators, *Blimp1*, *Prdm14* and *Ap2γ* were conserved between rat and mouse. Although, rat and mouse are genetically similar and share many common features in early embryonic development, such as formation of the epiblast into an epithelial cup prior to gastrulation (Huber 1915, Nichols & Smith 2009, Nichols & Smith 2011, Bedzhov et al. 2014, Irie et al. 2014), it remains possible that the rat and mouse differ in the key PGC regulators. In porcine and human cells, BMP and WNT signalling induce the expression of *Sox17* and *Blimp1* (Irie et al. 2015, Wang et al. 2016, Kobayashi et al. 2017). Elevated levels of *Sox17* were identified by single-cell RNA sequencing in both embryonic hPGCs and *in vitro* derived PGCLCs, while the knockdown of *Sox17* in human IPSCs undergoing the PGCLC differentiation protocol reduced the number of TNAP positive cells and the expression of key PGC markers (e.g. *Blimp1*) (Irie et al. 2015). Elevated *Sox17* expression has also been detected in porcine derived PGCLCs compared to the pig IPSCs (Wang et al. 2016), potentially emphasising a role for SOX17 in the formation of pig PGCs. Although *Sox17* may play a crucial role in the generation of PGCs in species which produce bilaminar discs during embryogenesis (Irie et al. 2015, Wang et al. 2016, Kobayashi et al. 2017), it is difficult to say whether it would play a similar role in rodents who produce epithelium cups instead (Huber 1915, Nichols & Smith 2009, Nichols & Smith 2011, Bedzhov et al. 2014, Irie et al. 2014) without further investigation.

The second strategy taken to improve the differentiation of rat ESCs toward a germ cell fate was to restrict differentiation into the somatic cell lineages. By uncoupling somatic cell differentiation, it was hoped that the rat cells would become more available to the PGC inductive signals in the differentiation medium by losing a potential differentiation route, thus improving the efficiency of germ cell fate determination. Loss of the OTX2 transcription factor in mouse ESCs decreases the proportion of cells able to differentiate into the somatic cell lineages and increases the efficiency of germ cell determination both *in vitro* and *in vivo* (Zhang et al. 2018). Knocking out *Otx2* expression in rat cells decreased the expression of somatic cell differentiation gene markers when cells were induced to differentiate. However, increased expression of both PGC transcription factors and PGC-specific marker genes were present in only a single *Otx2* knock-out clone when subjected to the "Hayashi" PGCLC differentiation protocol. Although these results match what has been reported for *Otx2* knock-out cell lines generated from other model organisms (Acampora et al. 1998, Rhinn et al. 1998, Tseng et al. 2011, Zhang et al. 2018), it is not enough to conclude that the loss of *Otx2* expression is beneficial for rat germline determination. The results however do support future investigations into the potential antagonistic role of *Otx2* in rat PGCLC fate determination and the benefits of its removal during PGC differentiation.

Combining PGC transcription factor overexpression while preventing somatic cell differentiation may improve the efficiency of rat ESC differentiation into the germline. Overall, manipulation of the epiblast gene network of rat ESCs showed an improvement in the efficiency of differentiating rat cells into the germ cell fate. Cells subjected to an undirected embryoid body differentiation protocol showed the greatest induction in PGC-specific markers during transgene expression compared to those subjected to the "Hayashi" PGCLC differentiation protocol. This suggests that the protocol developed in mouse is sub-optimal for rat ESC differentiation into the germline. Additionally, this highlights one of the crucial issues with *in vitro* experimental research, despite the *in vitro* culture conditions being designed to mimic the niche *in vivo* environment of the embryo, these conditions are not identical to those the cells would experience within a developing rat embryo. To fully interrogate whether the implemented strategies do improve rat germ cell fate determination, it would be necessary to inject these manipulated cells into rat embryos to form chimaeric animals.

Improved rat ESC engraftment into the germline of the donor embryo would confirm the experimental approach used was beneficial for increasing the efficiency of rat ESC differentiation into the germline.

7.3 Future work

During this investigation, it was determined that directed differentiation of rat ESCs towards the epiblast and germ cell fate *in vitro* cannot be accomplished following the same protocol as mouse ESCs. Efficient induction of mouse ESCs into PGCLCs is thought to require transition through an EpiLC phase, where cells become responsive to the PGCLC induction signals (Hayashi et al. 2011, 2013). The difficulties in activating the PGCLC programme in *in vitro* cultured rat cells may have been related to the inefficient differentiation of rat ESCs into the EpiLC cell fate, reducing the number of cells which enter a PGC inductive state and therefore limiting the number of cells which can be successfully directed into the germ cell fate (Figure 7.3.1). Future investigations should compare the states of *in vitro* and *in vivo* rat cells to identify any distinct differences between the two, opening potential avenues of research for improving the efficiency of differentiating rat ESCs into PGCLCs.

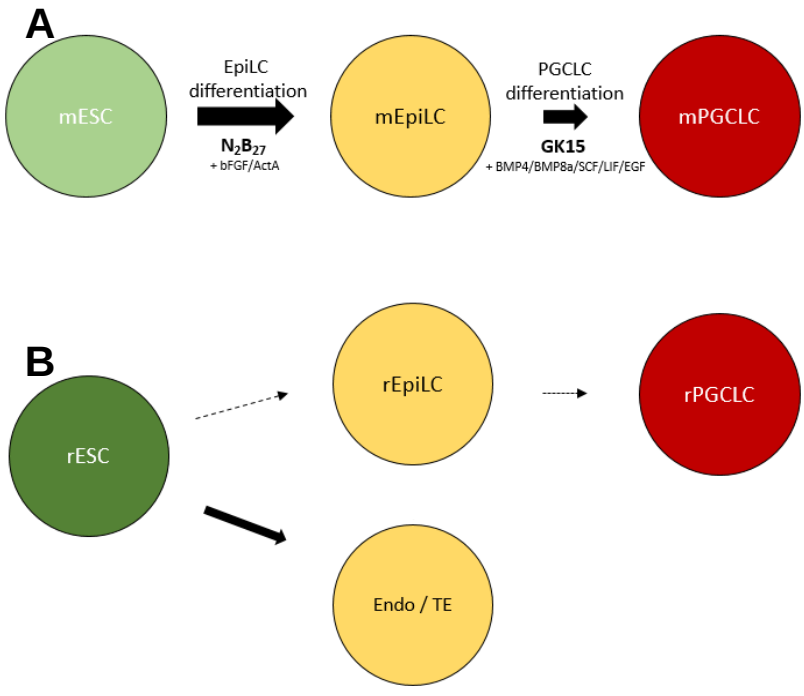

***Figure 7.3.1: Models of the rodent ESC-PGCLC differentiation**. A) Differentiation of mouse ESCs (mESCs) into PGCLCs in culture based on development of "Hayashi" PGCLC differentiation protocol. B) Hypothesised model of rat ESC differentiation when subjected to the "Hayashi" PGCLC differentiation protocol. Endo = Endoderm, TE = Trophectoderm*

Gene expression profiling such as single-cell RNA sequencing would prove useful in better understanding how the pluripotent state of the rat ESCs compares to the *in vivo* rat ICM. Additionally, the epigenetic status of our rat ESCs could be explored further using gold standard techniques such as bisulfite sequencing or ChIP-Seq. Analysing the epigenetic status of rat ESCs would help identify whether the presence or absence of repressive and active epigenetic markers on gene promotor/enhancer elements of pro-epiblast or germ cell regulators is different to those of the rat epiblast or mouse ESCs, reducing the efficiency of generating rat PGCLCs. With a better understanding of the state of the rat ESCs, it would be possible to tailor the culture conditions of our rat ESCs to direct them into a state which better mimics the pre-implantation epiblast prior to PGC specification, potentially making the cells more responsive to differentiation cues and thereby improve the efficiency of differentiation out of the naïve state and towards the epiblast and/or germline. HDAC inhibitors have been used to induce a naïve state in human pluripotent stem cells that is closer to the ground state pluripotency observed from strains of mouse ESCs (Guo et al. 2017). Significantly, HDAC-treated cells did not efficiently differentiate into certain lineages such as definitive endoderm (Guo et al. 2017).

Introducing HDAC inhibitors into the culture medium of rat ESCs might be useful for directing the differentiation towards the germline by not only ensuring the rat ESC genome is in a more epigenetically accessible state prior to differentiation, but also by potentially restricting rat ESC differentiation into unwanted cell lineages such as definitive endoderm, increasing the proportion of rat cells which adopt a germ cell fate. Resetting rat ESCs into a more naïve state might also make it easier to prime cells for differentiation into the epiblast/PGC cell fates due to the less repressive epigenetic state of the cells.

An important assumption in this project was that the key PGC regulators would be conserved between mouse and rat. Expression of the PGC transcription factors required for mouse PGC determination were detected in the genital ridges of rat embryos, and so it seemed reasonable to explore their potential role in rat PGC specification by inducing their overexpression. Future investigations could explore their role in rat germline determination further by generating knock-out rat ESC lines lacking the expression of *Blimp1*, *Prdm14* and/or *Ap2γ.*

If these factors shared a similar importance to PGC specification as described in the mouse, then it would be expected that germline transmission of the rat ESCs would be comprised when the cells are injected into an embryo to form chimaeric animals. Additionally, single-cell RNA sequencing of rat *in vivo* PGCs during development should be performed and compared to similar data generated from other species such as mice and humans. This multispecies comparison could assist in identifying the network of factors present during rat PGC specification and highlight factors which could be manipulated to improve the efficiency of directing differentiation into the germ cell fate. Comparing this data to that generated from the *in vitro* rat cells subjected to the “Hayashi” differentiation protocol would also assist in determining whether rat ESCs were being successfully directed towards a PGC cell fate, and what stage of PGC development the *in vitro* generated cells more closely resemble.
Many of the experimental approaches used in this project did increase the expression of germ cell-specific markers in differentiating rat ESCs, suggesting that with refinement, these strategies could provide the basis for improving the efficiency of generating rat PGCLCs. The efficiency of PGC-specific marker induction was greatest in rat cell lines inducing the expression of either *Blimp1* and *Prdm14* or *Blimp1* and *Ap2γ* from incorporated Tet-On piggyBac transposon vectors.
One of the key advantages of this *in vitro* system is the ability to induce transgene expression at any time by introducing doxycycline into the culture medium.
This system can be used to identify at what stage during *in vitro* rat PGCLC differentiation does overexpression of PGC regulators improve the efficiency rat PGC differentiation. This can be accomplished by inducing transgene expression at different stages throughout the PGCLC differentiation protocol and then identify the order and/or time point of expression which best induces germ cell fate determination. However, this system is more difficult to translate into the *in vivo* system, due to its reliance on external intervention to function.
Therefore, manipulation of the epiblast gene network of rat ESCs using a HDR-approach would be a more favourable strategy to implement in the future when transitioning into the *in vivo* system. An unintended outcome of incorporating a transgene cassette downstream of the *Brachyury* promotor was inducing the complete knock-out of *Brachyury*.

It is reported that generation of CRISPR/Cas9 induced knock-out cell lines is more efficient than CRISPR HDR knock-ins (Kimura et al. 2015, Jin & Li 2016), signifying there is a high probability that any isolated rat cell clone harbouring an incorporated transgene cassette also will have an NHEJ-induced mutation of the other *Brachyury* allele. BRACHYURY null mice are embryonic lethal at ~E10.5 due to reduced posterior mesoderm formation and impaired notochord and allantois development (Aramaki et al. 2013). However, prior to this, loss of functional BRACHYURY protein also reduces the sustained expression of the key PGC transcription factors during the late streak stages (~E7.0), considerably reducing the survival of developing PGCs (Aramaki et al. 2013). On this basis, it has been suggested that *Brachyury* expression is critical for the sustained expression of the PGC regulators during PGC specification. An alternative 'rewiring' strategy to the one presented could be to target the 3' end of the *Brachyury* gene instead of the transcriptional start site. A gene cassette would be designed with a 2A peptide at its 5' end, ensuring polycistronic expression of the endogenous *Brachyury* gene as well as the transgenes contained in the cassette. The CRISPR/Cas9 cut site could be within the terminal exon of the *Brachyury* gene, with any missing nucleotides from the *Brachyury* sequence being replaced within the template vector. This strategy would reduce the chance of unintended indel formation within the gene disrupting endogenous gene expression and ensure full translation of the *Brachyury* transcript whilst also making sure termination does not occur before the introduced transgenes have also been translated.

The reduced effectiveness of this method compared to the doxycycline-induced vectors may also have been related to the use of the relatively late epiblast marker *Brachyury* to drive transgene expression (Rivera-Pérez & Magnuson 2005).

The *Brachyury* gene was chosen as a suitable target for inducing *Blimp1* transgene expression due to it being linked with both the differentiation of epiblast cells (Rivera-Pérez & Magnuson 2005) and PGC specification (Aramaki et al. 2013), ensuring transgene expression occurred when rat cells were most likely to be susceptible to PGC differentiation cues. However, other gene targets could be considered such as FGF5 and OTX2. As *Otx2* is expressed during the EpiLC transitionary phase (Yang et al. 2014, Buecker et al. 2014, Murakami et al. 2016), and knock-out of the *Otx2* gene had a positive influence on PGC transcription factor expression in mouse (Zhang et al. 2018), this would be an appropriate alternative for driving transgene expression during differentiation out of the naïve ESC state.

Using a similar strategy as that for HDR template insertion into the *Brachyury* locus, PGC transcription factor transgene cassettes could be inserted downstream of the *Otx2* promotor, reducing the number of cells entering the somatic fate whilst driving differentiation towards the PGC lineage.

An alternative approach could be the use of bacterial (BAC) or yeast (YAC) artificial chromosome DNA constructs. BACs and YACs have been used to introduce large gene cassettes into the genome of pre-implantation embryos including the regulatory elements necessary to drive gene expression, ensuring that transgene expression closely matches endogenous gene expression (Schedl et al. 1996, Headon & Overbeek 1999, Rostovskaya et al. 2012, Jung et al. 2016). These constructs can be transmitted through the germ line (Schedl et al. 1996, Headon & Overbeek 1999, Jung et al. 2016), and in the case of BACs, have been successfully incorporated into the rat genome previously using CRISPR/Cas9 gene editing and piggyBac transposition (Jung et al. 2016). Phenotypic changes during mouse embryo development have been shown to be induced by transgene expression from a YAC vector (Schedl et al. 1996, Headon & Overbeek 1999), showcasing the potential of these constructs to drive cellular differentiation of edited cells. A BAC/YAC vector could be incorporated into the genome of rat ESCs, inducing the expression of *Blimp1* in combination with either *Prdm14* or *Ap2γ* using the regulatory elements of an epiblast gene such as *Brachyury* or *Otx2*. When induced to differentiate, the edited cells would drive the expression of the PGC regulators when endogenous epiblast gene expression occurs, potentially assisting the directed differentiation of the cells towards the germ cell fate.

A major technical issue encountered during this investigation was the sensitivity of rat ESCs to single cell sorting. The survival of rat ESCs post FACs was poor, with a high proportion of the surviving clones being karyotypically abnormal (outside the normal range). Rat ESCs can be cultured after colony dissociation (Buehr et al. 2008, Ying et al. 2008), but ESCs carrying genetic abnormalities are normally prevented from contributing to the germline (Liu et al. 1997, Longo et al. 1997), potentially reducing the efficiency of ESC transmission into the germline. Human stem cells are reported to be sensitive to manipulation *in vitro*, reducing the cell recovery and survival of cells after FACs (Hoffman & Carpenter 2005). Human cells cultured in the presence of Y-27632 (ROCK inhibitor) for 24 hours post FACs have been shown to have a greater survival rate, recover faster and generate fewer karyotypically abnormal clones (Emre et al. 2010).

Rat ESCs cultured in DMEM/F12 medium supplemented with Y-27632 have been shown to have improved colony forming efficiency and reduced spontaneous differentiation during standard culture compared to 2i+LIF conditions (Yaoyao et al. 2017). It would therefore be interesting to determine whether the addition of Y-27632 or any other cell survival factor could prove beneficially for isolating a greater number of healthy rat ESCs harbouring the desired genome edit post FACs.

As there is limited published literature on the markers of rat PGCs, it would also be beneficial to identify a greater selection of potential markers to purify PGCLCs generated from rat ESCs. Although the isolation of PGCLCs has been accomplished by staining pools for the presence of C-KIT (Yamaji et al. 2010) and Tissue Non-specific Alkaline Phosphatase (TNAP) (Hayashi et al 2011), sequencing techniques such as microarrays performed on mouse PGCs have identified a greater number of germ-cell related genes which have proven useful for identification of mouse PGCs (Davood et al. 2011). Screening rat PGCs for germ cell-specific surface markers could improve the purification of rat PGCLCs from a differentiated pool of cells by providing alternative targets for antibody selection and FACs sorting. Another solution to using cell surface markers to identify PGCLCs could be the use of reporter cell lines. Cells harbouring a *Nanos3*-fluroscent protein reporter have been used to monitor differentiation of mammalian cells into the PGC lineage both *in vitro* and *in vivo* (Yamaji et al. 2010, Irie et al 2015, Kobayashi et al. 2017). Attempts were made to generate a rat ESC *Nanos3*-mCherry reporter cell line during this investigation, however, failure to identify gRNAs able to induce DSBs in the *Nanos3* locus meant this this was not accomplished.

Modelling germ cell fate determination *in vitro* is a powerful tool to generate insights into the molecular mechanisms which drive and regulate differentiation into the germline. This knowledge would be invaluable to translate this into potential future cell therapies and fertility treatments in humans. Additionally, cell banking of *in vitro* pluripotent cell-derived gametes will be an invaluable contribution to the conservation of endangered species, as well as potentially reduce lengthy breeding programmes and increase the efficiency of generating livestock animals with desirable characteristics such as increased produce yield or improved disease resistance.

Chapter 8 Bibliography

Acampora D, Di Giovannantonio L.G, Simeone A. (2013) Otx2 is an intrinsic determinant of the embryonic stem cell state and is required for transition to a stable epiblast stem cell condition. *Development*. 140: 43-55.

Acampora D, Di Giovannantonio LG, Di Salvio M, Mancuso P, Simeone A. (2009) Selective inactivation of Otx2 mRNA isoforms reveals isoform-specific requirement for visceral endoderm anteriorization and head morphogenesis and highlights cell diversity in the visceral endoderm. *Mechanisms of development*. 126: 882 – 897

Acampora D, Di Giovannantonio LG, Garofalo A, Nigro V, Omodei D, Lombardi A, Zhang J, Chambers I, Simeone A. (2017) Functional Antagonism between OTX2 and NANOG Specifies a Spectrum of Heterogeneous Identities in Embryonic Stem Cells. *Stem Cell Reports*. 9(5): 1642–1659.

Aitman TJ, Critser JK, Cuppen E, Dominiczak A, Fernandez-Suarez XM, Flint J, Gauguier D, Geurts AM, Gould M, Harris PC, Holmdahl R, Hubner N, Izsvák Z, Jacob HJ, Kuramoto T, Kwitek AE, Marrone A, Mashimo T, Moreno C, Mullins J, Mullins L, Olsson T, Pravenec M, Riley L, Saar K, Serikawa T, Shull JD, Szpirer C, Twigger SN, Voigt B, Worley K. (2008) Progress and prospects in rat genetics: a community view. *Nat Genet*. 40(5): 516-522.

Auerbach W, Dunmore JH, Fairchild-Huntress V, Fang Q, Auerbach AB, Huszar D, Joyner AL. (2000) Establishment and chimera analysis of 129/SvEv- and C57BL/6-derived mouse embryonic stem cell lines. *Biotechniques. 29(5):1024-8, 1030, 1032.*

Auman HJ, Nottoli T, Lakiza O, Winger Q, Donaldson S, Williams T. (2002) Transcription factor AP-2gamma is essential in the extra-embryonic lineages for early postimplantation development. *Development*. 129(11):2733-2747.

Bagci H, Fisher AG. (2013) DNA Demethylation in Pluripotency and Reprogramming: The Role of Tet Proteins and Cell Division. *Cell Stem Cell*. 13(3): 265-269.

Bao S, Leitch HG, Gillich A, Nichols J, Tang F, Kim S, Lee C, Zwaka T, Li X, Surani MA. (2012) The Germ Cell Determinant Blimp1 Is Not Required for Derivation of Pluripotent Stem Cells. *Cell Stem Cell.* 11: 110–117.

Bedzhov I, Graham SJ, Leung CY, Zernicka-Goetz M. (2014) Developmental plasticity, cell fate specification and morphogenesis in the early mouse embryo. *Philos Trans R Soc Lond B Biol Sci.* 369(1657): 20130538.

Bikoff EK, Morgan MA, Robertson EJ. (2009) An expanding job description for Blimp-1/PRDM1. *Curr Opin Genet Dev*. 19(4):379-385.

Blair K, Wray J, Smith A. (2011) The liberation of embryonic stem cells. *PLoS Genet*. 7(4):e1002019.

Blair K, Leitch HG, Mansfield W, Dumeau CÉ, Humphreys P, Smith AG. (2012) Culture parameters for stable expansion, genetic modification and germline transmission of rat pluripotent stem cells. *Biol Open*. 1(1): 58–65.

Blais EM, Rawls KD, Dougherty BV, Li ZI, Kolling GL, Ye P, Wallqvist A, Papin JA. (2007) Reconciled rat and human metabolic networks for comparative toxicogenomics and biomarker predictions. *Nat. Commun*. 8:14250.

Boroviak T, Stirparo GG, Dietmann S, Hernando-Herraez I, Mohammed H, Reik W, Smith A, Sasaki E, Nichols J, Bertone P. (2018) Single cell transcriptome analysis of human, marmoset and mouse embryos reveals common and divergent features of preimplantation development. *Development*. 145: dev167833.

Brons IG, Smithers LE, Trotter MW, Rugg-Gunn P, Sun B, Chuva de Sousa Lopes SM, Howlett SK, Clarkson A, Ahrlund-Richter L, Pedersen RA, Vallier L. (2007) Derivation of pluripotent epiblast stem cells from mammalian embryos. *Nature*. 448(7150):191-5.

Buecker C, Srinivasan R, Wu Z, Calo E, Acampora D, Faial T, Simeone A, Tan M, Swigut T, Wysocka J. (2014) Reorganization of enhancer patterns in transition from naive to primed pluripotency. *Cell Stem Cell* 14, 838–853.

Buehr M, Meek S, Blair K, Yang J, Ure J, Silva J, McLay R, Hall J, Ying QL, Smith A. (2008). Capture of authentic embryonic stem cells from rat blastocysts. Cell. 135, 1287–1298.

Buehr M, Nichols J, Stenhouse F, Mountford P, Greenhalgh CJ, Kantachuvesiri S, Brooker G, Mullins J, Smith AG. (2003). Rapid Loss of Oct-4 and Pluripotency in Cultured Rodent Blastocysts and Derivative Cell Lines. *Biol. Repro*. 68, 222-229.

Buhr N, Carapito C, Schaeffer C, Kieffer E, Van Dorsselaer A, Viville S. (2008) Nuclear proteome analysis of undifferentiated mouse embryonic stem and germ cells. *Electrophoresis*. 29(11):2381-90.

Burns KH, Owens GE, Fernandez JM, Nilson JH, Matzuk MM. (2002) Characterization of Integrin Expression in the Mouse Ovary. *Biology of Reproduction*. 67(3): 743–751.

Butcher E.O. (1929) The development of the somites in the white rat (*Mus norvegicus albinus*) and the fate of the myotomes, neural tube, and the gut in the tail. *Amer. J. Anat.* 44**:** 381-439.

Cai KQ, Capo-Chichi CD, Rula ME, Yang DH, Xu XX. (2008) Dynamic GATA6 Expression in Primitive Endoderm Formation and Maturation in Early Mouse Embryogenesis. *Developmental dynamics*. 237: 2820–2829

Casanova EA, Okoniewski MJ, Cinelli P. (2012) Cross-Species Genome Wide Expression Analysis during Pluripotent Cell Determination in Mouse and Rat Preimplantation Embryos *PLoS One*. 7(10): e47107.

Chambers I, Colby D, Robertson M, Nichols J, Lee S, Tweedie S, Smith A. (2003). Functional expression cloning of Nanog, a pluripotency sustaining factor in embryonic stem cells. *Cell*. 113, 643-655.

Chambers I, Silva J, Colby D, Nichols J, Nijmeijer B, Robertson M, Vrana J, Jones K, Grotewold L, Smith A. (2007) Nanog safeguards pluripotency and mediates germline development. *Nature.* 450: 1230–1234.

Chazaud C, Oulad-Abdelghani M, Bouillet P, Décimo D, Chambon P, Dollé P. (1996). AP-2.2, a novel gene related to AP-2, is expressed in the forebrain, limbs and face during mouse embryogenesis. *Mech. Dev.* 54*,* 83-94.

Chen D, Liu W, Lukianchikov A, Hancock GV, Zimmerman J, Lowe MG, Kim R, Galic Z, Irie N, Surani MA, Jacobsen SE, Clark AT. (2017) Germline competency of human embryonic stem cells depends on eomesodermin. Biol Reprod. 97(6):850-861.

Chen HH, Welling M, Bloch DB, Muñoz J, Mientjes E, Chen X, Tramp C, Wu J, Yabuuchi A, Chou YF, Buecker C, Krainer A, Willemsen R, Heck AJ, Geijsen N. (2014) DAZL Limits Pluripotency, Differentiation, and Apoptosis in Developing Primordial Germ Cells. *Stem Cell Reports*. 3: 892–904.

Chia NY, Chan YS, Feng B, Lu X, Orlov YL, Moreau D, Kumar P, Yang L, Jiang J, Lau MS, Huss M, Soh BS, Kraus P, Li P, Lufkin T, Lim B, Clarke ND, Bard F, Ng HH. *(*2010*).* A genome-wide RNAi screen reveals determinants of human embryonic stem cell identity*.* *Nature* 468*:* 316– 20*.*

Chu LF, Surani MA, Jaenisch R, Zwaka TP. (2011) Blimp1 Expression Predicts Embryonic Stem Cell Development in vitro. *Current Biology.* 21:1759–1765.

Cong L, Ran FA, Cox D, Lin S, Barretto R, Habib N, Hsu PD, Wu X, Jiang W, Marraffini LA, Zhang F. (2013) Multiplex genome engineering using CRISPR/Cas systems. *Science*. 339:819–823

Czechanski A, Byers C, Greenstein I, Schrode N, Donahue LR, Hadjantonakis AK, & Reinholdt LG. (2014). Derivation and characterization of mouse embryonic stem cells from permissive and nonpermissive strains. *Nature protocols*, *9*(3), 559-74.

D'Amour KA, Agulnick AD, Eliazer S, Kelly OG, Kroon E, Baetge EE. (2005) Efficient differentiation of human embryonic stem cells to definitive endoderm. *Nat Biotechnol*. 23(12):1534-41.

Davies OR, Lin CY, Radzisheuskaya A, Zhou X, Taube J, Blin G, Waterhouse A, Smith AJ, Lowell S. (2013) Tcf15 Primes Pluripotent Cells for Differentiation. *Cell Rep*. 3(2): 472–484.

Dudley BM, Runyan C, Takeuchi Y, Schaible K, Molyneaux K. (2007) BMP signaling regulates PGC numbers and motility in organ culture. *Mech Dev*. 124(1):68-77.

Durcova-Hills G, Adams IR, Barton SC, Surani MA, McLaren A. (2006) The role of exogenous fibroblast growth factor-2 on the reprogramming of primordial germ cells into pluripotent stem cells. *Stem Cells.* 24, 1441-1449

Eckert D, Buhl S, Weber S, Jäger R, Schorle H. (2005) The AP-2 family of transcription factors. *Genome Biol*. 6(13):246.

Eckert D, Biermann K, Nettersheim D, Gillis AJ, Steger K, Jäck HM, Müller AM, Looijenga LH, Schorle H. (2008) Expression of BLIMP1/PRMT5 and concurrent histone H2A/H4 arginine 3 dimethylation in fetal germ cells, CIS/IGCNU and germ cell tumors. *BMC Dev Biol*. 8:106. doi: 10.1186/1471-213X-8-106.

Eggan K, Akutsu H, Loring J, Jackson-Grusby L, Klemm M, Rideout WM 3rd, Yanagimachi R, Jaenisch R (2001) Hybrid vigor, fetal overgrowth, and viability of mice derived by nuclear cloning and tetraploid embryo complementation.

Emre N, Vidal JG, Elia J, O'Connor ED, Paramban RI, Hefferan MP, Navarro R, Goldberg DS, Varki NM, Marsala M, Carson CT. (2010) The ROCK inhibitor Y-27632 improves recovery of human embryonic stem cells after fluorescence-activated cell sorting with multiple cell surface markers. *PloS one*. 5(8), e12148.

Encinas G, Zogbi C, Stumpp T. (2012) Detection of Four Germ Cell Markers in Rats during Testis Morphogenesis: Differences and Similarities with Mice. *Cells Tissues Organs.* 195:443-455.

Evans MJ, Kaufman MH. (1981) Establishment in culture of pluripotential cells from mouse embryos. Nature. 292(5819):154-6.

Fog CK, Galli GG, Lund AH. (2012) PRDM proteins: important players in differentiation and disease. *Bioessays*. 34(1):50-60.

Geurts, AM, Cost GJ, Freyvert Y, Zeitler B, Miller JC, Choi VM, Jenkins SS, Wood A, Cui X, Meng X, Vincent A, Lam S, Michalkiewicz M, Schilling R, Foeckler J, Kalloway S, Weiler H, Ménoret S, Anegon I, Davis GD, Zhang L, Rebar EJ, Gregory PD, Urnov FD, Jacob HJ, Buelow R.. (2009). Knockout Rats via Embryo Microinjection of Zinc-Finger Nucleases. *Science.* 325, 433.

Gardner RL. (1985) Clonal analysis of early mammalian development. *Philos Trans R Soc Lond B Biol Sci*. 312(1153):163-78.

Gibbs RA, Weinstock GM, Metzker ML, Muzny DM, Sodergren EJ, Scherer S, Scott G, Steffen D, Worley KC, Burch PE (2004) Genome sequence of the Brown Norway rat yields insights into mammalian evolution. *Nature*. 428:493–521.

Glover JD, Taylor L, Sherman A, Zeiger-Poli C, Sang HM, McGrew MJ. (2013) A Novel Piggybac Transposon Inducible Expression System Identifies a Role for Akt Signalling in Primordial Germ Cell Migration. *PLOS ONE* 8(11): e77222.

Günesdogan U, Magnúsdóttir E, Surani MA. (2014) Primordial germ cell specification: a context-dependent cellular differentiation event [corrected]. *Philos Trans R Soc Lond B Biol Sci.* 369: 1657.

Guo G, Yang J, Nichols J., Hall JS, Eyres I, Mansfield W, and Smith, A. (2009). Klf4 reverts developmentally programmed restriction of ground state pluripotency. Development 136, 1063– 1069.

Guo G, von Meyenn F, Rostovskaya M, Clarke J, Dietmann S, Baker D, Sahakyan A, Myers S, Bertone P, Reik W, Plath K, Smith A. (2017) Epigenetic resetting of human pluripotency. *Development*. 144(15):2748-2763.

Habibi E, Brinkman AB, Arand J, Kroeze LI, Kerstens HH, Matarese F, Lepikhov K, Gut M, Brun-Heath I, Hubner NC, Benedetti R, Altucci L, Jansen JH, Walter J, Gut IG, Marks H, Stunnenberg HG. (2013) Whole-genome bisulfite sequencing of two distinct interconvertible DNA methylomes of mouse embryonic stem cells. Cell Stem Cell. 13(3):360-9.

Hayashi K, Ogushi S, Kurimoto K, Shimamoto S, Ohta H, Saitou M (2012) Offspring from oocytes derived from in vitro primordial germ cell-like cells in mice. *Science*. 338(6109):971-5.

Hayashi K, Saitou M. (2013) Generation of eggs from mouse embryonic stem cells and induced pluripotent stem cells. *Nature Protocols*. 8: 1513–1524.

Hayashi K. Ohta H. Kurimoto K. Aramaki S. Saitou M. (2011) Reconstitution of the mouse germ cell specification pathway in culture by pluripotent stem cells. *Cell*. 146: 519-532.

Headon DJ, Overbeek PA. (1999) Involvement of a novel Tnf receptor homologue in hair follicle induction. *Nat Genet*. 22(4):370-4.

Hochedlinger K (2011) Embryonic Stem Cells: Testing the Germ-Cell Theory. *Current Biology*. 21(20) R850-R852.

Hoffman LM, Carpenter MK. (2005) Characterization and culture of human embryonic stem cells. *Nat Biotechnol*. 23(6):699-708.

Home P, Ray S, Dutta D, Bronshteyn I, Larson M, Paul S. (2009) GATA3 Is Selectively Expressed in the Trophectoderm of Peri-implantation Embryo and Directly Regulates *Cdx2* Gene Expression. *J*. Biol. Chem. 284: 28729-28737.

Hong J, He H, Bui P, Ryba-White B, Rumi M.A, Soares MJ, Dutta D, Paul S, Kawamata M, Ochiya T. (2013) A focused microarray for screening rat embryonic stem cell lines. Stem Cells Dev. 22: 431–443.

Høyer P, Byskov A, Møllgård K. (2005) Stem cell factor and c-Kit in human primordial germ cells and fetal ovaries. *Mol. Cell Endocrinol.* 234:1–10.

Hsu PD, Lander ES, Zhang F. (2014). Development and Applications of CRISPR-Cas9 for Genome Engineering. *Cell*. 157(6): 1262–1278.

Huber GC. (1915) The Development of the Albino Rat (Mus norvegicus albinus). *J Morphol*. 26(2).

Huang Y, Osorno R, Tsakiridis A, Wilson V. (2012) *In Vivo* differentiation potential of epiblast stem cells revealed by chimeric embryo formation. *Cell Rep*. 2(6):1571-8.

Iannaccone PM, Taborn GU, Garton RL, Caplice MD, Brenin DR. (1994) Pluripotent Embryonic Stem Cells from the Rat Are Capable of Producing Chimeras. *Developmental Biology.* 163(1) 288-292.

Imreh MP, Gertow K, Cedervall J, Unger C, Holmberg K, Szöke K, Csöregh L, Fried G, Dilber S, Blennow E, Ahrlund-Richter L. (2006) In vitro culture conditions favoring selection of chromosomal abnormalities in human ES cells. *J Cell Biochem*. 99(2):508-16.

Irie N, Weinberger L, Tang WW, Kobayashi T,Viukov S, Manor YS, Dietmann S, Hanna JH, Surani MA. (2015) SOX17 Is a Critical Specifier of Human Primordial Germ Cell Fate. *Cell* 160(1-2): 253–268.

Irie N, Tang WWC, and Surani MA. (2014) Germ cell specification and pluripotency in mammals: a perspective from early embryogenesis. *Reprod Med Biol*. 13(4): 203–215.

Izsvåk Z, FrÖhlich J, Grabundzija I, Shirley JR, Powell HM, Chapman KM, Ivics Z, Hamra FK. (2010). Generating knockout rats by transposon mutagenesis in spermatogonial stem cells. *Nat. Methods.* 7, 443-445.

Jacob H. (1999) Functional genomics and rat models. *Genome Res*. 9, 1013–1016.

Jin LF, Li JS. (2016) Generation of genetically modified mice using CRISPR/Cas9 and haploid embryonic stem cell systems. *Dongwuxue Yanjiu*. 37(4): 205–213.

John SA, Garrett-Sinha LA. (2009) Blimp1: a conserved transcriptional repressor critical for differentiation of many tissues. *Exp Cell Res*. 315(7):1077-1084.

Jung CJ, Ménoret S, Brusselle L, Tesson L, Usal C, Chenouard V, Remy S, Ouisse LH, Poirier N, Vanhove B, de Jong PJ, Anegon I. (2016) Comparative Analysis of piggyBac, CRISPR/Cas9 and TALEN Mediated BAC Transgenesis in the Zygote for the Generation of Humanized SIRPA Rats. *Sci Rep*. 6: 31455.

Kemper CH, Peters PW. (1987) Migration and proliferation of primordial germ cells in the rat. *Teratology*. 36(1):117-24

Keshet E, Lyman SD, Williams DE, Anderson DM, Jenkins NA, Copeland NG, Parada LF. (1991) Embryonic RNA expression patterns of the c-kit receptor and its cognate ligand suggest multiple functional roles in mouse development. *EMBO J*. 10, 2425–2435.

Kim M, Rhee JK, Choi H, Kwon A, Kim J, Lee GD, Jekarl DW, Lee S, Kim Y, Kim TM. (2017) Passage-dependent accumulation of somatic mutations in mesenchymal stromal cells during in vitro culture revealed by whole genome sequencing. *Sci Rep*. 7(1):14508.

Kimura Y, Oda M, Nakatani T, Sekita Y,Monfort A, Wutz A, Mochizuki H, Nakano T (2015) CRISPR/Cas9-mediated reporter knock-in in mouse haploid embryonic stem cells. *Sci Rep*. 5: 10710.

Kobayashi T, Zhang H, Tang WWC, Irie N, Withey S, Klisch D, Sybirna A, Dietmann S, Contreras DA, Webb R, Allegrucci C, Alberio R, Surani MA. (2017) Principles of early human development and germ cell program from conserved model systems. *Nature*. 546(7658):416-420.

Kojima Y, Sasaki K, Yokobayashi S, Sakai Y, Nakamura T, Yabuta Y, Nakaki F, Nagaoka S, Woltjen K, Hotta A, Yamamoto T, Saitou M. (2017) Evolutionarily Distinctive Transcriptional and Signaling Programs Drive Human Germ Cell Lineage Specification from Pluripotent Stem Cells. Cell Stem Cell. 2017 Oct 5; 21(4):517-532

Krehbiel R.H. (1962) Distribution of ova in the rat uterus. *Anat. Rec.* 143**:** 239-241.

Kuckenberg P, Buhl S, Woynecki T, van Fürden B, Tolkunova E, Seiffe F, Moser M, Tomilin A, Winterhager E, Schorle H. (2010) The transcription factor TCFAP2C/AP-2gamma cooperates with CDX2 to maintain trophectoderm formation. *Mol Cell Biol*. 30(13):3310-20.

Kurimoto K, Yabuta Y, Ohinata Y, Shigeta M, Yamanaka K, Saitou M (2008). Complex genome-wide transcription dynamics orchestrated by Blimp1 for the specification of the germ cell lineage in mice. Genes Dev 22: 1617–1635.

Kurokawa D, Takasaki N, Kiyonari H, Nakayama R, Kimura-Yoshida C, Matsuo I, Aizawa S. (2004) Regulation of Otx2 expression and its functions in mouse epiblast and anterior neuroectoderm. *Development.* 131: 3307-3317.

Labosky PA, Barlow DP, Hogan BL. (1994). Mouse embryonic germ (EG) cell lines: transmission through the germline and differences in the methylation imprint of insulin-like growth factor 2 receptor (Igf2r) gene compared with embryonic stem (ES) cell lines. *Development.* 120, 3197-3204.

Lawson KA, Meneses JJ, Pedersen RA (1991) Clonal analysis of epiblast fate during germ layer formation in the mouse embryo. *Development*. 113(3):891-911.

Leitch HG, Blair K, Mansfield W, Ayetey H, Humphreys P, Nichols J, Surani MA, Smith A. (2010). Embryonic germ cells from mice and rats exhibit properties consistent with a generic pluripotent ground state. *Development* 137, 2279-2287.

Leitch HG, McEwen KR, Turp A, Encheva V, Carroll T, Grabole N, Mansfield W, Nashun B, Knezovich JG, Smith A, Surani MA, Hajkova P. (2013) Naive pluripotency is associated with global DNA hypomethylation. *Nat Struct Mol Biol*. 20(3):311-6.

Li P, Tong C, Mehrian-Shai R, Jia L, Wu N, Yan Y, Maxson RE, Schulze EN, Song H, Hsieh CL, Pera MF, Ying QL. (2008) Germline competent embryonic stem cells derived from rat blastocysts. *Cell*. 135(7):1299-310.

Li TD, Feng GH, Li YF, Wang M, Mao JJ, Wang JQ, Li X, Wang XP, Qu B, Wang LY, Zhang XX, Wan HF, Cui TT, Wan C, Liu L, Zhao XY, Hu BY, Li W, Zhou Q. (2017) Rat embryonic stem cells produce fertile offspring through tetraploid complementation. *Proc Natl Acad Sci U S A*. 114(45):11974-11979.

Liu X, Wu H, Loring J, Hormuzdi S, Disteche CM, Bornstein P, Jaenisch R. (1997) Trisomy eight in ES cells is a common potential problem in gene targeting and interferes with germ line transmission. *Dev Dyn*. 209(1):85-91

Liu Z, Chen O, Wall JBJ, Zheng M, Zhou Y, Wang L, Ruth Vaseghi H, Qian L, Liu J. (2017) Systematic comparison of 2A peptides for cloning multi-genes in a polycistronic vector. *Sci Rep*. 7: 2193.

Longo L, Bygrave A., Grosveld FG, Pandolfi PP. (1997) The chromosome make-up of mouse embryonic stem cells is predictive of somatic and germ cell chimaerism*. Transgenic Res.* 6, 321–328.

Mali P, Yang L, Esvelt KM, Aach J, Guell M, DiCarlo JE, Norville JE, Church GM. (2013) RNA-guided human genome engineering via Cas9. *Science*. 339:823–826.4.

Mandelbaum J, Bhagat G, Tang H, Mo T, Brahmachary M, Shen Q, Chadburn A, Rajewsky K, Tarakhovsky A, Pasqualucci L, Dalla-Favera R. (2010) BLIMP1 is a tumor suppressor gene frequently disrupted in activated B cell-like diffuse large B cell lymphoma. *Cancer Cell*. 18(6):568-79.

Martin GR. (1981) Isolation of a pluripotent cell line from early mouse embryos cultured in medium conditioned by teratocarcinoma stem cells. *Proc Natl Acad Sci U S A*. 78(12):7634-8.

Matsui Y, Zsebo K, Hogan BL. (1992) Derivation of pluripotential embryonic stem cells from murine primordial germ cells in culture. *Cell*. 70(5):841-7.

Meek S, Wei J, Sutherland L, Nilges B, Buehr M, Tomlinson SR, Thomson AJ, Burdon T. (2013) Tuning of β-catenin activity is required to stabilize self-renewal of rat embryonic stem cells. *Stem Cells*. 31(10): 2104-15.

Meyenn F, Berrens RV, Andrews S, Santos F, Collier AJ, Krueger F, Osorno R, Dean W, Rugg-Gunn PJ, and Reik W. (2016) Comparative Principles of DNA

Methylation Reprogramming during Human and Mouse In Vitro Primordial Germ Cell Specification. *Developmental Cell.* 39: 104–115.

Mikkola M, Olsson C, Palgi J, Ustinov J, Palomaki T, Horelli-Kuitunen N, Knuutila S, Lundin K, Otonkoski T, Tuuri T. (2006) Distinct differentiation characteristics of individual human embryonic stem cell lines. *BMC Dev Biol*. 6:40.

Murakami K, Günesdogan U, Zylicz JJ, Tang WWC, Sengupta R, Kobayashi T, Kim S, Butler R, Dietmann S, Surani MA (2016) NANOG alone induces germ cells in primed epiblast in vitro by activation of enhancers. *Nature*. 529: 403–407.

Nagamatsu G, Kosaka T, Kawasumi M, Kinoshita T, Takubo K, Akiyama H, Sudo T, Kobayashi T, Oya M, Suda T. (2011) A germ cell-specific gene, Prmt5, works in somatic cell reprogramming. *J. Biol. Chem*. 286: 10641-10648.

Nakaki F, Hayashi K, Ohta H, Kurimoto K, Yabuta Y, Saitou M. (2013) Induction of mouse germ-cell fate by transcription factors in vitro. *Nature*. 501(7466):222-226.

Nakaki F, Saitou M. (2014) PRDM14: a unique regulator for pluripotency and epigenetic reprogramming. *Trends Biochem Sci*. 39(6): 289-98.

Nicholas JS, Hall BV. (1942) Experiments on developing rats. II. The development of isolated blastomeres and fused eggs. *J. Exp. Zool*. 90**:** 441-460.

Nichols J, Smith A, Buehr M. (1998) Rat and mouse epiblasts differ in their capacity to generate extraembryonic endoderm. *Reproduction, Fertility and Development*. 10(8) 517 – 526.

Nichols J, Smith A. (2009) Naive and primed pluripotent states. *Cell Stem Cell*. 4(6):487-92.

Nichols J, Smith A. (2011) The origin and identity of embryonic stem cells. *Development.* 138, 3-8.

Ohinata Y, Ohta H, Shigeta M, Yamanaka K, Wakayama T, Saitou M. (2009) A signaling principle for the specification of the germ cell lineage in mice. *Cell.* 137(3):571-84.

Ohinata Y, Payer B, O'Carroll D, Ancelin K, Ono Y, Sano M, Barton SC, Obukhanych T, Nussenzweig M, Tarakhovsky A, Saitou M, Surani MA. (2005) Blimp1 is a critical determinant of the germ cell lineage in mice. *Nature*. 436(7048):207-213.

Ouhibi N, Sullivan NF, English J, Colledge WH, Evans MJ, Clarke NJ. (1995). Initial culture behaviour of rat blastocysts on selected feeder cell lines. *Mol. Reprod. Dev*. 40, 311-324.

OüRahilly R, Müller F. (1987) Developmental Stages in Human Embryos. *Washington, DC: Carnegie. Institution of Washington;* (Publication 637). *Proc Natl Acad Sci U S A*. 98(11):6209-14.

Rao TP, Kühl M. (2010) An Updated Overview on Wnt Signaling Pathways: A Prelude for More. *Circulation Research* 106: 1798–1806.

Ray S, Dutta D, Rumi MA, Kent LN, Soares MJ, Paul S. (2009) Context-dependent Function of Regulatory Elements and a Switch in Chromatin Occupancy between GATA3 and GATA2 Regulate *Gata2* Transcription during Trophoblast Differentiation. *J. Biol. Chem.* 284*:* 4978–4988

Resnick JL, Bixler LS, Cheng L, Donovan PJ. (1992) Long-term proliferation of mouse primordial germ cells in culture. Nature. 359(6395):550-1.

Rhinn M, Dierich A, Shawlot W, Behringer RR, Le Meur M, Ang SL. (1998) Sequential roles for Otx2 in visceral endoderm and neuroectoderm for forebrain and midbrain induction and specification. *Development*, 125: 845-856

Richardson BE, Lehmann R (2010) Mechanisms guiding primordial germ cell migration: strategies from different organisms. *Nat Rev Mol Cell Biol.* 11(1):37-49*.*

Rivera-Pérez JA, Magnuson T. (2005) Primitive streak formation in mice is preceded by localized activation of Brachyury and Wnt3. *Dev Biol*. 288(2):363-71.

Rocchietti-March M, Weinbauer GF, Page DC, Nieschlag E, Gromoll J. (2000) Dazl protein expression in adult rat testis is up-regulated at meiosis and not hormonally regulated*. International journal of andrology*. 23: 51-56.

Rossant J. (2008) Stem cells and early lineage development. *Cell*. 132(4):527-31.

Rostovskaya M, Fu J, Obst M, Baer I, Weidlich S, Wang H, Smith AJ, Anastassiadis K, Stewart AF. (2012) Transposon-mediated BAC transgenesis in human ES cells. *Nucleic Acids Res*. 40(19): e150.

Sabour D, Araúzo-Bravo MJ, Hübner K, Ko K, Greber B, Gentile L, Stehling M, Schöler HR. (2011) Identification of genes specific to mouse primordial germ cells through dynamic global gene expression. *Human Molecular Genetics*, 20(1): 115–125

Saitou M, Payer B, Lange UC, Erhardt S, Barton SC, Surani MA. (2003) Specification of germ cell fate in mice. *Philos Trans R Soc Lond B Biol Sci.* 358(1436):1363-70.

Schäfer S, Anschlag J, Nettersheim D, Haas N, Pawig L, Schorle H. (2011) The role of BLIMP1 and its putative downstream target TFAP2C in germ cell development and germ cell tumours. *Int J Androl*. 34(4):e152-159.

Schedl A, Ross A, Lee M, Engelkamp D, Rashbass P, van Heyningen V, Hastie ND. (1996) Influence of PAX6 gene dosage on development: overexpression causes severe eye abnormalities. *Cell*. 86(1):71-82.

Schlafke S, Enders AC. (1963) Observations on the fine structure of the rat blastocyst. *J Anat*. 97(Pt 3): 353–360.5.

Silva J, Barrandon O, Nichols J, Kawaguchi J, Theunissen TW, Smith A. (2008) Promotion of reprogramming to ground state pluripotency by signal inhibition. PLoS Biol. 6:e253.

Smits BMG, Mudde JB, van de Belt J, Verheul M, Olivier J, Homberg J, Guryev V, Cools AR, Ellenbroek BA, Plasterk RHA, Cuppen E. (2006). Generation of gene knockouts and mutant models in the laboratory rat by ENU-driven target-selected mutagenesis. *Pharmacogenet. Genomics.* 16, 159-169.

Stewart CL, Gadi I, Bhatt H. (1994). Stem cells from primordial germ cells can reenter the germ line. *Dev. Biol.* 161, 626-628.

Stranzinger GF. (1996). Embryonic stem-cell-like cell lines of the species rat and Bovinae. *Int. J. Exp. Pathol.* 77, 263-267.

Streeter GL. (1942) Developmental horizons in human embryos. Description of age group XI, 13–20 somites, and age group XII, 21–29 somites. Contrib. Embryol. 30:211–245.

Sugawara A, Goto K, Sotomaru Y, Sofuni T, Ito T. (2006) Current status of chromosomal abnormalities in mouse embryonic stem cell lines used in Japan. *Comp Med*. 56(1):31-4.

Tada S, Era T, Furusawa C, Sakurai H, Nishikawa S, Kinoshita M, Nakao K, Chiba T, Nishikawa S. (2005) Characterization of mesendoderm: a diverging point of the definitive endoderm and mesoderm in embryonic stem cell differentiation culture. *Development*. 132(19):4363-74.

Takahashi S, Kobayashi S, Hiratani I. (2018) Epigenetic differences between naïve and primed pluripotent stem cells. *Cell Mol Life Sci*. 2018; 75(7): 1191–1203.

Tam PP, Zhou SX. (1996). The allocation of epiblast cells to ectodermal and germ-line lineages is influenced by the position of the cells in the gastrulating mouse embryo. *Dev. Biol*. 178, 124–132.

Tarkowski AK. (1962). Interspecific transfers of eggs between rat and mouse. *J. Embryol. Exp. Morphol*. 10**:** 476-495.

Tesar PJ, Chenoweth JG, Brook FA, Davies TJ, Evans EP, Mack DL, Gardner RL, McKay RD. (2007) New cell lines from mouse epiblast share defining features with human embryonic stem cells. Nature. 448(7150):196-9.

Tseng WF, Jang TH, Huang CB, Yuh CH. (2011) An evolutionarily conserved kernel of gata5, gata6, otx2 and prdm1a operates in the formation of endoderm in zebrafish. *Developmental Biology.* 357(2): 541-557

Ueda S, Kawamata M, Teratani T, Shimizu T, Tamai Y, Ogawa H, Hayashi K, Tsuda H, Ochiya T. (2008) Establishment of Rat Embryonic Stem Cells and Making of Chimera Rats. *PLoS ONE*. 3(7): e2800.

Vassilieva S, Guan K, Pich U, Wobus AM. (2000). Establishment of SSEA-1- and Oct-4-expressing rat embryonic stem-like cell lines and effects of cytokines of the IL-6 family on clonal growth. *Exp. Cell Res*. 258, 361-373

Veillard AC, Marks H, Bernardo AS, Jouneau L, Laloë D, Boulanger L, Kaan A, Brochard V, Tosolini M, Pedersen R, Stunnenberg H, Jouneau A. (2014) Stable methylation at promoters distinguishes epiblast stem cells from embryonic stem cells and the in vivo epiblasts. *Stem Cells Dev.* 23(17):2014–2029.

Vincent SD, Dunn NR, Sciammas R, Shapiro-Shalef M, Davis MM, Calame K., Bikoff EK, Robertson EJ. (2005) The zinc finger transcriptional repressor Blimp1/Prdm1 is dispensable for early axis formation but is required for specification of primordial germ cells in the mouse. *Development*. 132: 1315-1325.

Wang H, Xiang J, Zhang W, Li J, Wei Q, Zhong L, Ouyang H, Han J. (2016) Induction of Germ Cell-like Cells from Porcine Induced Pluripotent Stem Cells. *Scientific Reports*. 6, 27256.

Ward C, Stern P, Willington M, Flenniken A. (2002) Efficient germline transmission of mouse embryonic stem cells grown in synthetic serum in the absence of a fibroblast feeder layer. *Lab Invest*. 82:1765-7.

Ware CB, Siverts LA, Nelson AM, Morton JF, Ladiges WC. (2003) Utility of a C57BL/6 ES line versus 129 ES lines for targeted mutations in mice. Transgenic Res. 12(6):743-6.

Weber S, Eckert D, Nettersheim D, Gillis AJ, Schäfer S, Kuckenberg P, Ehlermann J, Werling U, Biermann K, Looijenga LH, Schorle H. (2010) Critical function of AP-2 gamma/TCFAP2C in mouse embryonic germ cell maintenance. Biol Reprod. 82(1):214-23.

Welling M, Geijsen N. (2013) Uncovering the true identity of naïve pluripotent stem cells. *Trends Cell Biol*. 23(9):442-448.

Werling U, Schorle H. Transcription factor gene AP-2 gamma essential for early murine development. (2002) *Mol Cell Biol* 2002; 22:3149–3156

Williams RL, Hilton DJ, Pease S, Willson TA, Stewart CL, Gearing DP, Wagner EF, Metcalf D, Nicola NA, Gough NM. (1988) Myeloid leukaemia inhibitory factor maintains the developmental potential of embryonic stem cells. *Nature*. 336(6200):684-7.

Winnier G, Blessing M, Labosky PA, Hogan BL. (1995) Bone morphogenetic protein-4 is required for mesoderm formation and patterning in the mouse. *Genes & Dev*. 9: 2105-2116.

Wongtrakoongate P, Jones M, Gokhale PJ, Andrews PW. (2013) STELLA Facilitates Differentiation of Germ Cell and Endodermal Lineages of Human Embryonic Stem Cells. *PLoS One*. 8(2): e56893.

Wu C, Bauer JS, Juliano RL, McDonald JA. *(*1993*).* The alpha 5 beta 1 integrin fibronectin receptor, but not the alpha 5 cytoplasmic domain, functions in an early and essential step in fibronectin matrix assembly. *J. Biol. Chem.* 268*:* 21883–*21888.*

Yamaji M, Seki Y, Kurimoto K, Yabuta Y, Yuasa M, Shigeta M, Yamanaka K, Ohinata Y, Saitou M (2008) Critical function of Prdm14 for the establishment of the germ cell lineage in mice. *Nat Genet* 40: 1016–1022.

Yamaji M, Tanaka T, Shigeta M, Chuma S, Saga Y, Saitou M. (2010) Functional reconstruction of NANOS3 expression in the germ cell lineage by a novel transgenic reporter reveals distinct subcellular localizations of NANOS3. *Reproduction.* 139 (2): 381–393.

Yamaji M, Ueda J, Hayashi K, Ohta H, Yabuta Y, Kurimoto K, Nakato R, Yamada Y, Shirahige K, Saitou M. (2013) PRDM14 ensures naive pluripotency through dual regulation of signaling and epigenetic pathways in mouse embryonic stem cells. *Cell Stem Cell*. 12(3):368-82.

Yang SH, Kalkan T, Morissroe C, Marks H, Stunnenberg H, Smith A, Sharrocks AD. (2014) Otx2 and Oct4 drive early enhancer activation during embryonic stem cell transition from naive pluripotency. *Cell Rep*. 7: 1968-1981.

Yaoyao Chen, Sonia Spitzer, Sylvia Agathou, Ragnhildur Thora Karadottir, and Austin Smith (2017) Gene Editing in Rat Embryonic Stem Cells to Produce In Vitro Models and In Vivo Reporters. *Stem Cell Reports*. 9(4): 1262–1274.

Yasunaga M, Tada S, Torikai-Nishikawa S, Nakano Y, Okada M, Jakt LM, Nishikawa S, Chiba T, Era T, Nishikawa S. (2005) Induction and monitoring of definitive and visceral endoderm differentiation of mouse ES cells. *Nat Biotechnol*. 23(12):1542-50.

Yeom YI, Fuhrmann G, Ovitt CE, Brehm A, Ohbo K, Gross M, Hübner K, Schöler HR. (1996) Germline regulatory element of Oct-4 specific for the totipotent cycle of embryonal cells. *Development.* 122(3):881-94.

Ying QL, Nichols J, Chambers I, Smith A. (2003) *BMP induction of Id proteins suppresses differentiation and sustains embryonic stem cell self-renewal in collaboration with STAT3*. *Cell* 115, 281–292.

Ying QL, Wray J, Nichols J, Batlle-Morera L, Doble B, Woodgett J, Cohen P, Smith A. (2008) The ground state of embryonic stem cell self-renewal. *Nature*. 453(7194):519-23.

Zhang J, Zhang M, Acampora D, Vojtek M, Yuan D, Simeone A, Chambers I. (2018) OTX2 restricts entry to the mouse germline. *Nature.* 562: 595–599.

*Zhang Z, Morla A, Vuori K, Bauer J, Juliano R, Ruoslahti E. (*1993*).* The alpha v beta 1 integrin functions as a fibronectin receptor but does not support fibronectin matrix assembly and cell migration on fibronectin. *J. Cell Biol.* 122*:*235–242.

Zhao X, Lv Z, Liu L, Wang L, Tong M, Zhou Q. (2010) Derivation of embryonic stem cells from Brown Norway rats blastocysts. *J Genet Genomics*. 37(7):467-73.

Chapter 9 Appendix

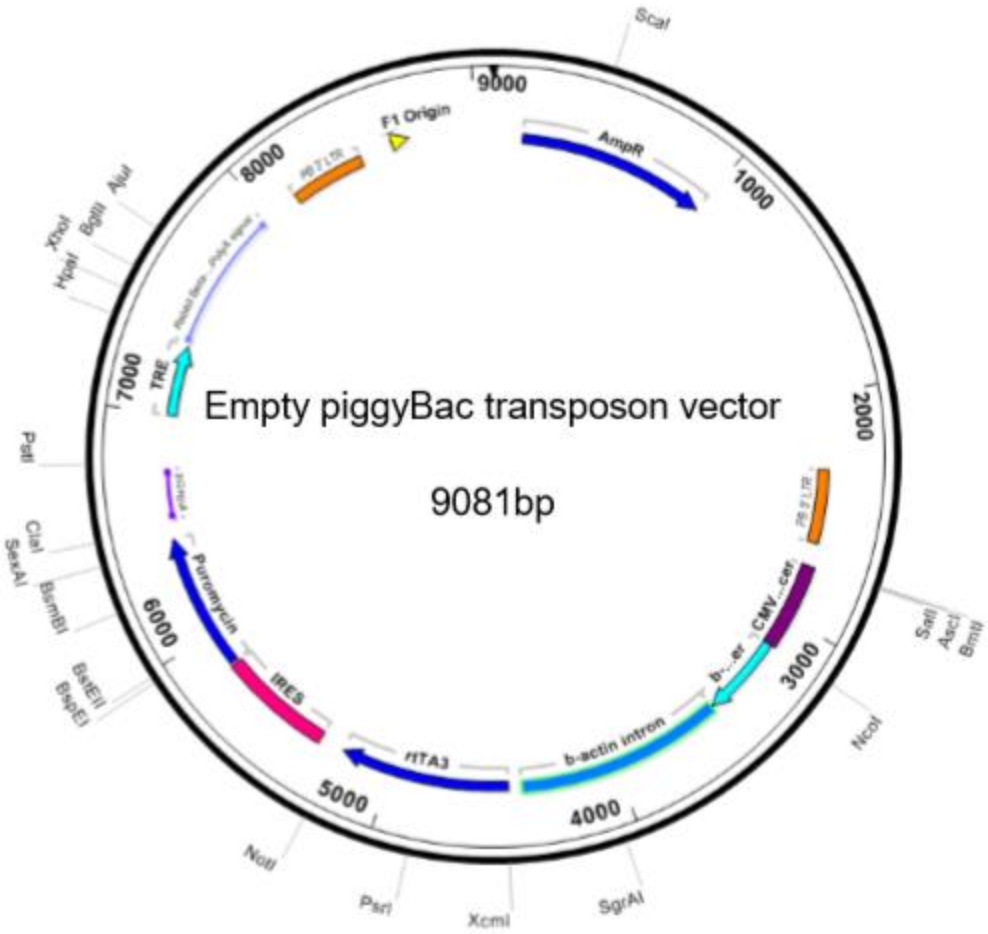

Figure A 1. Tet-EMPTY vector map

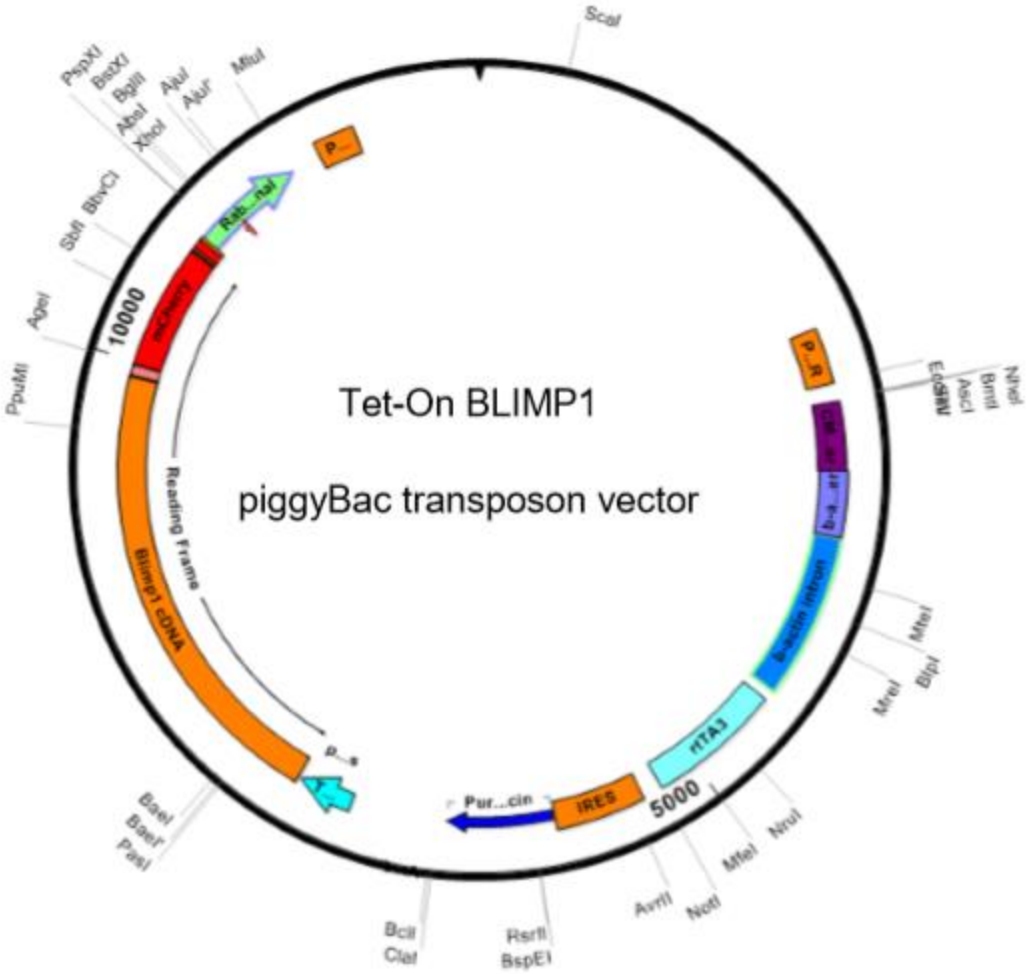

Figure A 2. Tet-BLIMP1 vector map

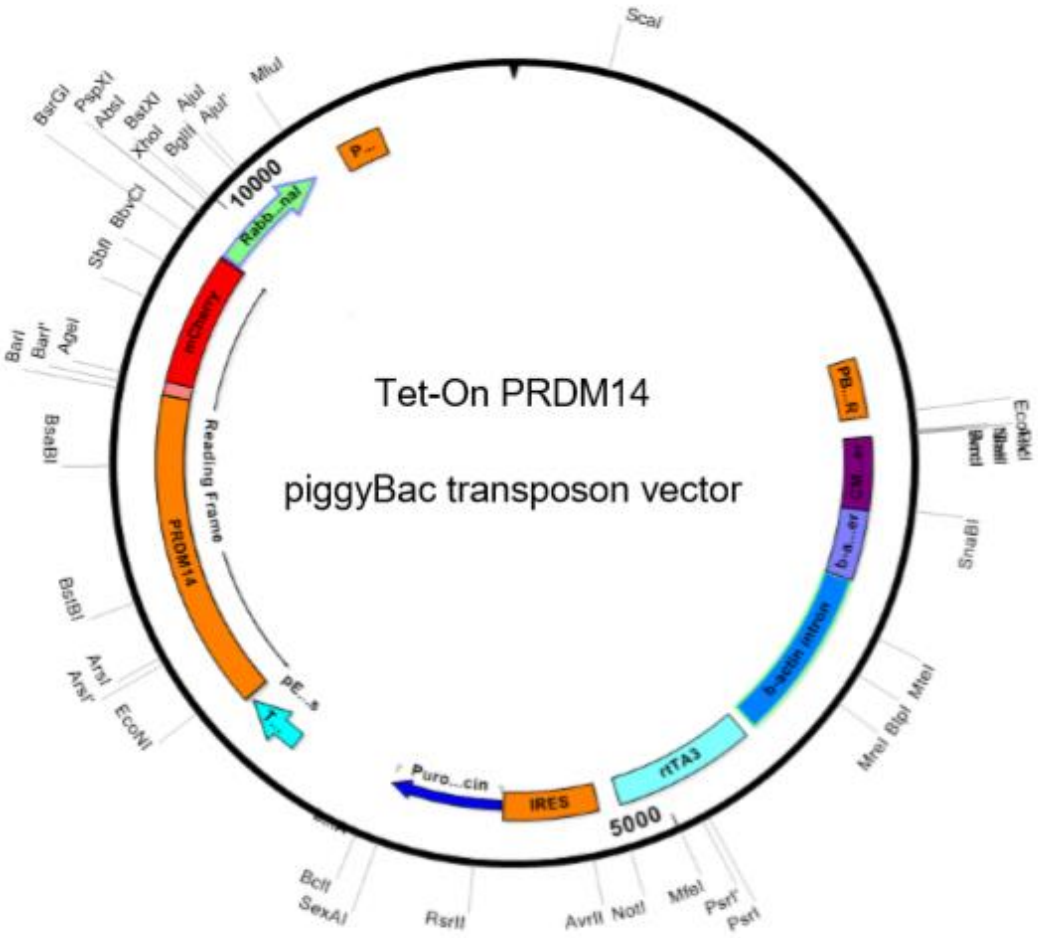

Figure A 3. Tet-PRDM14 vector map

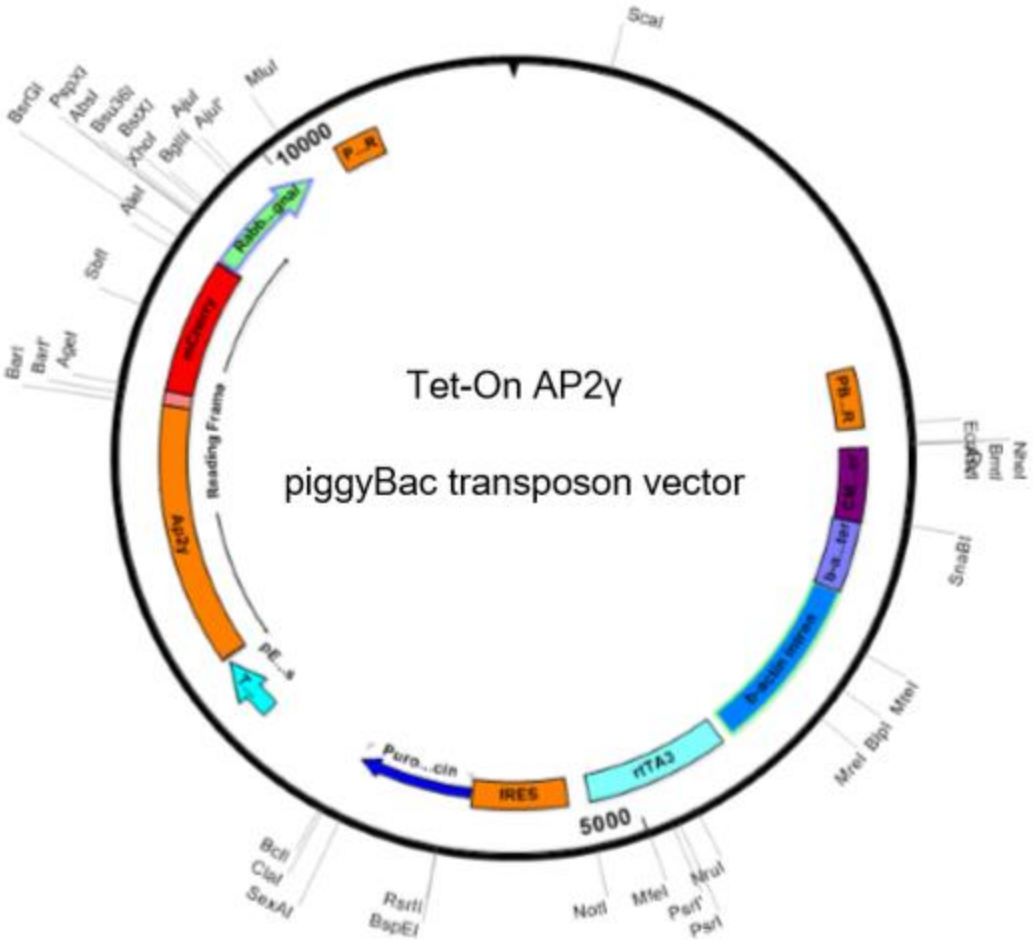

Figure A 4. Tet-AP2γ vector map

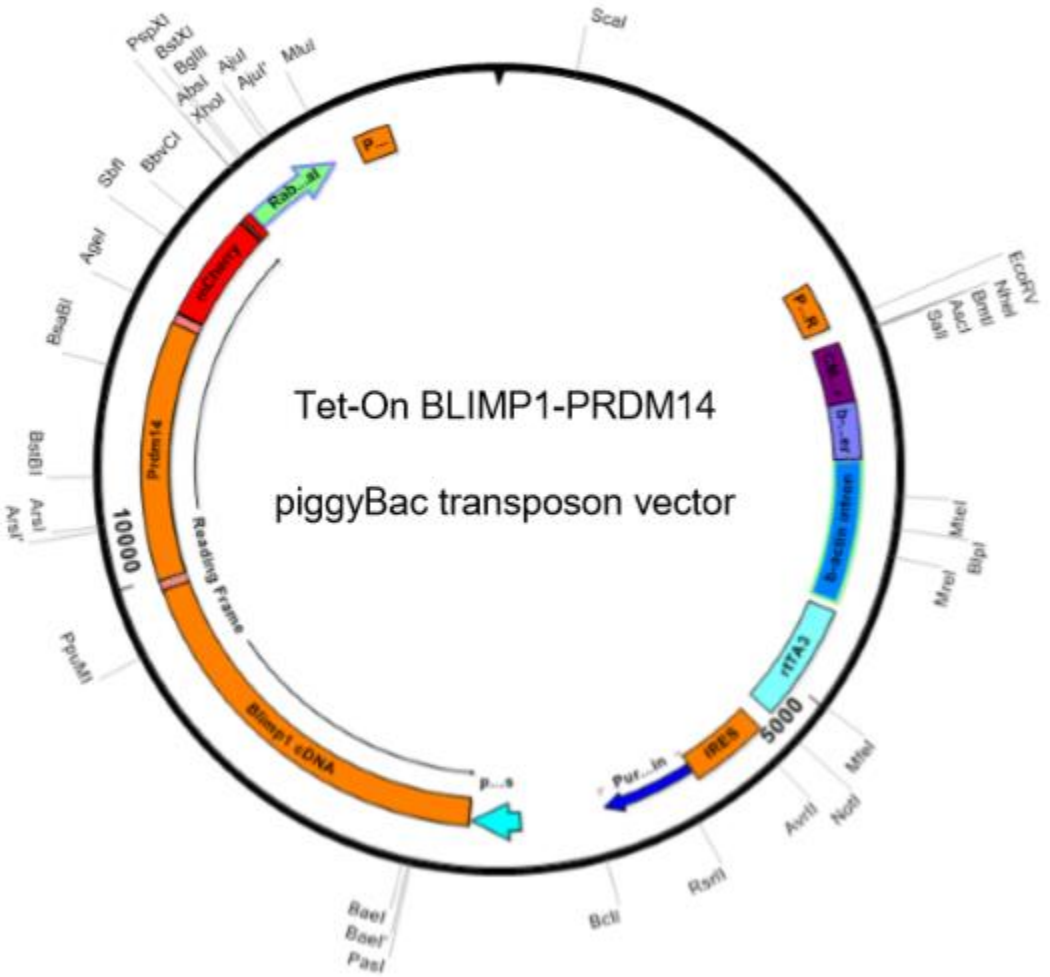

Figure A 5. Tet-BLIMP1-PRDM14 vector map

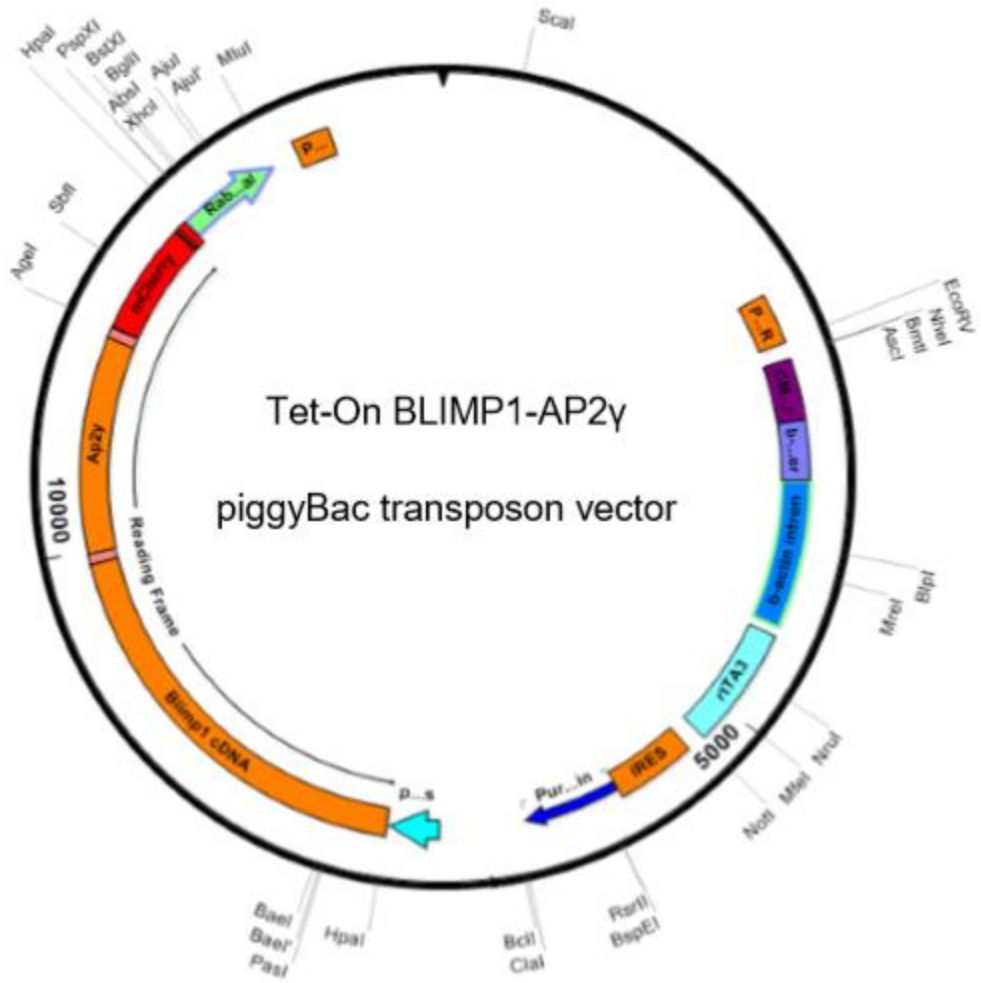

Figure A 6. Tet-BLIMP1-AP2γ vector map

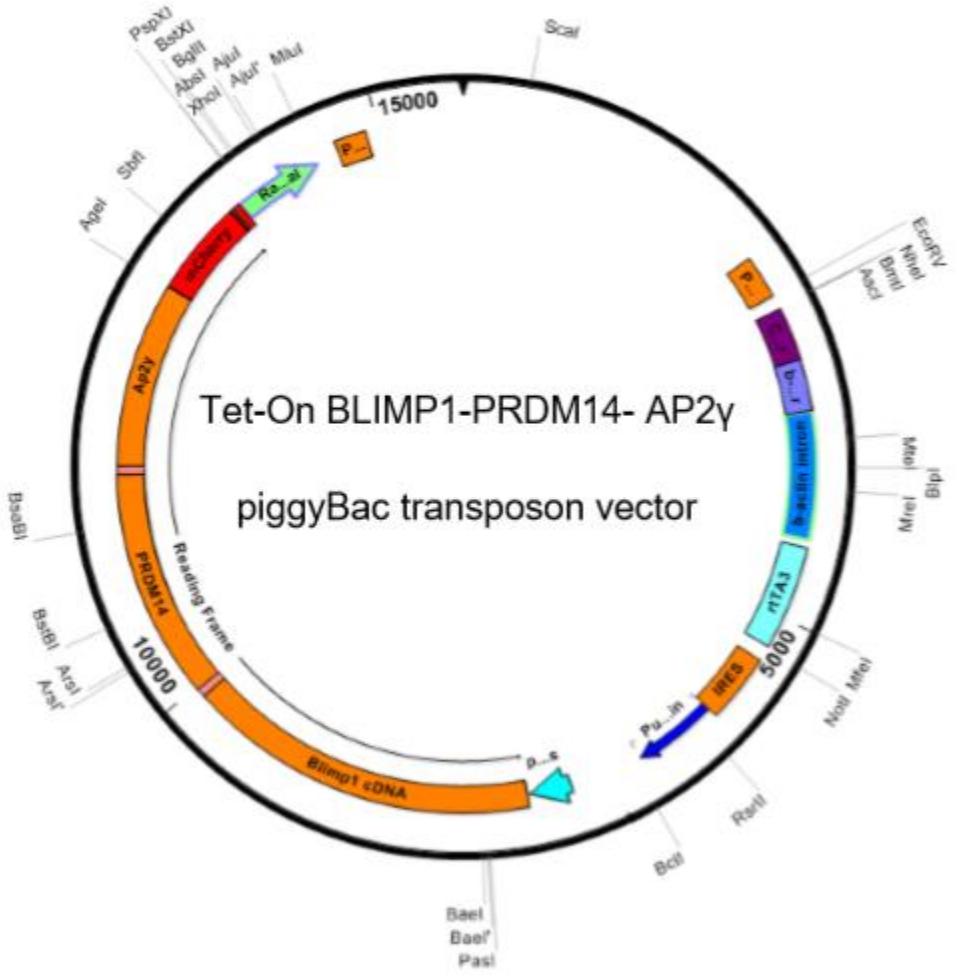

Figure A 7. Tet-BLIMP1-PRDM14-AP2γ vector map

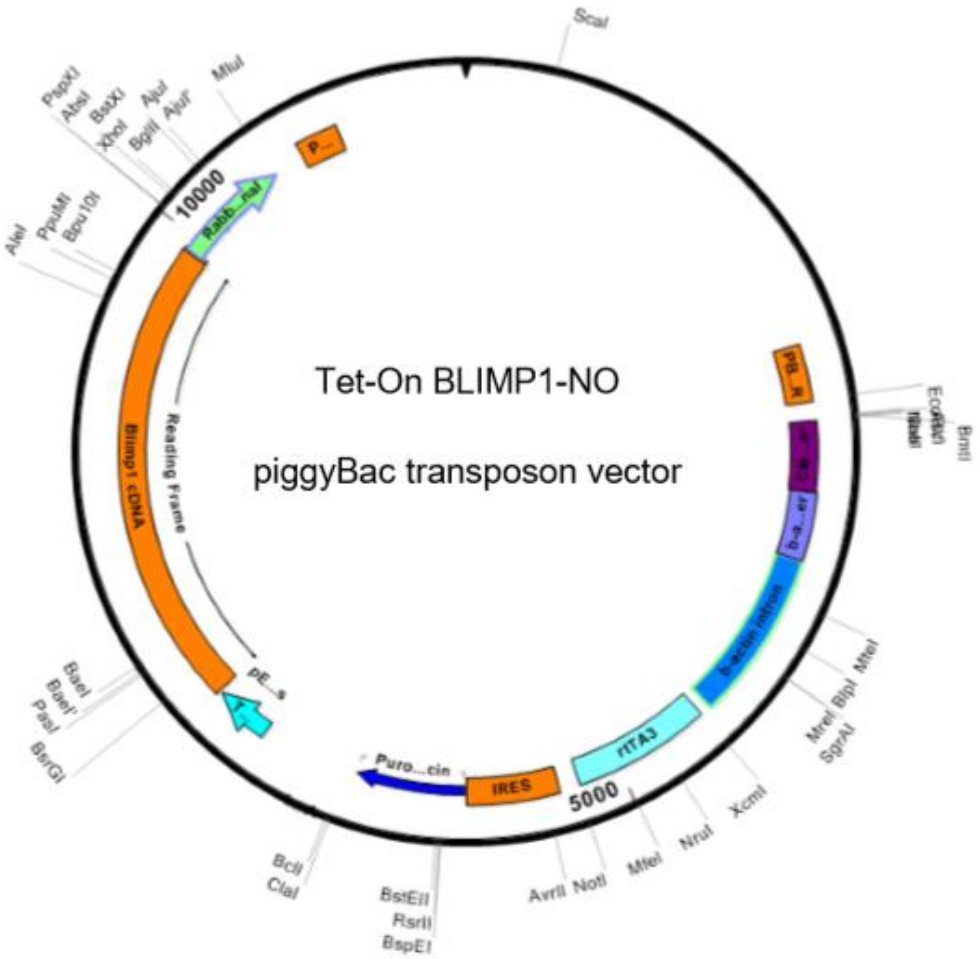

Figure A 8. Tet-BLIMP1-NO vector map

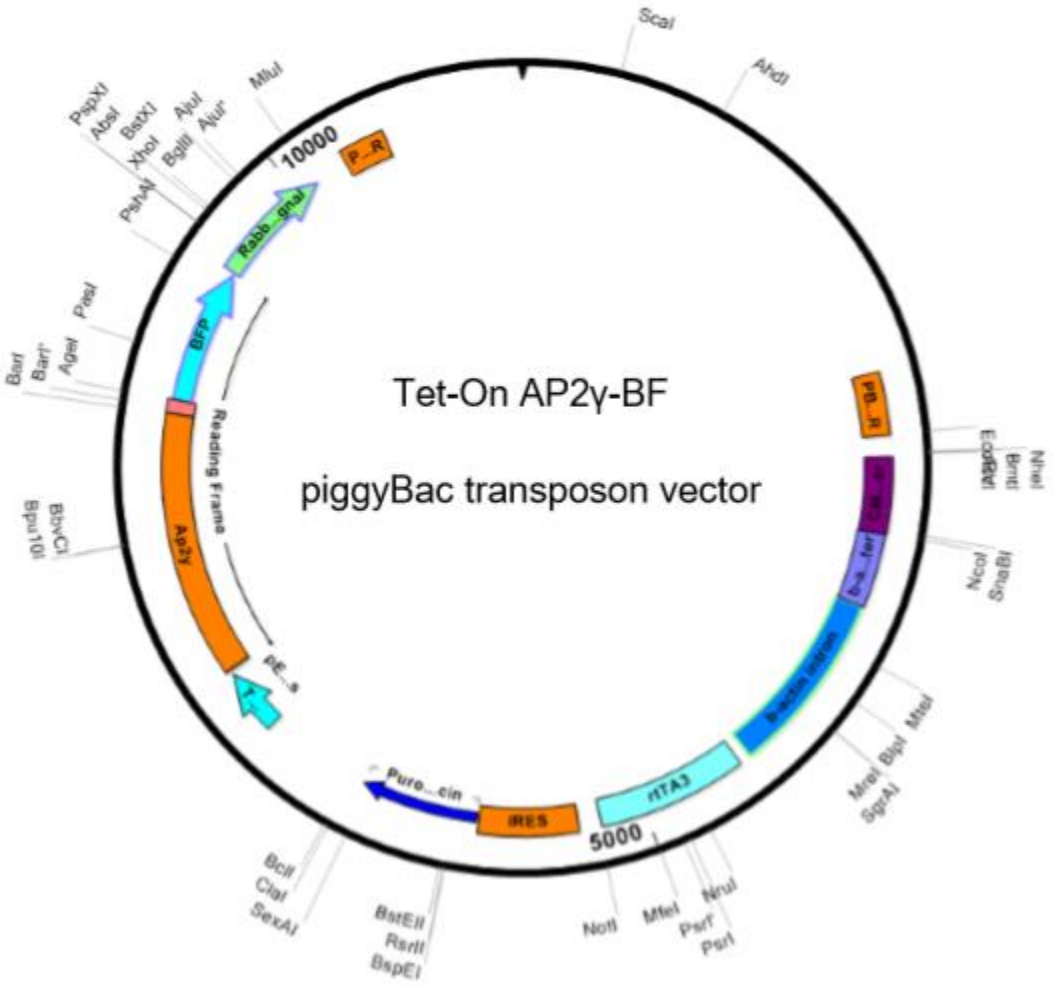

Figure A 9. Tet-AP2γ-BF vector map

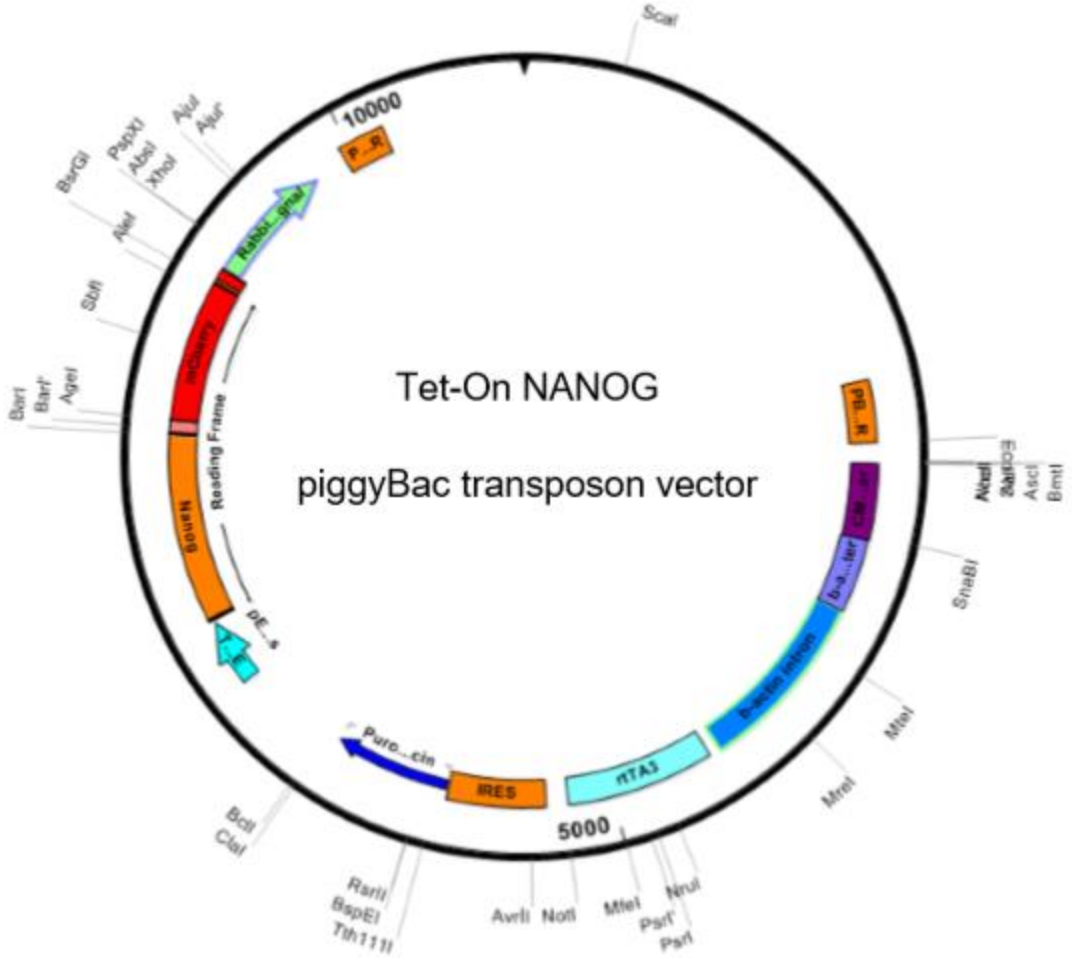

Figure A 10. Tet-NANOG vector map